Characterization of *Populus x canescens* LysM Receptor-Like Kinases CERK1-1 and CERK1-2 and their Role in Chitin Signaling

Dissertation

zur Erlangung des mathematisch-naturwissenschaftlichen Doktorgrades

"Doctor rerum naturalium"

der Georg-August-Universität Göttingen

im Promotionsprogramm Biologie

der Georg-August University School of Science (GAUSS)

vorgelegt von

Mascha Milenka Muhr

aus Soest

Göttingen, 2022

Betreuungsausschuss

1. Betreuer: **Prof. Dr. Volker Lipka**
Zellbiologie der Pflanze,
Albrecht-von-Haller Institut für Pflanzenwissenschaften

2. Betreuer: **PD Dr. Thomas Teichmann**
Zellbiologie der Pflanze,
Albrecht-von-Haller Institut für Pflanzenwissenschaften

Mitglieder der Prüfungskommission

Referent: **PD Dr. Thomas Teichmann**
Zellbiologie der Pflanze,
Albrecht-von-Haller Institut für Pflanzenwissenschaften

Korreferent: **Prof. Dr. Andrea Polle**
Forstbotanik und Baumphysiologie,
Büsgen-Institut

Weitere Mitglieder der Prüfungskommission

Prof. Dr. Volker Lipka
Zellbiologie der Pflanze,
Albrecht-von-Haller Institut für Pflanzenwissenschaften

Prof. Dr. Ivo Feußner
Biochemie der Pflanze,
Albrecht-von-Haller Institut für Pflanzenwissenschaften

Prof. Dr. Christiane Gatz
Molekularbiologie und Physiologie der Pflanze,
Albrecht-von-Haller Institut für Pflanzenwissenschaften

PD Dr. Marcel Wiermer
Molekularbiologie der Pflanze-Mikroben Interaktion,
Albrecht-von-Haller Institut für Pflanzenwissenschaften

Tag der mündlichen Prüfung: 07.03.2022

Promovierenden-Erklärung

der Georg-August-Universität Göttingen

Die Gelegenheit zum vorliegenden Promotionsvorhaben ist mir nicht kommerziell vermittelt worden. Insbesondere habe ich keine Organisation eingeschaltet, die gegen Entgelt Betreuerinnen und Betreuer für die Anfertigung von Dissertationen sucht oder die mir obliegenden Pflichten hinsichtlich der Prüfungsleistungen für mich ganz oder teilweise erledigt.

Hilfe Dritter wurde bis jetzt und wird auch künftig nur in wissenschaftlich vertretbarem und prüfungsrechtlich zulässigem Ausmaß in Anspruch genommen. Insbesondere werden alle Teile der Dissertation selbst angefertigt; unzulässige fremde Hilfe habe ich dazu weder unentgeltlich noch entgeltlich entgegengenommen und werde dies auch zukünftig so halten.

Die Ordnung zur Sicherung der guten wissenschaftlichen Praxis an der Universität Göttingen wurde von mir beachtet.

Eine entsprechende Promotion wurde an keiner anderen Hochschule im In- oder Ausland beantragt; die eingereichte Dissertation oder Teile von ihr wurden nicht für ein anderes Promotionsvorhaben verwendet.

Mir ist bekannt, dass unrichtige Angaben die Zulassung zur Promotion ausschließen bzw. später zum Verfahrensabbruch oder zur Rücknahme des erlangten Grades führen.

Solingen, den

Mascha Muhr

Summary

Poplar trees have been established as a model organism to study woody perennial plants. The first fully sequenced tree species was *Populus trichocarpa*. Nevertheless, for experiments in the laboratory often other *Populus* species are used that are less recalcitrant to transformation than *Populus trichocarpa*. Amongst others, *Populus x canescens*, a natural hybrid of *P. tremula* x *P. alba*, is a species that is much easier transformable.

Due to their fast growth and easy propagation, poplars are also of commercial interest for the pulp and paper industry and serve as a renewable energy resource for the production of biofuel and biogas. Poplars can be planted in short rotation coppices and produce a high amount of biomass within a few years. However, poplar plantations suffer from different pathogens that significantly impair plant growth. Rust fungi of the genus *Melampsora* are a class of pathogens responsible for major biomass losses due to infection-induced early defoliation as well as a decrease of stem height and stem diameter.

Plants recognize microbes with the help of receptor complexes that are specific for pathogen-associated molecular patterns (PAMPs). The detection of PAMPs leads to defense reactions like the activation of mitogen-activated protein kinase (MAPK) signaling cascades to activate defense genes and the generation of reactive oxygen species (ROS). Lysin motif receptor-like kinases (LysM-RLKs) and lysin motif receptor-like proteins (LysM-RLPs) play a crucial role for the recognition of fungal pathogens. They are able to bind different N-acetylglucosamine containing molecules and thus also bind the β-1,4-linked N-acetylglucosamine homopolymer chitin which is the major component of the fungal cell wall.

Plant receptors that are involved in chitin perception are best studied in Arabidopsis and rice. In Arabidopsis, chitin is detected by a receptor complex consisting of the LysM-RLK CHITIN ELICITOR RECEPTOR KINASE 1 (AtCERK1) and two other LysM-RLKs, LYK4 and LYK5. In rice the LysM-RLP CHITIN ELICITOR BINDING PROTEIN (OsCEBiP) is the major chitin receptor. However, chitin-triggered responses are dependent on association of OsCEBiP with OsCERK1.

In this thesis, LysM-RLKs or LysM-RLPs that play a role for chitin perception in poplar were identified. A phylogenetic analysis revealed that the *Populus trichocarpa* genome encodes homologs of all known LysM-RLKs and LysM-RLPs described in the model organisms *Arabidopsis thaliana*, *Oryza sativa*, *Medicago truncatula* and *Lotus japonicus*. Mass spectrometry analyses of chitin affinity purified protein samples from *Populus trichocarpa* and

Populus x canescens were performed to identify LysM-RLKs or LysM-RLPs with a potential function in chitin binding and perception. Poplar *CERK1* turned out to be the main candidate for a key component of the poplar chitin receptor. *In-silico* analyses of the protein domains of the two paralogous *CERK1* genes, *PcCERK1-1* and *PcCERK1-2*, which are present in *Populus x canescens,* suggested that both genes encode functional LysM-RLKs with kinase activity. A functional analysis evaluating the role of the *PcCERK1* paralogs in ROS burst and MAPK activation was carried out with complementation studies of a chitin-insensitive Arabidopsis *Atcerk1* mutant and CRISPR/Cas9 generated knockout mutants in poplar. Complementation could only be accomplished for the *PcCERK1-2* gene that partially restored the chitin-triggered MAPK activation of *Atcerk1*. However, the results from the poplar knockout mutants suggest a function for both *PcCERK1* genes in both chitin signaling processes. As possible reason for the lack of complementation ability of *PcCERK1-1* and the lack of ROS burst complementation for *PcCERK1-2*, amino acid substitutions between AtCERK1 and PcCERK1-1/PcCERK1-2 are discussed that might lead to conformational changes and thus impair interaction of PcCERK1 proteins with downstream components of the Arabidopsis signal transduction.

Poplar leaves of *Pccerk1-1* and *Pccerk1-2* single knockouts both had a normal ROS burst response after chitin treatment whereas in the *Pccerk1-1 Pccerk1-2* double knockout mutant the chitin-triggered ROS burst was completely abolished. Therefore, a redundant function for both genes mediating the generation of ROS after chitin perception was concluded. MAPK activation in chitin elicitor treated leaf samples was shown to be predominantly dependent on *PcCERK1-1.* In the *Pccerk1-1* single knockout the chitin-triggered MAPK response was strongly impaired while the *Pccerk1-2* single knockout showed a wildtype-like response. The slight residual MAPK activation in the *Pccerk1-1* single knockout was supposed to be caused by *PcCERK1-2* since in the double knockout the ability for chitin-induced MAPK signaling was entirely lost. In leaves *PcCERK1-1* has been shown to be significantly higher expressed than *PcCERK1-2*. Thus, functional analyses and expression data indicate that chitin signaling in *Populus x canescens* is mainly mediated by *PcCERK1-1*.

In addition to the generation of gene knockouts the overexpression of a kinase dead *Pccerk1-1* variant was tested as an alternative strategy for functional analysis. The overexpression was supposed to exhibit a dominant negative effect on chitin signaling. The response to chitin in regard to MAPK and ROS burst signaling was only slightly reduced in a *Pccerk1-1_LOF* (LOF: loss of function) overexpressor line. This was probably due to a low expression level of the

Pccerk1-1_LOF variant since in Arabidopsis *Atcerk1_LOF* overexpressor lines chitin-triggered ROS and MAPK activation was completely abolished. Another reason might be the presence of homodimeric receptor complexes involving the second paralog PcCERK1-2 that still have signal transduction capacity. Nevertheless, the results indicate that PcCERK1-1 has the kinase activity predicted by *in-silico* analyses and that this kinase activity is important for signal transduction.

In conclusion, the results of this thesis show that both *PcCERK1* genes are involved in chitin-triggered defense responses. *PcCERK1-1* and *PcCERK1-2* have maintained redundant functions in chitin-triggered ROS burst. In contrast to this, *PcCERK1* paralogs show a functional diversification in chitin-triggered MAPK activation, which mainly depends on *PcCERK1-1*.

Zusammenfassung

Pappeln sind als ein Modell-Organismus für die Forschung an Bäumen etabliert. *Populus trichocarpa* war die erste vollständig sequenzierte Baumart. Trotzdem werden im Labor häufig andere Pappelarten für Experimente verwendet, da *Populus trichocarpa* nur schwer transformierbar ist. Zum Beispiel lassen sich Pappeln der Art *Populus x canescens* (eine natürliche Hybride aus *P. tremula* x *P. alba*) leichter unter Laborbedingungen kultivieren und transformieren.

Aufgrund ihres schnellen Wachstums und ihrer relativ einfachen Vermehrung sind Pappeln auch von wirtschaftlichem Interesse für die Holz-verarbeitende Industrie und werden als erneuerbare Energiequelle für die Produktion von Biotreibstoff und Biogas genutzt. Pappeln können in Kurzumtriebsplantagen angebaut werden und bereits innerhalb weniger Jahre eine große Menge an Biomasse produzieren. Allerdings besteht die Gefahr, dass der Befall mit Schädlingen das Wachstum der Bäume erheblich einschränkt. Rostpilze der Gattung *Melampsora* sind weit verbreitete Krankheitserreger, die zu den Hauptursachen für einen geringen Biomassezuwachs infizierter Pappelplantagen zählen, da der Befall mit diesen Pilzen einen verfrühten Blattabfall sowie ein vermindertes Stammwachstum bewirkt.

Pflanzen sind in der Lage schädliche Organismen mit Hilfe von Rezeptoren zu erkennen, die spezifisch für sogenannte Pathogen-assoziierte molekulare Muster sind (PAMPs). Die Erkennung solcher Pathogen-assoziierten molekularen Muster löst verschiedene Abwehrmechanismen aus. Ein Beispiel ist die Produktion von reaktiven Sauerstoffspezies (ROS) oder die Aktivierung von Mitogen-aktivierten Proteinkinase (MAPK) Signalkaskaden, um die Expression von Abwehrgenen zu initiieren. Lysin-Motiv Rezeptor-ähnliche Kinasen (LysM-RLKs) oder Lysin-Motiv Rezeptor-ähnliche Proteine (LysM-RLPs) spielen eine wesentliche Rolle für die Erkennung pilzlicher Erreger. Sie binden Moleküle, die N-Acetylglucosamin enthalten, und somit auch Chitin, ein Homopolymer aus β-1,4-glycosidisch verknüpften N-Acetylglucosamin, welches ein Hauptbestandteil der pilzlichen Zellwand ist.

Welche Rezeptoren in Pflanzen für die Chitinerkennung verantwortlich sind, ist am besten in Arabidopsis und Reis erforscht. In Arabidopsis besteht der Chitin-bindende Rezeptor-Komplex aus der LysM-RLK „CHITIN ELICITOR RECEPTOR KINASE 1“ (AtCERK1) und zwei weiteren LysM-RLKs, LYK4 und LYK5. In Reis ist das LysM-RLP „CHITIN ELICITOR BINDING PROTEIN“ (OsCEBiP)

essentiell für die Chitin-Erkennung. Allerdings ist auch in Reis die LysM-RLK OsCERK1 ein wichtiger Co-Rezeptor von OsCEBiP.

In dieser Dissertation wurde untersucht, welche LysM-RLKs oder LysM-RLPs eine Rolle für die Chitin-vermittelte Immunantwort in der Pappel spielen. Es konnte mit Hilfe einer phylogenetischen Analyse gezeigt werden, dass das Genom von *Populus trichocarpa* für homologe Proteine von allen bereits bekannten LysM-RLKs und LysM-RLPs aus den vier verschiedenen Modelorganismen *Arabidopsis thaliana*, *Oryza sativa*, *Medicago truncatula* und *Lotus japonicus* kodiert. Um von diesen homologen Proteinen diejenigen zu identifizieren, die die Fähigkeit haben Chitin zu binden, wurde die potentielle Chitin-Affinität der Zielproteine zur Aufreinigung von Proteinproben genutzt, welche anschließend mittels Massenspektrometrie analysiert wurden. Es wurden dabei sowohl Proben von *Populus trichocarpa* als auch von *Populus x canescens* verwendet. Es stellte sich heraus, dass *CERK1* auch in der Pappel ein Hauptkandidat unter den LysM-RLKs ist, welche wahrscheinlich an der Chitinerkennung beteiligt sind. *In-silico* Analysen der Protein-Domänen von zwei paralogen *CERK1* Genen, *PcCERK1-1* und *PcCERK1-2*, aus *Populus x canescens,* weisen für beide Gene darauf hin, dass diese potentiell funktionale LysM-RLKs mit Kinaseaktivität sind. Daher wurde die Funktion untersucht, die diese Paraloge in der Chitin-induzierten Produktion von ROS und MAPKinasen-Aktivierung haben. Dafür wurden einerseits Komplementationsstudien in der Arabidopsis-Mutante *Atcerk1,* welche nicht mehr in der Lage ist, auf Chitin zu reagieren, durchgeführt und andererseits Pappelmutanten untersucht, in denen beide Gene durch Gen-Knockouts ausgeschaltet wurden. In der *Atcerk1* Mutante konnte mit dem *PcCERK1-2* Gen nur teilweise die durch Chitin ausgelöste MAPK-Aktivierung wiederhergestellt werden. Die Ergebnisse der Pappel-Knockout-Mutanten deuten jedoch auf eine Funktion beider *PcCERK1*-Gene bei der Chitin-Signalübertragung hin. Als mögliche Gründe für die fehlende Fähigkeit von PcCERK1-1 die *Atcerk1* Linie zu komplementieren und von PcCERK1-2 den ROS burst von *Atcerk1* wiederherzustellen, werden Aminosäuresubstitutionen zwischen AtCERK1 und PcCERK1-1/PcCERK1-2 diskutiert, die möglicherweise die Konformation des Proteins derart verändern, dass die Signalweiterleitung vom Rezeptor nicht mehr möglich ist, da die Bindung der dafür notwendigen Arabidopsis-Interaktionspartner beeinträchtigt ist.

Für die *Pccerk1-1* und *Pccerk1-2* Einzel-Knockouts in der Pappel wurde jeweils eine normale ROS-Burst-Reaktion nach der Chitinbehandlung nachgewiesen, während in der *Pccerk1-1 Pccerk1-2* Doppel-Knockout-Mutante gar kein ROS-Burst mehr sichtbar war. Daher wurde für

beide Gene auf eine redundante Funktion bei der Erzeugung von ROS nach Chitin-Wahrnehmung geschlossen. Im Gegensatz dazu, konnte nachgewiesen werden, dass die MAPK-Aktivierung in mit Chitin behandelten Blattproben überwiegend von *PcCERK1-1* abhängt. In den *Pccerk1-1* Einzel-Knockout Pflanzen war die durch Chitin ausgelöste MAPK-Reaktion stark beeinträchtigt, während die *Pccerk1-2* Einzel-Knockout Pflanzen immer noch eine wildtypähnliche Reaktion aufwiesen. Das schwache MAPK-Restsignal im *Pccerk1-1* Einzel-Knockout wurde vermutlich durch *PcCERK1-2* verursacht, da die Doppel-Knockout Pflanzen gar keine Chitin-induzierte MAPK-Aktivierung aufwiesen. Interessanterweise zeigte eine Expressionsanalyse, dass *PcCERK1-1* in Blättern signifikant höher exprimiert wird als *PcCERK1-2*. Somit deuten die Ergebnisse der Funktionsanalyse und die Expressionsdaten darauf hin, dass die Chitinperzeption im Wesentlichen durch *PcCERK1-1* vermittelt wird.

Als Alternative zu der Erstellung der Knockout Pflanzen wurde getestet, ob die Überexpression eines modifizierten *PcCERK1-1* Gens mit funktionsloser Kinasedomäne (*Pccerk1-1_LOF;* LOF: loss of function) einen dominant negativen Effekt auf die Chitin-vermittelte Signalweiterleitung hat. Es konnte jedoch nur eine geringfügig verminderte Signalstärke für ROS-Burst oder MAPKinase Aktivierung festgestellt werden. Vermutlich liegt dies an einer zu niedrigen Expressionsrate von *Pccerk1-1_LOF*, da derselbe Versuch in Arabidopsis in den *Atcerk1_LOF* Überexpressions-Linien zu einem kompletten Verlust der Chitin-induzierten ROS Produktion und MAPK-Aktivierung führte. Außerdem könnten auch homodimere Rezeptorkomplexe mit PcCERK1-2 immer noch funktional sein. Allerdings liefert dieses Experiment trotzdem einen Hinweis darauf, dass PcCERK1-1 tatsächlich die bereits durch die *in-silico* Analyse vermutete Kinaseaktivität aufweist und diese wichtig für die Signalweiterleitung ist.

Zusammenfassend zeigen die Ergebnisse dieser Arbeit, dass beide *PcCERK1* Gene an durch Chitin ausgelösten Abwehrreaktionen beteiligt sind. *PcCERK1-1* und *PcCERK1-2* scheinen beide eine redundante Funktion für die ROS Produktion zu haben. Im Gegensatz dazu hat eine funktionale Diversifizierung der Paraloge hinsichtlich MAPK-Aktivierung stattgefunden, welche hauptsächlich durch *PcCERK1-1* vermittelt wird.

List of abbreviations

α	anti / alpha
Ω	Ohm
°C	degree Celsius
µg	microgramm
µl	microliter
µm	micrometer
µM	micromolar
µmol	micromol
A. thaliana	*Arabidopsis thaliana*
A. tumefaciens	*Agrobacterium tumefaciens*
AcN	acetonitrile
AM	arbuscular mycorrhizal
AP	alkaline phosphatase
APS	ammonium persulfate
At	*Arabidopsis thaliana*
ATP	adenosine triphosphate
Avr	avirulence
bp	base pairs
BAR	bialaphos resistance gene
BIK1	BOTRYTIS-INDUCED KINASE 1
BLASTP	Basic Local Alignment Search Tool (for protein sequences)
BSA	bovine serum albumin
C6mer	chitin hexamer
Ca^{2+}	calcium
Cas9	CRISPR-associated protein 9
CDPK	Ca^{2+}-dependent protein kinase
CEBiP	CHITIN ELICITOR BINDING PROTEIN
CERK1	CHITIN ELICITOR RECEPTOR LIKE KINASE 1
CO	chitooligosaccharides
CRISPR	clustered regularly interspaced short palindromic repeats
DNA	desoxyribonucleic acid
DTT	dithiothreitol
E. coli	*Escherichia coli*
EDR1	ENHANCED DISEASE RESISTANCE 1
EDTA	ethylenediaminetetraacetic acid
EFR	ELONGATION FACTOR TU RECEPTOR
ER	endoplasmic reticulum
ESTs	expressed sequence tags
et al.	et alii (and others)
ETI	effector-triggered immunity
ETS	effector-triggered susceptibility
FA	formic acid

FAD	flavin adenine dinucleotide
flg22	22-amino acid peptide of the conserved N-terminal part of flagellin
FLS2	FLAGELLIN SENSITIVE 2
FT2	FLOWERING LOCUS T2
g	gram or gravitation
GFP	green fluorescence protein
GlcNAc	N-acetylglucosamine
GPI anchor	glycosylphosphatidylinositol anchor
gRNA	guide RNA
h	hours
H_2O_2	hydrogen peroxide
HEPES	4-(2-hydroxyethyl)-1-piperazineethanesulfonic acid
HR	hypersensitive cell death response
Hyg	hygromycin
IAM	iodoacetamide
ISR	induced systemic resistance
Kan	kanamycin
KOH	potassium hydroxide
l	liter
LB	Luria-Bertani
LCO	lipo-chitooligosaccharides
LHY1	LATE ELONGATED HYPOCOTYL 1
LHY2	LATE ELONGATED HYPOCOTYL 2
Lj	*Lotus japonicus*
LOF	loss of function
LRR	leucine rich repeat
LTF1	LIGNIN BIOSYNTHESIS-RELATED TRANSCRIPTION FACTOR 1
LYK	LYSIN MOTIF RECEPTOR-LIKE KINASE
LYM	LYSIN MOTIF RECEPTOR-LIKE PROTEIN
LYP	LYSIN MOTIF CONTAINING PROTEIN
LysM	lysin motif
LysM-RLKs	lysin motif receptor-like kinases
LysM-RLPs	lysin motif receptor-like proteins
M	molar
m	meter
MAMPs	microbe-associated molecular patterns
MAPK	mitogen-activated protein kinase
MAPKK	mitogen-activated protein kinase kinase
MAPKKK	mitogen-activated protein kinase kinase kinase
MeOH	methanol
Mg	magnesium
$MgCl_2$	magnesium chloride
$MgSO_4$	magnesium sulfate
min	minute(s)
ml	milliliter
mm	millimeter

mM	millimolar
MS	Murashige and Skoog medium
Mt	*Medicago truncatula*
Myc factor	mycorrhization factor
MYR1	MYC FACTOR RECEPTOR 1
N. benthamiana	*Nicotiana benthamiana*
Na_2MoO_4	sodium molybdate
NaCl	sodium chloride
NADPH	nicotinamide adenine dinucleotide phosphate
NaF	sodium fluoride
NB-LRR	nucleotide binding leucine rich repeat
NFP	NOD FACTOR PERCEPTION
NFR	NOD FACTOR RECEPTOR
NFRe	epidermal NOD FACTOR RECEPTOR
NH_4HCO_3	ammonium hydrogencarbonate
$(NH_4)_2SO_4$	ammonium sulfate
nM	nanomolar
nm	nanometer
Nod factor	nodulation factor
O_2	dioxygen
O_2^-	superoxide
OD	optical density
Os	*Oryza sativa*
PAD3	PHYTOALEXIN DEFICIENT 3
PAMPs	pathogen-associated molecular patterns
PBL	PBS1-LIKE PROTEIN
Pc	*Populus x canescens*
PGN	peptidoglycan
PKA-Cα	PROTEIN KINASE A catalytic subunit alpha isoform
PR1	PATHOGENESIS-RELATED PROTEIN 1
PRR	pattern recognition receptor
Pt	*Populus trichocarpa*
PTI	pattern-triggered immunity
PVDF	polyvinylidene difluoride
PVPP	polyvinylpolypyrrolidone
QTL	quantitative trait loci
RBOHD	respiratory burst oxidase homolog D
RBOHs	respiratory burst oxidase homologs
RKS1	RESISTANCE-RELATED KINASE 1
RLCK	RECEPTOR-LIKE CYTOPLASMIC KINASE
RNA	ribonucleic acid
ROS	reactive oxygen species
rpm	rounds per minute
s	second(s)
SD	standard deviation
SDS	sodium dodecyl sulfate

SDS-PAGE	sodium dodecyl sulfate polyacrylamide gel electrophoresis
SEM	standard error of the mean
SERK1	SOMATIC EMBRYOGENESIS RECEPTOR KINASE 1
SOD	SUPEROXIDE DISMUTASE
Spec	spectinomycin
SRC	short rotation coppice
TBS-T	tris buffered saline tween
T-DNA	transfer-DNA
TEMED	tetramethylethylenediamine
TF	transcription factor
U	unit
V	volt
YEB	yeast extract beef
ZAR1	HOPZ-ACTIVATED RESISTANCE 1

Table of contents

1. Introduction

1.1 Poplar in research and economy

1.1.1. Poplar as a model tree

Poplar has been established as a model organism for woody perennial species. *Populus trichocarpa* was the first fully sequenced tree species (Tuskan et al., 2006). For several reasons poplar is a suitable model to perform molecular studies in trees. Poplar has a relatively small genome size compared to other trees (Tuskan et al., 2006). Also, poplar trees grow very fast and are easy to propagate vegetatively via stem cuttings on soil as well as in *in vitro* culture. In addition, different transformation protocols are available to generate transgenic lines. Another advantage is the availability of expressed sequence tags (ESTs) and that many quantitative trait loci (QTL) were already mapped that could be combined with the new genome sequence information. Finally, the occurrence of a considerable genetic variation in natural populations allows to study the genetic bases of adaptions to the environment or variation in tree morphology (Bradshaw et al., 2000; Taylor, 2002).

The key advantage in comparison to the main model organism Arabidopsis (an annual herbaceous pant) is the possibility of studying biological processes that are of major importance or even unique for trees. This includes for example wood development, adaption to seasonal climate changes, transition from juvenile to mature states and long-term exposure to beneficial as well as pathogenic microorganisms due to the longer life span of several decades (Jansson and Douglas, 2007).

1.1.2 Poplar and its economic use

For economic purposes, poplar trees are planted in short rotation coppices (SRC) that are harvested within 2-7 years depending on the intended use (Dimitriou and Rutz, 2015). Poplar plantations can be also established on polluted soils (e.g. contaminated with heavy metals or pesticides) as they are well suited for phytoremediation (Yadav et al., 2010; Castro-Rodríguez et al., 2016). Apart from the application in the pulp and paper industry (Stanton et al., 2002; Yang et al., 2006; Christersson, 2008) the use of poplars as a renewable energy resource is of increasing interest. Poplar wood chips can either be directly burned in combustion and

heating systems (Dimitriou and Rutz, 2015) or serve as a feedstock for the production of biofuel and biogas (Sannigrahi et al., 2010; Littlewood et al., 2014; Aghaalikhani et al., 2017).

Many attempts have been made to genetically modify specific traits of poplar to increase economic productivity of poplar plantations (reviewed in Thakur et al., 2021). The introduction of resistance genes into susceptible poplar lines should minimize yield losses caused by pathogen infection and ensure a better pest control. The damage of insects, for example, could be reduced by transgenic poplars containing the *Bacillus thuringiensis* endotoxin (Yang et al., 2016; Liu et al. 2016a; Ding et al., 2017; Xu et al. 2019). Symptoms caused by the bacterium *Xanthomonas populi* were significantly less severe in transgenic *P. tremula x P. alba* plants that express the synthetic antimicrobial peptide D4E1 (Mentag et al., 2003). Resistance towards fungal pathogens was improved, for instance, by the over-expression of transcription factors PtoWRKY60, PtrWRKY18 and PtrWRKY35 (Ye et al., 2014; Jiang et al., 2017) or heterologous expression of the *Trichoderma harzianum* endochitinase gene *ech*42 in *Populus nigra x Populus maximowiczii* (Noël et al., 2005). Transgenic poplar plants expressing herbicide tolerance genes such as the bialaphos resistance (BAR) gene which encodes for the enzyme phosphinothricin acetyltransferase should make weed control easier (Confalonieri et al., 2000; Bonadei et al., 2012; Lebedev et al., 2016). Research on enhanced drought and salinity tolerance has also been performed. Amongst others, one approach was to minimize the effect of salinity stress induced production of reactive oxygen species (ROS). The overexpression of a superoxide dismutase (SOD) gene from *Tamarix androssowii (TaMnSOD)* that was supposed to act as a ROS scavenger could significantly enhance growth of the transgenic lines under salt stress conditions (Wang et al., 2010). The transformation of transcription factors was also tested. Transgenic poplars expressing the dehydration-responsive element binding (DREB)-like transcription factor *AhDREB1* from the halophyt *Atriplex hortensis*, for example, were shown to have higher survival rates as well as enhanced photosynthetic rates under salt stress (Du et al., 2012; Guo et al., 2019). Finally, a lot of studies also dealt with the improvement of wood quality for paper manufacturing and biofuel production. Wood is made up of three major components: cellulose, hemicellulose and lignin. The cell wall polymer lignin has a negative impact on wood utilization because it needs to be removed during the manufacturing process of bioethanol or paper in order to allow for enzymatic hydrolysis of cellulose (Baucher et al., 2003; Welker et al., 2015). Various attempts have been made to modify the lignin content by altering the gene expression of

regulatory enzymes that are part of the lignin biosynthesis pathway, like for instance the downregulation of the caffeoyl-CoA 3-O-methyltransferase (CCoAOMT) gene (Meyermans et al., 2000; Zhong et al., 2000; Lu et al., 2004; Wang et al., 2012). The authors of a recent study also developed a cell-type specific modification of lignin to prevent growth defects that can occur as a negative side effect in lignin content altered plants. Gui et al. (2020) introduced a phosphorylation insensitive variant of the lignin biosynthesis-related transcription factor 1 (LTF1) either under control of a vessel-specific promoter or of a fiber-specific promoter into poplar. Phosphorylation of LTF1 is needed to end suppression of lignin biosynthesis genes. Thus, the modified phosphorylation-null variant of LTF1 is continuously inhibiting lignin biosynthesis. Vessel specific suppression of lignin biosynthesis resulted in dwarfism whereas the fibre-specific suppression of lignin biosynthesis showed normal growth performance despite the desired reduction of lignin content in fibre cells (decreased by 43 %) that facilitated saccharification.

However, even though many promising lines which display an improvement of important traits could be generated, the commercialization of these transgenic lines is still a problem. So far worldwide only two genetically engineered varieties of poplar that exhibit enhanced insect resistance are commercially available in China (Wang et al., 2018). Drawbacks are for example strict regulations of genetically modified organisms combined with a low market acceptance. Many traits are also regulated by multiple genes in a complex network and thus additional research is necessary to ensure the long-term stability of modified traits (Thakur et al., 2021).

1.1.3 *Melampsora* as a major pathogen of poplar

Biomass losses due to pathogen infection are one of the major problems for an efficient use of poplar plantations. In particular biotrophic rust fungi of the genus *Melampsora* are responsible for severe annual growth losses that can reach up to 50 % (Pinon and Frey, 2005). These pathogens have a complex life cycle with five different spore types including a host change. Their sexual cycle starts in spring on larch needles with haploid pycniospores. After fusion of opposite mating types, dikaryotic aeciospores are generated that are distributed by wind and can then infect the leaves of poplar trees. The germination of aeciospores leads to the formation of uredinia on the abaxial side of the leaf which are visible as orange pustules

and are the typical disease symptom. Uredinia harbor urediniospores which are responsible for the major damage caused by *Melampsora* infection of poplar since they are reproduced in several vegetative cycles. Large amounts of spores are dispersed by wind and thus the infection can spread rapidly to uninfected tissue. In autumn, teliospores are developed in senescent leaves that overwinter in fallen leaves on the ground. In spring these spores undergo karyogamy and meiosis and thus generate basidiospores that are again transmitted by wind to larch needles and can start the cycle again (Hacquard et al., 2011).

Poplar cultivars exhibit different susceptibility towards *Melampsora* rust infection and Poplar-*Melampsora* interactions can be thus classified into incompatible or compatible interactions. In an incompatible interaction, *Melampsora* colonization of leaves is inhibited by the plant through activation of defense responses. Compatible *Melampsora* strains are successful in invading their host (Laurans and Pilate, 1999). The proliferation of the fungus inside the leaf tissue negatively affects mesophyll integrity and gas exchange through stomata which subsequently leads to a strongly impaired ability to fix carbon through photosynthesis (Jiang et al., 2016; Eberl et al., 2018; Gortari et al., 2018). As a consequence, trees suffer from premature defoliation and reduced growth that manifests in a decrease of stem height and basal stem diameter (Widin and Schipper 1981; Benetka et al., 2011; Dillen et al., 2013; Verlinden et al., 2013). Control of rust infection is therefore necessary to prevent significant biomass yield losses for financial viability of poplar plantations. Hence, understanding the difference between compatible and incompatible interactions has been a subject of studies. In particular gene expression profiles gave valuable insight into Poplar-*Melampsora* interactions and revealed also a number of pathogen-defense genes that might play a role for immunity (Rinaldi et al., 2007; Miranda et al., 2007; Azaiez et al., 2009; Duplessis et al., 2009; Hacquard et al., 2011). Genome mapping disclosed also several disease resistance loci. In *Populus deltoides*, for instance, three major resistance loci for *Melampsora larici populina*, namely *R1*, *Rus* and *MER*, are found in close proximity to each other on chromosome 19 (Yin et al., 2004; Jorge et al. 2005; Bresson et al., 2011; Wei et al., 2020). Another example is the resistance locus *MXC3* in *Populus trichocarpa* that is associated with total resistance towards *Melampsora columbiana* (Stirling et al., 2001; Yin et al., 2004).

However, there have been no studies in poplar so far that deal with the specific receptors recognizing *Melampsora* rust fungi and initiating plant immune responses. This thesis should shed light on receptor systems for the fungal cell wall polymer chitin that probably could be

used to improve poplar pathogen response in the future and lead to the development of strategies inhibiting fungal pathogen entry.

1.2 The plant immune system

1.2.1 Pattern triggered immunity (PTI) and effector triggered immunity (ETI)

In contrast to animals, which possess an adaptive immune system with specialized mobile defender cells that can distinguish between endogeneous and foreign cells derived from pathogens, plants solely rely on an innate immune system where each cell has the capability to initiate defense mechanisms on its own (Ausubel, 2005). During evolution of plants, this innate immune system has developed two layers of defence. The first layer of defense is the pattern-triggered immunity (PTI) (Jones and Dangl, 2006). Pathogen-associated molecular patterns (PAMPs) are recognized by plasma membrane localized pattern recognition receptors (PRRs) (Macho and Zipfel, 2014). PAMPs are defined as essential components that occur in a whole pathogen class and are often crucial for the survival of the pathogen. Common examples are the bacterial derived PAMPs flagellin, elongation factor Tu and peptidoglycan as well as the fungal cell wall polymer chitin (Boller and Felix, 2009). Two major classes of PRRs are built by leucine-rich repeats receptors (LRR receptors) and lysin motif domain containing receptors (LysM receptors). Their extracellular binding domain determines the specificity for a certain PAMP. LRR receptors typically sense proteinaceous ligands like the bacterial flagellin peptide flg22. LysM receptors detect N-acetylglucosamine containing glycan patterns, such as chitin and peptidoglycan (Desaki et al., 2018a). PAMP perception triggers numerous immune responses summarized in Figure 1 (modified after Ortiz-Morea et al., 2020). These include for example the activation of signaling cascades to initiate defense gene expression, the production of reactive oxygen species and the strengthening of the cell wall through callose deposition (Ortiz-Morea et al. 2020).

In order to overcome PTI, adapted pathogens have developed effectors that interfere with PTI responses. This can lead to effector-triggered susceptibility (ETS) (Jones and Dangl, 2006). One well studied effector protein is for example the AvrPto effector from *Pseudomonas syringae*. AvrPto directly inhibits the kinase domain of the *Pseudomonas* detecting PRR and, thus, can block immune signaling (Xiang et al., 2008). Another *Pseudomonas syringae*

effector, HopAI1, is able to dephosphorylate mitogen-activated protein kinases thereby inactivating the downstream signaling cascades for initiation of defense gene expression (Zhang et al., 2007).

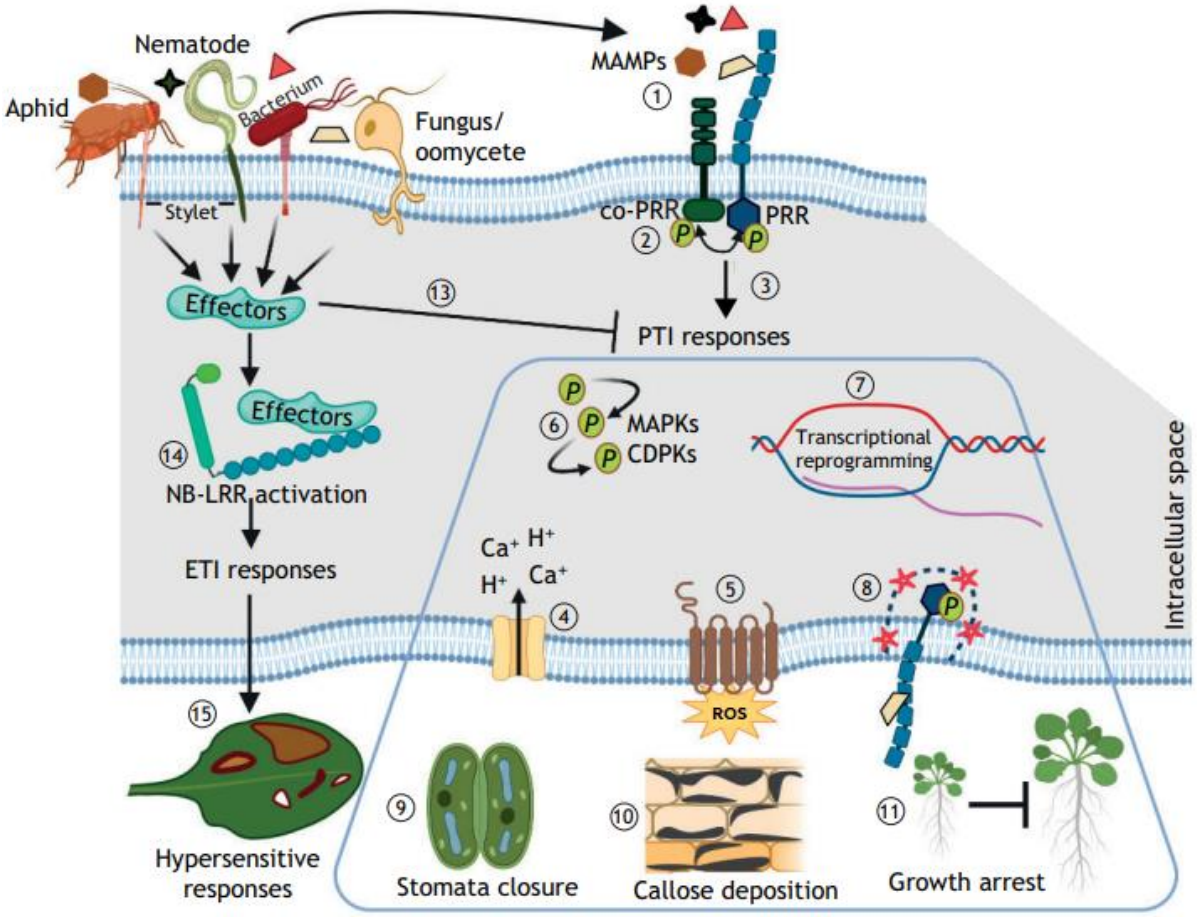

Figure 1: Plant immune responses triggered by perception of microbe-associated molecular patterns. Pathogen derived microbe-associated molecular patterns (MAMPs) are detected at the cell surface by the extracellular domain of pattern recognition receptors (PRRs) (1). Usually, signaling is activated by heterodimerization with a co-receptor and phosphorylation of intracellular kinase domains of the receptor complex (2). This leads to the initiation of pattern triggered immunity (PTI) (3) which is summarized in the blue box. Early and fast responses are the opening of ion channels for calcium influx (4), the generation of reactive oxygen species (ROS) in the extracellular space (5) and phosphorylation of mitogen-activated protein kinases (MAPKs) as well as Ca^{2+}-dependent protein kinases (CDPKs) (6) followed by signaling cascades that lead to the activation of defense genes by transcriptional reprogramming (7). PTI responses are regulated by removal of activated PRRs from the plasma membrane by endocytosis (8). If the elicitor of PTI is still present later responses include the closure of stomata (9), callose deposition (10) to impair the intracellular growth of invading pathogens and finally a growth arrest (11).
Some pathogens have evolved specific effector proteins to suppress PTI responses resulting in Effector triggered susceptibility (ETS) (13). However, plants in turn can adapt to these effectors with intracellular nucleotide-binding domain leucine-rich repeat proteins (NB-LRRs) (14). NB-LRR proteins are able to recognize specific effector proteins and activate effector-triggered immunity (ETI) which leads in most cases to a hypersensitive cell death response (15). Modified after Ortiz-Morea et al. (2020).

Plants try to adapt to ETS with a second layer of defense that has been established during co-evolution: the effector triggered immunity (ETI). ETI often results in a hypersensitive cell death response (HR) at the infection site and thus prevents further proliferation of the pathogen (Jones and Dangl, 2006). ETI is mediated by intracellular nucleotide binding leucine rich repeat (NB-LRR) proteins. According to their N-terminal domain they are classified into two main groups with either a Toll/Interleukin-1 receptor domain (TIR-NB-LRR) or a coiled-coil domain (CC-NB-LRR) (Meyers et al., 2003). Interestingly, in poplar another NB-LRR subfamily exists which has an N-terminal BED domain (BED-NB-LRR) that putatively codes for a zinc-finger DNA-binding domain. BED-NB-LRRs are absent in other dicot plants and could only be identified so far in rice (Kohler et al., 2008; Germain and Séguin, 2011).

While PRRs recognize common PAMPs the NB-LRR proteins are usually specialized for recognition of specific effector proteins (Jones and Dangl, 2006). The perception of an effector can also require pairs of NB-LRR proteins that are genetically linked together and are assembled within a heterodimeric complex (Williams et al., 2014; Saucet et al., 2015). Apart from the direct detection of effectors, NB-LRRs are also able to indirectly sense effectors. This indirect recognition is described with the help of the guard model. The effector target, the so-called guardee, is an essential host protein for the induction of defense mechanisms. Effector mediated modifications of the guardee are detected by NB-LRR proteins and induce plant defense responses. Indirect recognition enables NB-LRR proteins to monitor the effect of several different effectors on the same guardee (Dangl and Jones, 2001). The guard model was later replaced by the decoy model. Decoys mimic certain plant defense components but have no function in host defense by themselves. Pathogen effectors can not distinguish between the decoy and their original host target protein. Thus, effector binding leads to alterations on the decoy that are monitored by their respective NB-LRRs to initiate defense responses (van der Hoorn and Kamoun, 2008).

In general, NB-LRRs can be divided into sensor and helper NB-LRRs. Sensor NB-LRRs are involved either in direct recognition of the effector or the detection of the modified decoy. Helper NB-LRRs are important to mediate downstream signaling of sensor NB-LRRs to initiate cell death. Unlike the permanently built NB-LRR pairs, helper NB-LRRs do not seem to physically interact with their appropriate sensor NB-LRR and can exhibit redundant functions for several sensor NB-LRRs (Wu et al., 2017; Jubic et al., 2019).

Recently it has been discovered that NB-LRR activation induces the building of so-called plant resistosomes that consist of several NB-LRR proteins which build an oligomeric complex (Dangl and Jones, 2019; Saur et al., 2021). The first example of such a resistosome was discovered during studies on the interaction of the NB-LRR HOPZ-ACTIVATED RESISTANCE 1 (ZAR1) with the effector protein AvrAC from *Xanthomonas campestris* or rather its host target protein PBS1-LIKE PROTEIN 2 (PBL2). In Arabidopsis, ZAR1 was shown to exist in a preformed complex with RESISTANCE-RELATED KINASE 1 (RKS1). ZAR1 is able to detect the uridylation of PBL2 caused by the effector AvrAC (Wang et al., 2015). This uridylated version of PBL2 is recruited to ZAR1-RKS1 that subsequently assembles into a wheel like pentamer: the ZAR1 resistosome (Wang et al., 2019a; Wang et al., 2019b). Plant resistosomes are able to integrate into the plasma membrane where they are supposed to disrupt plasma membrane integrity and/or serve as an ion channel (possibly for calcium influx) to influence ion homeostasis. Both have the potential to trigger cell death responses or activation of stress-induced defense signaling (Wang et al., 2019b; Saur et al., 2021).

Interestingly, recent studies identified that PTI and ETI immune responses can not be seen as two distinct pathways conferring immunity but that a close PTI-ETI crosstalk is necessary for robust plant immunity. PAMP triggered PRR signaling has been shown to be important for ETI-associated responses. In turn, ETI is considered as a potentiation of PTI (Ngou et al., 2021; Yuan et al., 2021a; Yuan et al., 2021b).

1.2.2 Plant immune responses triggered by PAMP perception

1.2.2.1 ROS burst signaling

Reactive oxygen species (ROS) play a role in different cellular processes. They are not only by-products of the normal metabolism in peroxisomes, chloroplasts and mitochondria but also serve as signaling molecules. Depart from adaption to abiotic stresses they have an impact on developmental and growth processes (Suzuki et al., 2011). Additionally, they are very important for plant immunity. Plants respond to pathogen attack within minutes with an apoplastic transient ROS burst during PTI. The ROS burst of ETI responses starts also with a fast transient ROS production but includes a strong second peak after several hours that is more sustained than the first (Levine et al., 1994; Draper, 1997; Yuan et al., 2021a; Yuan et

al., 2021b). ROS can either have a direct toxic effect on the invading pathogen or act as second messenger molecule to trigger further immune responses (Qi et al., 2017).

At the plasma membrane the major ROS generating enzymes are nicotinamide adenine dinucleotide phosphate (NADPH) oxidases. Due to their structural and functional homology to mammalian NADPH oxidases, they are called respiratory burst oxidase homologs (RBOHs) (Torres and Dangl, 2005). RBOHs have two Ca^{2+}-binding EF-hand motifs at the N-terminus and a flavin adenine dinucleotide (FAD)- and NADPH-binding site at the C-terminus. The core C-terminal region is built by six transmembrane domains and the functional oxidase domain (Figure 2; modified after Suzuki et al., 2011). Arabidopsis encodes for ten RBOH genes which were named alphabetical RBOHA to RBOHJ (Torres and Dangl, 2005). Among these, RBOHD seems to play the prior role in plant immunity since the PAMP-triggered ROS production in the Arabidopsis *rbohD* mutant was shown to be nearly completely abolished (Torres et al., 2002; Nühse et al., 2007).

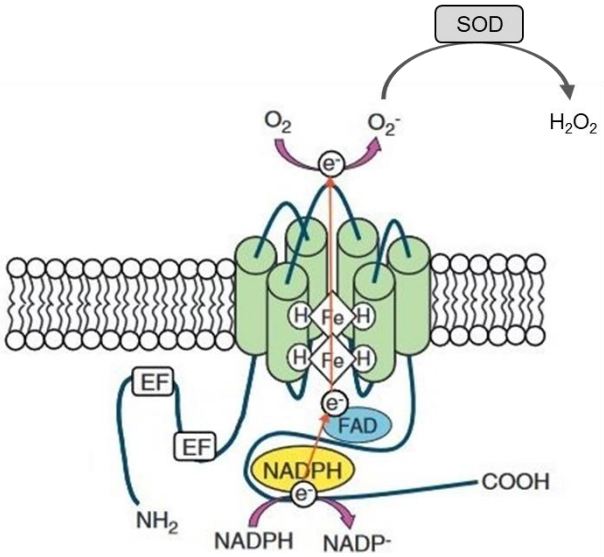

Figure 2: Structure of plant NADPH oxidases. NADPH oxidases reside at the plasma membrane. The N-terminus has two EF hand motifs (EF) that serve as Ca^{2+} binding sites. At the C-terminus a flavin adenine dinucleotide (FAD)- and nicotinamide adenine dinucleotide phosphate (NADPH)-binding site assists in electron transfer. The conserved core region consists of six transmembrane α-helices (green cylinders) and two heme groups (H-Fe-H). Oxygen (O_2) is reduced by electron transfer into the superoxide radical (O_2^-). Superoxide can be further transferred by the enzyme superoxide dismutase (SOD) into the more stable hydrogen peroxide (H_2O_2). Modified after Suzuki et al. (2011).

Activation of PAMP-induced ROS production was shown to be dependent on the presence of Ca^{2+} (Ogasawara et al., 2008) and phosphorylation of RBOHD by Ca^{2+}-dependent protein kinases (CPKs) (Dubiella et al., 2013). However, RBOHD can also be activated in a calcium

independent manner by receptor-like cytoplasmic kinases (RLCKs). In Arabidopsis RBOHD is phosphorylated by the RLCK BOTRYTIS-INDUCED KINASE 1 (BIK1). BIK1 was shown to be strongly associated with the PRRs for flagellin (FLAGELLIN SENSITIVE 2 (FLS2)), elongation factor Tu (ELONGATION FACTOR TU RECEPTOR (EFR)) and chitin (CHITIN ELICITOR RECEPTOR LIKE KINASE 1 (CERK1)), and thus directly links PAMP perception with ROS activation (Kadota et al, 2014; Zhang et al., 2010). Calcium dependent and independent regulation of RBOHD might act together since BIK1 mediated phosphorylation of RBOHD was suggested to increase the sensitivity of RBOHD to Ca^{2+} based regulation (Kadota et al., 2015).

1.2.2.2 MAPK signaling

Mitogen-activated protein kinases (MAPKs) are involved in a broad range of signaling pathways including pathogen signaling, abiotic stress responses, phytohormone signaling and developmental processes. They are activated by a sequential cascade: MAPK kinase kinases (MAPKKK) activate MAPK kinases (MAPKK) that finally activate their respective MAPKs (Colcombet and Hirt, 2008). The genome of Arabidopsis encodes 20 MAPKs, 10 MAPKKs and 60 putative MAPKKKs. The presence of only half as many MAPKKs as MAPKs points out that activation of multiple MAPKs by one MAPKK is very likely (Ichimura et al., 2002). Hitherto, only few of them have been characterized for their contribution to a specific signaling pathway. It turned out that especially three MAPKs, namely MPK3, MPK4 and MPK6 play a major role in many of the diverse signaling cascades (Colcombet and Hirt, 2008). They are also involved in PAMP triggered immunity where two different signaling cascades could be identified so far in Arabidopsis (Figure 3).

The first one consists of the MAPKKK MEKK1, the two MAPKKs MKK1 and MKK2, and the MAPK MPK4 (Gao et al., 2008; Qiu et al., 2008a). It was suggested that this MAPK cascade is strongly involved in ROS homeostasis. MPK4 has been proposed to negatively regulate plant innate immunity by downregulation of H_2O_2 levels (Gao et al., 2008; Pitzschke et al., 2009).

The second MAPK signaling cascade was shown to be a positive regulator for plant immune responses. It is involved in the production of phytoalexins which serve as antimicrobial compounds, pathogen-induced stomata closure, ethylene biosynthesis and activation of defense genes (Liu and Zhang, 2004; Mao et al., 2011; Li et al., 2012a; Lassowskat et al., 2014; Su et al., 2017). This MAPK phosphorylation cascade is composed of the two MAPKKs MKK4

and MKK5, and the two MAPKs MPK3 and MPK6 (Asai et al., 2002). Which MKKK is acting upstream of MKK4 and MKK5 has not been fully unraveled. Originally, Asai et al. (2002) proposed that the MAPKKK MEKK1 initiates the signaling cascade. However, since in the *mekk1* background flg22 activation of MPK3 and MPK6 was not abolished a functional redundancy for MEKK1 activity was assumed (Ichimura et al., 2006; Suarez-Rodriguez et al., 2007). A study by Bi et al. (2018) suggests that the MKKKs MKKK3 and MKKK5 play a major role in that respect. The *mapkkk3 mapkkk5* double mutants were strongly impaired in MPK3/6 activation after treatment with the PAMPs flagellin, chitin or elf18. Nevertheless, the remaining slight MPK3/6 activation hints also here to the presence of additional MAPKKK family members that might be involved in pattern-triggered MPK3/6 activation.

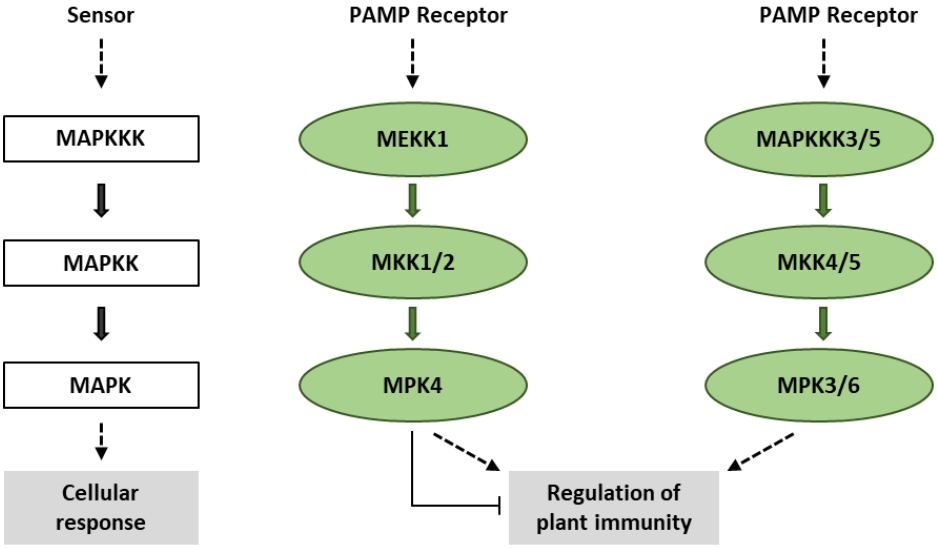

Figure 3: Mitogen-activated protein kinase (MAPK) signaling cascades activated by recognition of plant pathogens. MAPK signaling cascades consist of a MAPK kinase kinase (MAPKKK) that activates a MAPK kinase (MAPKK) that finally activates a MAPK. In Arabidopsis at least two different MAPK signaling cascades are activated upon recognition of pathogen-associated molecular patterns (PAMPs). The first one, which is made up of MEKK1, MKK1/MKK2 and MPK4, is supposed to be a negative regulator of plant immunity. The second one, which is composed of MAPKKK3/MAPKKK5, MKK4/MKK5 and MPK3/MPK6, was shown to be a positive regulator of plant immunity. (Illustration based on literature of Gao et al., 2008; Qiu et al., 2008a; Asai et al., 2002 and Bi et al., 2018.)

Recognition of PAMPs by PRRs and the activation of MAPK cascades are directly linked by receptor-like cytoplasmic kinases (RLCKs) (Tang et al. 2017). It was shown that in Arabidopsis the chitin recognition receptor CERK1 interacts with the RLCK PBL27 which phosphorylates MAPKKK5 upon chitin perception (Shinya et al., 2014; Yamada et al., 2016; Liu et al., 2018). However, other studies could not confirm the participation of PBL27, and suggested that

instead six other RLCKs (PBL19, PBL20, PBL37, PBL38, PBL39 and PBL40) act fully redundant in mediating chitin-induced MAPKKK5 phosphorylation (Bi et al., 2018; Rao et al., 2018). Contradicting results seem to be due to different chitin oligomers used in the studies and different plant growth conditions (Yamaguchi et al., Supplemental data in Bi et al. (2018)). One explanation for the discrepancy was that several receptor complexes for chitin recognition with overlapping functions might exist that differentiate between the chitin variants. Therefore, PBL27 as well as the other six RLCKs possibly both play a role.

1.2.2.3 Callose deposition

The deposition of callose, a natural (1,3)-β-glucan cell wall polymer, represents an unspecific defense response which occurs ubiquitously in all plants after attack of various pathogens including bacteria, fungi and viruses at the site of infection. The callose deposition leads to the formation of papillae which are not only building a physical barrier but are also enriched with additional components which should slow down pathogen entry. Amongst others, this includes for example phenolic compounds, reactive oxygen species and cell wall proteins like peroxidases (Underwood, 2012; Voigt, 2014). Specifically for the defense against biotrophic fungi that develop feeding structures called haustoria, penetration failure in incompatible interactions was associated with rapid callose deposition (Bayles et al., 1990). In successful defense reactions, papillae formed underneath the fungal appressorium inhibit the growth of the penetration peg and further differentiation into haustoria or could build a complete encasement around already established haustoria (Underwood, 2012). Another mechanism to inhibit colonization and spread of pathogens to other tissues by callose deposition is the closure of plasmodesmata. For instance, in soybean the deposition of callose at plasmodesmata near the site of infection was shown to inhibit movement of the soybean mosaic virus to neighboring cells (Li et al., 2012b).

Regulation of pathogen-induced callose deposition appears to be governed by distinct signaling pathways. This was suggested by Luna et al. (2011) who observed differences between flg22-induced and chitosan-induced callose deposition. For both, the generation of ROS had a potentiating effect on callose production. However, flg22-induced callose deposition seems to be controlled by a RBOHD-dependent H_2O_2 production whereas chitosan-induced callose deposition appears to be controlled by a RBOHD-independent H_2O_2

production. In addition, also growth conditions were shown to influence the capacity to deposit callose. Dependent on the availability of light, sucrose or vitamins, abscisic acid had either a positive effect or a negative effect on callose deposition (Luna et al., 2011). Thus, it was proposed that signaling pathways for regulation of callose deposition are determined by the environmental conditions and the eliciting PAMP.

1.2.2.4 Activation of defense genes

Upon pathogen recognition, the initiation of defense signaling induces a transcriptional reprogramming that favors defense over other cellular processes, e.g. growth and development (Buscaill and Rivas, 2014). Transcription factors (TFs) play a major role in modulation of gene expression. The family of WRKY TFs is very well characterized and known to play an important role for defense gene activation. They are named after their DNA-binding region, which has a highly conserved WRKYGQK peptide sequence also designated as the WRKY domain. In Arabidopsis the WRKY TF superfamily consists of 74 members (Pandey and Somssich, 2009). WRKY TFs can either be positive or negative regulators of plant defense gene expression since *wrky* knockout mutants show either enhanced susceptibility or enhanced resistance towards pathogen infection (Pandey and Somssich, 2009). WRKY TFs are mainly activated by the MAPK signaling cascade and, in some cases, are also associated with NB-LRR proteins (Ishihama and Yoshioka, 2012). Downstream targets of WRKY TFs are difficult to analyse and only a few direct targets could be identified thus far. Two examples are the PHYTOALEXIN DEFICIENT 3 (PAD3) gene which is a key enzyme for the biosynthesis of the antimicrobial compound camalexin and is activated by AtWRKY33 (Qiu et al., 2008b) and PATHOGENESIS-RELATED PROTEIN 1 (PR1), which is negatively regulated by AtWRKY48 (Xing et al., 2008).

PR1 belongs to a whole class of pathogenesis-related (PR) proteins that play a crucial role in plant defense responses. PR proteins have been categorized into 17 families and encode for instance many hydrolytic enzymes like β-1,3-glucanases and several types of chitinases for degradation of fungal cell walls as well as enzymes with membrane permeabilizing functions. The accumulation of PR proteins is known to be induced rapidly after pathogen attack and is therefore an indispensable component of innate immune responses. PR genes can thus also serve as marker genes for defense signaling (Jain and Khurana, 2018).

1.3 LysM RLKs/RLPs and MAMP perception

1.3.1 General structure of lysin motif receptor-like kinases and lysin motif receptor-like proteins

Lysin motif receptor-like kinases (LysM-RLKs) and lysin motif receptor-like proteins (LysM-RLPs) are PRRs, which detect microbe-associated molecular patterns (MAMPs) that are either derived from pathogens (also called pathogen-associated molecular patterns (PAMPs)) or from symbionts. Dependent on the MAMPs that are perceived, downstream signaling pathways lead to induction of defense responses or establishment of symbiosis with beneficial microbes like rhizobia and myccorhiza. Like the other PRRs, LysM-RLKs and LysM-RLPs, are plasma membrane bound and act as hetero-oligomeric complexes. Some LysM-RLKs thus can share dual functions in detection of different MAMPs due to complex formation with different co-receptors (Buendia et al., 2018). The extracellular domain, which recognizes the MAMP, is composed of three lysin motifs (LysM) that are designated after their identification in bacterial autolysin proteins. These three LysM are separated by two cysteine residues that are present as a conserved CxC motif (Buendia et al., 2018) and were shown to be involved in the formation of disulfide bridges which are necessary for correct folding of the ectodomain (Lefebvre et al., 2012; Liu et al., 2012a).

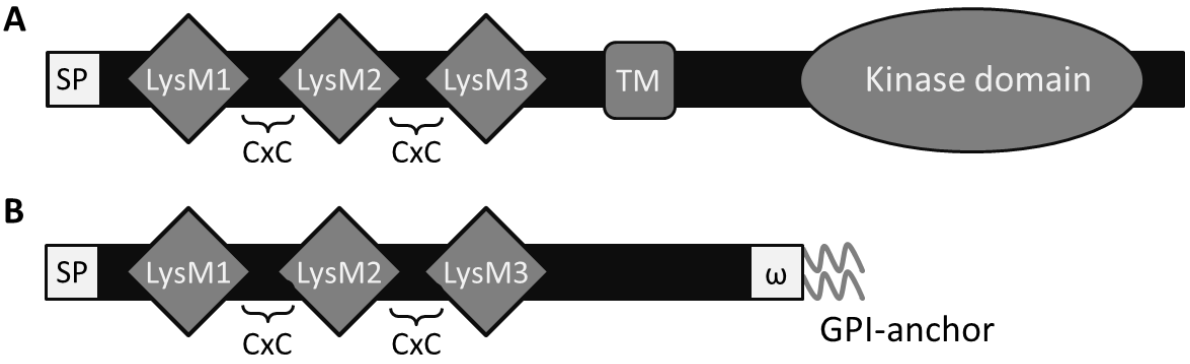

Figure 4: Schematic representation of plant lysin motif receptor-like kinases (LysM-RLKs) and lysin motif receptor-like proteins (RLPs). A) LysM-RLKs are characterized by three LysM domains in their extracellular domain which are separated by two cysteine residues in a conserved CxC motif. In addition, they have a transmembrane domain and an intracellular kinase domain which can be either active or inactive. **B)** LysM-RLPs have as well three LysM domains separated by a CxC motif in their extracellular domain. They lack an intracellular signaling domain and are attached to the plasma membrane with a glycosylphosphatidyl-inositol anchor (GPI-anchor). The omega site serves as a GPI attachment signal. **SP:** signal peptide; **LysM:** lysin motif; **TM:** transmembrane domain; **ω**: omega site. (Illustration based on the shemes by Arrighi et al. 2006, Petutschnig et al. 2014 and Awwanah 2020.)

LysM-RLKs are anchored at the plasma membrane by a transmembrane domain and are characterized by an intracellular kinase domain which can be either active or inactive (Figure 4A). LysM-RLPs lack intracellular domains. Instead of a transmembrane domain they are usually attached to the plasma membrane with a glycosylphosphatidylinositol anchor (GPI-anchor) (Figure 4B).

1.3.1.1 The lysin motif

The term lysin motif originates from the discovery in several bacterial autolysin proteins that cause cell lysis by hydrolyzation of bacterial cell walls (Birkeland, 1994). Later it was discovered that this motif is widely distributed and can be also found in eukaryotes including animals, insects, fungi and plants (Buist et al., 2008). The presence of this domain in eukaryotic proteins was suspected to be a result of horizontal gene transfer from bacteria (Bateman and Bycroft, 2000). The LysM domain is built up by 44 to 65 amino acids and is characterized by a βααβ secondary structure where the two helices are packed onto the same side of a two-stranded anti-parallel β sheet (Figure 5; modified after Bateman and Bycroft, 2000).

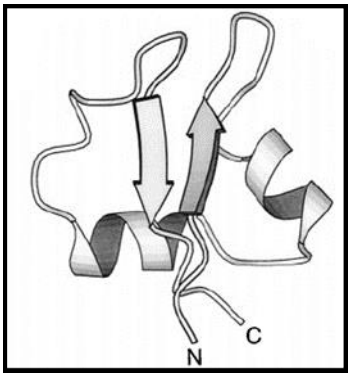

Figure 5: 3D structure of a LysM domain. LysM domains are typically folded in a βααβ structure. Both α helices are packed onto the same side of a two-stranded anti-parallel β sheet. Modified after Bateman and Bycroft (2000).

LysM domains bind to different types of N-acetylglucosamine (GlcNAc)-containing molecules. Therefore, the LysM receptors of plants can recognize for example the bacterial cell wall polymer peptidoglycan (PGN), chitooligosaccharides (CO) derived from fungal cell walls and lipo-chitooligosaccharides (LCO) secreted from bacteria or arbuscular mycorrhizal fungi which serve as symbiotic signals (Gust et al., 2012). Plants need to distinguish between this various

GlcNAc containing molecules to either induce symbiosis or immune signaling. However, the contribution of structural characteristics in the LysM domain for this discrimination remained unclear for a long time. A recent study in *Lotus japonicus* finally unraveled that slight differences in the first of the three LysM domains of plant LysM-RLKs are sufficient for the binding of different MAMPs. Two small regions of 6 residues each, define the ligand specificity for either chitin octamers (CO8) or LCOs (Bozsoki et al., 2020). The second LysM domain determines specificity for different LCO components in LysM receptors for symbiosis signals (Radutoiu et al., 2007; Bensmihen et al., 2011).

Adaptive pathogens evolved effector proteins to bypass pathogen recognition and activation of PAMP induced immune signaling. Interestingly, also some effector molecules carry LysM domains. The LysM-containing effector Ecp6 from the tomato leaf mould pathogen *Cladosporium fulvum,* for example, is proposed to directly compete for chitin binding with the PRR receptor. Because the effector acts like a scavenger protein for fungal cell-wall derived chitin fragments it thus prevents their recognition by the host immune receptors (de Jonge et al., 2010).

1.3.1.2 The kinase domain

Most eukaryotic protein kinases are either specific for phosphorylation of serine/threonine residues or tyrosine residues. Plant RLKs belong to the serine/ threonine class of protein kinases (Walker, 1994). Among the eukaryotic protein kinase superfamily, specific regions are highly conserved. The catalytic core of all protein kinases has a characteristic bilobal fold in common (Figure 6, modified after Taylor and Kornev, 2011).

The N-lobe contains five β strands whereas the C-lobe shows a high proportion of α helices. Part of the N-lobe is the glycine-rich loop with a GxGxxGxV motif that is involved in ATP binding and is responsible for correct positioning of the γ-phosphate. Due to its function, the glycine-rich loop is also known as phosphate-binding loop (P-loop).

The C-lobe contains several loop structures that are essential for binding the protein substrate and initiating the phosphotransfer reaction. The first one is the catalytic loop that harbors the H/YRD motif and directs the γ-phosphate of ATP to the protein substrate. The magnesium (Mg)-binding loop with a conserved DFG motif interacts with one of the ATP bound magnesium ions and is followed by the activation loop and P+1 loop. These three loops are

referred to as activation segment. The activation loop contains a phosphorylation site that needs to be phosphorylated either by autophosphorylation or by transphosphorylation by another kinase. This will subsequently cause a conformational change that is mandatory for catalytic activity. The P+1 loop with its APE motif serves as a key contact site between the substrate and the kinase. It accommodates the P+1 residue of the substrate which means the residue immediately after the serine, threonine or tyrosine that will be phosphorylated (Taylor and Kornev, 2011; Taylor et al., 2012).

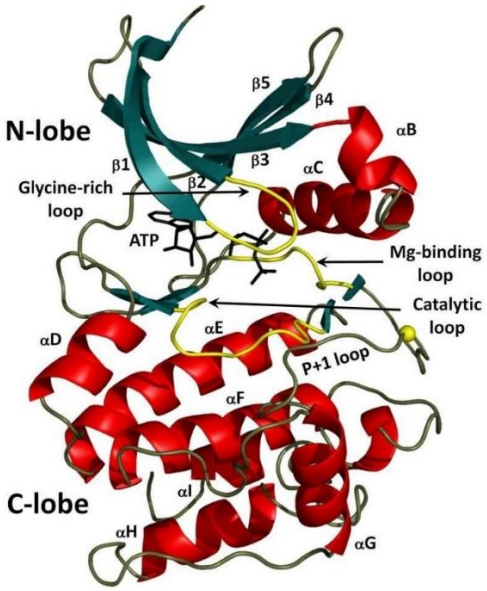

Figure 6: Structure of the catalytic core of the Protein Kinase A (PKA). The N-lobe has five characteristic β strands (blue) and two short α helices (red). The C-lobe consists mainly of α helices. Important loop structures for protein kinase activity are colored yellow. Modified after Taylor and Kornev (2011).

The catalytic core of all protein kinases can be divided into twelve subdomains which are designated with roman numerals. Kinase subdomains I-IV are part of the N-terminal lobe, subdomain V serves as a linker region between the two lobes and the larger C-lobe is built by subdomains VIA and VIB as well as subdomains VII–XI (Hanks and Hunter, 1995).

Hanks and Hunter (1995) identified twelve invariant residues within the catalytic core of protein kinases which are correlated with kinase activity. These essential amino acids are assigned on the protein sequence of the Protein Kinase A catalytic subunit alpha isoform (PKA-Cα). Gly^{50} and Gly^{52} are part of the glycine rich loop in kinase subdomain I. Lys^{72} in subdomain II forms an essential salt bridge with Glu^{91} in subdomain III. Asp^{166} and Asn^{171} belong to the catalytic loop in subdomain VIB. Asp^{184} and Gly^{186} are part of the Mg-binding loop in subdomain VII. Glu^{208} in subdomain VIII forms an ion pair with Arg^{280} in subdomain XI

that is important to stabilize the large C-lobe. Asp^{220} helps stabilizing the catalytic loop by hydrogen bonds. The last invariant residue is Gly^{225} in subdomain IX with so far unknown function.

Based on their kinase domain, plant LysM-RLKs can be divided into two groups. The first one has a catalytically active kinase domain and can exhibit autophosphorylation. Model organisms like *Medicago truncatula*, *Lotus japonicus*, *Arabidopsis thaliana* and *Oryza sativa* have at least one LysM-RLK that is able to autophosphorylate via dimerization (Fliegmann et al., 2016; Madsen et al., 2011; Liu et al., 2012a; Squeglia et al., 2017). The other group of plant LysM-RLKs was identified to have an inactive kinase domain and signal transduction was thus shown to be dependent on receptor complex formation with one of the catalytically active LysM-RLKs (Buendia et al., 2018). The inactive kinase domains of LysM-RLKs lack either some of the conserved residues in the glycine rich loop and the DFG motif (Cao et al., 2014; Awwanah, 2020) or are even characterized by a complete absence of the activation and P+1 loop (Madsen et al., 2003; Arrighi et al., 2006) and are therefore also called pseudokinases. For the Arabidopsis LysM-RLKs the classification into active and pseudokinases is illustrated in Figure 7 (modified after Tanaka et al, 2013).

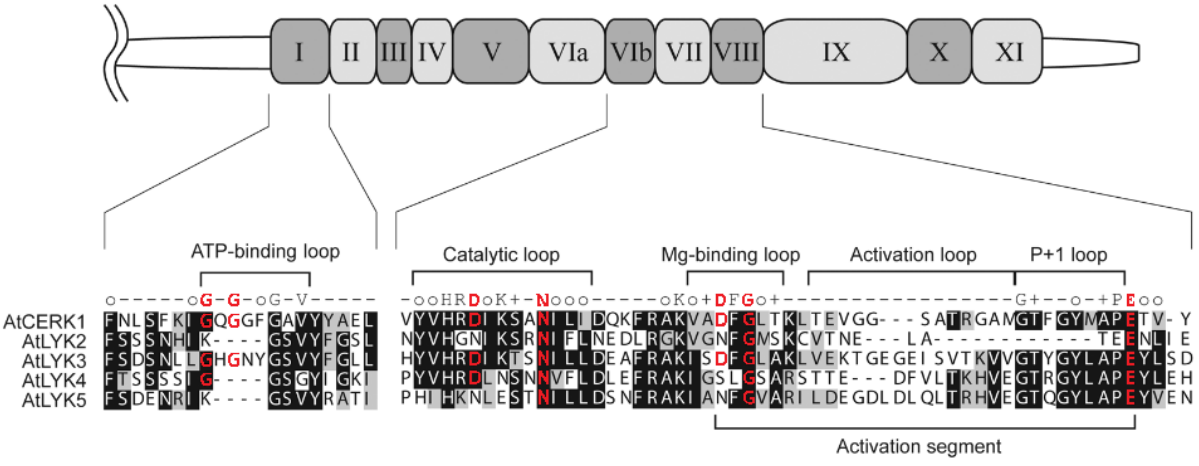

Figure 7: Comparison of the kinase domains of the five Arabidopsis lysin motif receptor-like kinases. Roman numerals designate the twelve kinase subdomains. Kinase subdomain I and VIb to VIII that contain important structures for protein kinase activity are shown in detail. The consensus line shows invariant residues essential for kinase activity (uppercase letters in red), nearly invariant residues (uppercase letters), conserved nonpolar residues (o) and conserved small residues with near neutral polarity (+) of the eukaryotic protein kinase superfamily according to Hanks and Hunter (1995). Only AtCERK1 and AtLYK3 are active kinases due to the presence of all invariant residues. Modified after Tanaka et al. (2013).

1.3.1.3 GPI-anchor

The glycosylphosphatidylinositol (GPI)-anchor is a complex glycolipid structure, which allows stable attachment of GPI-anchored proteins to the extracellular leaflet of the plasma membrane (Figure 8; modified after Desnoyer and Palanivelu, 2020). Its posttranslational addition to the C-terminus of many eukaryotic proteins occurs in the endoplasmic reticulum (ER). GPI-anchored proteins at first exist as a protein precursor. A special sequence about 30 residues upstream of the C-terminus builds the so-called omega site followed by a spacer region and a hydrophobic tail. The hydrophobic segment and spacer region of the C-terminus is cleaved from the protein precursor by a GPI transamidase complex. Subsequently the pre-assembled GPI-anchor is covalently attached. The mature protein finally consists of the GPI-anchor directly added to the omega site (Desnoyer and Palanivelu, 2020).

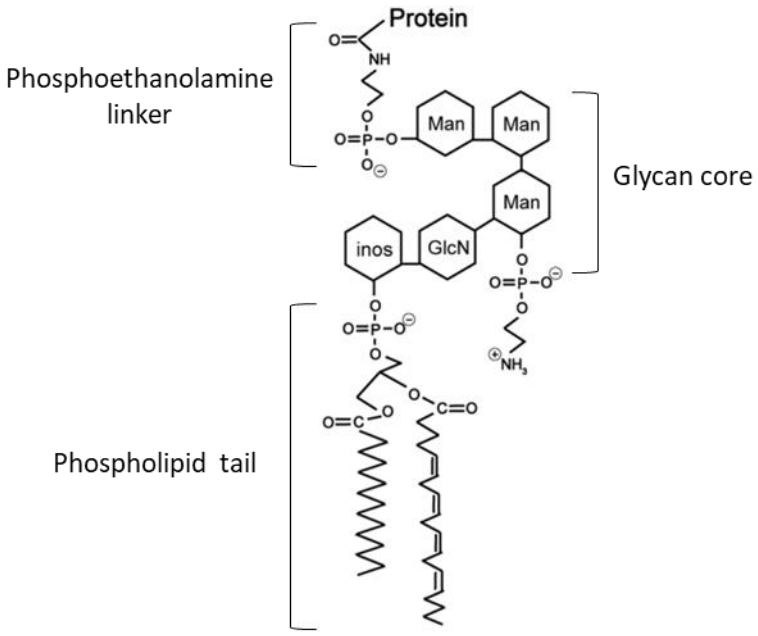

Figure 8: Structure of the glycosylphosphatidylinositol (GPI)-anchor. A phosphoethanolamine linker connects the GPI-anchor with the C-terminus of the protein. The conserved glycan core consists of three mannose (Man), one glucosamine (GlcN) and one myo-inositol (inos) residue. The glycan core can be additionally modified with diverse sugars or phosphoethanolamine groups. The phospholipid tail of the GPI-anchor is also variable. Modified after Desnoyer and Palanivelu (2020).

1.3.2 LysM RLKs/RLPs in pathogen perception

1.3.2.1 Perception of chitin

Chitin perception is best studied in the model plants Arabidopsis and *Oryza sativa*. The major chitin receptor identified in rice is the LysM-RLP CHITIN ELICITOR BINDING PROTEIN (CEBiP). Chitin-induced ROS burst and defense gene expression was nearly abolished in suspension-cultured *cebip* cells (Kaku et al., 2006; Kouzai et al., 2014a). It was shown that OsCEBiP preferential binds to heptamer and octamer chitin oligosaccharides with high affinity (Hayafune et al., 2014). In addition, knockdown mutants of the LysM-RLK CHITIN ELICITOR RECEPTOR LIKE KINASE 1 (CERK1) were highly impaired in chitin-triggered immune responses (Shimizu et al., 2010). However, OsCERK1 itself has no chitin binding activity despite the presence of LysM-domains (Shinya et al., 2012; Liu et al., 2016b). Binding of one chitin molecule induced the dimerization of OsCEBiP which is supposed to subsequently lead to the formation of a signalling complex by recruitment of OsCERK1 (Figure 9a) (Shimizu et al., 2010; Hayafune et al., 2014). OsLYP4 and OsLYP6, two other LysM-RLPs, were also reported to have a function in sensing fungal chitin. Nevertheless, their contribution to chitin signaling was significantly less than that of OsCEBiP and the degree in which they are involved in chitin signaling still needs to be elucidated (Liu et al., 2012b). In Arabidopsis, chitin perception depends on the LysM-RLK AtCERK1. Knockout mutants of AtCERK1 are insensitive to chitin and, thus, lack immune responses like chitin-induced activation of MAPK signaling cascades or chitin-triggered ROS burst (Miya et al. 2007; Petutschnig et al., 2014). All three LysM motifs were predicted to be important for chitin recognition because only the full length ectodomain was shown to be capable of chitin binding (Petutschnig et al., 2010). Chitin binding induces the homodimerization of CERK1 and allows autophosphorylation of its kinase domain, which is necessary for signal transduction (Liu et al., 2012a).

Two other LysM-RLKs, AtLYK4 and AtLYK5, are also involved in the perception of chitin and are supposed to form a hetero-oligomeric complex with CERK1 (Figure 9b) (Cao et al., 2014; Xue et al., 2019). They both have an inactive kinase domain and thus signaling relies on kinase activity of CERK1. AtLYK5 was suggested to be the primary chitin binding receptor since its chitin binding affinity significantly exceeded that of CERK1 (Cao et al., 2014). Because chitin-triggered ROS burst and MAPK activation was slightly reduced in *Atlyk4* single mutants and strongly impaired in *Atlyk5* single mutants, whereas in the *Atlyk4 Atlyk5* double mutant they

were completely abolished, AtLYK4 and AtLYK5 were supposed to share redundant functions (Cao et al., 2014). Protein interaction studies showed partially contradicting results. Xue et al. (2019) determined an interaction of CERK1-LYK5 and LYK5-LYK4 proteins but failed to provide evidence for a possible CERK1-LYK4 interaction. Therefore, AtLYK4 was supposed by them to be not functionally redundant but act instead as a LYK5-associated co-receptor or scaffold protein to enhance chitin-induced signaling. In contrast to this, Wang et al. (2020a) observed in similar interaction studies for both, AtLYK4 as well as AtLYK5, an interaction with AtCERK1. In the presence of chitin, interaction of AtLYK4/AtLYK5 with AtCERK1 could be significantly increased. Furthermore, interaction of CERK1 with LYK4 appeared to be similar strong like the interaction of CERK1 and LYK5. In addition, also Erwig et al. (2017) reported that AtCERK1 is able to directly phosphorylate AtLYK4 and AtLYK5 *in vitro*. Taken together, a fully redundant function for AtLYK4 and AtLYK5 in a hetero-oligomeric complex with CERK1 is still plausible.

Recently, CERK1-dependent chitin perception in Arabidopsis was shown to trigger induced systemic resistance (ISR) against the cabbage looper *Trichoplusia ni* (Vishwanathan et al., 2020). ISR was observed in diverse host plants of arbuscular and ectomycorrhizal fungi and thus thought to be a consequence of host colonization (Gange et al., 2005; Liu et al., 2007; Cameron et al., 2013; Kaling et al., 2018). However, in the nonmycorrhizal plant Arabidopsis ISR was missing in the *cerk1* mutant and inoculation with the heat killed ectomycorrhizal fungus *Laccaria bicolor* or chitin was sufficient for establishment of ISR. This indicates that rather the recognition of conserved molecular patterns like chitin is responsible for ISR induction and that ISR is not like previously assumed an outcome of symbiotic interactions (Vishwanathan et al., 2020).

Interestingly, an Arabidopsis homolog of OsCEBiP, LYSIN MOTIF DOMAIN-CONTAINING GLYCOSYLPHOSPHATIDYLINOSITOL-ANCHORED PROTEIN 2 (AtLYM2), can also bind chitin oligosaccharides with a high affinity but does not induce chitin-triggered immune responses like ROS burst or defense gene expression (Shinya et al., 2012). Instead, it was reported to have a function in chitin-triggered immunity by mediating the closure of plasmodesmata and thus limiting the molecular flux between cells. Since AtLYM2 was not required for CERK1-mediated chitin-triggered defense responses these two pathways are considered to be independent from each other (Faulkner et al., 2013). Further evidence for an independent regulation was given by a study from Cheval et al. (2020) which identified that RBOHD activation for ROS production is regulated by phosphorylation of different serine residues

during AtLYM2-mediated and CERK1-mediated chitin signaling. Nevertheless, the AtLYM2 mediated chitin-triggered plasmodesmata closure was also dependent on AtLYK4 and AtLYK5 (Cheval et al., 2020).

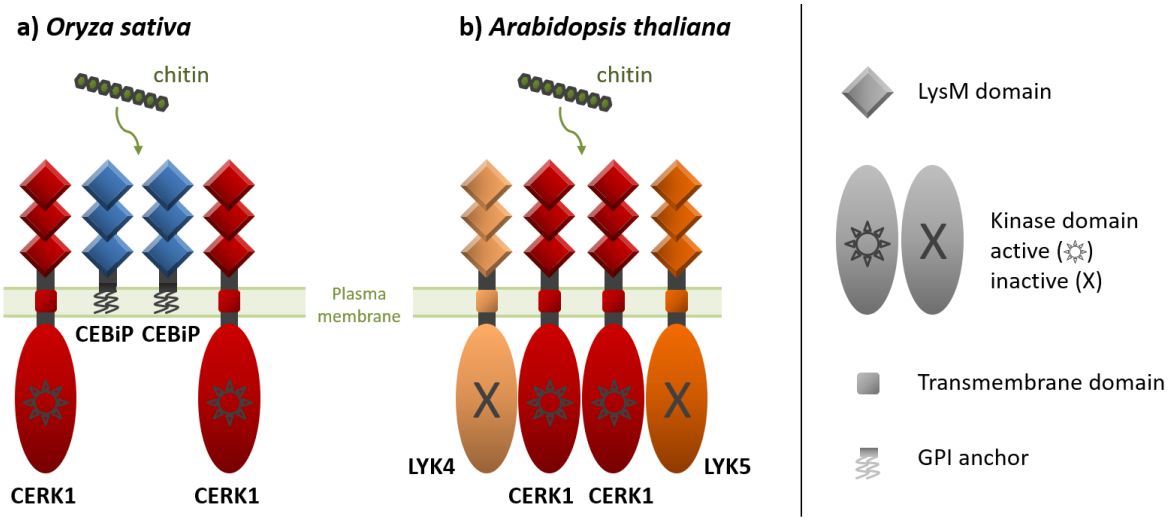

Figure 9: Chitin perception in rice and Arabidopsis. a) The major chitin receptor in rice is OsCEBiP, a LysM-RLP that has no intracellular domains and is attached to the membrane with a glycosylphosphatidylinositol anchor (GPI-anchor). Upon chitin binding a receptor complex with OsCERK1 is built. In contrast to AtCERK1, no chitin binding capacity could be detected for OsCERK1 and oligomerization with OsCEBiP is essential for signal transduction. **b)** In Arabidopsis, chitin perception relies on the LysM-RLKs AtCERK1, AtLYK4 and AtLYK5. Since AtLYK4 and AtLYK5 are LysM-RLKs with an inactive kinase domain signaling is mediated by kinase activity of AtCERK1. (Illustration based on literature of Miya et al., 2007; Petutschnig et al., 2010; Cao et al., 2014; Shimizu et al., 2010; Hayfune et al., 2014 and Wang et al., 2020a.)

1.3.2.2 Perception of peptidoglycan

CERK1 can form different ligand-induced heterooligomeric receptor complexes. Depart from its function in chitin perception, it was also predicted to be a component of the receptor complex recognizing bacterial peptidoglycan (PGN). Willmann et al. (2011) showed that, unlike the chitin sensing AtLYM2, the two other Arabidopsis homologs of OsCEBiP, AtLYM1 and AtLYM3, directly bind to PGN. In addition, *lym1* and *lym3* knockout mutants as well as *cerk1* knockout mutants were insensitive to peptidoglycan and had an enhanced susceptibility to bacterial infection. Since no PGN binding for AtCERK1 was detected, it was assumed that AtCERK1 serves only as a co-receptor for PGN-triggered signal transduction. Because the phenotypes of single *lym1* or *lym3* and double *lym1 lym3* mutants were indistinguishable the authors concluded that they do not share redundant functions. Thus, AtLYM1 and AtLYM3,

need to act together in one and the same complex to mediate PGN perception (Figure 10b) (Willmann et al., 2011).

In rice the LysM-RLPs OsLYP4 and OsLYP6 are identified as PGN receptors in addition to their function in chitin signaling (Liu et al., 2012b). Similar to Arabidopsis the OsCERK1 kinase is essential for signaling and supposed to form a complex with OsLYP4 and OsLYP6 (Figure 10a) (Ao et al., 2014; Kouzai et al., 2014b).

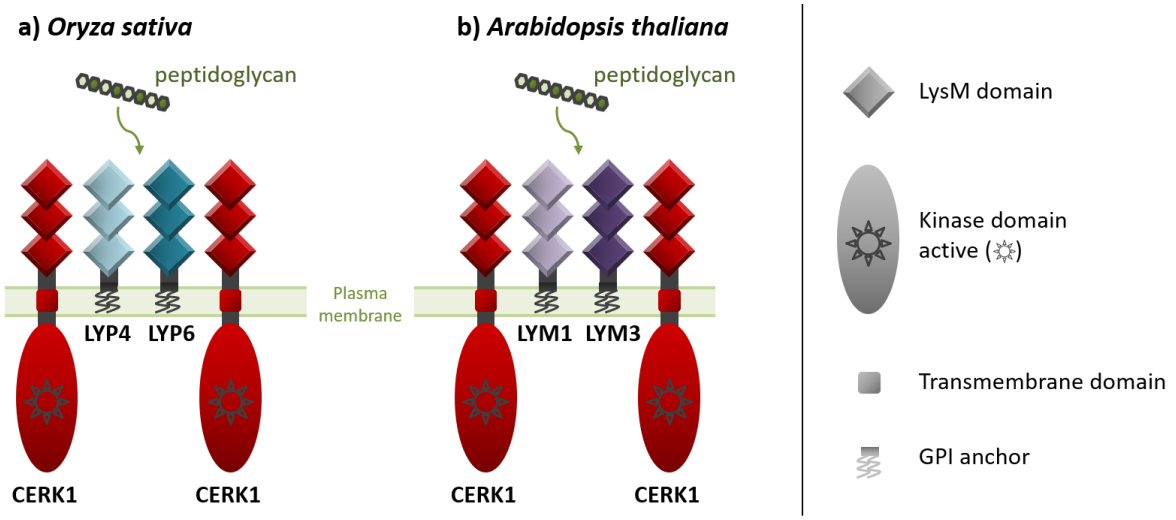

Figure 10: Peptidoglycan perception in rice and Arabidopsis. a) In rice the LysM-RLPs OsLYP4 and OsLYP6 are binding to peptidoglycan. Signaling is mediated by the co-receptor OsCERK1. **b)** Similarly, in Arabidopsis two peptidoglycan binding LysM-RLPs, AtLYM1 and AtLYM3, are associated with AtCERK1. (Illustration based on literature of Willmann et al., 2011; Ao et al., 2014 and Kouzai et al., 2014b.)

1.3.3 LysM-RLKs/RLPs in symbiosis establishment

1.3.3.1 Perception of Nod factors

Nodulation (Nod) factors are signaling molecules secreted from rhizobia to establish root nodule symbiosis in leguminous plants. Nod factors are lipo-chitooligosaccharides (LCOs) that consist of short-chain chitin oligomers (CO3-CO5) with a fatty acid chain at the non-reducing terminal end. They are structurally very diverse dependent on structural variation of the acyl chain and various additional modifications of the chito-oligosaccharide backbone. Nod factors are unique for each rhizobial strain and major determinants of the host range (Dénarié et al., 1996).

In *Medicago truncatula* the LYSM-RLKs NOD FACTOR PERCEPTION (MtNFP) and LYSIN MOTIF RECEPTOR-LIKE KINASE 3 (MtLYK3) were identified as Nod factor receptors (Figure 11a) (Ben Amor et al., 2003; Limpens et al., 2003). MtNFP has an inactive kinase domain due to the lack of several invariant amino acids in the activation loop and the DFG motif (Arrighi et al., 2006). Heteromerization with the kinase active MtLYK3 was, therefore, shown to be necessary to allow signalling (Pietraszewska-Bogiel et al., 2013; Moling et al., 2014).

In *Lotus japonicus* NOD FACTOR RECEPTOR 1 (LjNFR1) and NOD FACTOR RECEPTOR 5 (LjNFR5) are essential receptors to initiate Nod factor symbiosis signaling (Figure 11b) (Radutoiu et al., 2003). LjNFR5 is structurally very similar to MtNFP and does not contain an activation loop (Madsen et al., 2003). LCO-triggered signaling in *Lotus* relies on the active kinase domain of the co-receptor LjNFR1 (Madsen et al., 2011). Recently, Murakami et al. (2018) reported, that a third LysM-RLK is involved in Nod factor perception in *Lotus japonicus*. The epidermal LysM receptor LjNFRe, which is primarily expressed in the outer root cell layer, is also able to phosphorylate LjNFR5 and *nfre* knockout mutants were shown to build fewer nodules. It was suggested that LjNFRe amplifies Nod factor signaling in root epidermal cells.

Unexpectedly, in non-legume plants, Nod factors are detected as well. In Arabidopsis, the perception is supposed to depend on the LysM-RLK AtLYK3. Recognition of rhizobial Nod factors leads to the suppression of PTI (Liang et al., 2013). For what reason non-legume plants like Arabidopsis perceive LCOs is still an open question. One hypothesis is that suppression of plant innate immunity signaling was initially the first function of LCOs used by pathogens to promote susceptibility. Later co-evolution leads to the emergence of rhizobia that use LCOs as molecules to induce symbiosis (Liang et al., 2014). However, this theory does not explain why non-legumes should have maintained receptors for LCO perception that repress innate immunity (Limpens et al., 2015). Indeed, negative regulation of defense responses is part of a successful symbiotic interaction (Mithöfer, 2002). Expression profiling in *Medicago* and *Lotus* showed that early responses to rhizobia include induction of defense gene expression, which is subsequently suppressed during nodule formation (Kouchi et al., 2004; El Yahyaoui et al., 2004). Interestingly, in contrast to Arabidopsis, in *Medicago* a block of pathogen-induced ROS burst after recognition of LCOs did not result in higher susceptibility towards pathogens or reduced expression of immunity-associated genes. This hints towards a mechanism that has evolved in symbiotic plants to maintain parallel defense mechanisms independently from ROS production (Rey et al., 2019).

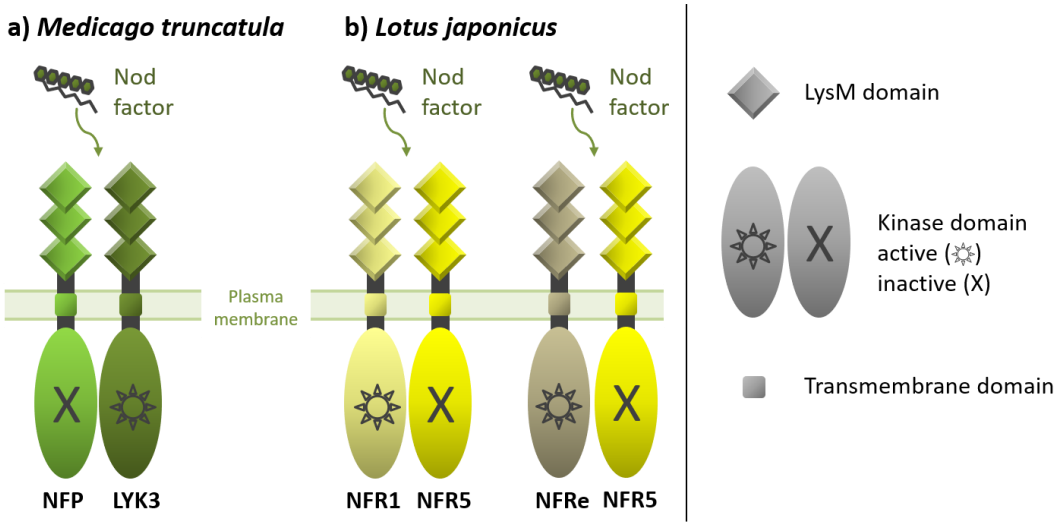

Figure 11: Nod factor perception in *Medicago* and *Lotus*. a) In *Medicago truncatula* Nod factor perception is mediated by a receptor complex composed of MtNFP and MtLYK3. **b)** In *Lotus japonicus* LjNFR1, LjNFR5 and to a lesser extend also LjNFRe are important for Nod factor perception. In contrast to LjNFR1, LjNFRe signaling capacity is restricted to the outer root cell layer. (Illustration based on literature of Ben Amor et al., 2003; Limpens et al., 2003; Radutoiu et al., 2003; Madsen et al., 2011; Pietraszewska-Bogiel et al., 2013; Moling et al., 2014 and Murakami et al., 2018.)

1.3.3.2 Perception of Myc factors

Arbuscular mycorrhizal (AM) fungi secrete at least two different classes of signalling molecules to initiate symbiosis. These are either short-chain chitooligosaccharides (CO4/CO5) or Myc-LCOs (Maillet et al., 2011; Genre et al., 2013). In rice, the receptor complex for perception of Myc factors to enable arbuscular mycorrhization is proposed to consist of the LysM-RLK MYC FACTOR RECEPTOR 1 (OsMYR1, also known as OsLYK2/OsNFR5) and OsCERK1 as a co-receptor (Figure 12). *Osmyr1* and *Oscerk1* single mutants were significantly impaired in Myc factor responses and mycorrhizal colonization was reduced (Miyata et al., 2014; Zhang et al., 2015; Carotenuto et al., 2017, He et al., 2019). In addition it was shown that OsMYR1 exhibits a high affinity for CO4 binding, which induces OsMYR1 phosphorylation by OsCERK1 (He et al., 2019). However, there might be a redundant LysM receptor involved in Myc factor perception since the phenotype of *Osmyr1* mutants can be overcome by a very high inoculation with AM fungi spores (He et al., 2019). This also explains previous contradictive results obtained by Miyata et al. (2016) who initially could not observe a reduced mycorrhization of *Osmyr1* knockout mutants due to a very strong inoculation system that exceeded the natural conditions of spores by multiple times.

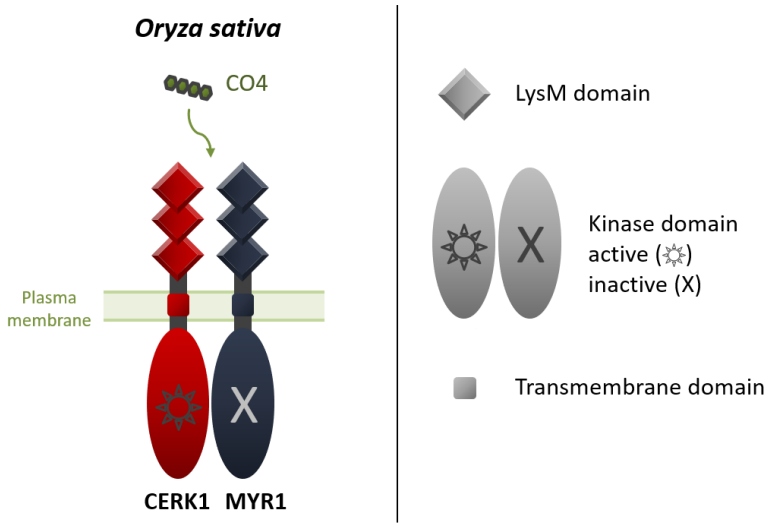

Figure 12: Perception of CO4 in rice. In rice short-chain chitooligosaccharides (CO4) derived from arbuscular mycorrhiza are perceived by the LysM-RLK OsMYR1 and its co-receptor OsCERK1. (Ilustration based on literature by Miyata et al., 2014; Zhang et al., 2015; Carotenuto et al., 2017 and He et al., 2019.)

In other model plants, the perception of AM symbiosis signals is still under debate. Studies in the model plant Arabidopsis cannot be performed since Arabidopsis do not establish a symbiosis with arbuscular mycorrhiza (Wang and Qiu, 2006). In *Lotus japonicus* and *Medicago truncatula* a study by Zhang et al. (2015) supposed that the same receptors that are involved in the perception of Nod factors, LjNFR1 and MtLYK3, play as well a role in perception of Myc-LCOs since *Ljnfr1* and *Mtlyk3* mutants showed reduced colonization. However, the authors suggested a functional redundancy with other LysM-RLKs due to the observation that stronger or prolonged inoculation with AM fungi spores can fully compensate the effect of the *Ljnfr1* or *Mtlyk3* mutants (Zhang et al., 2015). This might be also a reason why a participation of LjNFR1 or MtLYK3 in mycorrhization had been excluded by other studies (Radutoiu et al., 2003; Rasmussen et al., 2016; Feng et al., 2019). Instead, similar to the situation in rice, MtCERK1 (also known as MtLYK9) was proposed to play a dual role in AM symbiosis and immunity. MtCERK1 was shown to bind also to CO4 in addition to CO8 and mutants showed reduced levels of AM colonization. Nevertheless, reduction of mycorrhization shown for *Mtcerk1* mutants is less pronounced than the strong phenotype observed for *Oscerk1* mutants. Therefore, further research is necessary to unravel functional redundancies among receptor complexes for AM symbiosis signals in *Medicago* (Gibelin-Viala 2019; Feng et al., 2019).

1.4 Research Objectives

LysM-RLKs and LysM-RLPs are essential receptor components involved in the perception of chitin and initiation of defense responses. Their role in chitin signaling is well characterized in the model plants Arabidopsis and *Oryza sativa*. In Arabidopsis, the chitin receptor complex consists of the LysM-RLK AtCERK1 and the two LysM-RLKs AtLYK4 and AtLYK5 (Miya et al., 2007; Petutschnig et al., 2010; Cao et al., 2014). Since AtLYK4 and AtLYK5 both possess inactive kinase domains, signaling capacity depends on kinase activity of AtCERK1 (Liu et al., 2012a; Cao et al., 2014). In contrast to Arabidopsis, the LysM-RLK OsCERK1 in rice has no chitin binding affinity (Shinya et al., 2012; Liu et al., 2016b). Nevertheless, OsCERK1 is an important component of the chitin receptor complex and serves as a co-receptor for the LysM-RLP OsCEBiP which is the main chitin receptor identified in rice (Kaku et al., 2006; Shimizu et al., 2010; Kouzai et al., 2014a).

The aim of this thesis was the identification and characterization of chitin receptor components in the woody perennial poplar. For this purpose, an *in-silico* analysis in the poplar species *Populus trichocarpa* and *Populus x canescens* was carried out and revealed LysM-RLK and LysM-RLP homologs in the poplar genomes. Out of these candidates, encoded proteins which might play a role in chitin perception were identified with mass spectrometry using chitin affinity purified protein samples. As a result of this analysis, a focus of the work was set on CERK1 homologs and functional analysis of the two *CERK1* paralogs, *PcCERK1-1* and *PcCERK1-2*, of *Populus x canescens* was carried out. Complementation studies in a chitin insensitive Arabidopsis *cerk1* mutant and analyses of *Pccerk1-1* / *Pccerk1-2* single as well as double mutants were performed to confirm participation of poplar *CERK1* genes in chitin-triggered MAPK and ROS burst responses.

2. Material and Methods

2.1 Material

2.1.1 Plants

2.1.1.1 Arabidopsis lines

For generating the transgenic *Arabidopsis thaliana* lines used in this study (Tab. 1) the T-DNA insertion line *cerk1-2* (GABI-Kat 096F09) (Miya *et al.,* 2007) was used as a background. The ecotype Columbia-0 (Col-0) served as a wildtype reference. The *fls2c* mutant was obtained from Cyril Zipfel (Sainsbury Lab, Norwich, UK). For checking the expression levels of constructs in western blot the CERK1-GFP line of Petutschnig *et al.* (2014) was used.

Table 1: Transgenic *Arabidopsis thaliana* lines generated in this study.

Transgene	Back-ground	Vector	Selection marker bacteria	Selection marker plants
PcCERK1-1_mCitrine	*cerk1-2*	pGreenII-pAtCERK1-PcCERK1-1_mCitrine	Kan^R	$BASTA^{®R}$
PcCERK1-1_mCitrine	*cerk1-2*	pMDC7HA-pLexAop-35S-PcCERK1-1_mCitrine	$Spec^R$	Hyg^R
PcCERK1-2_mCitrine	*cerk1-2*	pGreenII-pAtCERK1-PcCERK1-2_mCitrine	Kan^R	$BASTA^{®R}$
Atcerk1_KinLOF	Col-0	pGreenII-p35S-Atcerk1_KinLOF	Kan^R	$BASTA^{®R}$

2.1.1.2 Poplar lines

As a wildtype reference and for generating transgenic lines (Tab. 2) the hybrid *P. x canescens* (*Populus tremula* x *Populus alba*) clone INRA 717-1B4 was used.

Table 2: Transgenic poplar lines generated in this study.

Transgene	Back-ground	Vector	Selection marker bacteria	Selection marker plants
Overexpression lines				
Pccerk1_KinLOF	*P. x can*	pK7WG2-p35S-Pccerk1_KinLOF	$Spec^R$	Kan^R
CRISPR/Cas9 knockout lines				
Pccerk1-1	*P. x can*	pYLCRISPR/Cas9P35s-N_Pccerk1-1	$Spec^R$	Kan^R
Pccerk1-2	*P. x can*	pYLCRISPR/Cas9P35s-N_Pccerk1-2	$Spec^R$	Kan^R
Pccerk1-1 Pccerk1-2	*P. x can*	C886p9ioR-35SCas_Pccerk1-1/Pccerk1-2*	$Spec^R$	Kan^R

* This vector was ordered from the DNA Cloning Service e.K (Hamburg, Germany) (www.dna-cloning.com)

2.1.2 Plant media

2.1.2.1 ½ MS medium

Table 3: 1/2 MS medium

Chemical compound	concentration
MS salts including vitamins	2,2 g/L
Saccharose	20,0 g/L
pH 5,8	
Kobe Agar	7,0 g/L

The pH value is adjusted with KOH.

2.1.2.2 Co-incubation medium

Table 4: Co-incubation medium

Chemical compound	concentration
MS salts including vitamins	2,2 g/L
Saccharose	20,0 g/L
pH 5,8	
Plant Agar	8,0 g/L

The pH value is adjusted with KOH.

2.1.2.3 Regeneration medium

Table 5: Regeneration medium

Chemical compound	concentration
MS salts including vitamins	2,2 g/L
Saccharose	20,0 g/L
pH 5,8	
Plant Agar	8,0 g/L
add after autoclavation:	
Pluronic F-68	0,01 %
Thidiazuron	0,01 µM
Cefotaxime	150 mg/L
Timentin	200 mg/L

The pH value is adjusted with KOH.

2.1.2.4 Selection medium

Table 6: Selection medium

Chemical compound	concentration
MS salts including vitamins	2,2 g/L
Saccharose	20,0 g/L
pH 5,8	
Plant Agar	8,0 g/L
add after autoclavation:	
Pluronic F-68	0,01 %
Thidiazuron	0,01 µM
Cefotaxime	150 mg/L
Timentin	200 mg/L
Kanamycin	50 mg/L

The pH value is adjusted with KOH.

2.1.2.5 Recall medium

Table 7: Recall medium

Chemical compound	concentration
MS salts including vitamins	2,2 g/L
Saccharose	20,0 g/L
pH 5,8	
Plant Agar	8,0 g/L
add after autoclavation:	
Cefotaxime	150 mg/L
Timentin	200 mg/L
Kanamycin	50 mg/L

The pH value is adjusted with KOH.

2.1.3 Bacteria

2.1.3.1 Bacterial strains

E. coli: DH5-alpha, chemically competent cells

Agrobacterium tumefaciens: GV3101::pMP90, electrocompetent cells, Rif^R $Gent^R$

2.1.3.2 LB medium

Table 8: LB medium

Chemical compound	concentration
Peptone	1,0 %
Yeast extract	0,5 %
NaCl	1,0 %
pH 7,0	
optional: Agar	1,5 %

2.1.3.3 YEB medium

Table 9: YEB medium

Chemical compound	concentration
Peptone	0,5 %
Yeast extract	0,1 %
Beef extract	0,5 %
Sucrose	0,5 %
$MgSO_4$	2 mM
pH 7,0	
optional: Agar	1,5 %

2.1.3.4 Antibiotics

Table 10: Antibiotics used for bacteria selection.

Antibiotic	Stock concentration	Final concentration
Carbenicillin (Carb)	100 mg/ml	100 µg/ml
Spectinomycin (Spec)	50 mg/ml	50 µg/ml
Kanamycin (Kan)	50 mg/ml	50 µg/ml
Hygromycin (Hyg)	50 mg/ml	50 µg/ml
Gentamycin (Gent)	50 mg/ml	50 µg/ml
Rifampicin (Rif)	20 mg/ml	20 µg/ml

2.1.4 DNA isolation

2.1.4.1 DNA isolation buffer

Table 11: DNA isolation buffer

Chemical compound	concentration
Tris (pH 8,0)	0,2 M
NaCl	1,25 M
EDTA	0,025 M
SDS	0,5 %

2.1.5 Polymerase chain reaction

2.1.5.1 Polymerases

Table 12: DNA Polymerases

Polymerase	manufacturer	Units per µl
Phusion® High Fidelity DNA Polymerase	Thermo Fisher Scientific (Waltham, USA)	2 U/µl
GoTaq® DNA Polymerase	Promega (Fitchburg, USA)	5 U/µl

2.1.5.2 Oligonucleotides

All oligonucleotides were purchased from Thermo Fisher Scientific (Waltham, USA) and are listed in Tab. 13, Tab. 14 and Tab. 15 (see next page).

Table 13: Oligonucleotides used for cloning. The cloning was performed via Gibson Assembly (m_Citrine constructs) or overlap PCR (CRISPR/Cas9 constructs) and the overhang sequences are indicated in red. Primers used in PCR reactions are designated as forward (Fw) and reverse (Rv).

primer	sequence (5'-3')	purpose
pAtCERK1:PcCERK1-1_mCitrine		
530 Fw	GCGAATTGGGTACCGGCGCGGGCGCGCCTGTATGAAGA	amplification of *pAtCERK1* with vector pGreen overhang
531 Rv	AATCCTAATTTGGGATTCATTTTGAAGCTTCCTTAGATTCCCCA	amplification of *pAtCERK1* with PcCERK1-1 overhang
532 Fw	ATGAATCCCAAATTAGGATTTG	amplification of *PcCERK1-1*
533 Rv	CTCACCATCGCTCCAGCGTATCTTCCTGACATTAGATTGACA	amplification of *PcCERK1-1* with YAGA-m_Citrine overhang
542 Fw	TACGCTGGAGCGATGGTG	amplification of m_Citrine
543 Rv	ACTAGTGGATCCCCCGGG	amplification of m_Citrine
pLexA:PcCERK1-1_mCitrine		
736 Fw	GAAGCTAGTCGACTCTAGCCAAACAAAAAAAACAGAGA	amplification of *PcCERK1-1* with 5'UTR *AtCERK1* and vector pMDC7HA overhang
737 Rv	CACGGTTATACCTTTAAG	amplification of *PcCERK1-1* with 5'UTR AtCERK1
738 Fw	CTTAAAGGTATAACCGTG	amplification of second part *PcCERK1-1* with m_Citrine
739 Rv	GGGAGGCCTGGATCGACTAGCTACTTGTACAGCTCGTC	amplification of second part *PcCERK1-1* with m_Citrine and pMDC7HA overhang
pAtCERK1:PcCERK1-2_mCitrine		
530 Fw	GCGAATTGGGTACCGGCGCGGGCGCGCCTGTATGAAGA	amplification of *pAtCERK1* with vector pGreen overhang
559 Rv	AACCCTAATTTGGGATTCATTTTGAAGCTTCCTTAGATTCCCCA	amplification of *pAtCERK1* with *PcCERK1-2* overhang
560 Fw	ATGAATCCCAAATTAGGGTTAG	amplification of *PcCERK1-2*
561 Rv	CTCACCATCGCTCCAGCGTATCTTCCTGACATCAGATTGACA	amplification of *PcCERK1-2* with YAGA-m_Citrine overhang
542 Fw	TACGCTGGAGCGATGGTG	amplification of m_Citrine
543 Rv	ACTAGTGGATCCCCCGGG	amplification of m_Citrine

p35S:Pccerk1_LOF		
613 Fw	TCGACCTGCAGGCGGCCGCAATGAATCCCAAATTAGGATTTGG	amplification of *Pccerk1_LOF* first part with vector pK7WG2 overhang
612 Rv	ATGTCCATCTTATTAATGGCAGCT	amplification of *Pccerk1_LOF* first part
611 Fw	AGCTGCCATTAATAAGATGGACAT	amplification of *Pccerk1_LOF* second part
533 Rv	CTCACCATCGCTCCAGCGTATCTTCCTGACATTAGATTGACA	amplification of *Pccerk1_LOF* second part with YAGA_mCitrine overhang
542 Fw	TACGCTGGAGCGATGGTG	amplification of m_Citrine:T35S
301 Rv	ATAATTCGCGGTACCCGGGGATCCTGGTCACTGGATTTTGGTTTTA	amplification of m_Citrine:T35S with pK7WG2 overhang
CRISPR/Cas9 *Pccerk1-1*		
603 Fw	TAACTTCGGCGATGAATGAAGTTTTAGAGCTAGAAATAGCAAGTTAAA	F-Primer for gRNA. Carries 5' overhang for 20bp protospacer (red) for T1 gRNA targeting *PcCERK1-1*. For overlap PCR to fuse Promoter and gRNA
gR-R Rv	CGGAGGAAAATTCCATCCAC	Reverse primer for gRNA. Design by Ma et al., 2015. Used in first round of overlapping PCR. Forward primer carries specific gRNA sequence used as complementary overhang
U-F Fw	CTCCGTTTTACCTGTGGAATCG	Forward primer for U3/U6 promoters. Design by Ma et al., 2015. Used in first round of overlapping PCR. Reverse primer carries specific gRNA sequence used as complementary overhang
604 Rv	TTCATTCATCGCCGAAGTTATGACCAATGGTGCTTTGTAG	R-Primer for AtU3d promoter. Carries 5' overhang for 20bp protospacer (red) for T1 gRNA targeting *PcCERK1-1*. For overlap PCR to fuse Promoter and gRNA
605 Fw	TCGACTCAAAATGCAGCAAGTTTTAGAGCTAGAAATAGCAAGTTAAA	F-Primer for gRNA. Carries 5' overhang for 19bp protospacer (red) for T2 gRNA targeting PcCERK1-1. For overlap PCR to fuse Promoter and gRNA
gR-R Rv	CGGAGGAAAATTCCATCCAC	Reverse primer for gRNA. Design by Ma et al., 2015. Used in first round of overlapping PCR. Forward primer carries specific gRNA sequence used as complementary overhang
U-F Fw	CTCCGTTTTACCTGTGGAATCG	Forward primer for U3/U6 promoters. Design by Ma et al., 2015. Used in first round of overlapping PCR. Reverse primer carries specific gRNA sequence used as complementary overhang
606 Rv	TTGCTGCATTTTGAGTCGATGACCAATGTTGCTCCCT	R-Primer for AtU3b promoter. Carries 5' overhang for 19bp protospacer (red) for T2 gRNA targeting *PcCERK1-1*. For overlap PCR to fuse Promoter and gRNA
U-GAL Fw	ACCGGTAAGGCGCGCCGTAGTGCTCGACTAGTATGGAATCGGCAGCAAAGG	F-Primer for first gRNA expression cassette, used in 2nd PCR (overlap extension) as outer primer. Introduces Gibson assembly site for cloning into

		B-L site in destination vector pYLCRISPR/Cas9P35S-N. Additionally introduces SpeI site (blue). Design by Ma et al., 2015
Pgs-GA2 Rv	CAGGGAGCGGATAACAATTTCACACAGGCACATCCACTCCAAGCTCTTG	R-Primer for first gRNA expression cassette, used in 2nd PCR (overlap extension) as outer primer. Introduces Gibson assembly site 2 for fusion with second gRNA cassette. Design by Ma et al., 2015
U-GA2 Fw	GTGCCTGTGTGAAATTGTTATCCGCTCCCTGGAATCGGCAGCAAAGG	F-Primer for second gRNA expression cassette, used in 2nd PCR (overlap extension) as outer primer. Introduces Gibson assembly site 2 for fusion with first gRNA cassette. Design by Ma et al., 2015
Pgs-GAR Rv	TAGCTCGAGAGGCGCGCCAATGATACCGACGCGTATCCATCCACTCCAAGCTCTTG	R-Primer for last gRNA expression cassette, used in 2nd PCR (overlap extension) as outer primer. Introduces Gibson assembly site for cloning into B-R site in destination vector pYLCRISPR/Cas9P35S-N. Additionally introduces MluI site (blue). Design by Ma et al., 2015
CRISPR/Cas9 *Pccerk1-2*		
834 Fw	TCGAATCAAAGTGCAGAAAGTTTTAGAGCTAGAAATAGCAAGTTAAA	F-Primer for gRNA. Carries 5' overhang for 20bp protospacer (red) for T1 gRNA targeting *PcCERK1-2*. For overlap PCR to fuse Promoter and gRNA
gR-R Rv	CGGAGGAAAATTCCATCCAC	Reverse primer for gRNA. Design by Ma et al., 2015. Used in first round of overlapping PCR. Forward primer carries specific gRNA sequence used as complementary overhang
U-F Fw	CTCCGTTTTACCTGTGGAATCG	Forward primer for U3/U6 promoters. Design by Ma et al., 2015. Used in first round of overlapping PCR. Reverse primer carries specific gRNA sequence used as complementary overhang
835 Rv	TTTCTGCACTTTGATTCGATGACCAATGGTGCTTTGTAG	R-Primer for AtU3d promoter. Carries 5' overhang for 20bp protospacer (red) for T1 gRNA targeting PcCERK1-2. For overlap PCR to fuse Promoter and gRNA
836 Fw	TAACTTCGGCGATGAATGTGGTTTTAGAGCTAGAAATAGCAAGTTAAA	F-Primer for gRNA. Carries 5' overhang for 19bp protospacer (red) for T2 gRNA targeting *PcCERK1-2*. For overlap PCR to fuse Promoter and gRNA
gR-R Rv	CGGAGGAAAATTCCATCCAC	Reverse primer for gRNA. Design by Ma et al., 2015. Used in first round of overlapping PCR. Forward primer carries specific gRNA sequence used as complementary overhang
U-F Fw	CTCCGTTTTACCTGTGGAATCG	Forward primer for U3/U6 promoters. Design by Ma et al., 2015. Used in first round of overlapping PCR. Reverse primer carries specific gRNA sequence used as complementary overhang
837 Rv	CACATTCATCGCCGAAGTTATGACCAATGTTGCTCCCT	R-Primer for AtU3b promoter. Carries 5' overhang for 19bp protospacer (red) for T2 gRNA targeting *PcCERK1-2*. For overlap PCR to fuse Promoter and gRNA

U-GAL Fw	ACCGGTAAGGCGCGCCGTAGTGCTCGACTAGTATGGAATCGGCAGCAAAGG	F-Primer for first gRNA expression cassette, used in 2nd PCR (overlap extension) as outer primer. Introduces Gibson assembly site for cloning into B-L site in destination vector pYLCRISPR/Cas9P35S-N. Additionally introduces SpeI site (blue). Design by Ma et al., 2015
Pgs-GA2 Rv	CAGGGAGCGGATAACAATTTCACACAGGCACATCCACTCCAAGCTCTTG	R-Primer for first gRNA expression cassette, used in 2nd PCR (overlap extension) as outer primer. Introduces Gibson assembly site 2 for fusion with second gRNA cassette. Design by Ma et al., 2015
U-GA2 Fw	GTGCCTGTGTGAAATTGTTATCCGCTCCCTGGAATCGGCAGCAAAGG	F-Primer for second gRNA expression cassette, used in 2nd PCR (overlap extension) as outer primer. Introduces Gibson assembly site 2 for fusion with first gRNA cassette. Design by Ma et al., 2015
Pgs-GAR Rv	TAGCTCGAGAGGCGCGCCAATGATACCGACGCGTATCCATCCACTCCAAGCTCTTG	R-Primer for last gRNA expression cassette, used in 2nd PCR (overlap extension) as outer primer. Introduces Gibson assembly site for cloning into B-R site in destination vector pYLCRISPR/Cas9P35S-N. Additionally introduces MluI site (blue). Design by Ma et al., 2015

Table 14: Oligonucleotides used for diagnostic PCR of potentially transgenic poplar plants. Primers used in PCR reactions are designated as forward (Fw) and reverse (Rv).

primer	sequence (5‘-3‘)	purpose
248 Fw	CTACTTCTTTTTCTTAGCCTGTCC	Cas9 primer for pYLCRISPR/Cas9P35S-N used in diagnostic PCR to identify transgenic poplar plants
249 Rv	GAGACTGGTGAGATCGTTTG	Cas9 primer for pYLCRISPR/Cas9P35S-N used in diagnostic PCR to identify transgenic poplar plants
250 Fw	ATGGCTAAAATGAGAATATCACC	Primer for bacterial aadA kanamycin resistance gene used in diagnostic PCR to ensure absence of Argrobacteria in transgenic poplar plants transformed with vector pYLCRISPR/Cas9P35S-N
251 Rv	AGGCTTGATCCCCAGTAAG	Primer for bacterial aadA kanamycin resistance gene used in diagnostic PCR to ensure absence of Argrobacteria in transgenic poplar plants transformed with vector pYLCRISPR/Cas9P35S-N
70 Fw	TAGCTTCAAGTATGACGGGC	Primer for bacterial spectinomycin resistance gene used in diagnostic PCR to ensure absence of Argrobacteria in transgenic poplar plants transformed with vector pK7WG2 or C88p9ioR-35sCas

71 Rv	CGGTTCGTAAGCTGTAATGC	Primer for bacterial spectinomycin resistance gene used in diagnostic PCR to ensure absence of Argrobacteria in transgenic poplar plants transformed with vector pK7WG2 or C88p9ioR-35sCas
786 Fw	GGAGCTCCAGACAAGAAGTAC	Cas9 primer for C886p9ioR-35sCas used in diagnostic PCR to identify transgenic poplar plants
787 Rv	GAGGATAGCGTGCAGCTC	Cas9 primer for C886p9ioR-35sCas used in diagnostic PCR to identify transgenic poplar plants

Table 15: Oligonucleotides used for amplifying and sequencing of gRNA target sites in transgenic poplar lines. Primers used in PCR reactions are designated as forward (Fw) and reverse (Rv).

primer	sequence (5‘-3‘)	purpose
875 Fw	GATTTGGGTTTCTTCTTCTACTG	Forward primer to amplify target sites of gRNAs for *PcCERK1-1* in CRISPR/Cas9 lines (universal for both alleles)
876 Rv	ACAGTTGACACTCACATTAAGCTT	Reverse primer to amplify target sites of gRNAs for *PcCERK1-1* alba allele in CRISPR/Cas9 lines
875 Fw	GATTTGGGTTTCTTCTTCTACTG	Forward primer to amplify target sites of gRNAs for *PcCERK1-1* in CRISPR/Cas9 lines (universal for both alleles)
803 Rv	ACAGTTGACACTCACATTAAGCAC	Reverse primer to amplify target sites of gRNAs for *PcCERK1-1* tremula allele in CRISPR/Cas9 lines
877 Fw	GGTTAGGTTTTATTCTTCTGCTT	Forward primer to amplify target sites of gRNAs for *PcCERK1-2* in CRISPR/Cas9 lines (universal for both alleles)
800 Rv	AACTCCTGAGTAACATTGTTCTGT	Reverse primer to amplify target sites of gRNAs for *PcCERK1-2* alba allele in CRISPR/Cas9 lines
799 Fw	CTCAGTTTCTCTAGTTCATCTTCCT	Forward primer to amplify target sites of gRNAs for *PcCERK1*-2 in CRISPR/Cas9 lines (universal for both alleles)
879 Rv	CTAAAATTGAAACCAACGTTATACT	Reverse primer to amplify target sites of gRNAs for *PcCERK1-2* tremula allele in CRISPR/Cas9 lines

2.1.6 Agarose gel electrophoresis

2.1.6.1 50x TAE buffer

Table 16: 50x TAE buffer

Chemical compound	concentration
Tris	2 M
EDTA	50 mM
Acetic acid	5,7 % (v/v)

2.1.7 Protein extraction

2.1.7.1 Protein extraction buffer

Table 17: Protein extraction buffer

Chemical compound	concentration
Sucrose	250 mM
HEPES-KOH (pH 7,5)	100 mM
Glycerol	5 % (v/v)
Na_2MoO_4 x 2 H_2O	1 mM
NaF	25 mM
EDTA	10 mM
DTT	1 mM
Triton X-100	0,5 % (w/v)

2.1.7.2 Proteaseinhibitor Cocktail

Table 18: Protease inhibitor cocktail (100x)

Chemical compound	concentration
AEBSF (4-2-Aminoethyl Benzene Sulfonyl Fluoride)	1 g
Bestatin Hydrochloride	5 mg
Pepstatin A	10 mg
Leupeptin hemisulfate	100 mg
E-64 (Trans-Epoxysuccinyl-L-Leucylamido-(4-Guanidino)Butane)	10 mg
Phenanthroline (1, 10-phenanthroline monohydrate)	10 g

Solve reagents separately in dimethyl sulfoxide (DMSO) and combine together in a total volume of 200 ml. Aliquots can be stored at -20°C. Use 1:100.

2.1.8 SDS-polyacrylamide gel electrophoresis (SDS-PAGE)

2.1.8.1 Running gel buffer (10 %)

Table 19: Running gel buffer (10 %)

Chemical compound	concentration	Volume used for 250 ml
Tris pH 8.8	1 M	143,6 ml
SDS	10 %	3,79 ml

Filled up to a total volume of 250 ml with double distilled water.

2.1.8.2 Stacking gel buffer

Table 20: Stacking gel buffer

Chemical compound	concentration	Volume used for 250 ml
Tris pH 6.8	1 M	38,58 ml
SDS	10 %	3,06 ml

Filled up to a total volume of 250 ml with double distilled water.

2.1.8.3 Stacking gel

Table 21: Stacking gel

Chemical compound	concentration	Volume used for 10 ml
stacking gel buffer		8,16 ml
acrylamide / bisacrylamide	30 % / 0,8 %	1,66 ml
APS	10 %	0,05 ml
TEMED		0,005 ml

2.1.8.4 Running gel

Table 22: Running gel

Chemical compound	concentration	Volume used for 10 ml
running gel buffer		6,6 ml
acrylamide / bisacrylamide	30 % / 0,8 %	3,3 ml
APS	10 %	0,1 ml
TEMED		0,004 ml

2.1.8.5 4x SDS Loading Buffer

Table 23: 4x SDS loading buffer

Chemical compound	concentration
Tris (pH 6,8)	200 mM
DTT	400 mM
SDS	8 % (w/v)
Glycerol	40 % (v/v)
Bromphenolblue	0,1 % (w/v)

After mixing all compounds the loading buffer is dissolved in a 40 °C water bath. If stored in a freezer (-20 °C) each aliquot needs to be dissolved again in a 40 °C water bath before usage.

2.1.8.6 10x SDS Running Buffer

Table 24: 10x SDS running buffer

Chemical compound	concentration
Tris	250 mM
Glycine	2 M
SDS	1 % (w/v)

2.1.9 Western Blot

2.1.9.1 20x Transfer buffer

Table 25: 20x Transfer buffer

Chemical compound	concentration
Tris	1 M
Boric acid	1 M
pH 8,3	

2.1.9.2 Alkaline phosphatase buffer

Table 26: Alkaline phosphatase buffer

Chemical compound	concentration
Tris (pH 9,5)	100 mM
NaCl	100 mM
$MgCl_2$	50 mM

2.1.9.3 20x TBS-T buffer

Table 27: 20x TBS-T buffer

Chemical compound	concentration
Tris (pH 8,0)	200 mM
NaCl	3 M
Tween-20	1 % (v/v)

2.1.9.4 Antibodies

Table 28: Antibodies used in this study.

name of antibody	kind of antibody	used dilution	produced in	company
αGFP	primary	1:3000	rat, monoclonal	ChromoTek GmbH (Planegg-Martinsried, Germany)
αPhospho-p44/42 MAPK	primary	1:5000	rabbit, polyclonal	Cell Signaling Technology (Danvers, MA, USA)
α-rat lgG AP conjugate	secondary	1:5000	rabbit, polyclonal	Sigma-Aldrich (München, Germany)
α-rabbit lgG AP conjugate	secondary	1:5000	goat, polyclonal	Sigma-Aldrich (München, Germany)

2.1.10 Coomassie staining

2.1.10.1 Coomassie colloidal staining for SDS gels

Solution A: dissolve 40 g $(NH_4)_2SO_4$ in 380 ml bi-dest water and add 5 ml phosphoric acid (85 %)
Solution B: 1 g Coomassie Brilliant Blue G-250 dissolved in 20 ml bi-dest water

The amount to stain one gel consists of 20 ml Solution A and 400 µl Solution B mixed with 5 ml methanol.

2.1.10.2 Coomassie staining for PVDF membranes

Table 29: Coomassie staining solution

Chemical compound	concentration
Ethanol	45 % (v/v)
Acetic acid	10 % (v/v)
Comassie Brilliant Blue R-250	0,25 % (w/v)

Table 30: Destaining solution

Chemical compound	concentration
Ethanol	45 % (v/v)
Acetic acid	10 % (v/v)

2.2 Methods

2.2.1 Plant growth conditions

Poplar *in vitro* culture vessels as well as Arabidopsis plants were cultivated in a growth chamber (Johnson Controls, Milwaukee, WI, USA). The light was adjusted to 80 µmol/m²s, the temperature to 22° C / 18° C at day/night and the relative humidity to 60 %. Plants were incubated under long day conditions with a 16 h / 8 h day/night cycle or short day conditions with a 8 h / 16 h day/night cycle.

2.2.2 Poplar propagation

Poplar plants were grown *in vitro* in 580 ml glass vessels (J. WECK GmbH u. Co KG, Wehr, Germany) containing ½ MS medium (Tab. 3). Between the lid and the vessel, a fleece ring (Paramoll N260/200, Mank GmbH, Dernbach, Germany) was placed and the lid of the vessels was sealed with micropore band (3M GmbH, Neuss, Germany) to allow a gas exchange. Propagation of poplar plants was done with stem cuttings that were ideally done every six weeks. The stems were cut underneath each node and 5 internodes per vessel were placed 1 cm deep inside the media. Plants were cultivated in a growth chamber under long day conditions (2.2.1).

2.2.3 Transformation of plants

2.2.3.1 Transient transformation of *N. benthamiana*

100 ml YEB media (Tab. 9) were inoculated with the Agrobacteria containing the vector construct of interest and the appropriate antibiotics were added. The culture was incubated overnight and the next day the bacteria were pelleted by centrifugation at room temperature for 10 min at 4000 rpm. The bacteria were then resuspended in 30 ml 10 mM $MgCl_2$. The OD_{600} was adjusted with 10 mM $MgCl_2$ to 0.3. The solution was filled into a 1 ml syringe without needle and infiltrated in the abaxial side of the leaf of 5-week-old *N. benthamiana* plants. The plants are incubated under long day conditions. After three days a signal from the transiently transformed vector construct can be evaluated under the microscope.

2.2.3.2 Stable transformation of Arabidopsis

The genetic transformation of Arabidopsis was done with floral dip. Plants were grown under short day conditions (8 h light) for 4-5 weeks to build a strong rosette and were then transferred to long day conditions (16 h light) to induce the growth of flowers. Flowers can be cut once to break the apical dominance and increase the development of regrowing flowers.

Agrobacteria containing the vector construct of interest were prepared two days in advance of the floral dip. 5 ml YEB medium (Tab. 9) containing the appropriate antibiotics was inoculated with Agrobacteria from a glycerol stock and incubated over night at 28 °C and 180 rpm. The next day 4 ml of this overnight culture were used to inoculate 230 ml YEB medium containing only half of the usual antibiotic concentration. This culture was also incubated over night at 28 °C and 180 rpm. The culture is then centrifuged for 20 min at 4500 rpm at room temperature. The bacterial pellet was resuspended in 200 ml freshly prepared 5 % sucrose medium. The OD_{600} of the sucrose-bacteria solution should be adjusted to 0,8 and directly before the floral dip 0,05 % Silwet L-77 were added to help the bacteria stick to the plant. Plants were dipped once for up to 30 seconds until all flowers are sufficiently wetted with the bacterial solution. The pots were put back on a tray, watered and covered with an autoclave back to increase humidity. After an incubation over night at room temperature the plants were put back into long day conditions (16 h light). Developing seeds were harvested and screening for transformed seeds was performed with the appropriate selection marker.

2.2.3.3 Stable transformation of poplar

5 ml YEB medium (Tab. 9) including the appropriate antibiotics were inoculated with the bacterial culture that should be transformed into poplar and incubated over night at 28 °C and 180 rpm. The next day the overnight culture is transferred into a flask with 100 ml YEB medium without antibiotics and incubated at 28 °C and 200 rpm until a bacterial density (OD_{600}) between 0,25 and 0,8 is reached. The bacterial solution is mixed with 10 µl 200 mM acetosyringone and incubated again for 30 min at the same conditions. In the meantime, the plant material was prepared. For each transformation about twenty in vitro grown poplar plants were used. The leaves were completely removed and the stem was cut into little pieces

of around 0,5-1 cm. The plant material can be stored in sterile tap water until further processed. The stem cuttings were transferred into the bacterial culture and incubated for 30 min in the dark at 120 rpm to allow the bacteria attach to the plant. The stem cuttings were then removed from the bacterial culture and shortly dried on sterile filter paper. Afterwards they were spread on petri dishes with co-incubation medium (Tab. 4) and incubated at 22 °C for three days in the dark to allow transformation.

To remove the Agrobacteria from the stem cuttings they were washed with several washing steps which were all performed for 2 min. The first step was done with 150 ml sterile tap water. Next, they were washed three times in 150 ml sterile tap water containing 400 µg timentin. The last step was performed again with just 150 ml sterile tap water. After the washing the explants were spread on petri dishes with selection medium (Tab. 6) and incubated at 22 °C at low light conditions (10 µmol/m²s) in a growth cabinet (AR-66L/3, CLF Plant Climatics GmbH, Wertingen, Germany). The cuttings which have developed shoots (this can take two to six weeks) were transferred to glass vessels with recall medium (Tab. 7) and incubated at 22 °C at 20 µmol/m²s. If the shoots are high enough to be cut from the explant, they were transferred to a new glass vessel with recall medium to allow rooting. Only shoots which have developed from transgenic cells are able to build normal roots on the kanamycin containing medium and can be tested via PCR for their transgenic status. When the shoots are tested positively and reached a height of about 6 cm they were transferred to the growth chamber (2.2.1).

2.2.4 Selection of transgenic Arabidopsis

2.2.4.1 Basta® selection of transgenic Arabidopsis

Seeds were sown on soil and covered with a plastic lid to increase humidity for germination. After one week the seedlings are treated with a 0,1 % Basta® (Bayer CropScience AG, Monheim, Germany) solution. The dilution of the stock solution is done in tap water and is applied by spraying the whole plant tray. For safety reasons this step should be performed under the fume hood. The application of Basta® is repeated two or three times every second day. Surviving plants are successfully transformed and can be pricked into single pots.

2.2.4.2 In vitro selection of transgenic Arabidopsis

The in vitro selection was done on ½ MS (Tab. 3) agar plates containing the appropriate concentration of the selection marker (50 µg/ml hygromycin or 25 µg/ml phosphinothricin). Seeds were sterilized by washing with ethanol in a 1,5 ml tube. The seeds were incubated three times in 800 µl 70 % ethanol for 2 min on a wheel. Then a last washing step was done with 800 µl 100 % ethanol and the seeds were transferred together with the ethanol on a sterile filter paper in a petri dish. After drying for 10-15 min the seeds were transferred on the medium. Seedlings were grown under short-day conditions until resistant seedlings could be identified and transferred to soil.

2.2.5 Estradiol-spraying of plants

The stock solution of estradiol (50 mM) was prepared in ethanol and diluted with ethanol to a concentration of 5 mM for long term storage at -20 °C. The working solution (25 µM) was always freshly prepared before application and diluted in tap water. The application of estradiol was done by spraying the whole plant from above with a distance of 10 cm until everything was thoroughly wetted. To equalize the treatment for different plants the number of sprays for the first plant was counted and applied to the rest of the samples as well. For safety reasons this step was done under the fume hood. The protein expression level of the estradiol induced construct was always checked for each sample in parallel to the conducted experiment because levels might differ in the plant tissue.

2.2.6 DNA isolation

The leaf material (around 100 mg) was placed into a 2 ml tube with a 5 mm iron bead. After freezing the material in liquid nitrogen, it was homogenized in a TissueLyser LT (Qiagen, Venlo, Netherlands) for 2 min at 50 Hz. 300 µl of extraction buffer (Tab. 11) were added at room temperature and mixed. After 1 min incubation at room temperature the tube was centrifuged for 5 min at 11000 x g to get rid of the cell debris. The supernatant which contains the DNA was transferred to a 1,5 ml tube and the DNA was precipitated via mixing it with 300 µl isopropanol. After 5 min incubation at room temperature a second centrifugation at 11000 x g for 5 min took place. The supernatant was discarded and the DNA pellet dried at room temperature and then resuspended in 100 µl double distilled water.

2.2.7 Measurement of DNA concentrations

DNA concentrations were determined with the NanoDrop OneC Microvolume UV-Vis Spectrophotometer (Thermo Scientific, Waltham, USA). The purity of the sample was analysed with the ratio A260/A280 and should be around 1.8.

2.2.8 DNA sequencing

PCR products and DNA plasmids were premixed with the appropriate sequencing primer and send to Microsynth Seqlab (Göttingen, Germany) for sequencing. The resulting sequence was analysed with the software Geneious® 8.1.9 (Kearse et al., 2012).

2.2.9 Plasmid preparation

For plasmid preparation out of bacteria the NucleoSpin™ Plasmid Kit (Machery Nagel, Düren, Germany) was used according to the manufacturer's instructions.

2.2.10 Polymerase chain reaction

PCR products used for cloning were amplified with a proofreading polymerase (Tab. 31). For all other purposes a polymerase without proofreading function was used (Tab. 32). The amplification of PCR products was done with the program in Tab. 33.

Table 31: PCR mix used for cloning.

Chemical compound	Volume
5x Phusion® HF Buffer	10,0 µl
dNTPs (10mM)	1,0 µl
primer forward (10 µM)	1,5 µl
primer reverse (10 µM)	1,5 µl
Phusion® HF DNA Polymerase (2 U/µl)	0,2 µl
H_2O	34,8 µl

add 1 µl template DNA (10-50 ng)

Table 32: PCR mix used for colony PCR or general tests (e.g. Cas9 detection in potential transgenic poplar lines)

Chemical compound	Volume
10x DreamTaq Buffer	2,5 µl
dNTPs (10mM)	0,5 µl
primer forward (10 µM)	1,0 µl
primer reverse (10 µM)	1,0 µl
DreamTaq DNA Polymerase (5 U/µl)	0,1 µl
H_2O	14,9 µl

add 5 µl template DNA (10-50 ng or bacterial cells of one single colony diluted in 100 µl H_2O)

Table 33: General PCR program. T_m designates the melting temperature of the primers.

reaction step	temperature	time	
Initial denaturation	95 °C	3 min	
Denaturation	95 °C	30 s	35 cycles
Annealing	Tm-5 °C	30 s	
Elongation	72 °C	1 min/kb	
Final elongation	72 °C	10 min	

2.2.11 TA-cloning

TA-cloning was used to sequence transgenic poplar lines with several editing events in one and the same plant where overlapping chromatograms could not be resolved. Target sites of gRNA were amplified with PCR. The PCR product was run on an agarose gel (2.2.13) and DNA lanes were extracted (2.2.14). Afterwards adenine residues necessary for the cloning into the TA-cloning vector where added (Tab. 34).

Table 34: Addition of Adenine residues

Chemical compound	Volume
10x DreamTaq buffer	5,0 µl
dATPs (10mM)	1,0 µl
purified PCR product (250 ng)	x µl
DreamTaq DNA Polymerase (5 U/µl)	0,2 µl
H_2O	*ad* 50 µl

After a PCR clean-up with the NucleoSpin™ Gel and PCR clean-up Kit (Machery Nagel, Düren, Germany) the DNA fragments were ligated into the TA-cloning vector (pCR™2.1 vector, Thermo Fisher Scientific, Waltham, USA) (Tab. 35). The ligation was performed at room temperature for 1 h.

Table 35: Ligation into TA-cloning vector

Chemical compound	Volume
5x ExpressLink™ T4 DNA ligation buffer	2,0 µl
pCR™2.1 vector (50 ng)	2,0 µl
purified PCR product (150 ng)	x µl
ExpressLink™ T4 DNA Ligase (5 U/µl)	1,0 µl
H_2O	*ad* 10 µl

2.2.12 Gibson Assembly

For cloning DNA fragments into the vector of interest the NEBuilder® HiFi DNA Assembly Cloning kit (New England BioLabs, Ipswich, USA) was used according to the manufacturer's instructions.

2.2.13 Agarose gel electrophoresis

For DNA separation with agarose gel electrophoresis 1 % agarose gels were used. The agarose was dissolved by heating in a microwave in 1 x TAE buffer (Tab. 16). Afterwards it was cooled down to approximately 50 °C and 5 µl HDGreen™ DNA-Dye (Intas Science Imaging Instruments GmbH, Göttingen, Germany) per 100 ml agarose gel was added for visualizing DNA fragments. The gel electrophoresis was performed in a Sub-Cell GT cell (BioRad, Munich, Germany) filled with 1 x TAE buffer. Samples were mixed with 6x DNA loading dye prior to loading. As a marker the GeneRuler™ 1 kB or GeneRuler™ 100 bp DNA ladder (Thermo Fisher Scientific, Waltham, USA) was used according to the expected size of the DNA fragments. The gel was run at 90 - 120 V for 35 min. The analysis of the gel was done in a G:Box Genoplex Transilluminator at 312 nm and the imaging software of VWR (Radnor, PA, USA).

2.2.14 Extraction of DNA from agarose gels

For extracting DNA lanes from agarose gels the NucleoSpin™ Gel and PCR clean-up Kit (Machery Nagel, Düren, Germany) was used according to the manufacturer's instructions.

2.2.15 Transformation of bacteria

2.2.15.1 Transformation of E. coli with heat shock

Calcium competent *E. coli* cells (DH5-alpha) were thawed on ice. 2 µl of the vector of interest were gently mixed with 50 µl cells by inverting the tube. After an incubation of 30 min on ice the heat shock was done by placing the tube for 45 s in a 42 °C water bath. Afterwards the cells were cooled down for 2 min on ice and 250 µl LB medium (Tab. 8) were added. The bacteria were incubated for 60 min at 37 °C with 180 rpm. Petri dishes with LB media and the appropriate antibiotics for selection were meanwhile pre-warmed to 37 °C. The bacterial solution (20 µl and 200 µl) were spread on the plate with the help of a Drigalski spatula and incubated over night at 37 °C.

2.2.15.2 Transformation of Agrobacteria with electroporation

Electrocompetent *A. tumefaciens* cells (GV3101) were thawed on ice and 100 ng of the vector of interest were gently mixed with 50 µl cells. The cells were then pipetted into a cuvette for electroporation (1 mm gap width) which was pre-cooled on ice. The transformation was done with the MicroPulser Electroporator (BioRad, München, Germany) at 25 µF, 2.5 kV and 400 Ω. Directly after the electroporation 500 µl YEB (Tab. 9) medium without antibiotics were added and the solution transferred into a 2 ml tube. The bacteria were incubated at 28 °C and 180 rpm for two hours. Petri dishes with YEB media and the appropriate antibiotics for selection were meanwhile pre-warmed to 28 °C. The bacterial solution (20 µl and 200 µl) were spread on the plate with the help of a Drigalski spatula and incubated for two days at 28 °C.

2.2.16 Glycerol stocks of bacteria

Glycerol stocks serve for the long-term storage of bacteria at -80 °C. 5 ml YEB medium (Tab. 9) for Agrobacteria or 5 ml LB medium (Tab. 8) for *E. coli* were inoculated with bacteria from a plate by using a white pipette tip. Antibiotics were added according to the resistance of the

bacterial plasmids and the solution was incubated over night at 180 rpm at 28 °C for Agrobacteria and 37 °C for *E. coli*. 900 µl of the culture were mixed with 900 µl sterile glycerol (50 %) and stored in a freezer at -80 °C.

2.2.17 Protein isolation and quantification

2.2.17.1 Protein isolation for MS analyses

Chitin beads (New England Biolabs, Ipswich, USA) where washed one day prior to the experiment. The needed amount (500 µl for 10 g plant material) was transferred to a 15 ml tube. The solution was washed three times with 10 ml double distilled water with the help of a magnetic rack. The beads were allowed to bind for five minutes to the magnet before exchanging the solution for the next washing step. Washed beads were stored at 4°C.

Mortar and pistil were pre-cooled with liquid nitrogen. 10 g leaf material of soil grown plants were grinded in liquid nitrogen together with a spatula tip full of sand to a very fine powder. The powder should not thaw before the addition of extraction buffer (Tab. 17). Extraction buffer was prepared with protease-inhibitor cocktail (Tab. 18) and 0,5 % PVPP. For 10 g plant material 100 ml extraction buffer was used. The sample was thawed in the buffer and then divided into 50 ml tubes. To get rid of the cell debris and sand the tubes were centrifuged 10 min at 4 °C, 1000 rpm. The supernatant was filtered through 50 µm CellTrics® filters (Sysmex Deutschland GmbH, Norderstedt, Germany) into a new 50 ml tube. To the rest of the extract chitin magnetic beads were added and incubated for one hour on a wheel at 4°C. Chitin binding proteins should attach to the beads and are separated from the protein solution with the help of a magnetic rack. The chitin beads were washed two times with TBS-T buffer (Tab. 27), one time with TBS-T buffer containing 500 mM NaCl and again one time with just TBS-T buffer. To transfer the beads from the 50 ml tube to a 2 ml tube a blue pipette tip with cut end and 1 ml TBS-T buffer was used. The 2 ml tube was incubated on a magnetic rack and the buffer was exchanged with 100 µl 4x SDS buffer (Tab. 23) for elution. The SDS solution was incubated in a heat block at 95 °C to separate the chitin binding proteins from the beads. A tiny hole was punched with a syringe needle into the 2 ml tube and the tube was then transferred into a 15 ml tube. With a centrifugation step (4000 rpm, 4 °C) the beads are separated from the protein solution. The beads remain in the 2 ml tube while the solution can

pass the hole and is collected in the 15 ml tube. The protein solution is pipetted back to a 1,5 ml tube. In case there are still beads left in the protein solution it was incubated on a magnetic rack again and transferred into a new tube. This chitin pull down could then be processed via SDS gel electrophoresis for mass spectrometry analyses.

2.2.17.2 Protein isolation for MAPK assays

Total protein was extracted by grinding the frozen leaf material for two min at 50 Hz in a TissueLyser LT (Qiagen, Venlo, Netherlands) and adding 500 µl extraction buffer (Tab. 17) supplemented with a protease inhibitor cocktail (Tab. 18). The solution was mixed thoroughly on a vortex mixer. The cell debris was pelleted by centrifugation for 10 min, 11.000 x g, at 4 °C and the supernatant with the proteins was transferred to a new 1,5 ml tube. The amount of isolated proteins in each sample was determined with the Bradford assay and adjusted to the same amount for samples which should be compared in Western Blot analyses. 100 µl were mixed with SDS-loading buffer (Tab. 23) and stored at -20 °C.

2.2.17.3 Protein quantification with Bradford

To quantify the amount of proteins in a solution a standard curve with BSA was generated. For this purpose, a dilution series between 0 µg/ml and 15 µg/ml BSA was used. The amount of protein was determined with Bradford reagent (Carl Roth GmbH, Karlsruhe, Germany). 3 µl of each protein sample were mixed with 1 ml Bradford reagent and the absorption was measured at a wavelength of 595 nm. Protein concentrations were calculated based on the absorption of the standard curve.

2.2.18 ROS burst assay

A 96 well plate was prepared with 100 µl tap water in each well. Small leaf samples were filled in each well using a Ø 4 mm biopsy punch and incubated overnight to let the wound reaction pass by. The tap water was then exchanged with the treatment solution: 100 µM L-012 (a luminol analog) were mixed with 20 µg/ml Horse Radish Peroxidase and either 100 µg/ml chitin solution, 100 nM flg22 solution or water as a control. ROS detection was performed

with the TECAN Infinite® 200 PRO NanoQuant plate reader (Tecan Trading AG, Männedorf, Switzerland) for one hour with 1 min intervals. The integration time was set to 350 ms.

2.2.19 MAPKinase assay with leaves

Three Arabidopsis leaves of three different plants of the same genotype were pooled as one sample. The plants should be 3 to 5 weeks old. Leaves were incubated for three hours in tap water to let the wound reaction pass by. The water was then replaced with the treatment solution (10 µg/ml chitin solution, 10 nM flg22 solution or water as a control) and the sample was vacuum infiltrated for 10 min. 10 min post infiltration the sample was taken out of the solution, quickly dried by squeezing it gently on a tissue paper, transferred to a 2 ml tube and directly frozen in liquid nitrogen. Samples were stored at -20 °C until protein isolation was performed.

2.2.20 SDS-PAGE

The protein separation according to their molecular weight in SDS-PAGE was performed with gels with a thickness of 1,5 mm and a 10 % running gel concentration. The running gel (Tab. 22) was poured between glass plates and overlaid with isopropanol to achieve an even polymerization of the surface. After complete polymerization of the gel at room temperature the isopropanol was removed again. The stacking gel (Tab. 21) was poured on top and a comb was inserted immediately. After polymerization the gels were either stored in wet tissue paper at 4 °C or used directly for SDS-PAGE.

The gels were placed into the gel apparatus (Mini-PROTEAN® 3 system (BioRad, Munich, Germany)) and the tank was filled up with 1x SDS running buffer (Tab. 24). The samples for SDS-PAGE were always boiled for 5 min at 95 °C prior to loading to ensure that the SDS is denaturing the proteins and masking their intrinsic charge. The power supply (PowerPac™ HC (BioRad, Munich, Germany)) was set to 30 mA per gel. After the run, the gels for MS analyses were stained with Coomassie whereas the gels for MAPK analyses and protein expression analyses were processed further with Western blot.

2.2.21 Western Blot

Western Blot analyses was performed to detect specific proteins on the SDS-PAGE gels. Therefore, the proteins from the gels were transferred onto a PVDF membrane (0,45 µm pore size (Roth, Karlsruhe, Germany)) as follows. Before blotting the PVDF membrane was activated for 1 min in methanol and then temporarily stored in 1 x transfer buffer (Tab. 25) until usage. For each gel four Whatman papers were pre-wetted in 1 x transfer buffer. The blot was assembled within the western blot cassette by stacking a foam pad, two pre-wetted Whatman papers, the gel with the PVDF membrane on top, two pre-wetted Whatman papers and a foam pad. The PVDF membrane should face the anode to ensure that the proteins can bind to the membrane and do not diffuse into the wrong direction. The cassette was placed into the tank of the blotting apparatus (Trans-Blot® transfer cell (BioRad, Munich, Germany)) which was filled up with 1 x transfer buffer. Blotting was performed at 100 V for at least one hour at 4 °C.

Immunostaining was performed by first blocking the membrane with 3 % milk in 1 x TBST-T (Tab. 27) for 1 h on a shaker at room temperature. Afterwards the solution was removed and the membrane was incubated with the primary antibody (diluted 1:3000 in 3 % milk in 1 x TBST-T) over night at 4 °C on a shaker. The next day the membrane was washed six times for 15 min in 3 % milk in 1 x TBS-T to remove unbound primary antibody. The secondary antibody (diluted 1:5000 in 3 % milk in 1 x TBST-T) was incubated at room temperature for 3 h on a shaker. The washing of the membrane was repeated the same way as described above with 1 x TBS-T to remove unbound secondary antibody. The membrane was then incubated for 5 min in alkaline phosphatase (AP) buffer (Tab. 26). For detection of the antibody signal 500 µl of Immun-Star™ AP substrate (BioRad, Munich, Germany) was pipetted to the expected location of the protein and spread from this spot over the whole membrane. After a 15 min incubation in the dark the membranes were analysed with the ChemiDoc™ Touch Imaging System (Bio Rad, Munich, Germany).

2.2.22 Coomassie staining

2.2.22.1 Coomassie staining of PVDF membranes

The PVDF membranes were incubated for about 5 min in the Coomassie staining solution (Tab. 29). Then they were washed briefly in double distilled water to remove the surplus

solution and destained in destaining solution (Tab. 30) for about 3 min. The membranes were washed again briefly in double distilled water and were placed on a tissue paper to dry.

2.2.22.2 Coomassie staining of SDS gels

The stacking gel was removed and only the running gel was stained with Coomassie. Prior to the staining the running gel was washed two times in double distilled water for 5 min. Next it was transferred to the Coomassie colloidal staining solution (2.1.10.1) and incubated for 2 h on a shaker at room temperature. The Coomassie staining solution was exchanged with fresh solution and the incubation was continued overnight. The next day the background of the gel was destained with double distilled water which was exchanged several times if necessary.

2.2.23 Tryptic digestion of gel slices and purification for LC-MS/MS analyses

All reagents were used with MS-grade purity. If not mentioned differently all steps are conducted at room temperature. Protein LoBind tubes (Eppendorf, Hamburg, Germany) were used to prevent loss of proteins by attachment of proteins to the tube surface.

Gel slices were washed three times for 10 min in 1 ml water. The water was exchanged with 100 µl Acetonitrile (AcN) and incubated for 10 min. This step was repeated to ensure the complete removal of water. Gel slices should shrink in size and get a white color. The AcN was then removed and the gel slices dried in a speed vac for 10 min at 45 °C. 150 µl 10 mM DTT were added (diluted in 100 mM ammonium hydrogencarbonate (NH_4HCO_3)) and incubated for one hour at 56 °C in a heat block to reduce cysteine residues of the proteins. The DTT solution was exchanged with 150 µl 55 mM iodoacetamide (IAM) (diluted in 100 mM NH_4HCO_3) for alkylation of the reduced cysteine residues and incubated for 45 min in the dark. After taken off the IAM solution gel slices were washed in 500 µl 100 mM NH_4HCO_3 for 15 min. A second washing step was performed with 100 µl AcN for 15 min. In case the gel slices are still colored blue from the Coomassie staining an optional washing step with 50 % AcN and 50 % 100 mM NH_4HCO_3 was necessary which was followed again by a washing with 100 µl AcN for 15 min. The AcN was removed and the gel slices dried in a speed vac for 10 min at 45 °C. A trypsin solution was prepared by adding 80 µl resuspension buffer (50 mM acetic acid) to one vial of lyophilized trypsin (20 µg, Sequencing Grade Modified Trypsin) (Promega, Madison, USA) and further dilute this trypsin 1:20 in 50 mM NH_4HCO_3. For each sample 40 µl

of the trypsin solution was used plus an additional amount of 100 µl 50 mM NH_4HCO_3. The gel slices should take up this solution and trypsin digestion of the proteins into small peptides was performed via incubation overnight at 37 °C. The next day the supernatant was transferred to a new 2 ml tube. 100 µl 50 % AcN with 5 % formic acid (FA) were added to the gel slices and incubated for 30 min. The supernatant was pooled with the supernatant from the overnight incubation. The gel slices were incubated again for 10 min in 50 µl AcN and the supernatant was pooled with the previous supernatants. The pooled supernatants were dried in a speed vac at 45 °C until a dry protein pellet could be obtained. The pellet can be stored at 4 °C if necessary. It was resuspended in 50 µl water with 0,1 % FA.

The clean-up for MS analyses was performed via stage tipping. A stage tip was placed in a 2 ml tube with the help of a stage tip adapter. 100 µl methanol (MeOH) with 0,1 % FA was pipetted into the stage tip and centrifuged 2 min at maximal speed. The flow through was removed and 100 µl of 80 % AcN with 0,1 % FA was added and centrifuged at 10.000 rpm. The flow through was removed and the washing was continued with the addition of 100 µl water with 0,1 % FA. After a centrifugation at 10.000 rpm for 2 min this step was repeated once. The flow through was removed and the resuspended protein sample was loaded directly onto the stage tip. After a centrifugation for 5 min at 3000 rpm the flow through was loaded again to ensure that as much as possible protein is loaded to the C18 plug. The column was washed with 100 µl water with 0,1 % FA and centrifuged for 2 min at 10.000 rpm. The stage tip was afterwards transferred to a new 1,5 ml tube. 50 µl of 80 % AcN with 0,1 % FA was added to elute the proteins from the stage tip. After a centrifugation for 5 min at 3000 rpm the samples were dried in a speed vac at 45 °C until a dried pellet could be obtained.

2.2.24 MS analyses

The analyses of the MS samples were done in collaboration with Oliver Valerius (Institute of Microbiology and Genetics, Georg-August-University Göttingen, Germany) and Andrzej Majcherczyk (Büsgen-Institute, Georg-August-University Göttingen, Germany) on a Q Exactive™ HF Hybrid Quadrupol-Orbitrap™ mass spectrometer (Thermo Scientific, Waltham, USA) connected to an UltiMate™ 3000 RSLCnano system (Thermo Scientific, Waltham, USA). The evaluation of the results was done with the Proteome Discoverer 2.2 software (Thermo Scientific, Waltham, USA).

2.2.25 Confocal laser scanning microscopy

Confocal laser scanning microscopy was used to check the mCitrine expression of the transformed constructs in *N. benthamiana* and Arabidopsis leaves. Leaf discs were cut out with a biopsy punch (Ø 4 mm) and placed on an object slide. The leaf discs were wetted with a drop of double distilled water and covered with a cover glass. Microscopy was performed with a Leica TCS SP5 Confocal (Leica Microsystems, Wetzlar, Germany). The excitation wavelength of mCitrine is 514 nm and the expected emission at 525-560 nm. Chlorophyll autofluorescence was measured at an emission spectrum of 740-770 nm.

3. Results

3.1 Identification of candidate genes involved in chitin perception

3.1.1 Poplar responds to chitin with a ROS burst and the activation of a MAPK signaling cascade

Typical plant immune responses towards chitin are the production of ROS and the activation of a MAPK cascade (Macho and Zipfel 2014). To test if poplar leaves are responsive to chitin, the ROS burst and MAPK responses of poplar leaves towards chitin were tested in comparison to Arabidopsis as a control. The response to flg22 which is a peptide of the bacterial PAMP flagellin was monitored in both species for control as well.

For ROS burst analyses leaf discs were treated with the elicitor solution (chitin, flg22 or water as mock treatment) and analysed in a chemiluminescence assay. The results show that poplar leaves react with a chitin-triggered ROS production (Fig. 13). Interestingly, the poplar chitin response is induced earlier compared with Arabidopsis while the response to flg22 takes a similar time in both species.

For the analysis of MAPK activation leaf samples were infiltrated with the elicitor solution (chitin, flg22 or water as mock treatment). The total protein extracts were subsequently analysed via western blot with an antibody specifically detecting phosphorylated and thus activated MAPKs (Fig. 14). The kinetics of chitin-induced MAPK activation are similar in Arabidopsis and poplar. The phosphorylation of MAPKs was detected one minute after chitin treatment and the phosphorylation decreases after about fifteen minutes. Chitin induces a stronger activation of MAPKs in poplar than flg22 while in Arabidopsis the strength of the signal for chitin and flg22 is similar.

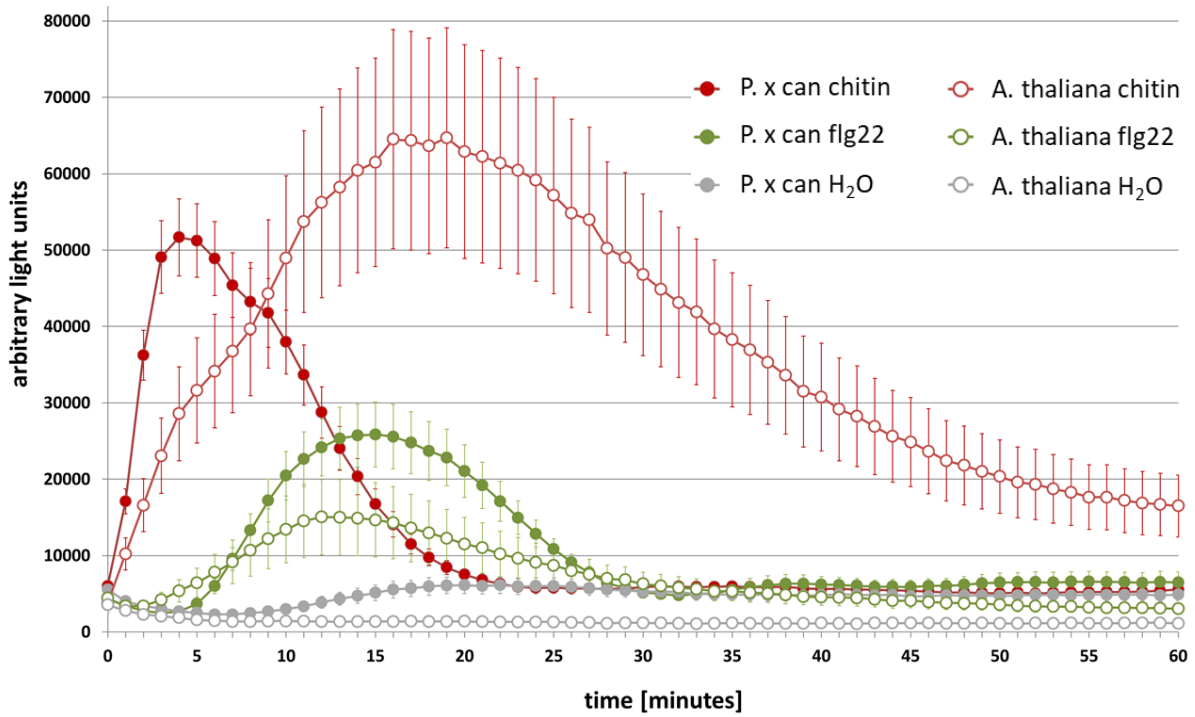

Figure 13: Chitin treatment triggers ROS burst in poplar. Leaf discs of *Populus x canescens* wildtype and Arabidopsis wildtype Col-0 were treated with either 100 µg/ml chitin solution, 100 nM flg22 solution or water as a control. To visualize ROS generation a luminol based assay was used. Data represent the mean of 8 leaf discs ± SEM.

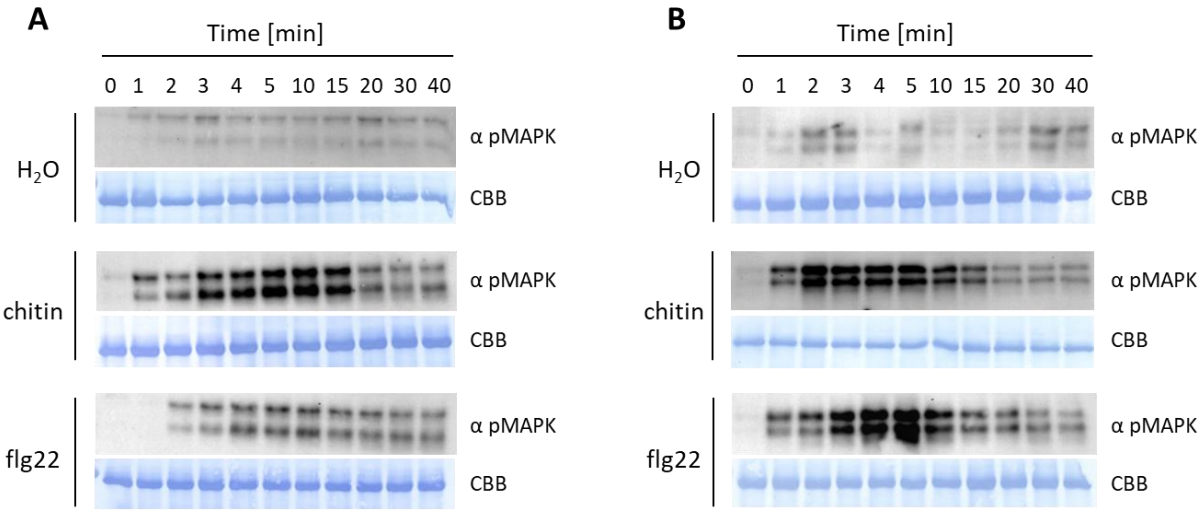

Figure 14: Chitin treatment triggers a MAPK response in poplar. A: poplar leaf samples of wildtype *Populus x canescens.* **B:** Arabidopsis leaf samples of wildtype Col-0. Leaf samples were infiltrated with either 10 µg/ml chitin solution, 10 nM flg22 solution or water as a control. After the indicated incubation time samples were harvested and phosphorylated MAPKs were detected in total protein extracts with a specific antibody. **CBB:** Coomassie Brilliant Blue-stained membranes.

3.1.2 A phylogenetic analysis identified a specific subset of potential chitin binding proteins in poplar

To discover possible candidate genes involved in chitin perception an *in-silico* search for poplar proteins similar to known LysM-RLKs and LysM-RLPs of other model species (*Arabidopsis thaliana*, *Oryza sativa*, *Medicago truncatula* and *Lotus japonicus*) was performed. Protein sequences of these species were used for a BLASTP search in the proteome database of *Populus trichocarpa* (www.phytozome.org; Goodstein et al., 2012). With the resulting protein sequences a phylogenetic tree was generated including these five species. Even though later experiments are conducted in the easier transformable and faster in vitro regenerating *Populus x canescens* the database of *Populus trichocarpa* was chosen due to its better annotated genome. Genes of *P. x canescens* corresponding to the identified genes in *P. trichocarpa* refer to the same clade (data not shown). Potential function of the poplar proteins in chitin binding or symbiosis as well as kinase activity or inactivity were assigned based on their homology to the well characterized LysM-RLKs and LysM-RLPs of the other four model species.

For the LysM-RLK homologs (Fig. 15) the group of putatively chitin binding and kinase active proteins is of special interest for this study. This group consist of proteins homologous to Arabidopsis and *Oryza sativa* CERK1 proteins. In both species CERK1 is part of the receptor complex detecting chitin (Petutschnig et al., 2010; Cao et. al, 2014; Kouzai et al., 2014a; Xue et al., 2019). In the poplar species *Populus trichocarpa* three homologs of the CERK1 gene were identified.

For the poplar LysM-RLK homologs of Arabidopsis AtLYK2 and AtLYK3 two and four copies could be detected, respectively. In Arabidopsis no chitin binding affinity is known for these two LysM-RLKs (Wan et al., 2012). Another group consists of potential chitin binding but kinase inactive proteins. Four copies of LYK4 homologs and two copies of LYK5 homologs are present in poplar. Studies in Arabidopsis show that LYK4 and LYK5 are co-receptors of CERK1 necessary for an effective chitin signal transduction (Wan et al., 2012; Cao et al., 2014; Erwig et al., 2017).

The last group of this phylogenetic tree contains symbiosis related genes. Four homologs of NFP genes have been identified in *Populus trichocarpa*. These are putative Nod factor binding receptor components and are predicted to have low or no chitin binding affinity.

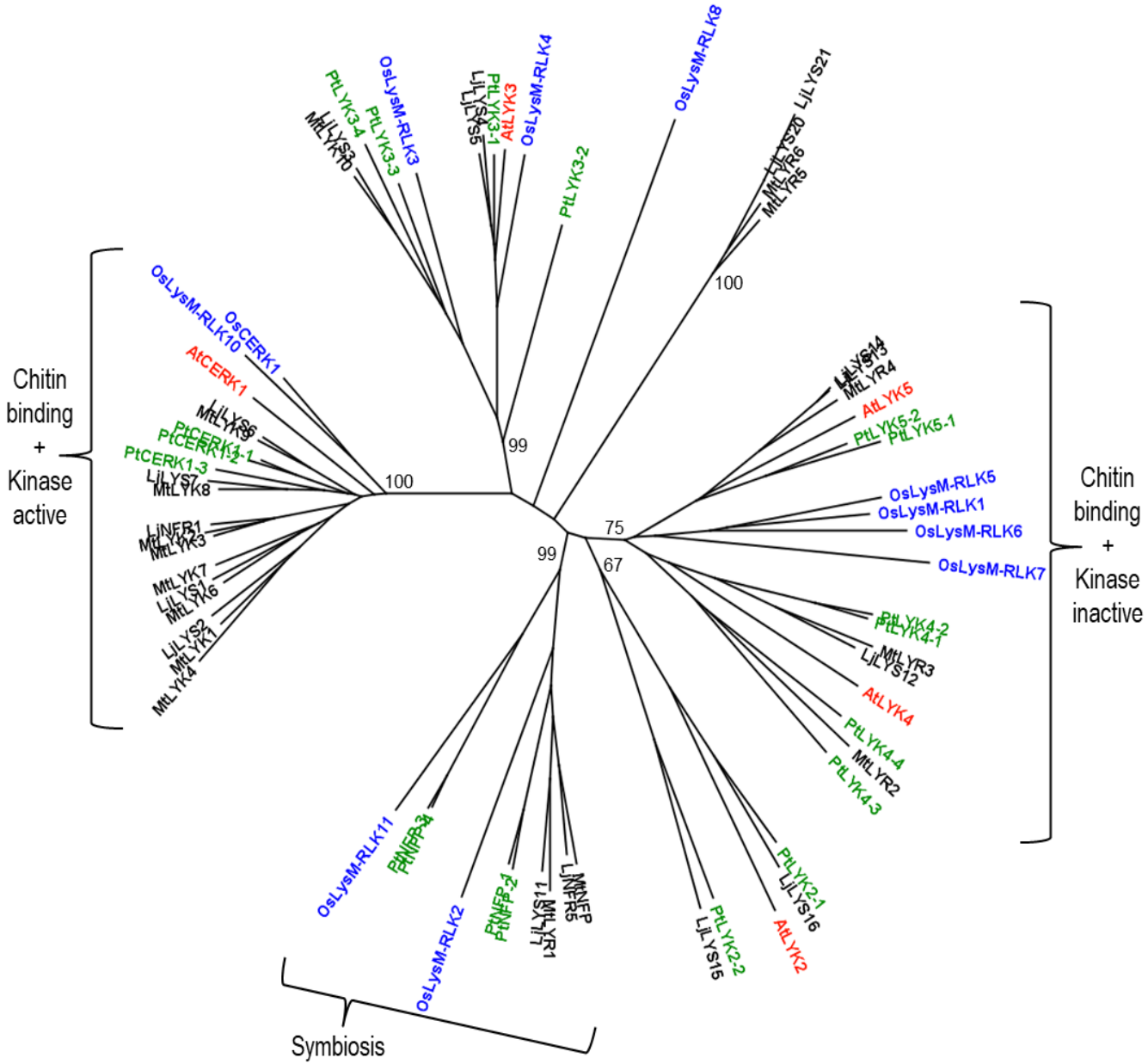

Figure 15: Several paralogs of lysin motif receptor-like kinases are present in poplar. The phylogenetic tree is based on full length protein sequences and was constructed with the Neighbor-Joining method of the software Geneious® 8.1.9 (Kearse et al., 2012). Numbers indicate bootstraps values performed with 1000 repetitions. The color code labels the different species: *Populus trichocarpa* proteins are shown in green, *Arabidopsis thaliana* proteins in red, *Oryza sativa* proteins in blue and *Medicago truncatula* and *Lotus japonicus* proteins are shown in black. According to their function in Arabidopsis, Rice, *Medicago* or *Lotus* the groups are clustered into chitin binding proteins with an active kinase domain, chitin binding proteins with an inactive kinase domain and symbiosis related genes.

The *in silico* analysis to identify LysM-RLP homologs in poplar (Fig. 16) revealed two homologs of AtLYM1/AtLYM3 which function in Arabidopsis in peptidoglycan recognition (Willmann et al., 2011) and two homologs of AtLYM2/OsCEBiP which are known to bind chitin in Arabidopsis and rice (Shinya et al., 2012; Kaku et al., 2006).

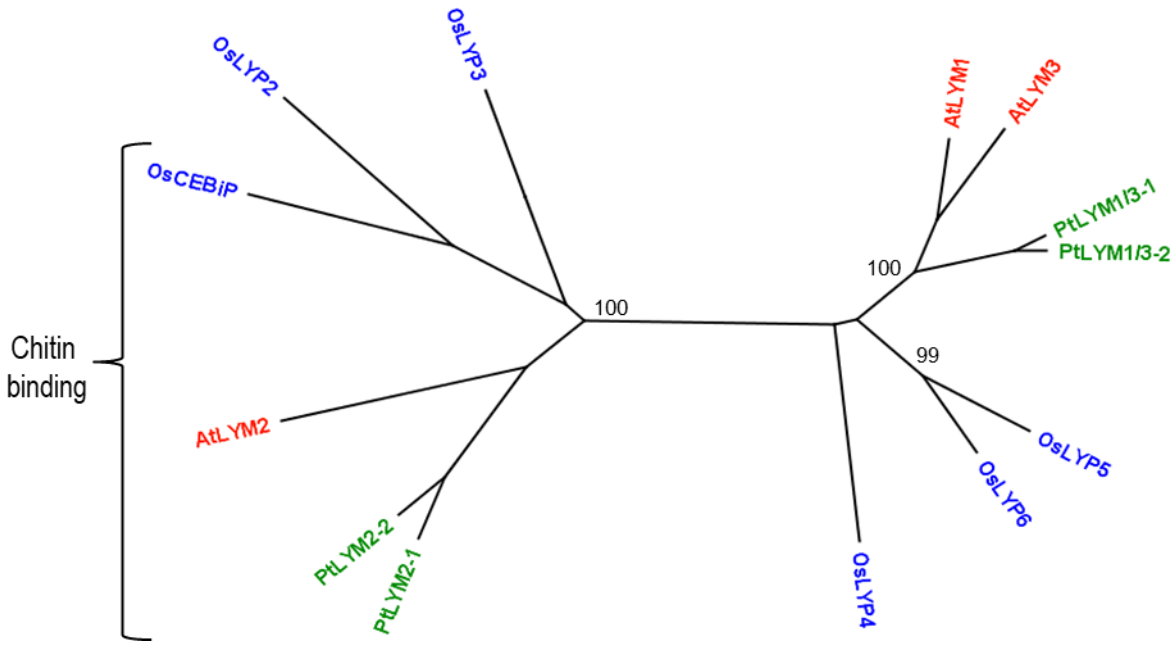

Figure 16: Several paralogs of lysin motif receptor-like proteins are present in poplar. The phylogenetic tree is based on full length protein sequences and was constructed with the Neighbor-Joining method of the software Geneious® 8.1.9 (Kearse et al., 2012). Numbers indicate bootstraps values performed with 1000 repetitions. The color code labels the different species: *Populus trichocarpa* proteins are shown in green, *Arabidopsis thaliana* proteins in red, and *Oryza sativa* proteins in blue. According to their function in Arabidopsis and rice a chitin binding capacity is also predicted for the LYM2 homologs of poplar.

3.1.3 An *in-silico* analysis of protein domains of poplar CERK1 suggests kinase activity

Since the focus of this thesis is the identification of CERK1 homologs in poplar only for these genes a further analysis was performed. For additional information on the domain structure and to support the hypothesis that the in chapter 3.1.2 identified poplar CERK1 homologs are kinase active an *in-silico* alignment with Arabidopsis CERK1 was performed (Fig. 17). The domain organization was determined based on the sequence homology to AtCERK1 using the InterProScan tool (Jones et al., 2014).

Sequencing of the *PtCERK1-2* gene in our department (Mo Awwanah, unpublished) showed single-nucleotide polymorphisms (SNPs) that differ from the database (www.phytozome.org; Goodstein et al., 2012) and result in premature stop codons thus identifying *PtCERK1-2* as a pseudogene. It was therefore excluded from the alignment.

In addition to sequences of *Populus trichocarpa* CERK1 also the protein sequences of the two *Populus x canescens* CERK1 homologs were included because in this thesis functional analysis is performed in *Populus x canescens*. Since the database of *Populus x canescens* (aspendb.uga.edu; Xue et al., 2015) has meanwhile been published but was still incomplete at the start of this thesis the sequences were obtained by sequencing in our department (Mo Awwanah, Supplemental Table 1).

Similar to other LysM-RLKs the data indicates the presence of three LysM domains in CERK1 proteins of both poplar species. Even though only the third LysM domain is predicted with the InterProScan tool the alignment with Arabidopsis CERK1 and the presence of the separating CxC motif indicates that the first and second LysM domain are existing as well. This is an essential requirement for a putative chitin binding function since in Arabidopsis all three LysM domains are necessary for chitin binding capacity (Petutschnig et al., 2010).

The presence of the highly conserved DFG motif as well as conservation of all invariant amino acids in the kinase domain (Hanks and Hunter, 1995) give a hint that all poplar CERK1 proteins are likely to be kinase active.

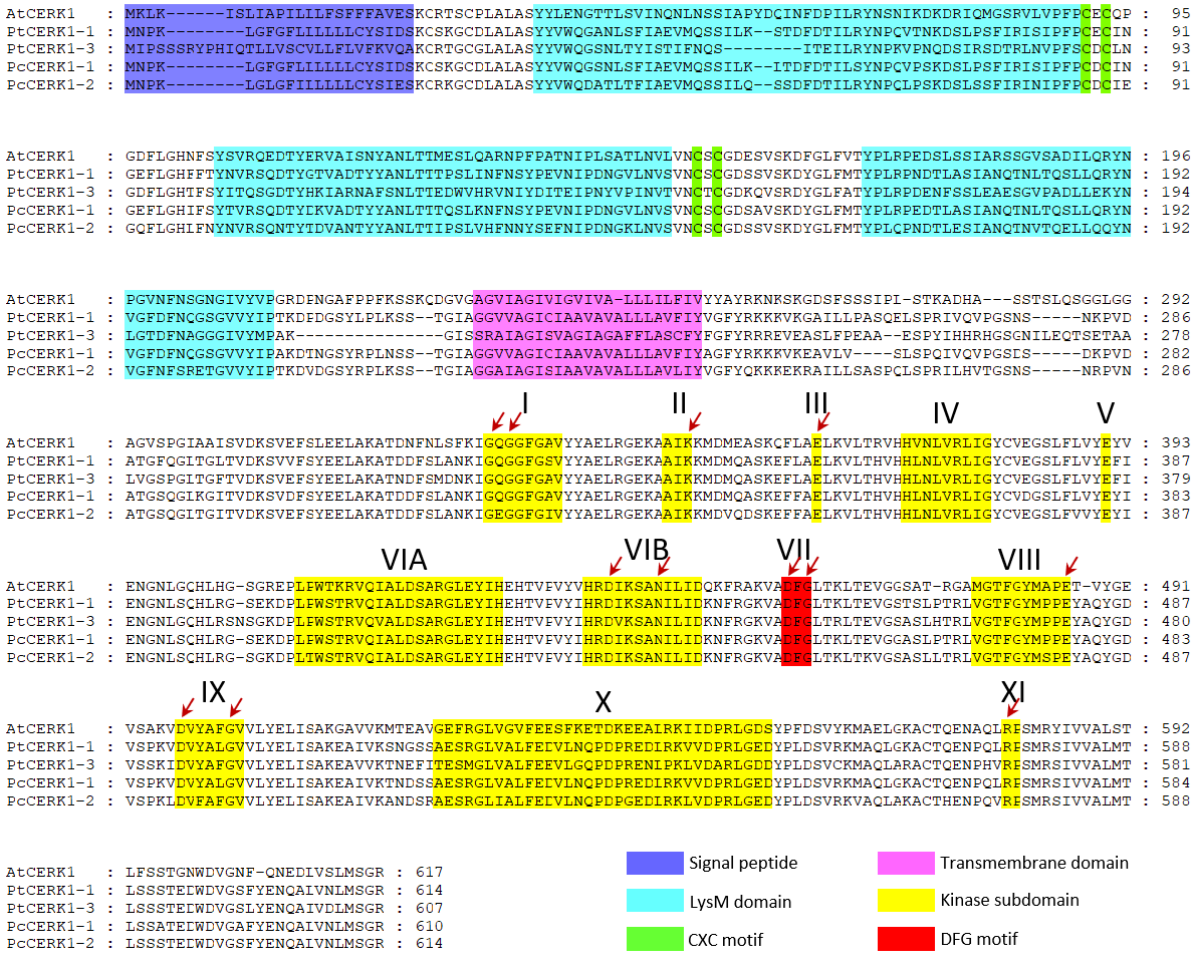

Figure 17: Poplar CERK1 proteins are likely to be kinase active. Alignment of full-length protein sequences were performed with the Clustal Omega software (Madeira et al., 2019). Sequences of CERK1 proteins from *Populus trichocarpa* (Pt) and *Populus x canescens* (Pc, tremula allele) were aligned with the Arabidopsis thaliana (At) CERK1 protein which is known to be kinase active. Invariant amino acids in the kinase domain according to Hanks and Hunter (1995) are indicated by red arrows and are conserved in the poplar CERK1 proteins as well. Signal peptides (dark blue), LysM domains (light blue) and transmembrane regions (pink) are assigned with InterProScan integrated in Geneious® 8.1.9 (Kearse et al., 2012). The presence of three LysM domains separated by a CxC motif (green) indicates chitin binding function of the poplar CERK1 ectodomains.

3.1.4 PcCERK1 genes are upregulated after chitin treatment

For the poplar *CERK1* genes there was no data about expression levels in various tissues in the web-based tool “Plant eFP Viewer” available (http://bar.utoronto.ca; Waese et al., 2017). In particular the expression of CERK1 genes in leaf material was of special interest since *Melampsora* as the model pathogen of poplar is infecting leaf tissue. To check whether CERK1 is expressed in poplar leaves and to test if the expression can be triggered by chitin the basic expression level and the inducibility after chitin treatment was tested via qPCR for

Populus x canescens PcCERK1-1 and *PcCERK1-2* (Mo Awwanah, unpublished). The data show that *PcCERK1-1* is significantly higher expressed than *PcCERK1-2* (supplemental Fig. 1) and both genes show a tendency to be upregulated after chitin treatment (supplemental Fig. 2).

3.1.5 A proteomic study showed that *CERK1-1* has the highest abundance among poplar LysM-RLKs identified with chitin affinity purification

The main objective of the proteomic study was to identify which of the LysM-RLK and LysM-RLP genes identified in the phylogenetic analysis (chapter 3.1.2) are indeed translated into proteins with chitin binding capacity. A particular focus was also here on CERK1. To check the abundance of CERK1 and other LysM-RLKs and LysM-RLPs, a mass spectrometry analysis was performed. As samples a total protein extraction from *Populus trichocarpa* or *Populus x canescens* leaves were used. The potential chitin binding capacity of candidate genes was utilized for purification. A detection thus also gives indirect evidence that the protein is able to bind chitin.

All genes with a potential chitin binding function (CERK1, LYK4, LYK5 and LYM2) were sequenced in our department again (Mo Awwanah, 2020 and Supplemental Table 1) to identify SNPs that differ from the database and result in an altered protein sequence. For protein identification via mass spectrometry the available protein databases of *P. trichocarpa* or *P. x canescens* (www.phytozome.org; Goodstein et al., 2012; aspendb.uga.edu; Xue et al., 2015) were supplemented with these additional sequences. Detected peptides were assigned to the corresponding candidate proteins of LysM-RLKs and LysM-RLPs identified in chapter 3.1.2..

The overall abundance of determined peptides for both poplar species was quite low compared to Arabidopsis. This might be due to a high content of phenolic compounds in poplar leaves which can interfere with protein isolation. Therefore, different purification steps were tested in addition to the standard protocol to reduce phenols in the total protein extract. This includes an additional purification with Dowex and Sephadex or addition of ascorbic acid to the buffer. As an alternative it was tried to enrich the amount of candidate proteins in the sample. This should be achieved by the input of double protein amount or the isolation of the microsomal fraction due to a predicted plasma membrane localization of candidate proteins. The elution of proteins from the chitin magnetic beads with a chitin

hexamer (C6-mer) was tested as well. This should lower the amount of unspecifically bound proteins eg. proteins that agglomerate on the magnetic bead instead of directly binding to the chitin.

In general, identified peptides were classified into two groups: unique peptides could only be assigned to one specific protein and therefore clearly identify its presence. In contrast, shared peptides could be assigned to two closely related proteins and thus it can not be distinguished from which of the two proteins the peptide originate.

The results for *Populus trichocarpa* show that PtCERK1-1 was detected in every sample with relatively high peptide counts compared to all other proteins (Fig. 18). This is in line with the literature as in Arabidopsis the CERK1 protein has also been shown together with LYK5 to exhibit a high chitin binding affinity (Petutschnig et al., 2010; Cao et al., 2014). Significantly more peptides are found in the microsomal fraction which is expected since the protein is likely to be membrane bound. No peptides related to PtCERK1-2 could be detected. Apart from the information in the genome database of *Populus trichocarpa* this gene was previously identified as a pseudogene (see chapter 3.1.3). Hence, this finding is another hint that supports this assumption. Peptides of PtCERK1-3 are significantly less abundant in the analysed samples than PtCERK1-1 peptides. Unique peptides of PtCERK1-3 could only be detected when the total protein extract was further purified for proteins of the microsomal fraction. In the other samples that are not enriched for membrane proteins only shared peptides with PtCERK1-1 are found (supplemental Fig. 3).

Out of four homologs of LYK4 only peptides for three candidate proteins have been identified (supplemental Fig. 4). For PtLYK4-1 exclusively shared peptides could be assigned. PtLYK4-2 and PtLYK4-4 were detected with unique peptides. Peptides for PtLYK4-3 are missing.

From two LYK5 homologs only PtLYK5-2 was found with unique peptides in the proteomic data (supplemental Fig. 5). Peptides for PtLYK5-1 failed to be determined. It is possible that PtLYK5-1 is not expressed in leaves because it could not be amplified in expression studies (Mo Awwanah, personal communication).

One unexpected finding was the presence of peptides unique for PtNFP-3 (supplemental Fig. 6). This candidate protein clusters in the phylogenetic analysis with proteins related to symbiosis (see chapter 3.1.2) and is assumed to bind Nod factors rather than chitin. This result indicates that it might exhibit a chitin binding activity as well.

Peptides derived from LysM-RLPs were found for PtLYM2 proteins (supplemental Fig. 7). PtLYM2-1 as well as the two splice variants of PtLYM2-2 (2-2.1 and 2-2.2) are all identified with unique peptides and with similar abundances.

The results of the mass spectrometry analysis of *Populus x canescens* chitin-affinity purified leaf proteins (Fig. 19) are similar to the results obtained from *Populus trichocarpa*. Out of two PcCERK1 homologs only PcCERK1-1 is identified with unique peptides whereas peptides corresponding to PcCERK1-2 are all shared (supplemental Fig. 8). This correlates with the significantly higher expression of *PcCERK1-1* compared with *PcCERK1-2* (chapter 3.1.4). Same as in *P. trichocarpa* the PcCERK1-1 peptides are more abundant than peptides of the other candidate proteins and are found in each sample.

In the group of PcLYK4 homologs unique peptides are determined for PcLYK4-1 and PcLYK4-2 (supplemental Fig. 9). Gene sequencing conducted in our department classified PcLYK4-3 and PcLYK4-4 as pseudogenes (Awwanah, 2020). Peptides for these proteins should therefore not appear in the mass spectrometry results. While this holds true for PcLYK4-3, PcLYK4-4 was identified with one and the same peptide in several measurements. The PcLYK4-4 pseudogene has several in frame stop codons. In principle the first part of the gene could be translated into a protein until the first premature stop codon arises. Nevertheless, the identified peptide appears

in an amino acid sequence after several stop codons and can thus not be part of a truncated PcLYK4-4 protein. It might be possible this peptide belongs to another unknown protein because the annotation of the genome database of *Populus x canescens* is still in progress.

Similar to *P. trichocarpa* only one homolog of PcLYK5 seems to be translated into a protein. Peptides for PcLYK5-1 were not detectable whereas PcLYK5-2 was identified in each measurement with unique peptides (supplemental Fig. 10). A Failure to determine peptides of PcLYK5-1 supports a classification as pseudogene due to in frame stop codons (Awwanah, 2020).

Peptides assigned to LysM-RLPs are found for all PcLYM2 proteins. PcLYM2-1 and the two splice variants of PcLYM2-2 were identified with unique peptides in the mass spectrometry measurements (supplemental Fig. 11).

Protein extraction	# 1	# 2	# 3	# 4	# 5	# 6	# 7	# 8	# 9	# 10	# 11	# 12	# 13	# 14
Protocol changes			microsomal fraction	microsomal fraction / C6mer elution			Dowex	Sephadex		Dowex + Ascorbic Acid		double protein amount	Sephadex	Sephadex / double protein amount
PtCERK1-1		4|4|11	7|7|31	7|7|49	6|7|9	3|4|4	6|8|8	5|6|6	2|2|4	8|9|19	4|4|4	4|4|6	1|1|1	3|3|4
PtCERK1-2														
PtCERK1-3			2|2|8	2|2|12	0|1|1	0|1|1	0|2|2	0|1|1		0|1|2				
PtLYK4-1													0|1|1	0|2|2
PtLYK4-2				1|1|4		1|1|1	2|2|2			1|1|2			1|2|3	2|4|5
PtLYK4-3														
PtLYK4-4					1|1|2						1|1|1	1|1|1	1|1|2	1|1|1
PtLYK5-1														
PtLYK5-2	1|1|1		2|2|8	4|4|14					3|3|9	4|4|14			1|1|1	
PtNFP-3		1|1|2	2|2|6	2|2|3										
PtLYM2-1	0|1|2			1|1|6	0|1|6	1|2|9	0|1|3	0|1|3	3|3|7	3|3|9	1|2|8	1|2|13	1|2|7	1|2|12
PtLYM2-2.1		1|1|2				2|2|2	1|1|1	1|1|1		1|1|2				
PtLYM2-2.2	1|2|3			1|1|4	1|2|9	2|3|9	1|2|5	1|2|5			0|1|6	0|1|7	0|1|5	0|1|10

Figure 18: Mass spectrometry analysis identified a specific subset of LysM-RLKs and LysM-RLPs in leaves of *Populus trichocarpa*. Proteins were extracted from leaf samples of *Populus trichocarpa* (Pt) and mass spectrometry was performed after chitin affinity purification. The protocol changes give information about purification steps carried out in addition to the standard protocol. These were performed to either reduce phenolic compounds (by addition of dowex, ascorbic acid and sephadex) or intended to enrich the presence of candidate proteins in the samples (microsomal fraction, chitin hexamer (C6mer) elution and double protein amount). Green and yellow color indicates peptides, which are unique for a protein and peptides shared with other proteins, respectively. The three-number code designates the number of unique peptides belonging specifically only to this protein (left), the number of distinct peptides found for this protein (middle) and the overall number of detected peptides including redundantly found peptides (right). A detailed list of detected peptides is provided in the appendix (supplemental Table 2-6).

Protein extraction	# 1	# 2	# 3	# 4	# 5	# 6	# 7	# 8	# 9
Protocol changes		microsomal fraction			Dowex + Ascorbic Acid		double protein amount	Sephadex	Sephadex / double protein amount
PcCERK1-1	2|3|6	7|10|23	2|5|8	6|8|19	4|5|12	2|2|2	5|8|10	2|2|2	3|4|6
PcCERK1-2	0|1|2	0|3|6	0|3|5	0|2|4	0|1|1		0|3|4		0|1|1
PcLYK4-1	2|2|4		1|2|3	2|2|5	1|1|6	1|2|3		1|3|3	0|1|1
PcLYK4-2	1|1|2		0|1|2			0|1|2		0|2|2	0|1|1
PcLYK4-3									
PcLYK4-4			1|1|2			1|1|2	1|1|1	1|1|3	1|1|2
PcLYK5-1									
PcLYK5-2	2|2|8	1|1|4	6|6|6	3|3|13	2|2|6	1|1|1	2|2|2	1|1|2	4|4|4
PcLYM2-1		3|4|14	0|1|3	0|1|4			0|2|2	0|1|1	0|1|4
PcLYM2-2.1	1|1|6		1|1|1	1|1|2					
PcLYM2-2.2		2|3|10	1|2|4	0|1|4			2|4|4	0|1|1	2|3|7

Figure 19: Mass spectrometry analysis identified a specific subset of LysM-RLKs and LysM-RLPs in leaves of *Populus x canescens*. Proteins were extracted from leaf samples of *Populus x canescens* (Pc) and mass spectrometry was performed after chitin affinity purification. The protocol changes give information about purification steps carried out in addition to the standard protocol. These were performed to either reduce phenolic compounds (by addition of dowex, ascorbic acid and sephadex) or intended to enrich the presence of candidate proteins in the samples (microsomal fraction and double protein amount). Green and yellow color indicates peptides, which are unique for a protein and peptides shared with other proteins, respectively. The three-number code designates the number of unique peptides belonging specifically only to this protein (left), the number of distinct peptides found for this protein (middle) and the overall number of detected peptides including redundantly found peptides (right). A detailed list of detected peptides is provided in the appendix (supplemental Table 7-10).

3.2 Complementation experiments with *PcCERK1-1* and *PcCERK1-2* in the chitin-insensitive Arabidopsis mutant *cerk1-2*

For a functional analysis of the putative poplar *CERK1* homologs a complementation study was performed. The two CERK1 genes of *Populus x canescens* (*PcCERK1-1* and *PcCERK1-2*) were transformed separately into the chitin-insensitve Arabidopsis mutant *cerk1-2*. The Arabidopsis CERK1 knockout mutant *cerk1-2* completely lacks the ability to respond with ROS generation or MAPK activation when treated with chitin (Miya et al. 2007; Petutschnig et al., 2014). Thus, in this complementation approach a reconstitution of these chitin-triggered responses by *PcCERK1-1* (chapter 3.2.1) or *PcCERK1-2* (chapter 3.2.2) were tested with one allele for each homolog.

3.2.1 *PcCERK1-1* is not able to restore the ROS burst or MAPK activity of the chitin insensitive Arabidopsis mutant *cerk1-2*

The *PcCERK1-1* gene was cloned into a vector construct for expression under control of the natural promoter of Arabidopsis *CERK1* and transformed into the Arabidopsis *cerk1-2* mutant. Transgenic lines could not be obtained for this *pAtCERK1:PcCERK1-1_mCitrine* construct probably due to cell death during early seed development. Therefore, a construct was cloned using an estradiol inducible promoter (*pLexA*) system. Gene expression is induced in a dose-dependent manner when estradiol is applied.

The estradiol inducibility of this *pLexA:PcCERK1-1_mCitrine* construct was first tested by transient expression in *N. benthamiana* (Fig. 20). As a negative control, either $MgCl_2$ buffer without any bacteria was infiltrated or plants were transformed with bacteria containing the *pLexA:PcCERK1-1_mCitrine* construct but sprayed with water instead of estradiol. As expected, the construct is not constitutively active. An mCitrine signal could only be observed after an estradiol application. The mCitrine signal is visible in several cell compartments including nucleus, cytoplasmic strands, endoplasmic reticulum and cell periphery. Since CERK1 was identified in localization studies of Arabidopsis and rice as a plasma membrane protein (Miya et al., 2007; Shimizu et al., 2010) for PcCERK1 a plasma membrane localization was expected as well. The applied dose of estradiol might therefore be not ideal and lead to a strong overexpression of the construct in *N. benthamiana* causing mislocalization of the protein.

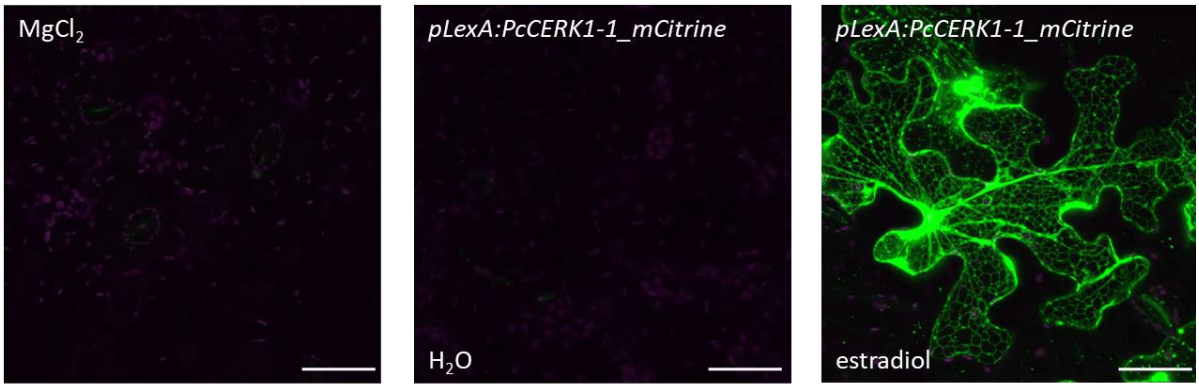

Figure 20: Estradiol-induced *pLexA:PcCERK1-1_mCitrine* expression in *N. benthamiana* results in strong mCitrine signals in several cell compartments. The *pLexA:PcCERK1-1_mCitrine* construct under control of an estradiol inducible promoter was transiently transformed into *N. benthamiana*. Leaves were sprayed with 25 µM estradiol or water as a control and incubated for 18 h. As a negative control, leaves were infiltrated with a $MgCl_2$ solution without agrobacteria. All images are z-stacks of 13 confocal images taken 1 µm apart. **Green:** *PcCERK1-1_mCitrine*; **magenta:** chloroplast autofluorescence. Scale bar = 50 µm.

For the complementation study in Arabidopsis the *pLexA:PcCERK1-1_mCitrine* construct was then stably transformed into the Arabidopsis *cerk1-2* mutant. Several transgenic lines were obtained. To examine the correct estradiol dose and incubation time a pre-test was carried out. Different concentrations ranging from 1 µM to 25 µM were applied to the leaf surface by spraying. Expression of the *pLexA:PcCERK1-1_mCitrine* construct was analysed after 1 h, 6 h and 24 h in total protein extracts via western blot (Fig. 21). The results show that independent of the applied estradiol doses one hour is not sufficient to induce the construct. After six hours a slight induction can be seen but there are apparently no differences in the signal strength between the applied doses of estradiol at this timepoint. The strongest induction of gene expression could be obtained after 24 h when applying 25 µM estradiol and was therefore used for further experiments.

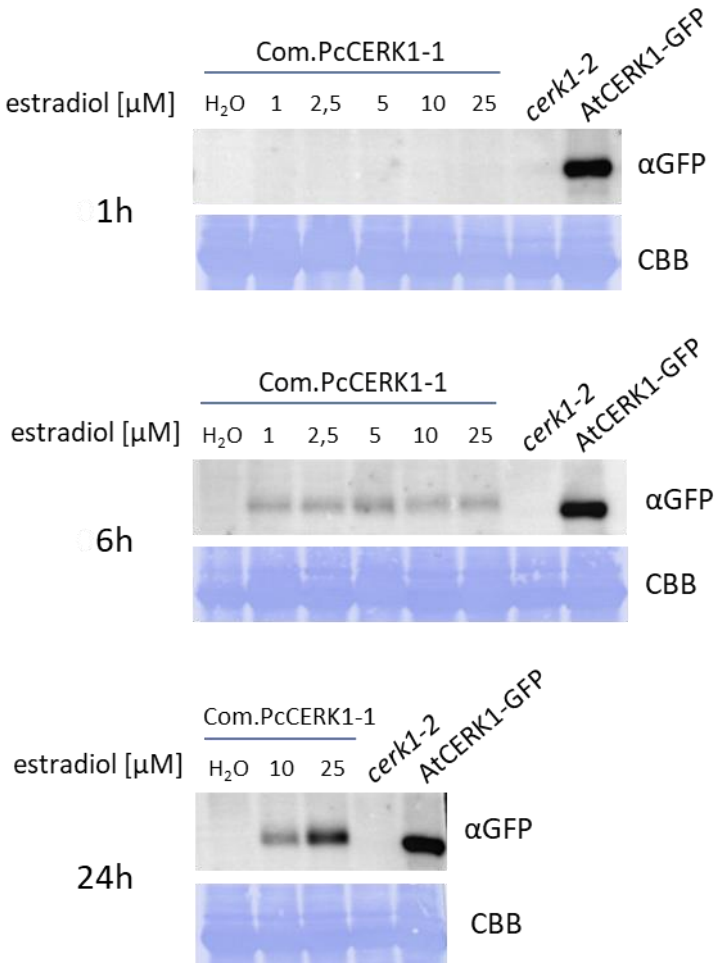

Figure 21: The expression of an estradiol inducible PcCERK1-1 construct is highly induced after application of 25 µM estradiol and an incubation time of 24 h. To investigate the correct dose to induce the estradiol inducible construct *pLexA:PcCERK1-1_mCitrine* different estradiol doses were tested. 1 h, 6 h, and 24 h after application a western blot analysis was performed to check the expression level via detection of the mCitrine-tag with an GFP antibody. **Com.PcCERK1-1:** *pLexA:PcCERK1-1_mCitrine* transformed into *cerk1-2* mutant; ***cerk1-2*:** Arabidopsis CERK1 knockout mutant that lacks chitin response; **AtCERK1-GFP:** *pAtCERK1:AtCERK1_GFP* transformed into *cerk1-2* mutant, used as a control for detection of PcCERK1-mCitrine fusions that are recognized by the GFP antibody; **CBB:** Coomassie Brilliant Blue-stained membrane.

The stably transformed Arabidopsis plants of *pLexA:PcCERK1-1_mCitrine* were analysed for subcellular localization of PcCERK1-1_mCitrine. Here, unlike the results in *N. benthamiana,* a PcCERK1-1_mCitrine signal is only present in the cell periphery (Fig. 22). This indicates cell membrane localization of PcCERK1-1_mCitrine, even though detection of the mCitrine signal was difficult and only few leaf cells showed a signal.

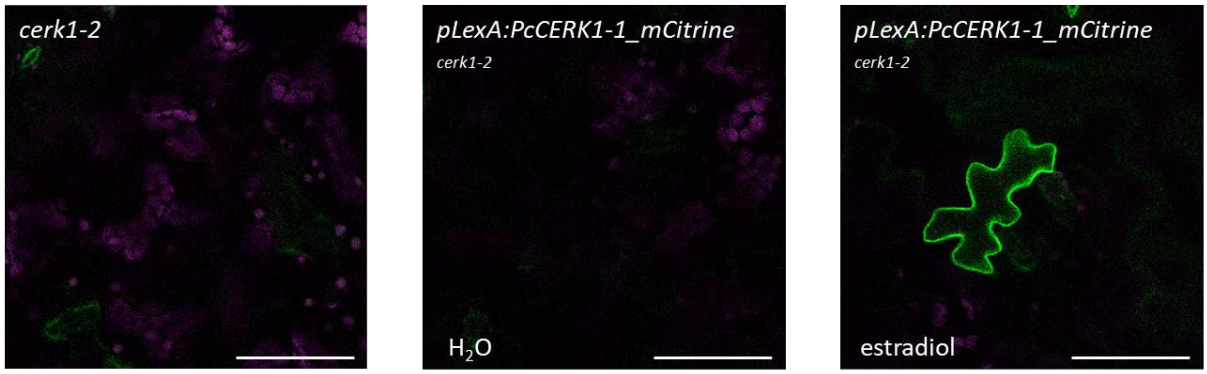

Figure 22: Estradiol-induced *pLexA:PcCERK1-1_mCitrine* expression in *A. thaliana* results in mCitrine signals in the cell periphery. The *PcCERK1-1_mCitrine* construct under an estradiol inducible promoter was stably transformed into the chitin insensitive Arabidopsis *cerk1-2* mutant. The mCitrine signal was measured after 18 h in leaves sprayed with 25 µM estradiol or water as a control. As a negative control leaves of the *cerk1-2* mutant were analysed as well. All images are single plane CLSM images. **Green:** *pLexA:PcCERK1-1_mCitrine*; **magenta:** chloroplast autofluorescence. Scale bar = 50 µm.

The complementation ability of *PcCERK1-1* was tested in the stable transgenic Arabidopsis lines with ROS burst and MAPK assays after application of estradiol. In parallel, an experiment with water sprayed samples was performed as a control. Western blot analysis was carried out to show that *pLexA:PcCERK1-1_mCitrine* expression was induced by estradiol and PcCERK1-1_mCitrine protein was produced.

As expected, plants sprayed with water did not exhibit any expression of *PcCERK1-1* and did not show a ROS burst (Fig. 23 A). For the estradiol sprayed plants two lines show a high amount of PcCERK1-1_mCitrine protein in western blots and the third line a low amount of PcCERK1-1_mCitrine protein. However only one of the *pLexA:PcCERK1-1_mCitrine* lines responds with a chitin-triggered ROS production. In this line the ROS burst is only slightly restored without the typical ROS burst peak (Fig. 23 B). The other two lines do not show complementation. The flagellin peaks are normal and not affected by applying estradiol to the plants (supplemental Fig. 12).

The investigation of the MAPK response after application of estradiol revealed no complementation ability for *PcCERK1-1* even though expression of *PcCERK1-1_mCitrine* is strongly induced in one line (Fig. 24 B). None of the lines shows a MAPK response when treated with chitin (Fig. 24 D) similar to the water sprayed controls (Fig. 24 C).

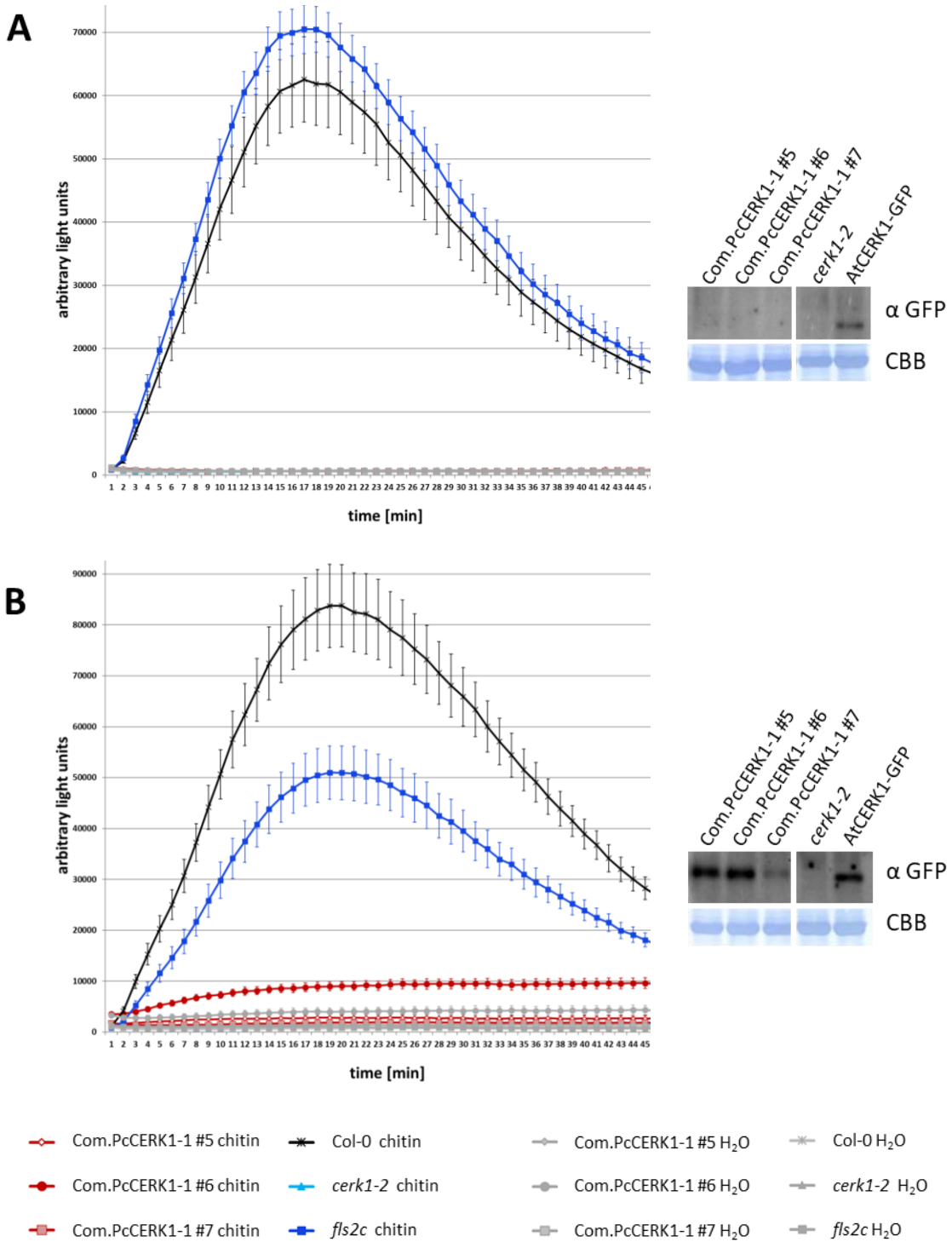

Figure 23: The estradiol inducible *PcCERK1-1* gene does not restore chitin-induced ROS burst of *cerk1*-2. Leaf discs were treated with 100 µg/ml chitin solution or water as a control. To visualize ROS generation a luminol based assay was used. Data represent the mean of 8 leaf discs ± SEM. To test if the *PcCERK1-1* gene expression was induced after applying estradiol a Western Blot was performed detecting the mCitrine tagged protein with a GFP antibody. **A:** samples sprayed with water; **B:** samples sprayed with 25 µM estradiol; **Com.PcCERK1-1 #5, #6, #7**: individual lines of *pLexA:PcCERK1-1_mCitrine* transformed into the *cerk1-2* mutant; **AtCERK1-GFP:** *pAtCERK1:AtCERK1_GFP* transformed into *cerk1-2* mutant, used as a control for detection of PcCERK1-mCitrine fusions that are recognized by the GFP antibody; **Col-0:** Arabidopsis wildtype; ***cerk1-2*:** Arabidopsis CERK1 knockout mutant that lacks chitin response; ***fls2c*:** Arabidopsis FLS2C knockout mutant that lacks flagellin response. **CBB:** Coomassie Brilliant Blue-stained membrane.

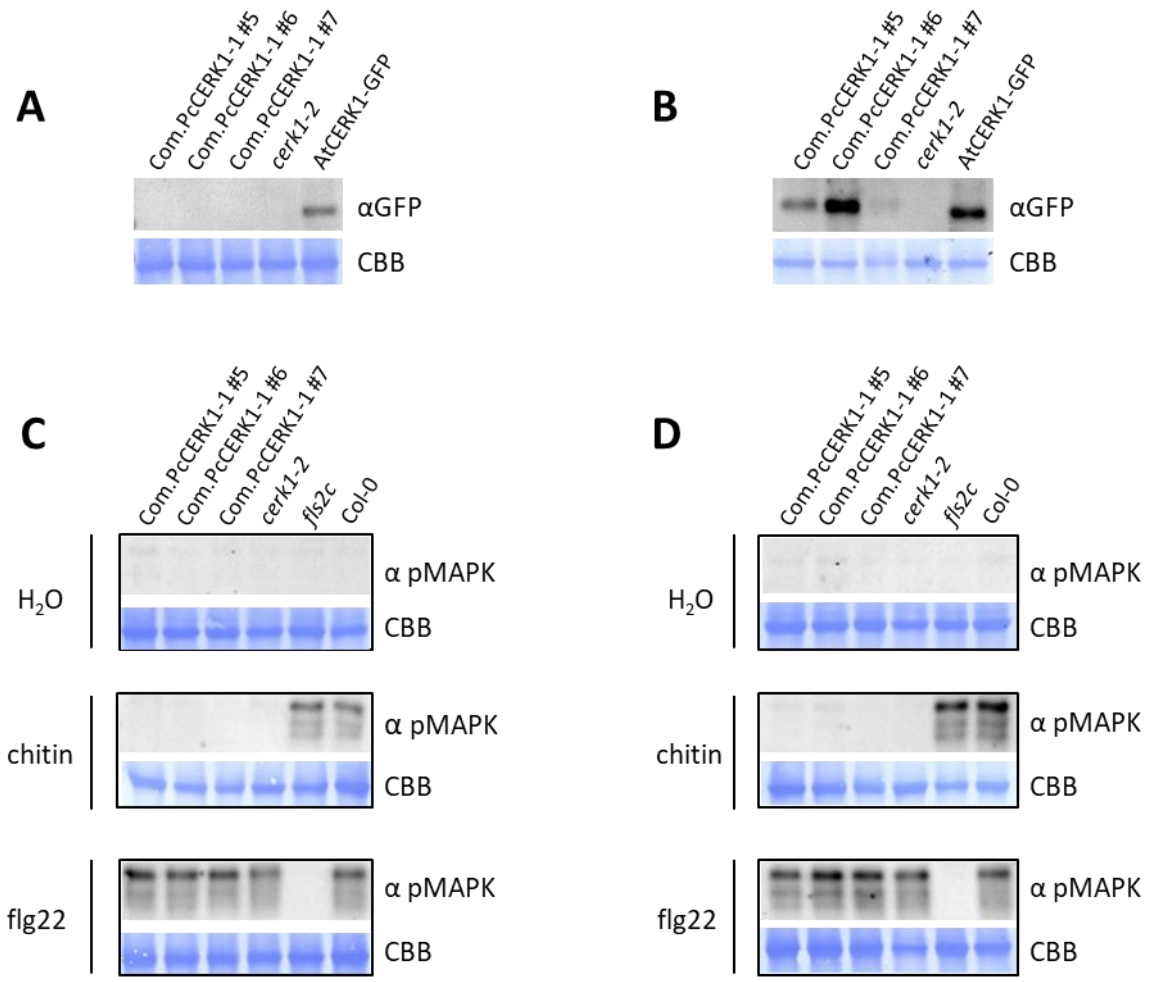

Figure 24: The estradiol inducible *PcCERK1-1* gene does not restore the chitin-induced MAPK activation of *cerk1-2*. A/B: Protein levels of *pLexA:PcCERK1-1_mCitrine* in transgenic lines treated with water (A) or estradiol (B) were detected with a GFP specific antibody. *pLexA:PcCERK1-1_mCitrine* is only detected after estradiol treatment. **C/D:** Two week old seedlings were treated with water (C) or 25 µM estradiol (D) and after 24 h infiltrated with either 10 µg/ml chitin solution, 10 nM flg22 solution or water as a control. After 12 min incubation time, samples were harvested and phosphorylated MAPKs were detected in total protein extracts with a specific antibody. **Com.PcCERK1-1 #5, #6, #7**: individual lines of *pLexA:PcCERK1-1_mCitrine* transformed into *cerk1-2* mutant; ***cerk1-2*:** Arabidopsis CERK1 knockout mutant that lacks chitin response; **AtCERK1-GFP:** *pAtCERK1:AtCERK1_GFP* transformed into *cerk1-2* mutant, used as a control for detection of PcCERK1-mCitrine fusions that are recognized by the GFP antibody; ***fls2c*:** Arabidopsis FLS2C knockout mutant that lacks flagellin response; **Col-0:** Arabidopsis wildtype; **CBB:** Coomassie Brilliant Blue-stained membranes.

3.2.2 *PcCERK1-2* is not able to restore the ROS burst but partially restores MAPK activity of the chitin insensitive Arabidopsis mutant *cerk1-2*

Analogous to the *PcCERK1-1* analysis, a complementation study in the Arabidopsis *cerk1-2* mutant that lacks the ability to respond to chitin was performed with the *PcCERK1-2* paralog for functional analysis. In contrast to *PcCERK1-1,* several stably transformed lines with the *PcCERK1-2* gene under control of the natural promoter of Arabidopsis CERK1 could be obtained. It was, therefore, not necessary to use an estradiol inducible promoter system. To test the subcellular localization of the *pAtCERK1:PcCERK1-2_mCitrine* construct it was analysed in transient expression in *N. benthamiana* (Fig. 25) and in the stably transformed Arabidopsis lines (Fig. 26).

In both experiments *PcCERK1-2_mCitrine* shows a signal in the cell periphery which is in line with the expected transmembrane localization of PcCERK1-2_mCitrine.

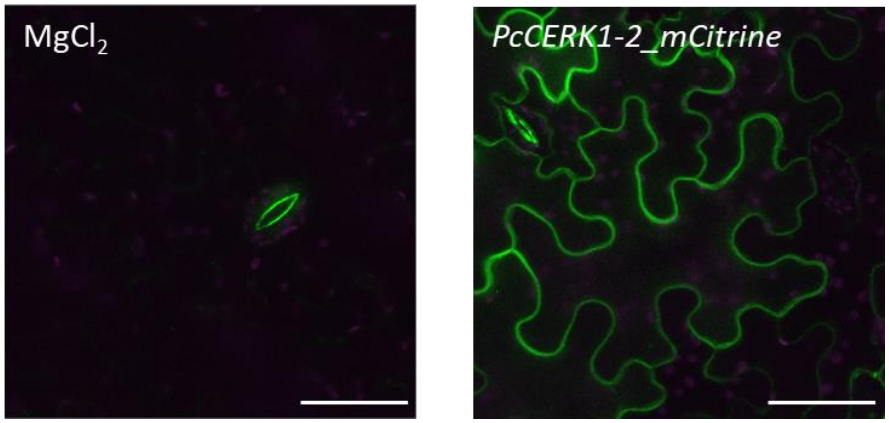

Figure 25: *PcCERK1-2_mCitrine* is localized in the cell periphery of *N. benthamiana* cells. The *pAtCERK1:PcCERK1-2_mCitrine* construct was transiently expressed in *N. benthamiana*. All images are z-stacks of 13 confocal images taken 1 µm apart. **Green:** *PcCERK1-2_mCitrine* (except autofluorescence stomata); **magenta:** chloroplast autofluorescence. Scale bar = 50 µm.

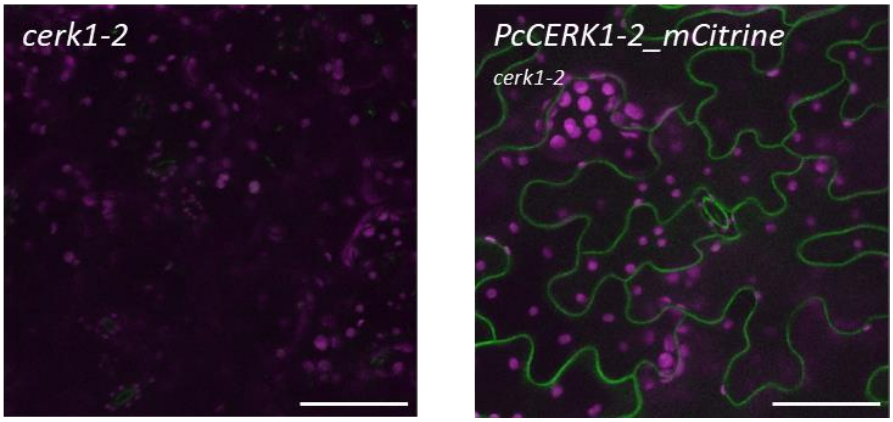

Figure 26: *PcCERK1-2_mCitrine* is localized in the cell periphery of *A. thaliana* cells. The *pAtCERK1:PcCERK1-2_mCitrine* construct was stably transformed into the A. thaliana *cerk1-2* mutant. All images are z-stacks of 7 confocal images taken 1 µm apart. Signal accumulation mode was used to make weak signals visible. **Green:** *PcCERK1-2_mCitrine;* **magenta:** chloroplast autofluorescence. Scale bar = 50 µm.

Complementation ability was tested in ROS burst and MAPK assays. The *PcCERK1-2* gene was not able to restore the chitin-triggered ROS burst (Fig. 27). Similar to Arabidopsis *cerk1-2* no signal was observed after chitin treatment whereas the flagellin response was normal (supplemental Fig. 13).

The results for the MAPK assay show that *PcCERK1-2* could only partially restore the chitin response of the Arabidopsis *cerk1-2* mutant (Fig. 28). A signal for phosphorylated MAPKs is visible for all three lines but with a weaker intensity compared with wildtype Col-0.

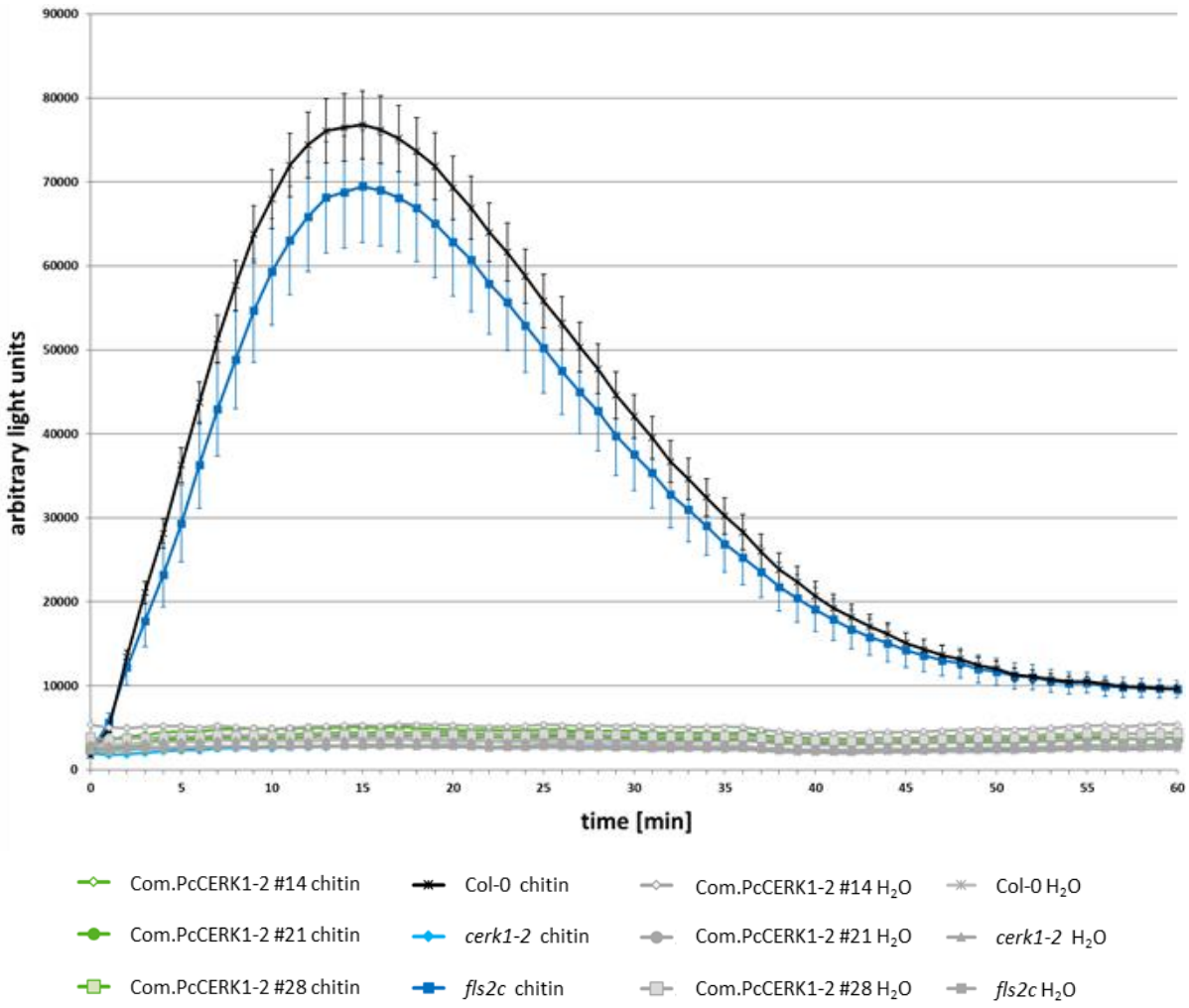

Figure 27: *PcCERK1-2* does not restore the ROS burst of the Arabidopsis *cerk1-2* mutant line. Leaf discs were treated with either 100 µg/ml chitin solution or water as a control. To visualize ROS generation a luminol based assay was used. Data represent the mean of 8 leaf discs ± SEM. **Com.PcCERK1-2 #14, #21, #28**: individual lines of *pAtCERK1:PcCERK1-2_mCitrine* transformed into *cerk1-2* mutant; **Col-0:** Arabidopsis wildtype; ***cerk1-2*:** Arabidopsis CERK1 knockout mutant that lacks chitin response; ***fls2c*:** Arabidopsis FLS2C knockout mutant that lacks flagellin response.

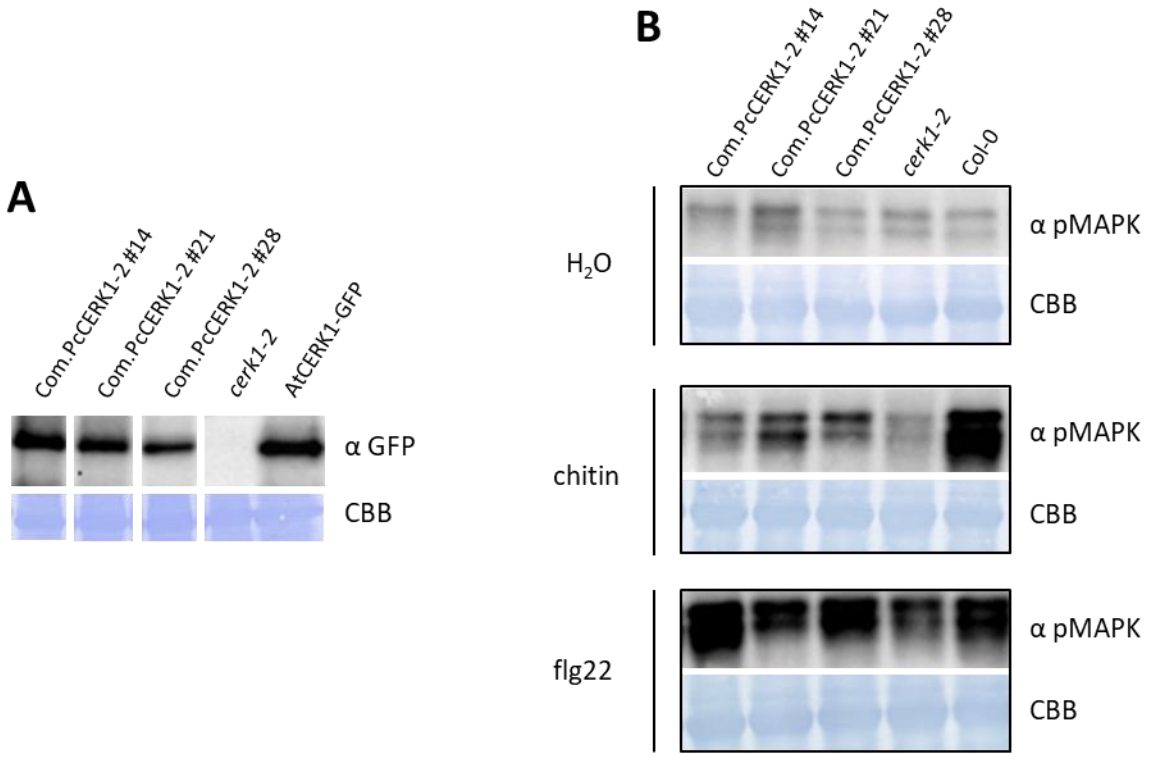

Figure 28: PcCERK1-2 partially restores the MAPK activation of Arabidopsis *cerk1-2*. A: Protein levels of the *pAtCERK1:PcCERK1-2_mCitrine* construct in transgenic Arabidopsis lines were detected with a GFP specific antibody. **B:** Leaf samples were infiltrated with either 10 µg/ml chitin solution, 10 nM flg22 solution or water as a control. After 10 min incubation time samples were harvested and phosphorylated MAPKs were detected in total protein extracts with a specific antibody. **Com.PcCERK1-2 #14, #21, #28**: individual lines of *pAtCERK1:PcCERK1-2_mCitrine* transformed into the Arabidopsis *cerk1-2* mutant; ***cerk1-2*:** Arabidopsis CERK1 knockout mutant that lacks chitin response; **AtCERK1-GFP:** *pAtCERK1:AtCERK1_GFP* transformed into *cerk1-2* mutant, used as a control for detection of PcCERK1-mCitrine fusions that are recognized by the GFP antibody; **Col-0:** Arabidopsis wildtype; **CBB:** Coomassie Brilliant Blue-stained membranes.

3.2.2.1 A protein model indicates amino acid positions that might interfere with complementation ability of the poplar *CERK1* genes in Arabidopsis

An open question is the reason for the lack of complementation ability of both poplar *PcCERK1* genes. An involvement of these genes in chitin-triggered ROS burst generation and MAPK activation was confirmed via analysis of the poplar *CERK1* single and double knockout lines (see chapter 3.3). Problems with the estradiol-inducible promoter system of *PcCERK1-1* might be one reason. However, heterologous expression of the *PcCERK1-2* gene with the natural *AtCERK1* promoter has been shown to restore the chitin-triggered MAPK activation of

Arabidopsis *cerk1-2*. It was hence expected that *PcCERK1-2* could restore the chitin-triggered ROS burst as well. Thus, the hypothesis put forward that downstream components of Arabidopsis that mediate ROS burst signal transduction do not interact with the poplar PcCERK1-2 receptor. A failure of downstream components to interact with PcCERK1-1 including those for MAPK seems to be possible as well. Therefore, the amino acid exchanges between the kinase domain of poplar CERK1 and Arabidopsis CERK1 were investigated to identify differences, which may be causal for altered binding of an interaction partner.

An alignment of both poplar CERK1 kinase domains with the Arabidopsis kinase domain of CERK1 was generated to analyse changes in the amino acid characteristics as well as changes in the presence of proline residues (Fig. 29). In particular a change in charge might affect the protein structure. Proline is known to introduce a kink in the secondary structure of proteins and is therefore directly influencing the folding of the protein (Barlow and Thornton, 1988). Complementation ability of the *PcCERK1* genes might be achieved by mutagenesis of these amino acids back to those present in Arabidopsis. Best candidates for testing the hypothesis are amino acid changes in important tertiary loop structures involved in substrate binding or amino acid changes in conserved kinase sub-domains.

It is expected that only residues on the surface of the protein interact with other cell components. To find out which amino acids in the alignment are surface exposed, the predicted 3D structure of the protein was analysed. Since neither the kinase domain structure of poplar CERK1 nor the kinase domain of Arabidopsis CERK1 has been resolved so far, a protein model was built by homology modelling. BRASSINOSTEROID INSENSITIVE 1-ASSOCIATED RECEPTOR KINASE 1 (BAK1) shares between 38,2 % and 39,4 % of amino acid sequence identity with PcCERK1-1, PcCERK1-2 and AtCERK1. BAK1 was chosen due to the highest ranking on the SWISS-MODEL server (https://swissmodel.expasy.org), a web-based protein homology modelling tool (Waterhouse et al., 2018). The modeling of PcCERK1-2 on BAK1 (PDB: 3ULZ; Yan et al., 2012) is displayed in Figure 30.

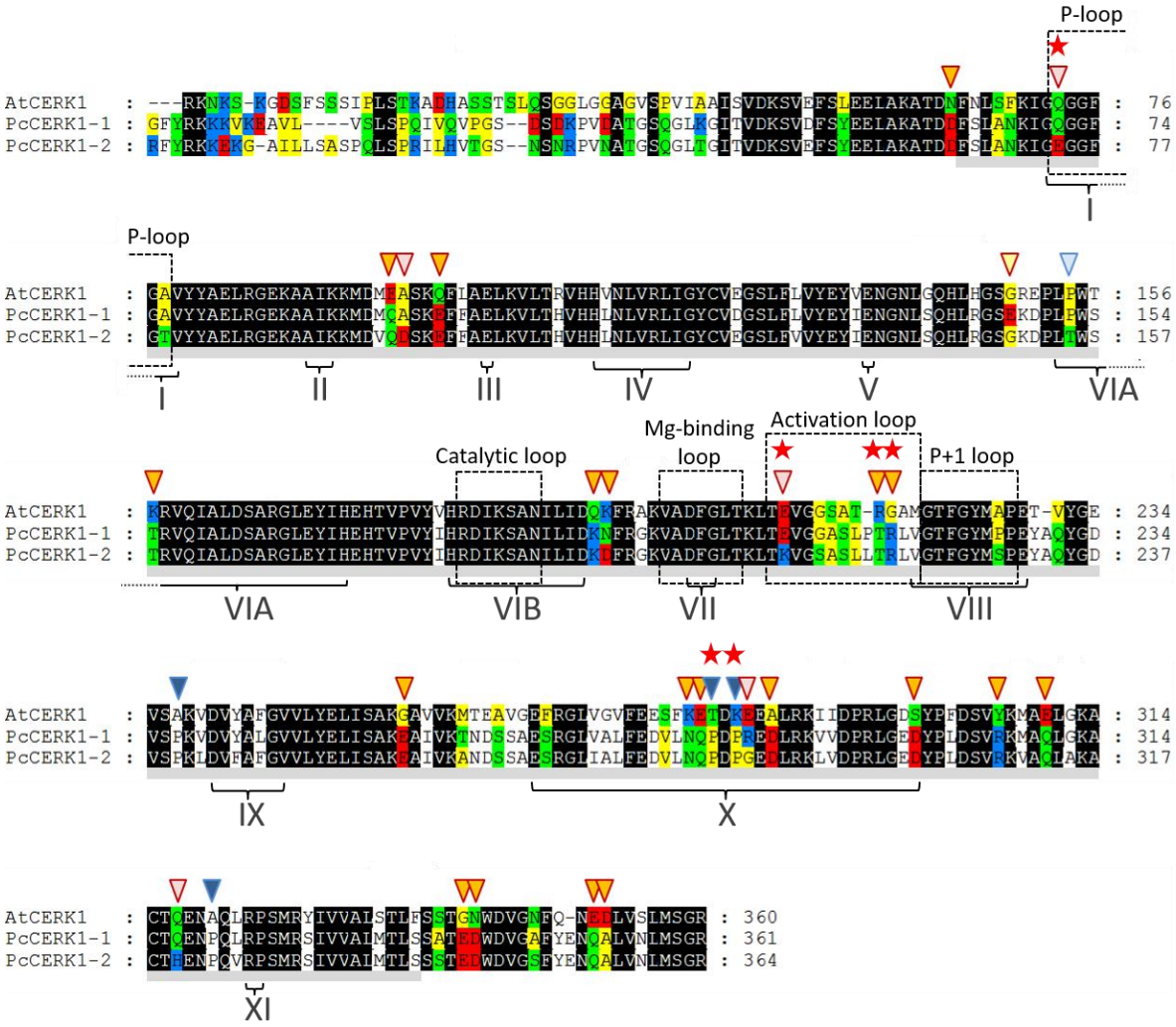

Figure 29: Analysis of differences between Arabidopsis and poplar CERK1 that might influence complementation ability. Alignment of the juxtamembrane and kinase domain of Arabidopsis CERK1 and *Populus x canescens* PcCERK1-1 and PcCERK1-2 to investigate changes in amino acid residues that might prevent binding of Arabidopsis interaction partners to the poplar protein. Differences in the amino acid characteristics between AtCERK1 and PcCERK1-1/PcCERK1-2 are colored as follows: red: acidic, green: polar, yellow: nonpolar, blue: basic. Black color indicates identity of amino acid residues between all three proteins. Colorless amino acids are either not different in characteristics or are excluded as possible mutation sites because they are not surface exposed. Triangles indicate a change in charge or change in proline which might influence the structure of the protein. The gray bar underneath the alignment designates the kinase domain. Roman numerals I-XI designate the kinase subdomains according to Hanks and Hunter (1995). Amino acids that are promising candidates for mutagenesis in order to gain complementation ability of PcCERK1 in Arabidopsis are marked with a red star.

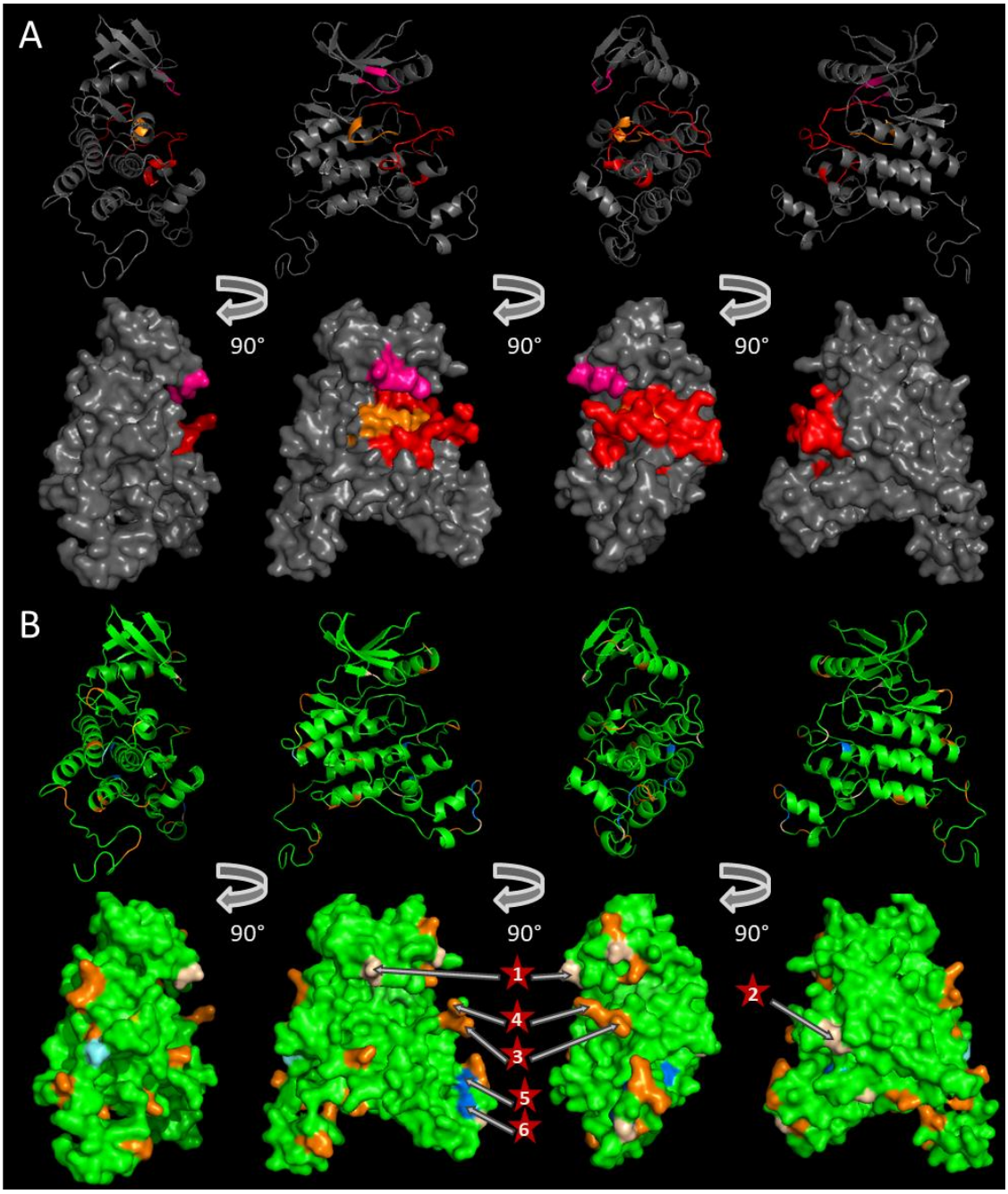

Figure 30: Modelling of PcCERK1-2 identified surface exposed amino acid positions that might be relevant for interaction with downstream components. The modelling was performed with the SWISS-MODEL server (https://swissmodel.expasy.org; Waterhouse et al., 2018) and then visualized in the PyMOL Molecular Graphics System, Version 2.3.4 (Schrödinger LLC, unpublished). The modeling intends to find surface exposed amino acids that could be mutagenized in order to gain complementation ability of PcCERK1-2 in Arabidopsis. **A:** The catalytic center for substrate binding is indicated in color: P-loop in magenta, catalytic loop in orange and activation segment (consisting of the Mg-binding-, activation- and P+1-loop) in red. **B:** Amino acids are colored according to the alignment scheme in Fig. 29 and represent a change in charge or change in proline when compared to Arabidopsis CERK1. The six best candidates for a mutagenesis are assigned with a red star. Numbers are given according to their appearance in the alignment of Fig. 29.

3.3 Analyses of poplar *PcCERK1-1* and *PcCERK1-2* knockout lines

PcCERK1 was identified in chapter 3.1 as the main candidate gene for a major component of the chitin receptor. To analyse the individual role of each of the *PcCERK1* genes in *Populus* x *canescens* (*PcCERK1-1* and *PcCERK1-2*) an overexpression approach of a kinase dead version of *PcCERK1-1* (chapter 3.3.1) and characterization of CRISPR/Cas9 knockouts of the individual genes (chapter 3.3.2 and 3.3.3) as well as the generation of a double knockout (chapter 3.3.4) were employed.

3.3.1 Analysis of the overexpression of a loss of function protein as an alternative strategy to the generation of CRISPR/Cas9 knockouts

In this thesis CRISPR/Cas9 knockout lines serve to analyse the gene function of the two *PcCERK1* genes in *Populus x canescens*. Since the generation of the CRISPR/Cas9 knockout lines is time consuming and it was not predictable that a double knockout will be successful as well another experiment has been carried out in parallel. As an alternative strategy the overexpression of a kinase dead version of PcCERK1-1 was tested. The kinase dead Pccerk1-1 protein should compete with the functional PcCERK1-1 protein and have a dominant negative effect on chitin signaling (Fig. 31). It might therefore interfere with signal transduction capacity of both poplar CERK1 proteins. Activation of CERK1 happens through autophosphorylation after dimerization of two CERK1 molecules (Liu et al., 2012a). Also in a heterodimer which is built up by a wildtype CERK1 and a kinase dead cerk1 the signal transduction capacity is supposed to be affected.

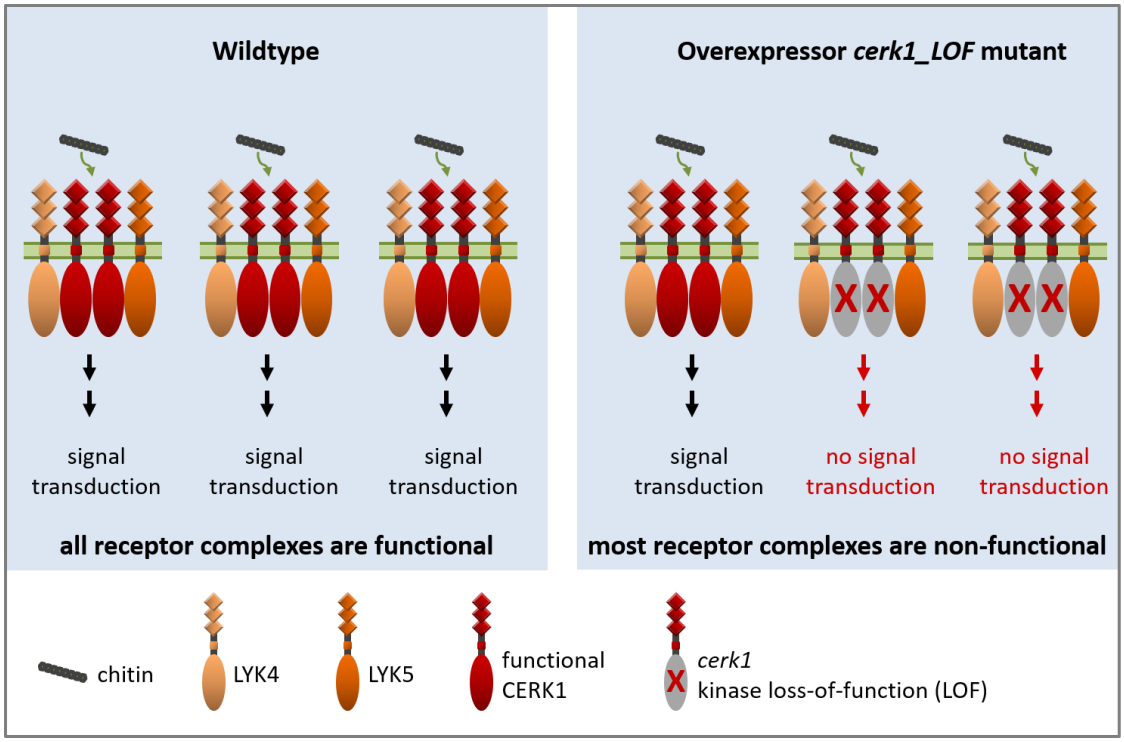

Figure 31: The overexpression of a cerk1 kinase loss-of-function protein should have a dominant negative effect on chitin signaling. The scheme displays the situation in Arabidopsis: a functional chitin receptor complex consists of two CERK1 proteins with LYK4 and LYK5 as co-receptors (Wan et al., 2012; Cao et al., 2014; Erwig et al., 2017). The overexpression of a cerk1_LOF protein should outcompete the functional CERK1. Incorporation of the cerk1_LOF variant should interfere with signal transduction capacity of the receptor complex and, as a consequence, most receptor complexes in the mutant are non-functional.

3.3.1.1 The overexpression of an Atcerk1 loss of function protein in Arabidopsis leads to an abolished chitin response

As a proof of principle, the overexpression of a kinase dead version of Arabidopsis CERK1 was first tested in Arabidopsis wildtype before the same mutation was introduced into the poplar protein (see chapter 3.3.1.2). A point mutation (K350N) in the kinase ATP binding site was introduced to obtain loss of CERK1 kinase activity as described in Petutschnig et al. (2010).

For AtCERK1 it is known that the protein is phosphorylated after chitin treatment and this phosphorylation is detectable in western blots as a band shift (Petutschnig et al., 2010). The chitin-triggered phosphorylation of AtCERK1 in the *p35S:Atcerk1_LOF* lines was abolished, but detectable in wildtype plants (Fig. 32).

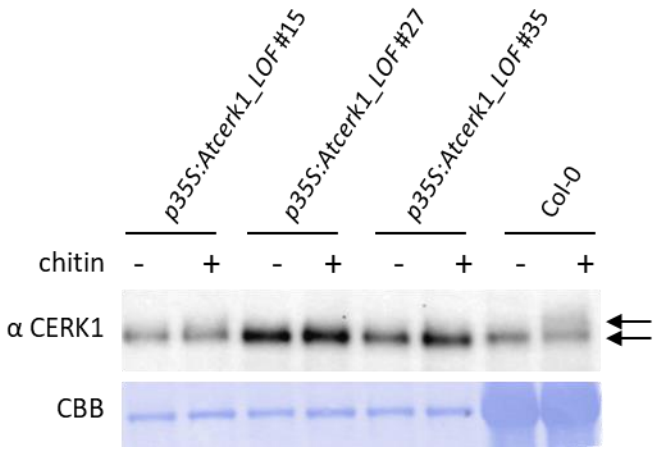

Figure 32: The Atcerk1 loss of function protein does not show chitin-triggered phosphorylation. Leaf samples were infiltrated with either 10 µg/ml chitin solution (+) or water (-). Expression of CERK1/cerk1_LOF was analysed in total protein extracts with a CERK1 specific antibody. Chitin-triggered CERK1 phosphorylation results in a band shift (Petutschnig et al., 2010). The band shift of the wildtype is indicated with arrows and is missing in the *p35S:Atcerk1_LOF* lines. To adjust the intensity of the CERK1 signal to the same level, wildtype protein was used in higher concentration. ***p35S:Atcerk1_LOF* #15, #27, #35**: individual lines overexpressing a kinase dead version of Arabidopsis CERK1; **Col-0**: Arabidopsis wildtype.

In addition, the chitin-induced ROS burst and MAPK responses of the *p35S:Atcerk1_LOF* lines were suppressed (Fig. 33 and Fig. 34) whereas the ROS burst triggered by flagellin was normal (supplemental Fig. 14).

These results show that the approach is suitable to be tested in poplar.

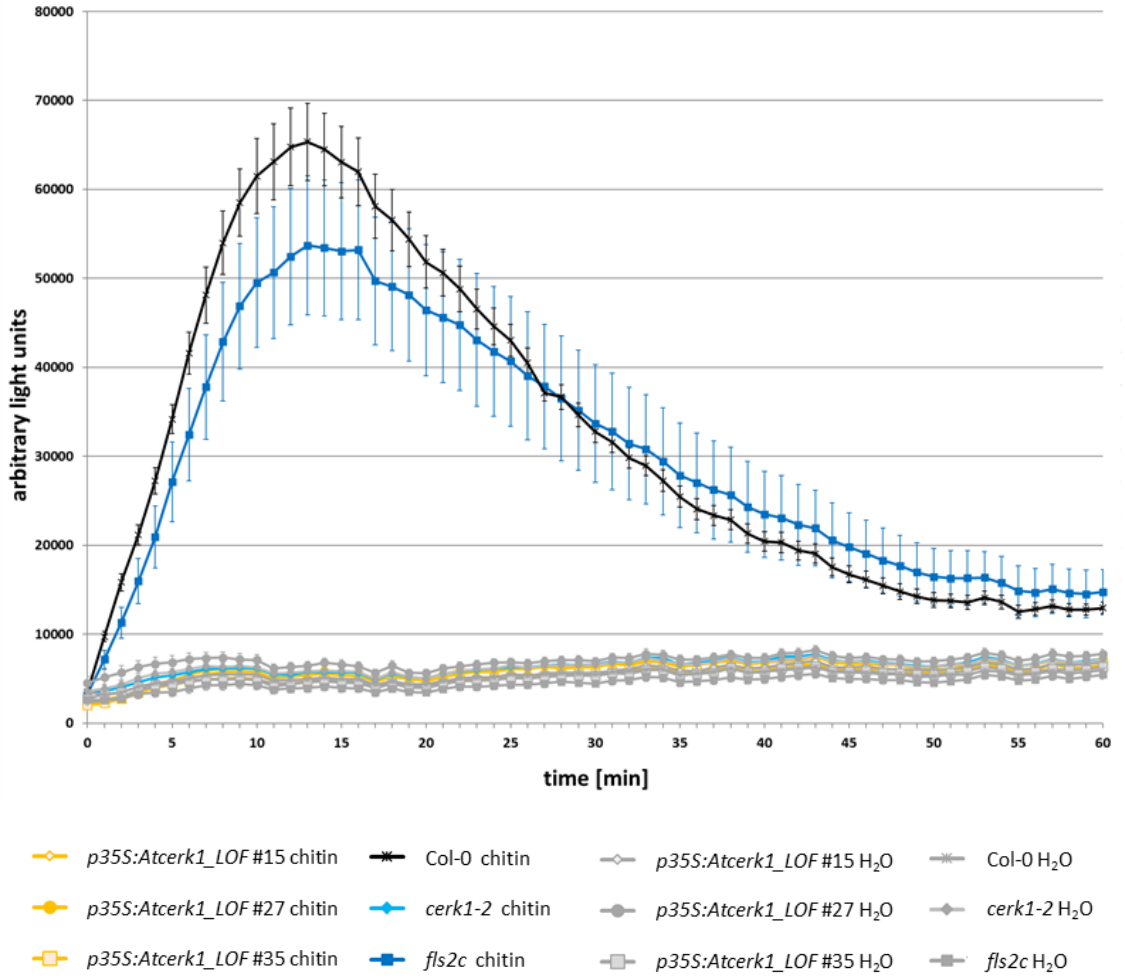

Figure 33: The overexpression of a cerk1 loss of function protein in Arabidopsis leads to abolishment of the chitin-induced ROS burst response. Leaf discs were treated with either 100 µg/ml chitin or water as a control. To visualize ROS generation a luminol based assay was used. Data represent the mean of 8 leaf discs ± SEM. ***p35S:Atcerk1_LOF* #15, #27, #35**: individual lines overexpressing a kinase dead version of Arabidopsis CERK1; **Col-0**: Arabidopsis wildtype; ***cerk1-2***: Arabidopsis CERK1 knockout mutant that lacks chitin response; ***fls2c***: Arabidopsis FLS2C knockout mutant that lacks flagellin response.

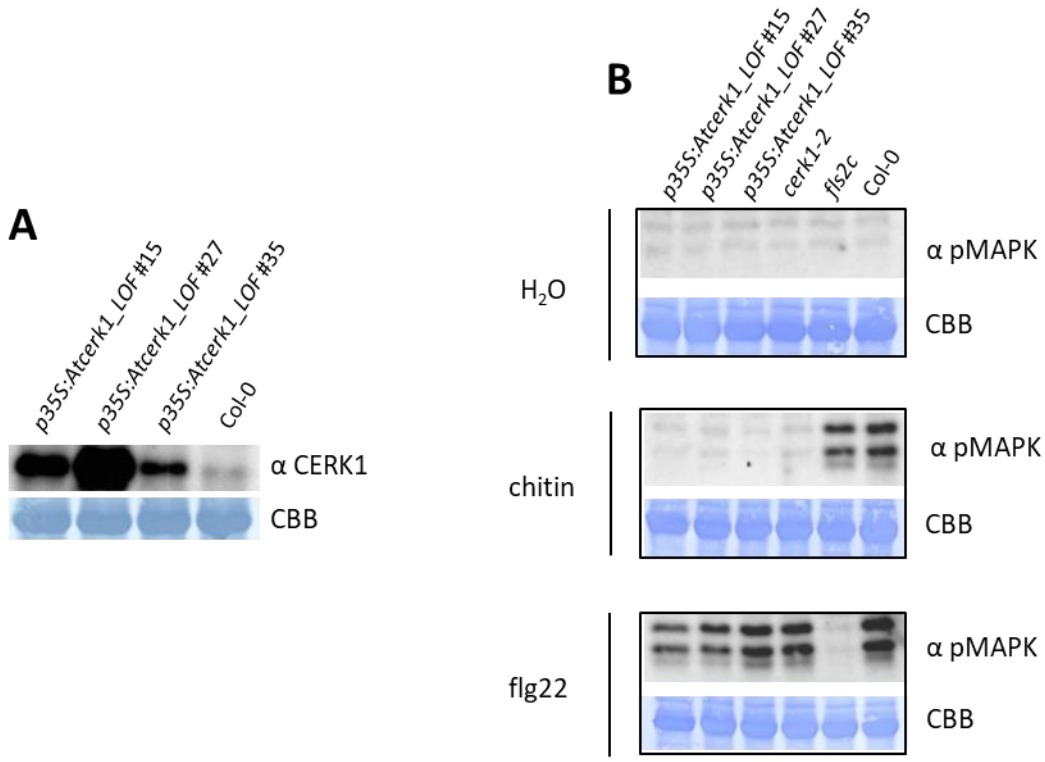

Figure 34: The overexpression of a cerk1 loss of function mutation in Arabidopsis leads to abolishment of the chitin-induced MAPK response. A: Expression levels of the cerk1_LOF in the *p35S:Atcerk1_LOF* lines compared to wildtype CERK1 in Col-0 were detected with a CERK1 specific antibody. **B:** Leaf samples were infiltrated with either 10 µg/ml chitin solution, 10 nM flg22 solution or water as a control. After 10 min incubation time samples were harvested and phosphorylated MAPKs were detected in total protein extracts with a specific antibody. ***p35S:Atcerk1_LOF* #15, #27, #35**: individual lines overexpressing a kinase dead version of Arabidopsis CERK1; **Col-0**: Arabidopsis wildtype; ***cerk1-2***: Arabidopsis CERK1 knockout mutant that lacks chitin response; ***fls2c***: Arabidopsis FLS2C knockout mutant that lacks flagellin response.

3.3.1.2 The overexpression of a Pccerk1-1 loss of function gene in poplar leads to a reduced chitin response

The proof of principle test in Arabidopsis showed that the overexpression of a kinase dead cerk1 protein is suitable to interfere with chitin-triggered signal transduction (see chapter 3.3.1.1). A poplar *p35S:Pccerk1-1_LOF* construct was cloned which introduces the same point mutation (K339N) into the kinase subdomain II of the encoded protein. Wildtype *Populus x canescens* was then transformed with this construct. The divergent numbering of the mutation results from the shorter poplar CERK1 protein length as compared to Arabidopsis.

In contrast to Arabidopsis *p35S:Atcerk1_LOF* lines, where the chitin-triggered ROS burst and MAPK response was completely abolished, the overexpression of a kinase dead version of

PcCERK1-1 in poplar only leads to a reduced response for ROS burst (Fig. 35) and MAPK (Fig. 36). The signal of the chitin-triggered response was weaker than in wildtype plants, but still visible in both assays. The flagellin response, used as a control, was not affected in *p35S:Pccerk1-1_*LOF lines (supplemental Fig. 15).

Due to a lack of a poplar CERK1 specific antibody, the expression level of the construct was not checked. Furthermore, it is not known whether the PcCERK1-2 protein exclusively forms homodimers and, therefore, does not interact with the mutant Pccerk1-1_LOF protein. Homodimers of intact PcCERK1-2 may reduce the impact of the overexpressed Pccerk1-1_LOF on chitin signaling.

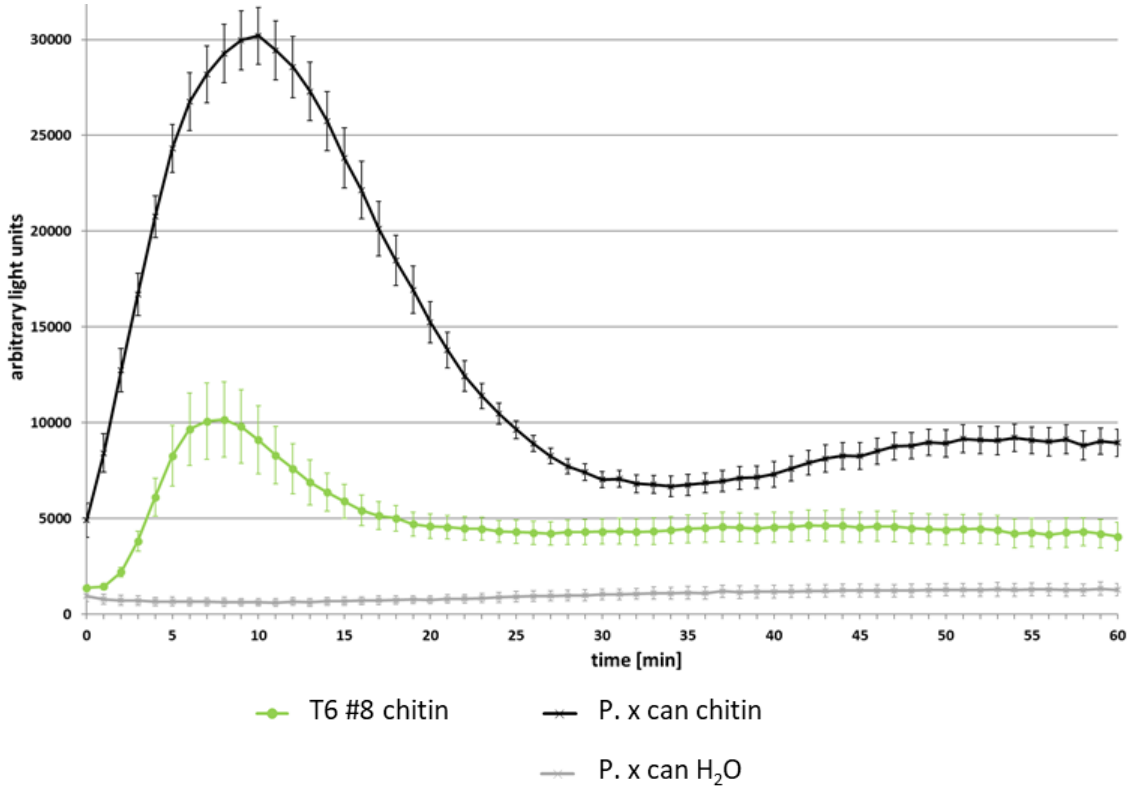

Figure 35: The overexpression of a Pccerk1-1 loss of function protein in wildtype leads to a reduced chitin-induced ROS burst response. Leaf discs were treated with either 100 µg/ml chitin solution or water as a control. To visualize ROS generation a luminol based assay was used. Data represent the mean of 8 leaf discs ± SEM. **T6 #8**: *p35S:Pccerk1-1_LOF* line overexpressing a kinase dead version of CERK1 in *Populus x canescens*; **P. x can**: wildtype *Populus x canescens*.

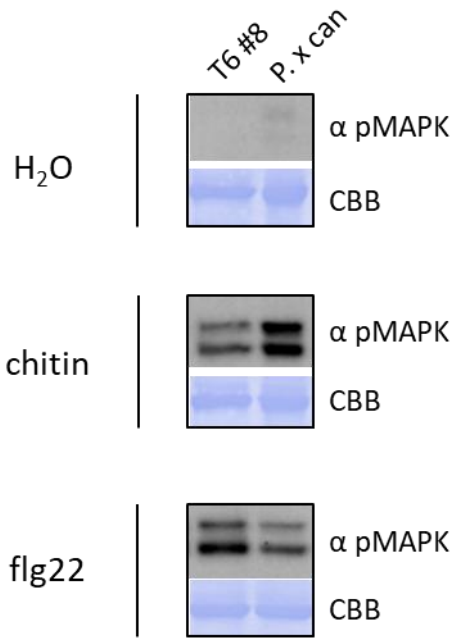

Figure 36: The overexpression of a Pccerk1-1 loss of function protein in wildtype leads to a slightly reduced chitin-induced MAPK response. Leaf samples were infiltrated with either 10 µg/ml chitin solution, 10 nM flg22 solution or water as a control. After 10 min incubation time samples were harvested and phosphorylated MAPKs were detected in total protein extracts with a specific antibody. **T6 #8**: *p35S:Pccerk1-1_LOF* line overexpressing a kinase dead version of CERK1 in *Populus x canescens*; **P. x can**: wildtype *Populus x canescens*; **CBB**: Coomassie Brilliant Blue-stained membranes.

3.3.2 *Pccerk1-1* CRISPR/Cas9 single knockout lines respond to chitin with ROS burst but have an impaired MAPK activation

To investigate the function of the *PcCERK1-1* gene in chitin signaling, CRISPR/Cas9 mediated knockouts were generated. The guide RNAs were designed to hit both alleles of the gene and target the first LysM domain of PcCERK1-1. Transgenic lines were analysed for their editing (Tab. 36 and supplemental Fig. 19) and the resulting editing effect (Tab. 37).

In line T5 #1b and T5 #5 the editing lead to a premature stop codon on both alleles which causes a loss of PcCERK1-1 functionality. Line T5 #17 had a premature stop codon on one allele while the other allele had a 19 amino acid long deletion in the LysM1 domain. Since in Arabidopsis all three CERK1 LysM domains are necessary to achieve chitin binding (Petutschnig et al., 2010) it is expected that a large deletion in one of the LysM domains also interferes with the functionality of the mutant PcCERK1-1 protein.

Table 36: Overview of CRISPR/Cas9 induced gene mutations in the *Pccerk1-1* single knockout lines. Lines were analysed with allele specific PCR and sequencing of the target sites. Corresponding chromatograms are shown in the appendix (supplemental Fig. 19).

	PcCERK1-1			
	***P. alba* allele**		***P. tremula* allele**	
Line	Editing		Editing	
	Target T1	Target T2	Target T1	Target T2
T5 #1b	- 1 bp	+ 1 bp	+ 1 bp	+ 1 bp
T5 #5	- 1 bp	- 42 bp (+2 bp subst.)	- 1 bp	+ 1 bp
T5 #17	- 1 bp	+ 1 bp (+2 bp subst.)	- 57 bp (T1-->T2)	

Table 37: Overview of CRISPR/Cas9 induced protein mutations in the *Pccerk1-1* single knockout lines. Lines were analysed with allele specific PCR and sequencing of the target site.

	PcCERK1-1	
	***P. alba* allele**	***P. tremula* allele**
Line	Editing effect	Editing effect
T5 #1b	premature stop codon	premature stop codon
T5 #5	premature stop codon	premature stop codon
T5 #17	premature stop codon	deletion of 19 aa in LysM1 domain

An involvement in chitin signaling was tested with ROS burst and MAPK assays. The chitin-triggered ROS burst was not impaired (Fig. 37) whereas the chitin-triggered MAPK response (Fig. 38) was strongly reduced. The ROS burst response to flagellin is normal (supplemental Fig. 16).

These results suggest that *PcCERK1-1* has its main function in mediating the chitin-induced MAPK response. The residual MAPK activation presumably results from the presence of the non-edited *PcCERK1-2* gene.

Thus, with respect to ROS burst either a redundant function of *PcCERK1-1* and *PcCERK1-2* is likely or the *PcCERK1-1* gene is not involved in ROS production.

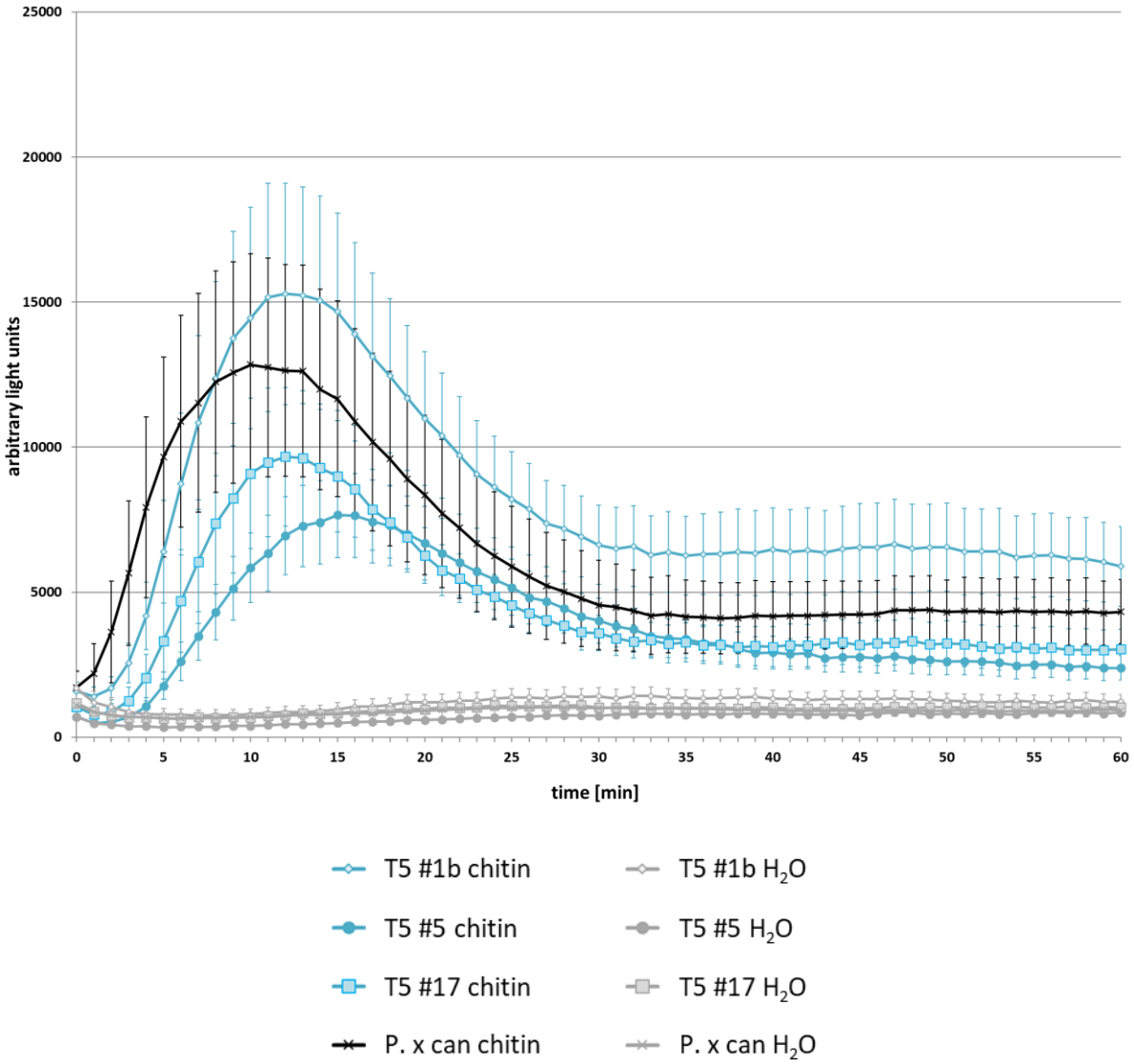

Figure 37: *Pccerk1-1* CRISPR/Cas9 knockout lines respond to chitin with a ROS burst. Leaf discs were treated with either 100 µg/ml chitin solution or water as a control. To visualize ROS generation a luminol based assay was used. Data represent the mean of 8 leaf discs ± SEM. **T5 #1b, T5 #5, T5 #17:** individual *Pccerk1-1* CRISPR/Cas9 knockout lines; **P. x can**: wildtype *Populus x canescens*.

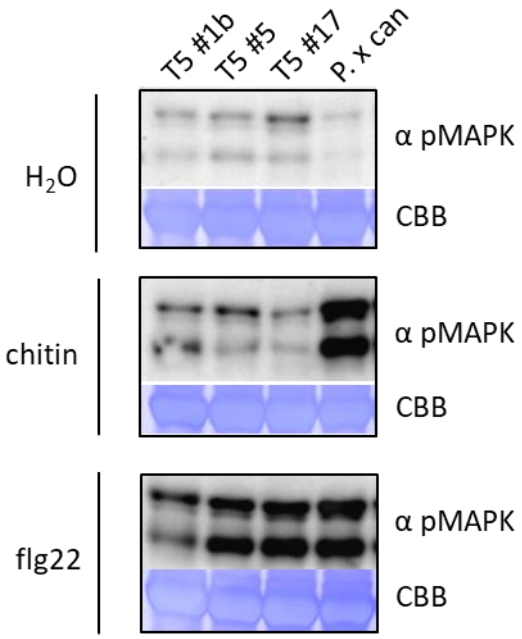

Figure 38: The chitin-induced MAPK response of *Pccerk1-1* CRISPR/Cas9 knockout lines is strongly impaired. Leaf samples were infiltrated with either 10 µg/ml chitin solution, 10 nM flg22 solution or water as a control. After 10 min incubation time, samples were harvested and phosphorylated MAPKs were detected in total protein extracts with a specific antibody. **T5 #1b, T5 #5, T5 #17**: individual *Pccerk1-1* CRISPR/Cas9 knockout lines; **P. x can**: wildtype *Populus x canescens;* **CBB**: Coomassie Brilliant Blue-stained membranes.

3.3.3 *Pccerk1-2* CRISPR/Cas9 single knockout lines still respond to chitin with normal ROS burst and normal MAPK activation

A CRISPR/Cas9 mediated knockout was also used to test the role of the *PcCERK1-2* gene in chitin signaling. Similar to the knockout of *PcCERK1-1* the guide RNAs were designed to hit both alleles of the gene and target the first LysM domain of *PcCERK1-2.* Only one line could be obtained with editing of both alleles (Tab. 38 and supplemental Fig. 20). On one allele the editing results in a premature stop codon while on the other allele a deletion of 19 amino acids in the LysM1 domain is observed (Tab. 39). Similar to line T5 #17, the deletion is most likely sufficient to interfere with functionality of the gene (see chapter 3.3.2).

Table 38: Overview of CRISPR/Cas9 induced gene mutations in the *Pccerk1-2* single knockout line. Lines were analysed with allele specific PCR and sequencing of the target site. The corresponding chromatogram is shown in the appendix (supplemental Fig. 20).

	PcCERK1-2			
	***P. alba* allele**		***P. tremula* allele**	
Line	Editing		Editing	
	Target T1	Target T2	Target T1	Target T2
T10 #3	- 1 bp	+ 1 bp	- 57 bp (T1-->T2)	

Table 39: Overview of CRISPR/Cas9 induced protein mutations in the *Pccerk1-2* single knockout line. Lines were analysed with allele specific PCR and sequencing of the target site.

	PcCERK1-2	
	***P. alba* allele**	***P. tremula* allele**
Line	Editing effect	Editing effect
T10 #3	premature stop codon	deletion of 19 aa in LysM1 domain

An involvement of *PcCERK1-2* in chitin signaling was tested with ROS burst and MAPK assays of the Pccerk1-2 knockout line. The ROS burst response after chitin (Fig. 39) and flagellin treatment was normal (supplemental Fig. 17). These findings are similar to the results of the *Pccerk1-1* single knockout and hint as well either towards a redundant function for both genes in ROS burst or indicate that *PcCERK1-2* is not involved in ROS production.

The chitin-triggered activation of the MAPK signaling cascade was not impaired as well (Fig. 40). This gives also further evidence to the hypothesis that *PcCERK1-1* is mainly responsible for MAPK signaling.

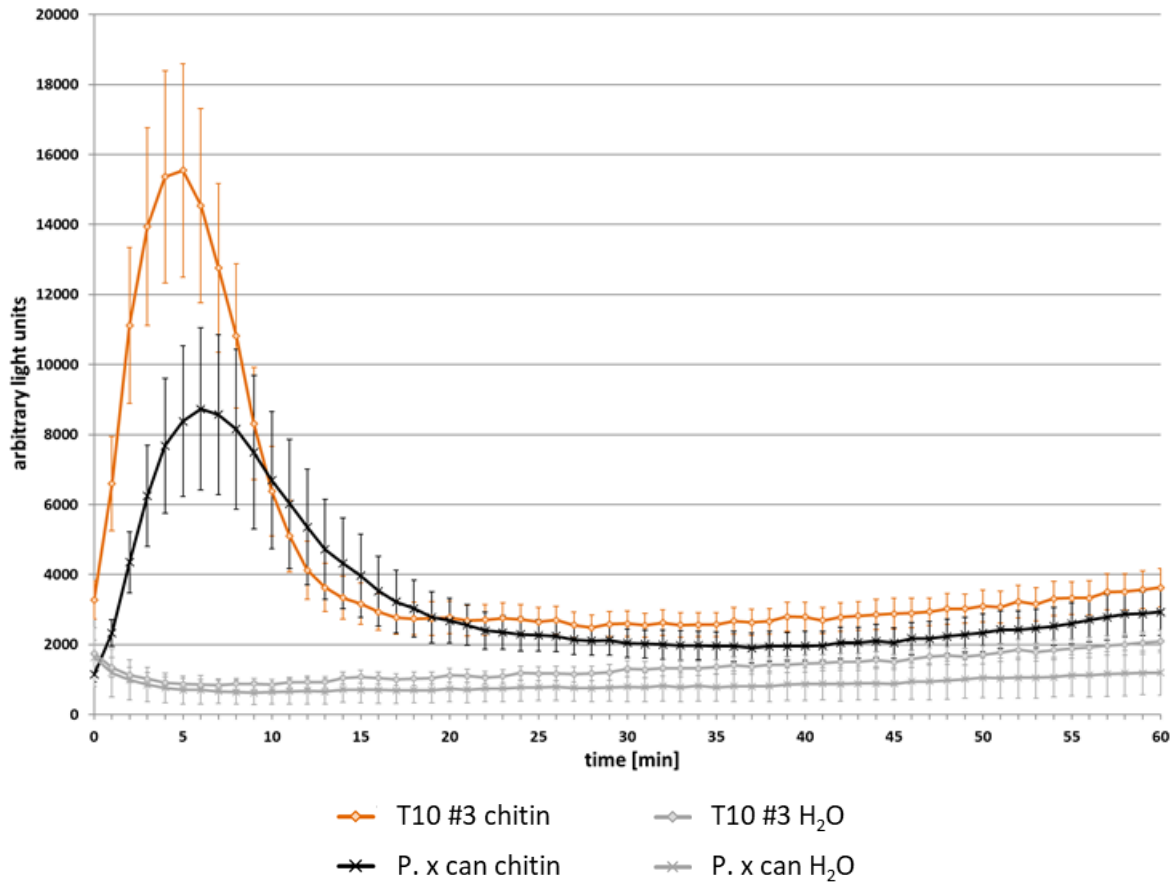

Figure 39: The *Pccerk1-2* CRISPR/Cas9 knockout line responds to chitin with ROS burst. Leaf discs were treated with either 100 µg/ml chitin or water as a control. To visualize ROS generation a luminol based assay was used. Data represent the mean of 8 leaf discs ± SEM. **T10 #3**: *Pccerk1-2* CRISPR/Cas9 knockout line; **P. x can**: wildtype *Populus x canescens*.

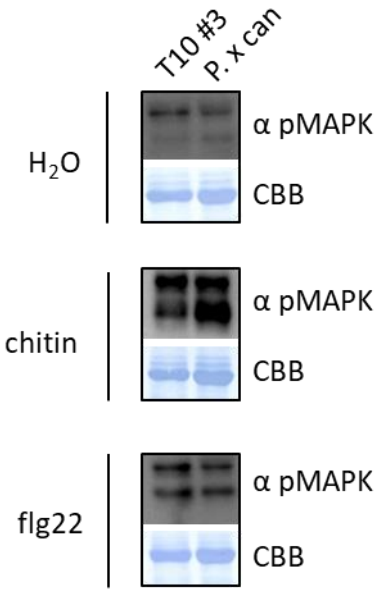

Figure 40: The chitin-induced MAPK response of a Pccerk1-2 CRISPR/Cas9 knockout line is not impaired. Leaf samples were infiltrated with either 10 µg/ml chitin solution, 10 nM flg22 solution or water as a control. After 10 min incubation time, samples were harvested and phosphorylated MAPKs were detected in total protein extracts with a specific antibody. **T10 #3**: *Pccerk1-2* CRISPR/Cas9 knockout line; **P. x can**: wildtype *Populus x canescens*; **CBB**: Coomassie Brilliant Blue-stained membranes.

3.3.4 The chitin response of *Pccerk1-1 Pccerk1-2* CRISPR/Cas9 double knockout lines is abolished

To investigate if both CERK1 orthologues have a redundant function in chitin signaling CRISPR/Cas9 mediated double knockouts of *PcCERK1-1* and *PcCERK1-2* were generated to compare the results with the single knockouts. The guide RNAs target the first LysM domain and were designed to hit both alleles of each gene. Transgenic lines were tested for their editing (Tab. 40 and supplemental Fig. 21). Highly chimeric tissue was observed for these lines leading to up to six different editing events on one allele. All editing causes a deletion of amino acids in the LysM1 domain or shifts the reading frame and introduces premature stop codons (Tab. 41).

Table 40: Overview of CRISPR/Cas9 induced gene mutations in the *Pccerk1-1 Pccerk1-2* double knockout lines. Lines were analysed with allele specific PCR. Subsequently a TA cloning of the amplified PCR fragment was performed and plasmids of individual clones were used to sequence the target site. Chimeric tissue leads to detection of different editing events in one and the same line. Corresponding chromatograms are shown in the appendix (supplemental Fig. 21).

	PcCERK1-1	
	***P. alba* allele**	***P. tremula* allele**
Line	Editing Target T1 / Target T2	Editing Target T1 / Target T2
T8 #19	- 1 bp / + 1bp - 6 bp / --	- 1 bp / -- - 2 bp / + 2bp - 51 bp / -- - 112 bp (T1-->T2) - 113 bp (T1-->T2) - 117 bp (T1-->T2)
T8 #20	- 15 bp / - 3 bp + 277 bp (+ 2 bp subst. and -2 bp) / --	- 1 bp / -- - 1 bp / - 1 bp - 20 bp / --
	PcCERK1-2	
	***P. alba* allele**	***P. tremula* allele**
Line	Editing Target T1 / Target T2	Editing Target T1 / Target T2
T8 #19	- 2 bp / -- - 5 bp / -- - 8 bp / -- - 114 bp (T1-->T2)	112 bp inverted (T1-->T2) - 2 bp / -- - 3 bp / - 4 bp - 4 bp / -- - 5 bp / -- - 112 bp (T1-->T2)
T8 #20	- 1 bp / - 6 bp	+ 1 bp / -- + 1 bp / - 3 bp + 1 bp / - 39 bp

Table 41: Overview of CRISPR/Cas9 induced protein mutations in the *Pccerk1-1 Pccerk1-2* double knockout lines. Lines were analysed with allele specific PCR. Subsequently a TA cloning was performed and plasmids of individual clones were used to sequence the target site. Chimeric tissue leads to detection of different editing events in one and the same line.

	PcCERK1-1	
	***P. alba* allele**	***P. tremula* allele**
Line	Editing effect	Editing effect
T8 #19	premature stop codon deletion of 2 aa in LysM1 domain	premature stop codon 39 aa different due to frame shift deletion of 17 aa in LysM1 domain premature stop codon premature stop codon deletion of 39 aa in LysM1 domain
T8 #20	deletion of 5 and 1 aa in LysM1 domain premature stop codon	premature stop codon premature stop codon premature stop codon
	PcCERK1-2	
	***P. alba* allele**	***P. tremula* allele**
Line	Editing	Editing
T8 #19	premature stop codon premature stop codon premature stop codon deletion of 38 aa in LysM1 domain	premature stop codon premature stop codon premature stop codon premature stop codon premature stop codon premature stop codon
T8 #20	premature stop codon	premature stop codon premature stop codon premature stop codon

Effects on chitin signaling were tested with ROS burst and MAPK assays. For both assays, the response to chitin was abolished (Fig. 41 and Fig. 42). The flagellin-triggered ROS burst was normal (supplemental Fig. 18).

The hypothesis that *PcCERK1-1* and *PcCERK1-2* have a redundant function in mediating chitin-triggered ROS burst could be verified with this result. It also approves the assumption that the residual signal intensity for the MAPK response in the *Pccerk1-1* single knockout lines results from the presence of the *PcCERK1-2* gene. Thus, an involvement in chitin signaling is confirmed for both genes.

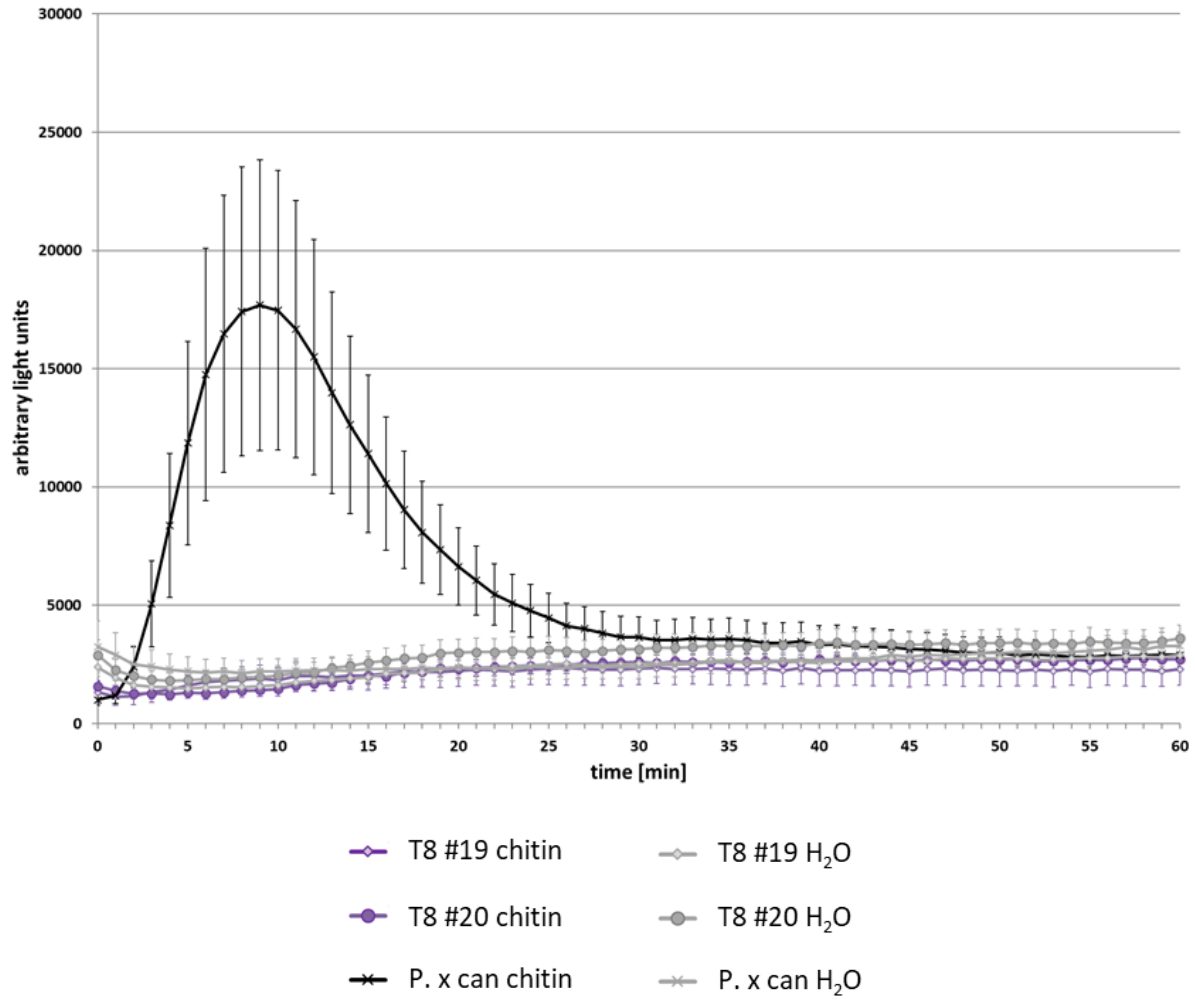

Figure 41*:* The chitin-triggered ROS burst response of *Pccerk1-1 Pccerk1-2* CRISPR/Cas9 double knockout lines is abolished. Leaf discs were treated with either 100 µg/ml chitin or water as a control. To visualize ROS generation a luminol based assay was used. Data represent the mean of 8 leaf discs ± SEM. **T8 #19, T8 #20**: individual *Pccerk1-1 Pccerk1-2* CRISPR/Cas9 double knockout lines; **P. x can**: wildtype *Populus x canescens*.

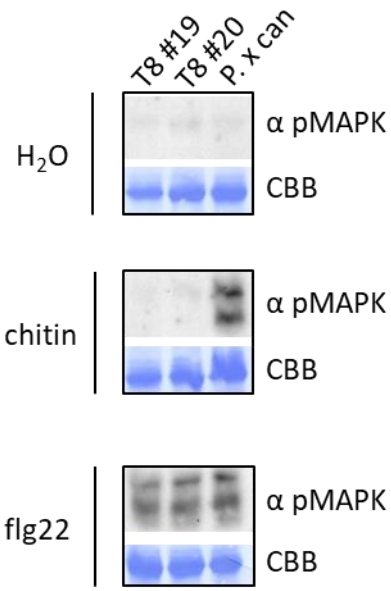

Figure 42: The chitin-induced MAPK response of *Pccerk1-1 Pccerk1-2* CRISPR/Cas9 double knockout lines is abolished. Leaf samples were infiltrated with either 10 µg/ml chitin solution, 10 nM flg22 solution or water as a control. After 10 min incubation time, samples were harvested and phosphorylated MAPKs were detected in total protein extracts with a specific antibody. **T8 #19, T8 #20**: individual *Pccerk1-1 Pccerk1-2* CRISPR/Cas9 double knockout lines; **P. x can**: wildtype *Populus x canescens*; **CBB**: Coomassie Brilliant Blue-stained membranes.

4. Discussion

4.1 Poplar is chitin responsive

Plants defend themselves against pathogens with diverse immune responses, including the production of reactive oxygen species (ROS) and the activation of mitogen-activated protein kinase (MAPK) signaling cascades to activate defense genes (Boller and Felix, 2009). They are able to recognize pathogens with the help of pathogen-associated molecular patterns (PAMPs) that are common for a whole pathogen class. These are for example chitin as a cell wall component of fungi or flagellin which is a protein of the bacterial flagellum that enables bacterial mobility (Chinchilla et al., 2007; Eckardt, 2008). For poplar, one of the major pathogens is *Melampsora* which is a fungus causing leaf rust (Hacquard et al., 2011).

This study aims towards identification of poplar genes and proteins involved in the perception of fungal chitin. Since infection by *Melampsora* urediniospores takes place at the abaxial side of the leaves (Rinaldi et al., 2007), leaf material was of particular interest for all experiments. At first, it was tested if poplar leaves are chitin responsive. The assays revealed that poplar is able to exhibit the typical chitin-triggered defense responses like ROS burst (Fig. 13) and MAPK activation (Fig. 14). The MAPK response was similar to Arabidopsis which was chosen as a control. For the ROS burst response, slightly different kinetics between these two species were observed. The ROS burst of poplar reaches its maximum peak significantly faster than Arabidopsis. This might be due to a general higher abundance of chitin receptor complexes in poplar. However, in this case not only the ROS burst but also MAPK activation should be triggered faster. Studies have shown that ROS production and MAPK activation are separate signaling pathways that are independent from each other (Segonzac et al., 2011; Xu et al., 2014). In addition, downstream pathways after chitin recognition at a receptor complex appear to be species specific. In Arabidopsis both pathways are mediated by different receptor-like cytoplasmic kinases (RLCKs). Chitin perception at a receptor complex is linked by the RLCK PBL27 with MAPK activation whereas RLCK BIK1 is responsible for the initiation of ROS burst (Zhang et al., 2010; Yamada et al., 2016). In contrast to that, in rice the RLCK OsRLCK185 is essential for both: MAPK and ROS burst signaling (Yamada et al. 2017; Kawasaki et al., 2017). In addition, the Rac/Rop GTPase OsRac1 is involved in an alternative pathway that mediates chitin-triggered ROS production and MAPK activation in rice (Akamatsu et al.,

2013; Kawasaki et al., 2017). Therefore, the faster ROS burst induction in poplar can be explained as the outcome of more efficient downstream signaling cascades, which are present in poplar but not in Arabidopsis. A higher abundance of RLCKs that mediate ROS burst responses or additional signaling components that lack in Arabidopsis could be possible reasons that positively influence signaling speed.

4.2 The paralog *CERK1-1* is the main candidate for a key component of the poplar chitin receptor

Lysin motif receptor-like kinases (LysM-RLKs) and lysin motif receptor-like proteins (LysM-RLPs) are known to be involved in the recognition of microbe-associated molecular patterns, like fungal chitin and bacterial peptidoglycan (Tanaka et al., 2013). In recent years the role that LysM-RLKs and LysM-RLPs play in pathogen immune responses or symbiosis were mainly studied in model organisms like Arabidopsis, *Oryza sativa*, *Lotus japonicus* and *Medicago truncatula* (Desaki et al., 2018a). Additional studies have been carried out in crops like tomato, wheat, cotton and pea (Liao et al., 2018; Lee at al., 2014; Wang et al., 2020b; Leppyanen et al., 2017). However, only little is known for woody perennials, for example apple, grape vine and mulberry (Zhou et al. 2018; Brulé et al. 2019; Lv et al. 2018) and in the woody perennial poplar the presence of LysM-RLKs and their function has not been investigated.

To check which LysM-RLKs or LysM-RLPs are encoded in the genome of poplar a phylogenetic analysis was performed with the database of the well annotated *Populus trichocarpa* genome. The phylogenetic tree of poplar proteins homologous to known LysM-RLKs and LysM-RLPs of Arabidopsis, Rice, Medicago and Lotus show that for each gene at least two or even up to four paralogs are existing in *Populus trichocarpa* (Fig. 15 and Fig. 16). This observation can be explained with a whole genome duplication event which has occurred in poplar around 8-13 million years ago (Tuskan et al., 2006).

In total there are 19 LysM-RLKs and four LysM-RLPs of which nine and two are clustered with proteins with a predicted chitin binding function, respectively. In particular, this includes paralogues of the LysM-RLKs CERK1, LYK4, LYK5 and the LysM-RLP AtLYM2/OsCEBiP.

In Arabidopsis AtCERK1 was identified as the major receptor for chitin-induced signaling (Miya et al., 2007; Petutschnig et al., 2010). Chitin signaling is dependent on receptor complex

formation by two AtCERK1 proteins which are associated with AtLYK4 and AtLYK5 (Cao et al., 2014; Xue et al., 2019). AtLYK4 and AtLYK5 show functional redundancy, though AtLYK5 plays the predominant role. This was concluded from experiments where *Atlyk5* knockout mutants are significantly more impaired in chitin-triggered immune responses than *Atlyk4* knockout mutants (Cao et al., 2014).

In rice the situation is slightly different. Here, OsCERK1 is not able to bind chitin and the AtLYM2 homolog OsCEBiP is the main receptor for chitin binding (Kaku et al., 2006; Shinya et al., 2012). However, also in rice OsCERK1 is part of the receptor complex and homodimerizes with OsCEBiP after chitin recognition to activate downstream signaling cascades (Shimizu et al., 2010). Remarkably, in Arabidopsis AtLYM2 contributes to chitin-triggered immunity by limiting the molecular flux of plasmodesmata rather than activating defense responses (Faulkner et al., 2013, Cheval et al., 2020).

To analyse if the potential poplar paralogs of LysM-RLKs and LysM-RLPs are expressed and translated into proteins, a mass spectrometry analysis was performed. The predicted chitin binding affinity was used for purification of candidate proteins. Mass spectrometry analyses was performed in *Populus trichocarpa* as well as in *Populus x canescens*.

Mainly peptides of the expected candidate proteins with a predicted function in chitin binding are found in mass spectrometry results (Fig. 18 and Fig. 19). Thus, a detection of CERK1, LYK4, LYK5 and LYM2 homologs in both poplar species was possible. Besides, one symbiosis related protein could be determined. Peptides were identified in the N-terminal as well as the C-terminal parts (supplemental Fig. 3-11) and therefore indicate that all of these genes are expressed into full length proteins.

Interestingly, the CERK1-1 proteins of *Populus trichocarpa* (PtCERK1-1) and *Populus x canescens* (PcCERK1-1) are the only proteins consistently found in all measurements with unique peptides. Additionally, peptide counts are higher compared with the other LysM-RLKs. Thus, it is one of the main candidate proteins that play a possible role in chitin perception. It needed to be elucidated whether it is also an important component of the chitin receptor complex similar to Arabidopsis and rice. The focus of this thesis is therefore the investigation of the involvement of the two *Populus x canescens* paralogs *PcCERK1-1* and *PcCERK1-2* in chitin signaling. Expression levels of LysM-RLK genes can be induced by chitin elicitor treatment. The Arabidopsis AtCERK1 and AtLYK5 genes, for example, exhibit a two-fold and nine-fold increase of gene expression in chitooctaose treated wild type plants, respectively

(Wan et al., 2008). Gene expression of *PcCERK1-1* and *PcCERK1-2* show a tendency to be up-regulated after chitin treatment as well (supplemental Fig. 2). Even though the difference is not statistically significant it gives another hint for a potential participation in chitin signalling. In contrast to the frequent detection of unique PcCERK1-1 peptides in the mass spectrometry results, there is no direct evidence for the presence of the PcCERK1-2 protein since only shared peptides were assigned. Compared with *PcCERK1-1* the *PcCERK1-2* gene is significantly lower expressed in leaves (supplemental Fig. 1). The detection of unique peptides was possibly prevented by the lower abundance because protein abundance and peptide identification by mass spectrometry was shown to be correlated (Washburn et al., 2001). Similar peptide abundances are visible for the two functional CERK1 paralogs of *Populus trichocarpa*. Unique peptides of the PtCERK1-3 protein (named PtCERK1-3 due to the presence of the pseudogene *PtCERK1-2*) are only detectable in the microsomal fraction. Thus, the overall detection level is considerable lower compared with PtCERK1-1 that is found with unique peptides in all measurements. This hints, analogous to the situation in *P. x canescens*, to different expression levels of *PtCERK1-1* and *PtCERK1-3* in the leaf samples which has not been experimentally tested so far.

A highly divergent expression pattern for two paralogous genes has also been described for the circadian clock genes *LATE ELONGATED HYPOCOTYL 1* and *2* (*LHY1 and LHY2*) in *Populus nigra*. *LHY2* was fivefold higher expressed in leaf and stem tissue than its paralog *LHY1*. The authors assumed that the higher transcript abundance of LHY2 indicate that *LHY2* has the major role in the *Populus* circadian clock system (Takata et al., 2009). Indeed, the single knockout of *LHY2* was sufficient to have an effect on photoperiodic growth regulation. *LHY2* has been shown to be involved in the downregulation of *FLOWERING LOCUS T2* (*FT2*) under short day conditions and in the *lhy2* knockout plants this repressive signaling on *FT2* was fully blocked (Ramos-Sánchez et al., 2019). Thus, the higher expression of *PcCERK1-1* suggests a higher impact of *PcCERK1-1* on the suspected chitin signaling function than *PcCERK1-2*. A deeper analysation of this issue is part of chapter 4.4. where functional analyses of the *PcCERK1* genes are described.

Regarding the other LysM-RLKs and LysM-RLPs found in mass spectrometry a function similar to Arabidopsis for the PcLYK4, PcLYK5 and PcLYM2 homologs was confirmed (Mo Awwannah, 2020).

LYK2 and LYK3 homologs as well as homologs of LYM1 or LYM3 proteins were not found in the mass spectrometry data. This is in line with the literature since these proteins seem not to be involved in chitin binding and detection. The biological function of LYK2 and LYK3 still remains unclear but there is no evidence for chitin binding capacity (Wan et al., 2012). LYM1 and LYM3 are specifically involved in peptidoglycan inducible defense responses and are not able to bind chitin (Willmann et al., 2011; Shinya et al., 2012). Out of four NFP paralogs that are putatively involved in symbiosis signaling one was found in *Populus trichocarpa*. However, the PtNFP-3 protein was detected only in three out of fourteen measurements and with only a low number of peptides compared to the other samples. NFP genes, like MtNFP from *Medicago truncatula* or LjNFR5 from *Lotus japonicus* are responsible for the recognition of Nod factors secreted from the symbiont (Mulder et al., 2006; Madsen et al., 2003). Thus, an identification of a symbiosis related gene in a chitin affinity purified sample was unexpected due to structurally differences between chitin and Nod factors. Even though both are composed of N-acetyl-D-glucosamine (GlcNAc), one difference between them is the length of the chitooligosaccharide chain. Nod factors are composed of three to five GlcNAc residues whereas chitin signaling is induced by longer oligomers (hexamer-octamer). In addition, Nod factors have in contrast to chitin a fatty acyl chain at the non-reducing terminal end and diverse other modifications like methylation, acetylation, fucosylation, carbamoyl groups or sulfations (D'Haeze and Holsters, 2002; Zipfel and Oldroyd, 2017). So far, there are no studies that describe the possible binding of chitin to a Nod factor receptor. However, Liu et al. (2012) showed that the CERK1 ectodomain is able to bind to the short chain chitooligosaccaride $(GlcNAc)_5$ but only the octamer $(GlcNAc)_8$ induces the necessary dimerization which is a prerequisite for chitin signalling. It is therefore conceivable that the PtNFP-3 protein binds to chitin unspecifically with a low affinity but that a possible chitin binding does not induce signaling.

4.3 PcCERK1 proteins have a typical LysM-RLK domain organization and are likely to be kinase active

The domain structure of the CERK1 proteins of *Populus trichocarpa* and *Populus x canescens* were compared in-silico with the domain structure of Arabidopsis CERK1. The analysis

revealed a typical LysM-RLK structure with three extracellular LysM domains, a transmembrane domain and an intracellular kinase domain (Fig. 17).

For the protein kinase superfamily twelve invariant amino acids in the kinase subdomains were reported to be correlated with enzyme activity (Hanks and Hunter, 1995). In particular, the Asp-Phe-Gly (DFG) motif in the activation loop is highly conserved among active kinases and assists in orientating the gamma phosphate of ATP for transfer (Hanks and Hunter, 1995). All invariant amino acids are present in Arabidopsis and poplar CERK1 proteins as well. For Arabidopsis CERK1 a kinase activity was already confirmed (Miya et al., 2007). Thus, the data suggests that the poplar CERK1 genes are also kinase active proteins.

4.4 PcCERK1 has a function in chitin signaling

As previously mentioned, the presence of two *PcCERK1* paralogs is the outcome of a whole genome duplication during evolution (Tuskan et al., 2006; Hou et al., 2019). It needs to be investigated whether the paralogs have a redundant function or if duplicated *PcCERK1* genes gained different functions or specifications during evolution. A sub- or neo-functionalization is quite common after a whole genome duplication because paralogs which are not silenced or eliminated afterwards are often affected by DNA mutations or changes in gene expression patterns (Force et al., 1999; Prince and Pickett, 2002).

Usually, paralogous genes with highly similar functions are most likely expressed in different tissues (Zhang, 2003). Semi-quantitative expression analyses in *Populus x canescens* revealed the presence of *PcCERK1-1* in leaves, roots, wood and developing xylem. *PcCERK1-2* is present in the same tissues as well as bark (personal communication, Mo Awwanah). The high overlap of tissues where both genes are expressed hints more towards a functional diversification.

The individual role of *PcCERK1-1* and *PcCERK1-2* and their function in chitin signaling was tested via complementation ability of an Arabidopsis *cerk1* knockout mutant and gene knockouts in poplar as discussed below.

Since the poplar species used in this study, *Populus x canescens,* is a hybrid between *Populus tremula* and *Populus alba* there are two different alleles representing the parental lines. The two individual alleles of PcCERK1-1 or PcCERK1-2 share each about 97 % amino acid sequence identity. In this study so far only one allele was tested in complementation experiments.

Between the two paralogs PcCERK1-1 and PcCERK1-2 there is an amino acid sequence identity of about 84 %.

4.4.1 Complementation studies in the chitin-insensitive Arabidopsis cerk1-2 mutant indicate chitin perception capacity of the poplar CERK1-2 paralog

To evaluate the function in chitin signaling of the two candidate genes *PcCERK1-1* and *PcCERK1-2* of *Populus x canescens* a complementation study in Arabidopsis was conducted. The Arabidopsis mutant *cerk1-2* serves as the background for transformation because it completely lacks the ability to respond to chitin with ROS burst or MAPK activation (Miya et al. 2007; Petutschnig et al., 2014).

4.4.1.1 Complementation experiments using *PcCERK1-1* were not successful

Transformation of the Arabidopsis *cerk1-2* mutant with a vector construct for expression of *PcCERK1-1* under control of the natural promoter of Arabidopsis *CERK1* did not result in transgenic lines. This is possibly a result of cell death in early seed development. Transient overexpression of Arabidopsis *CERK1* with a 35S promoter leads to necrosis due to cell death in *N. benthamiana* and was associated with its kinase activity (Pietraszewska-Bogiel et al., 2013; Suzuki et al., 2018). Difficulties with the constitutive expression of a *CERK1* gene under control of the 35S promoter were also described by Brulé et al. (2019). For one out of three CERK1 homologs of grapevine transgenic Arabidopsis lines could not be obtained. Gene toxicity was also here confirmed by transient expression in *N. benthamiana* which led to cell death necrosis. Cell death for *pAtCERK1:PcCERK1-1_mCitrine* in transiently transformed *N. benthamiana* was not observed (data not shown). Hence, the difficulties rather indicate that the signaling induced by PcCERK1-1 differs from the signaling induced by AtCERK1. Because the natural promotor of Arabidopsis was chosen to avoid overexpression in this heterologous gene expression system the results imply that the PcCERK1-1 protein somehow interacts stronger with the downstream signaling cascade. This would consequently lead to similar effects like an overexpression.

To obtain *PcCERK1-1* transgenic lines in the *Atcerk1*-2 background an estradiol inducible promoter was used. This vector system allows an estradiol dose dependent expression of the construct and was shown to be highly inducible in Arabidopsis and tobacco (Zuo et al., 2000).

During transient expression in *N. benthamiana*, using the estradiol-inducible system, PcCERK1-1_mCitrine was visible in several cell compartments including ER, nucleus, cytoplasmic strains and cell periphery (Fig. 20). LysM-RLKs are plasma membrane localized (Buendia et al., 2018). Studies of other CERK1 homologs in Arabidopsis, rice, apple and grapevine clearly confirmed this plasma membrane localization (Erwig et al., 2017; Shimizu et al., 2010; Zhou et al., 2018; Brulé et al., 2019). Therefore, the observation indicates a strong overexpression in transiently transformed cells. The applied estradiol concentration was probably chosen to high for the induction. Interestingly, also here necroses are not visible after three days post inoculation (data not shown). A strong overexpression was expected to induce cell death responses as described above. However, later timepoints were not analysed.

The expression of the estradiol inducible construct in the Arabidopsis *cerk1*-2 mutant resulted in a cell periphery localization of PcCERK1-1_mCitrine (Fig. 22). This suggests a plasma membrane localization and shows that in Arabidopsis the expression level is adequate to avoid effects of overexpression.

Inducibility of the *PcCERK1-1* gene in the Arabidopsis *cerk1*-2 mutant by estradiol was tested in parallel with the same leaf material used for the ROS burst or MAPK assays. For both assays at least two lines out of three exhibited a transgene expression. The chitin-induced ROS burst was not restored (Fig. 23). Even though one line showed a slight ROS induction the typical ROS burst peak was missing. Since for the other line with a transgene expression there was no signal visible at all, the observed slight ROS signal hints more towards a ROS production independently from the transgene expression. The *PcCERK1-1* gene was also not able to complement chitin-triggered MAPK activation (Fig. 24).

Poplar knockout data clearly pointed out an involvement of *PcCERK1-1* in chitin signaling (see chapter 4.4.2). Possible explanations for the lack of complementation ability are, therefore, discussed in chapter 4.4.1.3.

4.4.1.2 *PcCERK1-2* partially complements MAPK activation

In contrast to *PcCERK1-1,* for the *PcCERK1-2* gene a selection of transgenic Arabidopsis plants expressing *PcCERK1-2* under the control of the natural Arabidopsis CERK1 promotor was successful. The *pAtCERK1:PcCERK1-2_mCitrine* was visible in the cell periphery of *N. benthamiana* as well as A. thaliana cells which indicates a plasma membrane localization

(Fig. 25 and Fig. 26). The chitin-triggered ROS burst was not restored (Fig. 27) even though also here the data obtained from poplar knockout mutants imply a function of *PcCERK1-2* in ROS generation. For the MAPK activation after chitin treatment a slight signal was visible (Fig. 28). Thus, the complementation data show that *PcCERK1-2* can at least interact with the MAPK signaling components of Arabidopsis and is involved in MAPK signaling after chitin recognition.

4.4.1.3 Complementation ability might be achieved by site-directed mutagenesis

Poplar knockout data suggest that *PcCERK1-1* and *PcCERK1-2* are involved in chitin-triggered ROS burst sharing a redundant function. In addition, both *PcCERK1* genes have a function in chitin-induced MAPK signaling and it was shown that *PcCERK1-1* plays the prominent role in MAPK activation (see chapter 4.4.2).

The heterologous expression seems to be causative for the lack of complementation ability in Arabidopsis. Similar complementation studies with the other LysM-RLK genes *PcLYK4* and *PcLYK5* of *Populus x canescens* in the Arabidopsis double knockout mutant *Atlyk4 Atlyk5* showed that a complementation with these genes were possible even though it was only partial and did not reach full restoration of the wild-type phenotype (Awwanah, 2020). This indicates that in principle LysM-RLKs from poplar can achieve a complementation in Arabidopsis and that the cause for an impaired complementation are rather specific characteristics of the *PcCERK1* genes.

One possible explanation could be that the co-receptors for chitin signaling are not able to interact sufficiently with the PcCERK1 protein. In Arabidopsis the LysM-RLKs LYK4 and LYK5 are postulated to build a receptor complex with CERK1 for proper chitin signaling (Cao et al., 2014; Erwig et al. 2017; Xue et al., 2019). A dimerization of LYK4 and LYK5 with the poplar CERK1 may be possible but probably less effective. Since at least the MAPK response with the *PcCERK1-2* gene was restored in the Arabidopsis *cerk1* mutant another more likely explanation is that downstream components important for ROS signaling in Arabidopsis cannot interact with the poplar CERK1 protein. In Arabidopsis the receptor-like cytoplasmic kinase PBL27 is supposed to directly link chitin perception of CERK1 with the activation of MAPK signaling cascades (Shinya et al., 2014; Yamada et al., 2016).

For ROS burst activation the receptor-like cytoplasmic kinase BIK1 appears to be responsible for signal transduction. BIK1 is known to directly activate the NADPH oxidase RBOHD and was reported to be strongly associated with the leucine-rich repeat receptor kinases FLS2 and EFR (Kadota et al., 2014). However, Zhang et al. (2010) described that BIK1 is also able to associate with CERK1 and is involved in chitin-induced defense responses, like ROS burst and callose deposition. Taken together, it can be assumed that the *PcCERK1-2* gene in Arabidopsis is able to phosphorylate PBL27 which would explain the restoration of MAPK signaling but is somehow unable to phosphorylate BIK1 to initiate ROS burst signaling. With respect to lack of *PcCERK1-1* complementation ability it is likely that PcCERK1-1 neither interacts properly with PBL27 nor with BIK1.

Since LysM-RLKs like CERK1 are transmembrane proteins the interaction of downstream components for chitin signaling takes place at the cytoplasmic part which consists of the juxtamembrane and kinase domain. An in-silico alignment of the PcCERK1 juxtamembrane and kinase domain in comparison to AtCERK1 was performed to reveal differences in specific amino acid positions that might lead to an altered protein folding and possible prevent recognition of components for signal transduction in Arabidopsis (Fig. 29). The hypothesis was put forward that complementation ability of PcCERK1-1 and PcCERK1-2 in Arabidopsis can be achieved by mutagenesis of this amino acids back to the amino acids present in Arabidopsis CERK1. Specifically surface exposed amino acids have a potential impact on binding or interacting with a substrate. Therefore, a protein model of PcCERK1-2 was built in addition to have information about the 3D structure (Fig. 30). So far only the ectodomain of Arabidopsis CERK1 with the three LysM motifs has been crystalized (Liu et al., 2012). The modeling was thus performed with the kinase domain of BAK1 which was identified as the closest homology template.

According to the model and the sequence alignment six altered amino acid positions were identified that are supposed to have a high impact on the protein structure. The first one is a change in charge of PcCERK1-2 in the P-loop. Instead of the neutral amino acid glutamine the PcCERK1-2 protein has the acidic amino acid glutamic acid in this position. In addition, three changes in charge were found in the activation-loop. One of it is present only in PcCERK1-2 and two changes in charge directly next to each other are found in both, PcCERK1-1 and PcCERK1-2. The P-loop and the activation loop are both involved in the protein substrate interaction. Amino acid substitutions introducing a change in charge have direct influence on

electrostatic interactions and can thus alter substrate specificity (Wells et al., 1987; Exterkate et al., 1993). Already a single change in charge can have an impact on the conformation of a protein and its substrate specificity when it is part of the substrate binding site. This was for example observed for a bacterial ATP-binding cassette (ABC) transporter where the change of a nonpolar phenylalanine into a basic arginine introduces a new salt-bridge that slightly alters the confirmation of the binding pocket. This minor change was sufficient enough to enable the protein to bind the furanose form of D-galactose instead of the pyranose form (Maqbool et al., 2015). Another example for a change in substrate specificity has been demonstrated for the human type I and type II PHOSPHATIDYLINOSITOL PHOSPHATE (PIP) KINASES. Type I and type II PIP kinases both generate phosphatidylinositol-4,5-bisphosphate. However, they act in distinct pathways and use the stereoisomeric but different substrates phosphatidylinositol-4-phosphate or phosphatidylinositol-5-phosphate and are therefore functionally non-redundant. A single amino acid substitution in the activation loop exchanging a negatively charged glutamate with a nonpolar alanine for type I or vice versa for type II swapped their stereo-specific substrate recognition. The authors explained this by either changed electrostatic interactions with the substrate or that the negatively charged glutamate is part of an ion pair that stabilizes a specific confirmation of the activation loop (Kunz et al., 2002).

Two other altered amino acid positions that are of particular interest are changes in proline residues which are very close together and are in the kinase subdomain X. Since proline residues introduce a kink in the secondary structure (Barlow and Thornton, 1988), it can be expected that the folding of PcCERK1-1 and PcCERK1-2 is different from that of Arabidopsis CERK1 in this area. Even though the function of kinase subdomain X is still not completely unraveled it is known to be part of the C-terminal domain that allows binding of the peptide substrate and initiating the phosphotransfer (Hanks and Hunter, 1995). Hence, a possible conformational change would also impair substrate binding specificity.

Amino acid positions in the juxtamembrane domain were not taken into account. Except for the C-terminal part which is quite conserved, the juxtamembrane domain of poplar PcCERK1 and Arabidopsis AtCERK1 has only low sequence homology. A mutation of single sites is therefore probably not sufficient enough to see an effect. In addition, a recent study that compared the CERK1 juxtamembrane domains of Arabidopsis and rice concluded a functionally conserved role for the ability to trigger chitin-induced responses in Arabidopsis

even though overall sequence homology was similar to the one shown here for Arabidopsis and poplar. That means that AtCERK1 and OsCERK1 juxtamembrane domains shared a highly conserved C-terminal part with only a few amino acid exchanges and a significantly less conserved N-terminal part. Zhou et al. (2019) showed that a chimeric AtCERK1 receptor whose juxtamembrane domain was replaced with the juxtamembrane domain from OsCERK1 was still able to induce defense responses similar to wildtype AtCERK1. They identified that for both, AtCERK1 and OsCERK1, particularly only the C-terminal part of the CERK1 juxtamembrane domain is crucial for chitin-induced signaling. Thus, it can be assumed that the high sequence homology of the CERK1 C-terminal part of the juxtamembrane domain of PcCERK1 and AtCERK1 hints towards a conserved function as well. Apart from that, there seems to exist another unknown mechanism for the contribution of the juxtamembrane domain to chitin-induced signaling in Arabidopsis that is independent from sequence homology. Experiments where the juxtamembrane domain of Arabidopsis CERK1 was replaced with the juxtamembrane domain of two other RLKs, BAK1 and FLS2, showed that even with an overall low sequence homology of the juxtamembrane domains the ability to activate chitin-induced signaling was maintained (Zhou et al., 2019).

4.4.2 The poplar paralogs *PcCERK1-1* and *PcCERK1-2* exhibit a functional diversification in chitin signaling

CRISPR/Cas9 generated single and double knockout lines of *PcCERK1-1* and *PcCERK1-2* were used to analyse the individual role of these two genes in *P. x canescens* wildtype background. For all CRISPR/Cas9 knockouts only biallelic editing could be observed which means both alleles were edited but with different editing results on the *P. alba* and *P. tremula* allele (Tab. 36, Tab. 38 and Tab. 40). Biallelic editing is quite common for CRISPR/Cas9 generated knockouts in the first generation of transgenic plants (Belhaj et al., 2015). Usually, homozygous knockouts are achieved by self-pollination. In woody perennials, such as poplar, this is not possible due to a very long vegetative life cycle. The biallelic editing in the *Pccerk1-1* and *Pccerk1-2* single knockout plants caused loss-of function mutations on both alleles and, therefore, these lines are suitable for the evaluation of knockout effects. In most cases the editing leads to a loss of function due to premature stop codons. Some of the editing also results in a deletion of amino acids in the LysM1 domain (Tab. 37, Tab. 39). Bigger deletions

in a LysM domain should be sufficient to interfere with CERK1 function, since in Arabidopsis all three LysM domains were necessary for chitin binding (Petutschnig et al., 2010).

For the CRISPR/Cas9 *Pccerk1-1 Pccerk1-2* double knockouts chimeric tissue was observed which shows more than one, namely two to six editing events of each allele in the knockout plants (Tab. 40). In the literature, the safety of the CRISPR/Cas9 system in regard to multiple, successive editing of a gene is discussed controversially. There is some evidence that already edited alleles are usually not recognized anymore by the CRISPR/Cas9 system. Cutting of the target sequence (also referred to as protospacer sequence) that needs to be followed by a protospacer adjacent motif (PAM; generally 5' NGG) is very specific and does usually not tolerate more than three mismatches in the PAM proximal region (Hsu et al., 2013). Since the Cas9 protein cuts 3-4 bases apart from the PAM (Jinek et al., 2012) the recognition of the target sequence is thus automatically destroyed by bigger deletions or insertions. However, some studies have also shown that even small insertions or deletions of one base pair are sufficient to produce stable knockout lines. Stability tests of CRISPR/Cas9 induced mutations in the next generation revealed that new mutation types were only observed in chimeras with a wildtype allele. Otherwise, there was no detection of alterations or secondary modifications of an already mutated gene (Feng et al., 2014, Pan et al., 2016; Howells et al., 2018). Also a study specifically performed in poplar came to the conclusion that CRISPR/Cas9 edited genes do not underwent secondary editing. Bruegmann et al. (2019) evaluated several independent transgenic poplar lines after a period of seven month of vegetative propagation and did not observe any additional mutations. However, one issue discussed for the CRISPR/Cas9 system is the potential cutting of off-targets (Wolt et al., 2016). These are sequences which only differ from the gRNA target sequence in a few base pairs. Therefore, it still might be possible that an edited gene is cut again by the Cas9 protein when the initial editing does only lead to minor changes in the gene sequence. Yet, the occurrence of off-target editing seems to be very rarely happening in plants (Xie and Yang, 2013; Zhang et al., 2014; Jacobs et al., 2015; Li et al., 2019) and does not explain the high amount of different editing events in the *Pccerk1-1 Pccerk1-2* double knockouts plants. Therefore, a possible explanation for the multiple editing is that the initial cell from which the transgenic shoot has developed was successfully transformed with the Cas9 construct but editing of the target gene occurred later in the development of the shoot. Independent editing events in different cells of the shoot results in chimeric tissue which is a mosaic of cells which exhibit genetic differences of the

target gene. Nevertheless, also in the *Pccerk1-1 Pccerk1-2* lines most editing lead to premature stop codons or bigger deletions in the LysM1 domain (Tab. 41) and the prominent phenotype (the completely abolished chitin response discussed below) gives a hint that a double knockout could be successfully achieved in those lines. A repetition with non-chimeric lines should still be taken into account to verify these results because if the hypothesis is true that gene editing took place during shoot development, there is a high probability that the editing observed here is only specific for the tested leaf tissue. In other tissues the editing might be different including the possible presence of uncut wildtype alleles. Chimeras with wildtype alleles have been also recently described to arise frequently in CRISPR/Cas9 generated transgenic woody perennials like apple, pear and poplar that are regenerated from adventitious buds (Charrier et al., 2019; Ding et al., 2020). The number of transgenic plants with homogenous mutations could be increased with a second round of shoot regeneration (Ding et al. (2020); Malabarba et al., 2020). This would be also a simple method to generate non-chimeric lines from the double knockout lines of this thesis.

The analysis of the mutant lines revealed that the chitin-triggered ROS burst for *Pccerk1-1* and *Pccerk1-2* single knockout lines showed a wildtype-like response (Fig. 37 and Fig. 39). This suggests either that both genes do not participate in ROS production or that these genes have a redundant function and can fully compensate the loss of the other gene. The completely abolished ROS burst of the *Pccerk1-1 Pccerk1-2* double knockout (Fig. 41) showed clearly that a redundant function of *PcCERK1-1* and *PcCERK1-2* can be concluded for ROS burst responses. In contrast to this, the results for the chitin-triggered MAPK response hints towards a functional diversification of the *PcCERK1* genes. The ability to respond with a chitin-induced MAPKinase cascade is strongly impaired in the *Pccerk1-1* single knockout with only a very slight activation of MAPKinases visible (Fig. 38) while the *Pccerk1-2* single knockout line has still a wildtype-like MAPK response after chitin treatment (Fig. 40). In the double knockout the MAPK response is completely abolished (Fig. 42). This shows, that *PcCERK1-1* is primarily responsible for MAPK signaling. Thus, *PcCERK1-2* seems to be able to completely compensate the missing *PcCERK1-1* in ROS burst but only partially in MAPK response. Since *PcCERK1-1* is significantly higher expressed in wildtype the normal ROS burst of the *Pccerk1-1* single knockout line is possibly achieved by a higher expression of *PcCERK1-2* in this knockout line to compensate the missing *PcCERK1-1* gene. In the future, expression levels for both CERK1 paralogs should therefore be tested in the knockout mutants. Taken together, the results

highlight the *PcCERK1* genes as a major component of the chitin receptor complex in poplar similar as in other species. Both genes, *PcCERK1-1* as well as *PcCERK1-2* have a function in chitin signaling in poplar. *PcCERK1-1* seems to be the main gene for chitin signaling and more important regarding MAPK responses.

4.4.3 Overexpression of a kinase dead version of *PcCERK1-1* give a hint for kinase activity

As an alternative strategy to the CRISPR/Cas9 mediated knockout lines the overexpression of a kinase dead version of *PcCERK1* was tested. The overexpression of a kinase with inactivated kinase domain which competes with the wildtype protein should exhibit a dominant negative phenotype which resembles the phenotype of a null mutant. This was shown for example for the ENHANCED DISEASE RESISTANCE 1 (EDR1) protein kinase and SOMATIC EMBRYOGENESIS RECEPTOR KINASE 1 AND 2 (SERK1 and SERK2) (Tang and Innes, 2002; Gou et al., 2012). Here, the overexpression of a kinase dead version of *PcCERK1* should lead to a dominant negative effect on chitin signaling. A single point mutation of a conserved lysin residue in the ATP binding site of kinase subdomain II was introduced. This mutation already has been demonstrated to be sufficient for abolishment of kinase activity (Horn and Walker, 1994; Tang and Innes, 2002; Li et al., 2002; Petutschnig et al., 2010).

Before the application of this experimental strategy in poplar, a proof of principle test was performed in Arabidopsis. The mutated kinase dead Arabidopsis cerk1 led as expected to the lack of MAPK phosphorylation ability (Fig. 32) like previously described by Petutschnig et al. (2010). In addition, the overexpression in wildtype Arabidopsis plants resulted in a complete abolishment of chitin-induced ROS burst (Fig. 33) and MAPK responses (Fig. 34) which made it promising to apply this approach in poplar. However, in poplar the overexpression of a kinase dead cerk1-1 variant with the same mutation did not lead to such severe effects. The ROS burst (Fig. 35) and MAPK response (Fig. 36) was only slightly reduced. This could be due to a low expression level of the kinase dead variant in poplar since the dominant negative phenotype effect of a kinase inactive form was shown to be correlated with the expression level (Li et al., 2002). An antibody for the poplar CERK1 protein is not available so far and the CERK1 antibody for Arabidopsis was not able to bind (data not shown) to check the actual expression level in poplar transgenic plants.

In addition, it is also possible that the second paralog *PcCERK1-2* is responsible for a less significant effect. For Arabidopsis it is known that the chitin receptor complex consists of two CERK1 proteins building a homodimer which is associated with their co-receptors (Petutschnig et al., 2010; Liu et al., 2012; Cao et al., 2014). It is very likely that the chitin receptor complex in poplar needs also the CERK1 dimerization for signal transduction. It was not investigated if PcCERK1-1 and PcCERK1-2 can build heterodimers or if those proteins would be only able to build homodimers in such a receptor complex. That paralogous genes in poplar are able to build both hetero- and homodimers was for example described for the osmosensor *Histidine-Aspartate Kinase 1* (Héricourt et al., 2016). A possible homo-dimerization of PcCERK1-2 might therefore compensate the effect because these receptor complexes would still have a normal signal transduction capacity while only the PcCERK1-1 dimers with an incorporated Pccerk1-1_LOF protein are impaired in signal transduction. However, considering the results from the single knockout data in this case the redundant function of PcCERK1-2 for ROS generation should result in full restoration of ROS burst. Heterodimerization together with a low expression level of Pccerk1-1_LOF that still allows for some receptor activity is therefore the most plausible explanation.

In conclusion, even though the dominant negative effect on chitin signaling of the overexpressed kinase dead *Pccerk1-1* was not as prominent as in Arabidopsis, the results of the analysis indicate that the kinase domain of PcCERK1-1 is active and that kinase activity is as necessary for poplar CERK1 function like it is described for the Arabidopsis homolog (Petutschnig et al., 2010).

4.5 Conclusion

PcCERK1-1 and *PcCERK1-2* are predicted to be plasma membrane localized, kinase active LysM-RLKs. Both genes, *PcCERK1-1* as well as *PcCERK1-2* have a function in chitin signaling in poplar. They have redundant roles for ROS burst activation. Regarding the MAPK response, a functional diversification can be concluded. Here, *PcCERK1-1* seems to be of major importance and *PcCERK1-2* plays only a minor role. Taken together with the significantly higher abundance of *PcCERK1-1* transcript this gene seems to be primarily responsible for chitin signaling in poplar.

4.6 Outlook

For the poplar PcCERK1 genes a plasma membrane localization was predicted based on a fluorescence signal of the transgene in the cell periphery of Arabidopsis. To confirm a signal in the cell membrane a plasmolysis experiment or the co-transformation with a plasma membrane marker should be performed.

In this study the two homologs of PcCERK1 were shown to play a role in chitin signaling. LysM-RLKs usually function as hetero-oligomeric complexes (Buendia et al., 2018). In Arabidopsis a complex formation of the LysM-RLKs AtLYK5 and AtCERK1 was suggested (Cao et al., 2014, Xue et al., 2019). The chitin-induced AtLYK5 phosphorylation was shown to be dependent on CERK1 (Erwig et al., 2017). In addition, the LysM-RLK AtLYK4 shares a redundant function with AtLYK5 and is proposed to be a co-receptor or scaffold protein for AtLYK5-AtCERK1 complex formation and chitin-induced signaling (Cao et al., 2014; Xue et al., 2019). Another study in cotton also suggests a complex formation of GhCERK1 with GhLYK5 (Wang et al., 2020b). In *Populus x canescens* two PcLYK4 homologs and one PcLYK5 homolog were identified as functionally LysM-RLKs. An involvement in chitin signaling was confirmed via complementation ability of the chitin-insensitive Arabidopsis *Atlyk4/Atlyk5* double mutant (Awwanah, 2020). Furthermore, PcLYK5 was suggested to be a phosphorylation target of CERK1. Further experiments are needed, for example co-immunoprecipitation or bimolecular fluorescence complementation, to test if a hetero-oligomeric complex similar to Arabidopsis consisting of PcCERK1, PcLYK4 and PcLYK5 is formed.

To check the hypothesis that PcCERK1 has a kinase activity *in vitro* phosphorylation assays with the purified protein are necessary. The wild type kinase domain should be able to phosphorylate the artificial substrate myelin basic protein like it was described for the kinase domain of Arabidopsis CERK1 expressed in *E. coli* (Miya et al., 2007).

Prior to mutation of different sites in the kinase domain of PcCERK1 to unravel the lack of complementation ability in Arabidopsis a pre-experiment should be performed. The hypothesis that alterations in the kinase domain of PcCERK1 are the reason why Arabidopsis downstream components do not interact with the poplar receptor can be tested with a chimeric receptor complex of poplar CERK1 ectodomain and wildtype Arabidopsis kinase

domain. This chimeric receptor should be able to complement the phenotype of the chitin insensitive *cerk1-2* mutant. Otherwise, it should be considered that PcCERK1 is probable not able to induce chitin-triggered responses in Arabidopsis because of an impaired interaction with the ectodomains of the co-receptors AtLYK4 and AtLYK5.

Depart from differences in the protein structure, differences in the presence of phosphorylation sites should be taken into account. Phosphorylation of multiple sites is presumed to have a high impact on improving signal specificity (Swain and Siggia, 2002). After chitin recognition Arabidopsis CERK1 is autophosphorylated and this autophosphorylation is essential for the activation of immune signaling (Suzuki et al. 2016). PcCERK1 quite likely also autophosphorylates but potentially on different sites, compared with Arabidopsis AtCERK1, with the consequence that an interaction partner might not recognize the activated state in Arabidopsis.

Two different studies describe phosphorylation sites of serine, threonine and tyrosine residues in Arabidopsis CERK1 that are dependent on chitin treatment. Suzuki et al. (2016) tested 15 different in vivo phosphorylation sites including those identified by Petutschnig et al. (2010) for their biological function in chitin signaling. Complementation analyses in *cerk1* knockout mutants with cDNA of CERK1 mutated at predicted phosphosites revealed only three (T479, Y428 and T573) that play a direct role in chitin signaling. In addition, Liu et al. (2018) identified the phosphorylation site Y557 as important for CERK1-mediated chitin signaling. These four amino acid residues are all conserved in the *PcCERK1* genes as well. However, of the remaining eleven residues, seven of them are not conserved in the PcCERK1 genes. Suzuki et al. (2016) did not exclude that eventually additional phosphorylation sites might have an impact on chitin signaling as well since for some of the other phosphorylation sites they observed partial effects on chitin-induced gene expression. Besides protein structure changes it is, therefore, also conceivable that the missing of an important phosphorylation site is causative for the lack of PcCERK1 complementation ability.

Depart from its function in chitin sensing, poplar CERK1 may also be involved in mediating other signaling processes. For instance, it is known for Arabidopsis and *Oryza sativa* CERK1 that they also contribute to immune responses towards other pathogen-associated molecular patterns. Even though a direct binding of peptidoglycan (PGN) from bacteria to Arabidopsis CERK1 was not observed, it was shown that Arabidopsis CERK1 takes part in defense signaling

upon PGN recognition in a receptor complex with the LysM domain containing proteins LYM1 and LYM3 (Willmann et al., 2011). Similarly, OsCERK1 from Rice acts together with the LysM domain containing proteins LYP4/LYP6 to mediate PGN responses (Ao et al., 2014). In addition, in rice cells with mutated *Oscerk1* the response to bacterial lipopolysaccharides (LPS) was significantly diminished. However, this observation was specific for rice since the Arabidopsis mutants of *cerk1, lyk4, lyk5* and the triple mutant *lym1/2/3* still responded normally to LPS (Desaki et al., 2018b). On the other hand, Arabidopsis *Atcerk1* mutants were impaired in response to unbranched β-1,3-linked glucans which are besides chitin also a component of fungal cell walls (Mélida et al., 2018). It should be therefore considered to test the generated poplar knockouts of this thesis for their response to PGN, LPS and unbranched β-1,3-linked glucans as well.

Another process in which PcCERK1 might play a role is the development of mycorrhizal symbiosis. Poplars are able to establish symbiosis with ectomycorrhizal fungi as well as arbuscular mycorrhizal fungi (Danielsen et al., 2012; Liu et al., 2015). For several CERK1 homologs an involvement in both processes has been described: plant immunity as well as the contribution to symbiosis development. This was for example described for *Oryza sativa* OsCERK1 as well as *Pisum sativum* and *Medicago truncatula* CERK1-like receptor proteins (Miyata et al., 2014; He et al., 2019; Leppyanen et al., 2017; Gibelin-Viala et al., 2019). Interestingly in a study in *Solanum lycopersicum* different paralogs of CERK1 have subfunctionalized in their function. The tomato CERK1 paralog SlLYK12 plays a unique role for arbuscular mycorrhizal symbiosis whereas another tomato CERK1 paralog SlLYK1 is exclusively involved in chitin signaling (Liao et al., 2018). Since in *Populus x canescens PcCERK1-1* was identified to be the main gene for chitin signaling it should be analysed if *PcCERK1-2* has a main function in the establishment of symbiosis. In that regard it could be also tested if the expression of *PcCERK1-2* in roots is higher compared to the relatively low expression level in leaves.

As a long-term goal, a better understanding of chitin signaling in poplar should lead to strategies to improve the pathogen response towards the rust fungus *Melampsora*. A constitutive overexpression of CERK1 in poplar is most likely not feasible to enhance resistance. CERK1 overexpression might induce cell death as it was observed for Arabidopsis CERK1 in transient expression assays with *N. benthamiana* (Pietraszewska-Bogiel et al., 2013;

Suzuki et al., 2018). An alternative strategy would be an exchange of the CERK1 promoter with a promoter of a gene that is strongly induced by *Melampsora*. Hence, the cell death response due to overexpression of CERK1 would specifically occur at the sites of infection and directly interfere with *Melampsora* propagation. However, difficulties could arise when the chosen promoters are also activated by other processes. In *Populus trichocarpa* the sulfate transporter gene PtSultr3;5 (Potri.006G158900.1) was identified to exhibit a significantly strong induction after 48 hours post *Melampsora larici-populina* infection with both virulent and avirulent strains (Petre et al., 2012). On the other hand, PtSultr3;5 was also among the most induced transcripts in poplar roots during early interaction with the ectomycorrhizal fungus *Laccaria bicolor* (Felten et al., 2009) and is therefore probably also involved in the establishment of symbiosis. This example shows that careful evaluation of a promising *Melampsora* induced promoter is necessary before this approach can be applied.

5. References

Aghaalikhani, A., Savuto, E., Di Carlo, A., Borello, D., 2017. Poplar from phytoremediation as a renewable energy source: gasification properties and pollution analysis. Energy Procedia 142, 924–931. https://doi.org/10.1016/j.egypro.2017.12.148

Akamatsu, A., Wong, H.L., Fujiwara, M., Okuda, J., Nishide, K., Uno, K., Imai, K., Umemura, K., Kawasaki, T., Kawano, Y., Shimamoto, K., 2013. An OsCEBiP/OsCERK1-OsRacGEF1-OsRac1 Module Is an Essential Early Component of Chitin-Induced Rice Immunity. Cell Host & Microbe 13, 465–476. https://doi.org/10.1016/j.chom.2013.03.007

Ao, Y., Li, Z., Feng, D., Xiong, F., Liu, J., Li, J.-F., Wang, M., Wang, J., Liu, B., Wang, H.-B., 2014. OsCERK1 and OsRLCK176 play important roles in peptidoglycan and chitin signaling in rice innate immunity. Plant J 80, 1072–1084. https://doi.org/10.1111/tpj.12710

Arrighi, J.-F., Barre, A., Ben Amor, B., Bersoult, A., Soriano, L.C., Mirabella, R., de Carvalho-Niebel, F., Journet, E.-P., Ghérardi, M., Huguet, T., Geurts, R., Dénarié, J., Rougé, P., Gough, C., 2006. The *Medicago truncatula* Lysine Motif-Receptor-Like Kinase Gene Family Includes NFP and New Nodule-Expressed Genes. Plant Physiol. 142, 265–279. https://doi.org/10.1104/pp.106.084657

Asai, T., Tena, G., Plotnikova, J., Willmann, M.R., Chiu, W.-L., Gomez-Gomez, L., Boller, T., Ausubel, F.M., Sheen, J., 2002. MAP kinase signalling cascade in Arabidopsis innate immunity. Nature 415, 977–983. https://doi.org/10.1038/415977a

Ausubel, F.M., 2005. Are innate immune signaling pathways in plants and animals conserved? Nat Immunol 6, 973–979. https://doi.org/10.1038/ni1253

Awwanah, 2020. Characterization of *Populus x canescens* LysM-Receptor Like Kinases LYK4/LYK5 and LysM-Receptor Like Protein LYM2 and their Roles in Chitin Signaling. Doctoral thesis. Georg-August-University Göttingen

Azaiez, A., Boyle, B., Levée, V., Séguin, A., 2009. Transcriptome Profiling in Hybrid Poplar Following Interactions with *Melampsora* Rust Fungi. MPMI 22, 190–200. https://doi.org/10.1094/MPMI-22-2-0190

Barlow, D.J., Thornton, J.M., 1988. Helix geometry in proteins. Journal of Molecular Biology 201, 601–619. https://doi.org/10.1016/0022-2836(88)90641-9

Bateman, A., Bycroft, M., 2000. The structure of a LysM domain from *E. coli* membrane-bound lytic murein transglycosylase D (MltD). Journal of Molecular Biology 299, 1113–1119. https://doi.org/10.1006/jmbi.2000.3778

Baucher, M., Halpin, C., Petit-Conil, M., Boerjan, W., 2003. Lignin: Genetic Engineering and Impact on Pulping. Critical Reviews in Biochemistry and Molecular Biology 38, 305–350. https://doi.org/10.1080/10409230391036757

Bayles, C.J., Ghemawat, M.S., Aist, J.R., 1990. Inhibition by 2-deoxy-D-glucose of callose formation, papilla deposition, and resistance to powdery mildew in an ml-o barley mutant. Physiological and Molecular Plant Pathology 36, 63–72. https://doi.org/10.1016/0885-5765(90)90092-C

Belhaj, K., Chaparro-Garcia, A., Kamoun, S., Patron, N.J., Nekrasov, V., 2015. Editing plant genomes with CRISPR/Cas9. Current Opinion in Biotechnology 32, 76–84. https://doi.org/10.1016/j.copbio.2014.11.007

Ben Amor, B., Shaw, S.L., Oldroyd, G.E.D., Maillet, F., Penmetsa, R.V., Cook, D., Long, S.R., Denarie, J., Gough, C., 2003. The NFP locus of *Medicago truncatula* controls an early step of Nod factor signal transduction upstream of a rapid calcium flux and root hair deformation. Plant J 34, 495–506. https://doi.org/10.1046/j.1365-313X.2003.01743.x

Benetka, V., Černý, K., Pilařová, P., Kozlíková, K., 2011. Effect of *Melampsora larici-populina* on growth and biomass yield of eight clones of *Populus nigra*. J. For. Sci. 57, 41–49. https://doi.org/10.17221/51/2010-JFS

Bensmihen, S., de Billy, F., Gough, C., 2011. Contribution of NFP LysM Domains to the Recognition of Nod Factors during the *Medicago truncatula*/*Sinorhizobium meliloti* Symbiosis. PLoS ONE 6, e26114. https://doi.org/10.1371/journal.pone.0026114

Bi, G., Zhou, Z., Wang, W., Li, L., Rao, S., Wu, Y., Zhang, X., Menke, F.L.H., Chen, S., Zhou, J.-M., 2018. Receptor-Like Cytoplasmic Kinases Directly Link Diverse Pattern Recognition Receptors to the Activation of Mitogen-Activated Protein Kinase Cascades in Arabidopsis. Plant Cell 30, 1543–1561. https://doi.org/10.1105/tpc.17.00981

Birkeland, N.-K., 1994. Cloning, molecular characterization, and expression of the genes encoding the lytic functions of lactococcal bacteriophage ϕLCE: a dual lysis system of modular design. Can. J. Microbiol. 40, 658–665. https://doi.org/10.1139/m94-104

Boller, T., Felix, G., 2009. A Renaissance of Elicitors: Perception of Microbe-Associated Molecular Patterns and Danger Signals by Pattern-Recognition Receptors. Annu. Rev. Plant Biol. 60, 379–406. https://doi.org/10.1146/annurev.arplant.57.032905.105346

Bonadei, M., Zelasco, S., Giorcelli, A., Gennaro, M., Calligari, P., Quattrini, E., Carbonera, D., Balestrazzi, A., 2012. Transgene stability and agronomical performance of two transgenic Basta®-tolerant lines of *Populus alba.* Plant Biosystems - An International Journal Dealing with all Aspects of Plant Biology 146, 33–40. https://doi.org/10.1080/11263504.2011.641037

Bozsoki, Z., Cheng, J., Feng, F., Gysel, K., Vinther, M., Andersen, K.R., Oldroyd, G., Blaise, M., Radutoiu, S., Stougaard, J., 2017. Receptor-mediated chitin perception in legume roots is functionally separable from Nod factor perception. Proc Natl Acad Sci USA 114, E8118–E8127. https://doi.org/10.1073/pnas.1706795114

Bozsoki, Z., Gysel, K., Hansen, S.B., Lironi, D., Krönauer, C., Feng, F., de Jong, N., Vinther, M., Kamble, M., Thygesen, M.B., Engholm, E., Kofoed, C., Fort, S., Sullivan, J.T., Ronson, C.W., Jensen, K.J., Blaise, M., Oldroyd, G., Stougaard, J., Andersen, K.R., Radutoiu, S., 2020. Ligand-recognizing motifs in plant LysM receptors are major determinants of specificity. Science 369, 663–670. https://doi.org/10.1126/science.abb3377

Bradshaw, H.D., Ceulemans, R., Davis, J., Stettler, R., 2000. Emerging Model Systems in Plant Biology: Poplar (*Populus*) as A Model Forest Tree. Journal of Plant Growth Regulation 19, 306–313. https://doi.org/10.1007/s003440000030

Bresson, A., Jorge, V., Dowkiw, A., Guerin, V., Bourgait, I., Tuskan, G.A., Schmutz, J., Chalhoub, B., Bastien, C., Faivre Rampant, P., 2011. Qualitative and quantitative resistances to leaf rust finely

mapped within two nucleotide-binding site leucine-rich repeat (NBS-LRR)-rich genomic regions of chromosome 19 in poplar. New Phytologist 192, 151–163. https://doi.org/10.1111/j.1469-8137.2011.03786.x

Bruegmann, T., Deecke, K., Fladung, M., 2019. Evaluating the Efficiency of gRNAs in CRISPR/Cas9 Mediated Genome Editing in Poplars. IJMS 20, 3623. https://doi.org/10.3390/ijms20153623

Brulé, D., Villano, C., Davies, L.J., Trdá, L., Claverie, J., Héloir, M., Chiltz, A., Adrian, M., Darblade, B., Tornero, P., Stransfeld, L., Boutrot, F., Zipfel, C., Dry, I.B., Poinssot, B., 2019. The grapevine (*Vitis vinifera*) LysM receptor kinases VvLYK 1-1 and VvLYK 1-2 mediate chitooligosaccharide-triggered immunity. Plant Biotechnol J 17, 812–825. https://doi.org/10.1111/pbi.13017

Buendia, L., Girardin, A., Wang, T., Cottret, L., Lefebvre, B., 2018. LysM Receptor-Like Kinase and LysM Receptor-Like Protein Families: An Update on Phylogeny and Functional Characterization. Front. Plant Sci. 9, 1531. https://doi.org/10.3389/fpls.2018.01531

Buist, G., Steen, A., Kok, J., Kuipers, O.P., 2008. LysM, a widely distributed protein motif for binding to (peptido)glycans. Mol Microbiol 68, 838–847. https://doi.org/10.1111/j.1365-2958.2008.06211.x

Buscaill, P., Rivas, S., 2014. Transcriptional control of plant defence responses. Current Opinion in Plant Biology 20, 35–46. https://doi.org/10.1016/j.pbi.2014.04.004

Cameron, D.D., Neal, A.L., van Wees, S.C.M., Ton, J., 2013. Mycorrhiza-induced resistance: more than the sum of its parts? Trends in Plant Science 18, 539–545. https://doi.org/10.1016/j.tplants.2013.06.004

Cao, Y., Liang, Y., Tanaka, K., Nguyen, C.T., Jedrzejczak, R.P., Joachimiak, A., Stacey, G., 2014. The kinase LYK5 is a major chitin receptor in Arabidopsis and forms a chitin-induced complex with related kinase CERK1. eLife 3, e03766. https://doi.org/10.7554/eLife.03766

Carotenuto, G., Chabaud, M., Miyata, K., Capozzi, M., Takeda, N., Kaku, H., Shibuya, N., Nakagawa, T., Barker, D.G., Genre, A., 2017. The rice LysM receptor-like kinase OsCERK1 is required for the perception of short-chain chitin oligomers in arbuscular mycorrhizal signaling. New Phytol 214, 1440–1446. https://doi.org/10.1111/nph.14539

Castro-Rodríguez, V., García-Gutiérrez, A., Canales, J., Cañas, R.A., Kirby, E.G., Avila, C., Cánovas, F.M., 2016. Poplar trees for phytoremediation of high levels of nitrate and applications in bioenergy. Plant Biotechnol J 14, 299–312. https://doi.org/10.1111/pbi.12384

Charrier, A., Vergne, E., Dousset, N., Richer, A., Petiteau, A., Chevreau, E., 2019. Efficient Targeted Mutagenesis in Apple and First Time Edition of Pear Using the CRISPR-Cas9 System. Front. Plant Sci. 10, 40. https://doi.org/10.3389/fpls.2019.00040

Cheval, C., Samwald, S., Johnston, M.G., de Keijzer, J., Breakspear, A., Liu, X., Bellandi, A., Kadota, Y., Zipfel, C., Faulkner, C., 2020. Chitin perception in plasmodesmata characterizes submembrane immune-signaling specificity in plants. Proc Natl Acad Sci USA 117, 9621–9629. https://doi.org/10.1073/pnas.1907799117

Christersson, L., 2008. Poplar plantations for paper and energy in the south of Sweden. Biomass and Bioenergy 32, 997–1000. https://doi.org/10.1016/j.biombioe.2007.12.018

Chinchilla, D., Boller, T., Robatzek, S., 2007. Flagellin Signalling in Plant Immunity, in: Lambris, J.D. (Ed.), Current Topics in Innate Immunity, Advances in Experimental Medicine and Biology. Springer New York, New York, NY, pp. 358–371. https://doi.org/10.1007/978-0-387-71767-8_25

Colcombet, J., Hirt, H., 2008. Arabidopsis MAPKs: a complex signalling network involved in multiple biological processes. Biochemical Journal 413, 217–226. https://doi.org/10.1042/BJ20080625

Confalonieri, M., Belenghi, B., Balestrazzi, A., Negri, S., Facciotto, G., Schenone, G., Delledonne, M., 2000. Transformation of elite white poplar (*Populus alba L.*) cv. 'Villafranca' and evaluation of herbicide resistance. Plant Cell Reports 19, 978–982. https://doi.org/10.1007/s002990000230

Dangl, J.L., Jones, J.D.G., 2001. Plant pathogens and integrated defence responses to infection. Nature 411, 826–833. https://doi.org/10.1038/35081161

Dangl, J.L., Jones, J.D.G., 2019. A pentangular plant inflammasome. Science 364, 31–32. https://doi.org/10.1126/science.aax0174

Danielsen, L., Thürmer, A., Meinicke, P., Buée, M., Morin, E., Martin, F., Pilate, G., Daniel, R., Polle, A., Reich, M., 2012. Fungal soil communities in a young transgenic poplar plantation form a rich reservoir for fungal root communities. Ecol Evol 2, 1935–1948. https://doi.org/10.1002/ece3.305

de Jonge, R., Peter van Esse, H., Kombrink, A., Shinya, T., Desaki, Y., Bours, R., van der Krol, S., Shibuya, N., Joosten, M.H.A.J., Thomma, B.P.H.J., 2010. Conserved Fungal LysM Effector Ecp6 Prevents Chitin-Triggered Immunity in Plants. Science 329, 953–955. https://doi.org/10.1126/science.1190859

Dénarié, J., Debellé, F., Promé, J.-C., 1996. Rhizobium Lipo-Chitooligosaccharide Nodulation Factors: Signaling Molecules Mediating Recognition and Morphogenesis. Annu. Rev. Biochem. 65, 503–535. https://doi.org/10.1146/annurev.bi.65.070196.002443

Desaki, Y., Miyata, K., Suzuki, M., Shibuya, N., Kaku, H., 2018a. Plant immunity and symbiosis signaling mediated by LysM receptors. Innate Immun 24, 92–100. https://doi.org/10.1177/1753425917738885

Desaki, Y., Kouzai, Y., Ninomiya, Y., Iwase, R., Shimizu, Y., Seko, K., Molinaro, A., Minami, E., Shibuya, N., Kaku, H., Nishizawa, Y., 2018b. OsCERK1 plays a crucial role in the lipopolysaccharide-induced immune response of rice. New Phytol 217, 1042–1049. https://doi.org/10.1111/nph.14941

Desnoyer, N., Palanivelu, R., 2020. Bridging the GAPs in plant reproduction: a comparison of plant and animal GPI-anchored proteins. Plant Reprod 33, 129–142. https://doi.org/10.1007/s00497-020-00395-9

D'Haeze, W., Holsters, M., 2002. Nod factor structures, responses, and perception during initiation of nodule development. Glycobiology 12, 79R-105R. https://doi.org/10.1093/glycob/12.6.79R

Dillen, S.Y., Djomo, S.N., Al Afas, N., Vanbeveren, S., Ceulemans, R., 2013. Biomass yield and energy balance of a short-rotation poplar coppice with multiple clones on degraded land during 16 years. Biomass and Bioenergy 56, 157–165. https://doi.org/10.1016/j.biombioe.2013.04.019

Ding, L., Chen, Y., Wei, X., Ni, M., Zhang, J., Wang, H., Zhu, Z., Wei, J., 2017. Laboratory evaluation of transgenic *Populus davidiana × Populus bolleana* expressing Cry1Ac + SCK, Cry1Ah3, and Cry9Aa3 genes against gypsy moth and fall webworm. PLoS ONE 12, e0178754. https://doi.org/10.1371/journal.pone.0178754

Ding, L., Chen, Y., Ma, Y., Wang, H., Wei, J., 2020. Effective reduction in chimeric mutants of poplar trees produced by CRISPR/Cas9 through a second round of shoot regeneration. Plant Biotechnol Rep 14, 549–558. https://doi.org/10.1007/s11816-020-00629-2

Dimitriou, I., Rutz, D., 2015. Sustainable Short Rotation Coppice: A Handbook. WIP Renewable Energies. https://www.srcplus.eu/images/Handbook_SRCplus.pdf

Draper, J., 1997. Salicylate, superoxide synthesis and cell suicide in plant defence. Trends in Plant Science 2, 162–165. https://doi.org/10.1016/S1360-1385(97)01030-3

Du, N., Liu, X., Li, Y., Chen, S., Zhang, J., Ha, D., Deng, W., Sun, C., Zhang, Y., Pijut, P.M., 2012. Genetic transformation of *Populus tomentosa* to improve salt tolerance. Plant Cell Tiss Organ Cult 108, 181–189. https://doi.org/10.1007/s11240-011-0026-4

Dubiella, U., Seybold, H., Durian, G., Komander, E., Lassig, R., Witte, C.-P., Schulze, W.X., Romeis, T., 2013. Calcium-dependent protein kinase/NADPH oxidase activation circuit is required for rapid defense signal propagation. Proceedings of the National Academy of Sciences 110, 8744–8749. https://doi.org/10.1073/pnas.1221294110

Duplessis, S., Major, I., Martin, F., Séguin, A., 2009. Poplar and Pathogen Interactions: Insights from *Populus* Genome-Wide Analyses of Resistance and Defense Gene Families and Gene Expression Profiling. Critical Reviews in Plant Sciences 28, 309–334. https://doi.org/10.1080/07352680903241063

Eberl, F., Perreca, E., Vogel, H., Wright, L.P., Hammerbacher, A., Veit, D., Gershenzon, J., Unsicker, S.B., 2018. Rust Infection of Black Poplar Trees Reduces Photosynthesis but Does Not Affect Isoprene Biosynthesis or Emission. Front. Plant Sci. 9, 1733. https://doi.org/10.3389/fpls.2018.01733

Eckardt, N.A., 2008. Chitin Signaling in Plants: Insights into the Perception of Fungal Pathogens and Rhizobacterial Symbionts. Plant Cell 20, 241–243. https://doi.org/10.1105/tpc.108.058784

Eitas, T.K., Dangl, J.L., 2010. NB-LRR proteins: pairs, pieces, perception, partners, and pathways. Current Opinion in Plant Biology 13, 472–477. https://doi.org/10.1016/j.pbi.2010.04.007

El Yahyaoui, F., Küster, H., Ben Amor, B., Hohnjec, N., Pühler, A., Becker, A., Gouzy, J., Vernié, T., Gough, C., Niebel, A., Godiard, L., Gamas, P., 2004. Expression Profiling in *Medicago truncatula* Identifies More Than 750 Genes Differentially Expressed during Nodulation, Including Many Potential Regulators of the Symbiotic Program. Plant Physiol. 136, 3159–3176. https://doi.org/10.1104/pp.104.043612

Erwig, J., Ghareeb, H., Kopischke, M., Hacke, R., Matei, A., Petutschnig, E., Lipka, V., 2017. Chitin-induced and CHITIN ELICITOR RECEPTOR KINASE1 (CERK1) phosphorylation-dependent endocytosis of *Arabidopsis thaliana* LYSIN MOTIF-CONTAINING RECEPTOR-LIKE KINASE5 (LYK5). New Phytol 215, 382–396. https://doi.org/10.1111/nph.14592

Exterkate, F.A., Alting, A.C., Bruinenberg, P.G., 1993. Diversity of cell envelope proteinase specificity among strains of *Lactococcus lactis* and its relationship to charge characteristics of the substrate-binding region. Applied and Environmental Microbiology 59, 3640–3647. https://doi.org/10.1128/AEM.59.11.3640-3647.1993

Faulkner, C., Petutschnig, E., Benitez-Alfonso, Y., Beck, M., Robatzek, S., Lipka, V., Maule, A.J., 2013. LYM2-dependent chitin perception limits molecular flux via plasmodesmata. Proceedings of the National Academy of Sciences 110, 9166–9170. https://doi.org/10.1073/pnas.1203458110

Felten, J., Kohler, A., Morin, E., Bhalerao, R.P., Palme, K., Martin, F., Ditengou, F.A., Legué, V., 2009. The Ectomycorrhizal Fungus *Laccaria bicolor* Stimulates Lateral Root Formation in Poplar and Arabidopsis through Auxin Transport and Signaling. Plant Physiol. 151, 1991–2005. https://doi.org/10.1104/pp.109.147231

Feng, Z., Mao, Y., Xu, N., Zhang, B., Wei, P., Yang, D.-L., Wang, Z., Zhang, Z., Zheng, R., Yang, L., Zeng, L., Liu, X., Zhu, J.-K., 2014. Multigeneration analysis reveals the inheritance, specificity, and patterns of CRISPR/Cas-induced gene modifications in Arabidopsis. Proceedings of the National Academy of Sciences 111, 4632–4637. https://doi.org/10.1073/pnas.1400822111

Feng, F., Sun, J., Radhakrishnan, G.V., Lee, T., Bozsóki, Z., Fort, S., Gavrin, A., Gysel, K., Thygesen, M.B., Andersen, K.R., Radutoiu, S., Stougaard, J., Oldroyd, G.E.D., 2019. A combination of chitooligosaccharide and lipochitooligosaccharide recognition promotes arbuscular mycorrhizal associations in *Medicago truncatula*. Nat Commun 10, 5047. https://doi.org/10.1038/s41467-019-12999-5

Force, A., Lynch, M., Pickett, F.B., Amores, A., Yan, Y.L., Postlethwait, J., 1999. Preservation of duplicate genes by complementary, degenerative mutations. Genetics 151, 1531–1545.

Gange, A.C., Gane, D.R.J., Chen, Y., Gong, M., 2005. Dual colonization of *Eucalyptus urophylla* S.T. Blake by arbuscular and ectomycorrhizal fungi affects levels of insect herbivore attack. Agric Forest Ent 7, 253–263. https://doi.org/10.1111/j.1461-9555.2005.00268.x

Gao, M., Liu, J., Bi, D., Zhang, Z., Cheng, F., Chen, S., Zhang, Y., 2008. MEKK1, MKK1/MKK2 and MPK4 function together in a mitogen-activated protein kinase cascade to regulate innate immunity in plants. Cell Res 18, 1190–1198. https://doi.org/10.1038/cr.2008.300

Genre, A., Chabaud, M., Balzergue, C., Puech-Pagès, V., Novero, M., Rey, T., Fournier, J., Rochange, S., Bécard, G., Bonfante, P., Barker, D.G., 2013. Short-chain chitin oligomers from arbuscular mycorrhizal fungi trigger nuclear Ca2+ spiking in *Medicago truncatula* roots and their production is enhanced by strigolactone. New Phytol 198, 190–202. https://doi.org/10.1111/nph.12146

Germain, H., Séguin, A., 2011. Innate immunity: has poplar made its BED? New Phytologist 189, 678–687. https://doi.org/10.1111/j.1469-8137.2010.03544.x

Gibelin-Viala, C., Amblard, E., Puech-Pages, V., Bonhomme, M., Garcia, M., Bascaules-Bedin, A., Fliegmann, J., Wen, J., Mysore, K.S., Signor, C., Jacquet, C., Gough, C., 2019. The *Medicago truncatula* LysM receptor-like kinase LYK9 plays a dual role in immunity and the arbuscular mycorrhizal symbiosis. New Phytol 223, 1516–1529. https://doi.org/10.1111/nph.15891

Goodstein, D.M., Shu, S., Howson, R., Neupane, R., Hayes, R.D., Fazo, J., Mitros, T., Dirks, W., Hellsten, U., Putnam, N., Rokhsar, D.S., 2012. Phytozome: a comparative platform for green plant genomics. Nucleic Acids Research 40, D1178–D1186. https://doi.org/10.1093/nar/gkr944

Gortari, F., Guiamet, J.J., Graciano, C., 2018. Plant–pathogen interactions: leaf physiology alterations in poplars infected with rust (*Melampsora medusae*). Tree Physiology 38, 925–935. https://doi.org/10.1093/treephys/tpx174

Gou, X., Yin, H., He, K., Du, J., Yi, J., Xu, S., Lin, H., Clouse, S.D., Li, J., 2012. Genetic Evidence for an Indispensable Role of Somatic Embryogenesis Receptor Kinases in Brassinosteroid Signaling. PLoS Genet 8, e1002452. https://doi.org/10.1371/journal.pgen.1002452

Gui, J., Lam, P.Y., Tobimatsu, Y., Sun, J., Huang, C., Cao, S., Zhong, Y., Umezawa, T., Li, L., 2020. Fibre-specific regulation of lignin biosynthesis improves biomass quality in Populus. New Phytol 226, 1074–1087. https://doi.org/10.1111/nph.16411

Guo, Q., Lu, N., Sun, Y., Lv, W., Luo, Z., Zhang, H., Ji, Q., Yang, Q., Chen, S., Zhang, W., Li, Y., 2019. Heterologous Expression of the DREB Transcription Factor *AhDREB* in *Populus tomentosa* Carrière Confers Tolerance to Salt without Growth Reduction under Greenhouse Conditions. Forests 10, 214. https://doi.org/10.3390/f10030214

Gust, A.A., Willmann, R., Desaki, Y., Grabherr, H.M., Nürnberger, T., 2012. Plant LysM proteins: modules mediating symbiosis and immunity. Trends in Plant Science 17, 495–502. https://doi.org/10.1016/j.tplants.2012.04.003

Hacquard, S., Petre, B., Frey, P., Hecker, A., Rouhier, N., Duplessis, S., 2011. The Poplar-Poplar Rust Interaction: Insights from Genomics and Transcriptomics. Journal of Pathogens 2011, 1–11. https://doi.org/10.4061/2011/716041

Hanks, S.K., Hunter, T., 1995. The eukaryotic protein kinase superfamily: kinase (catalytic) domain structure and classification 1. FASEB j. 9, 576–596. https://doi.org/10.1096/fasebj.9.8.7768349

Hayafune, M., Berisio, R., Marchetti, R., Silipo, A., Kayama, M., Desaki, Y., Arima, S., Squeglia, F., Ruggiero, A., Tokuyasu, K., Molinaro, A., Kaku, H., Shibuya, N., 2014. Chitin-induced activation of immune signaling by the rice receptor CEBiP relies on a unique sandwich-type dimerization. Proceedings of the National Academy of Sciences 111, E404–E413. https://doi.org/10.1073/pnas.1312099111

He, J., Zhang, C., Dai, H., Liu, H., Zhang, X., Yang, J., Chen, X., Zhu, Y., Wang, D., Qi, X., Li, W., Wang, Z., An, G., Yu, N., He, Z., Wang, Y.-F., Xiao, Y., Zhang, P., Wang, E., 2019. A LysM Receptor Heteromer Mediates Perception of Arbuscular Mycorrhizal Symbiotic Signal in Rice. Molecular Plant 12, 1561–1576. https://doi.org/10.1016/j.molp.2019.10.015

Héricourt, F., Chefdor, F., Djeghdir, I., Larcher, M., Lafontaine, F., Courdavault, V., Auguin, D., Coste, F., Depierreux, C., Tanigawa, M., Maeda, T., Glévarec, G., Carpin, S., 2016. Functional Divergence of Poplar Histidine-Aspartate Kinase HK1 Paralogs in Response to Osmotic Stress. IJMS 17, 2061. https://doi.org/10.3390/ijms17122061

Horn, M.A., Walker, J.C., 1994. Biochemical properties of the autophosphorylation of RLK5, a receptor-like protein kinase from *Arabidopsis thaliana*. Biochimica et Biophysica Acta (BBA) - Protein Structure and Molecular Enzymology 1208, 65–74. https://doi.org/10.1016/0167-4838(94)90160-0

Hou, J., Wei, S., Pan, H., Zhuge, Q., Yin, T., 2019. Uneven selection pressure accelerating divergence of *Populus* and *Salix*. Hortic Res 6, 37. https://doi.org/10.1038/s41438-019-0121-y

Howells, R.M., Craze, M., Bowden, S., Wallington, E.J., 2018. Efficient generation of stable, heritable gene edits in wheat using CRISPR/Cas9. BMC Plant Biol 18, 215. https://doi.org/10.1186/s12870-018-1433-z

Hsu, P.D., Scott, D.A., Weinstein, J.A., Ran, F.A., Konermann, S., Agarwala, V., Li, Y., Fine, E.J., Wu, X., Shalem, O., Cradick, T.J., Marraffini, L.A., Bao, G., Zhang, F., 2013. DNA targeting specificity of RNA-guided Cas9 nucleases. Nat Biotechnol 31, 827–832. https://doi.org/10.1038/nbt.2647

Ishihama, N., Yoshioka, H., 2012. Post-translational regulation of WRKY transcription factors in plant immunity. Current Opinion in Plant Biology 15, 431–437. https://doi.org/10.1016/j.pbi.2012.02.003

Ichimura, K., Shinozaki, K., Tena, G., Sheen, J., Henry, Y., Champion, A., Kreis, M., Zhang, S., Hirt, H., Wilson, C., Heberle-Bors, E., Ellis, B.E., Morris, P.C., Innes, R.W., Ecker, J.R., Scheel, D., Klessig, D.F., Machida, Y., Mundy, J., Ohashi, Y., Walker, J.C., 2002. Mitogen-activated protein kinase cascades in plants: a new nomenclature. Trends in Plant Science 7, 301–308. https://doi.org/10.1016/S1360-1385(02)02302-6

Ichimura, K., Casais, C., Peck, S.C., Shinozaki, K., Shirasu, K., 2006. MEKK1 Is Required for MPK4 Activation and Regulates Tissue-specific and Temperature-dependent Cell Death in Arabidopsis. Journal of Biological Chemistry 281, 36969–36976. https://doi.org/10.1074/jbc.M605319200

Jacobs, T.B., LaFayette, P.R., Schmitz, R.J., Parrott, W.A., 2015. Targeted genome modifications in soybean with CRISPR/Cas9. BMC Biotechnol 15, 16. https://doi.org/10.1186/s12896-015-0131-2

Jansson, S., Douglas, C.J., 2007. *Populus*: A Model System for Plant Biology. Annu. Rev. Plant Biol. 58, 435–458. https://doi.org/10.1146/annurev.arplant.58.032806.103956

Jain, D., Khurana, J.P., 2018. Role of Pathogenesis-Related (PR) Proteins in Plant Defense Mechanism, in: Singh, A., Singh, I.K. (Eds.), Molecular Aspects of Plant-Pathogen Interaction. Springer Singapore, Singapore, pp. 265–281. https://doi.org/10.1007/978-981-10-7371-7_12

Jiang, Y., Ye, J., Veromann, L.-L., Niinemets, Ü., 2016. Scaling of photosynthesis and constitutive and induced volatile emissions with severity of leaf infection by rust fungus (*Melampsora larici-populina*) in *Populus balsamifera* var. *suaveolens*. Tree Physiol 36, 856–872. https://doi.org/10.1093/treephys/tpw035

Jiang, Y., Guo, L., Ma, X., Zhao, X., Jiao, B., Li, C., Luo, K., 2017. The WRKY transcription factors PtrWRKY18 and PtrWRKY35 promote *Melampsora* resistance in Populus. Tree Physiology 37, 665–675. https://doi.org/10.1093/treephys/tpx008

Jinek, M., Chylinski, K., Fonfara, I., Hauer, M., Doudna, J.A., Charpentier, E., 2012. A Programmable Dual-RNA-Guided DNA Endonuclease in Adaptive Bacterial Immunity. Science 337, 816–821. https://doi.org/10.1126/science.1225829

Jones, J.D.G., Dangl, J.L., 2006. The plant immune system. Nature 444, 323–329. https://doi.org/10.1038/nature05286

Jones, P., Binns, D., Chang, H.-Y., Fraser, M., Li, W., McAnulla, C., McWilliam, H., Maslen, J., Mitchell, A., Nuka, G., Pesseat, S., Quinn, A.F., Sangrador-Vegas, A., Scheremetjew, M., Yong, S.-Y., Lopez, R., Hunter, S., 2014. InterProScan 5: genome-scale protein function classification. Bioinformatics 30, 1236–1240. https://doi.org/10.1093/bioinformatics/btu031

Jorge, V., Dowkiw, A., Faivre-Rampant, P., Bastien, C., 2005. Genetic architecture of qualitative and quantitative *Melampsora larici-populina* leaf rust resistance in hybrid poplar: genetic mapping and QTL detection. New Phytologist 167, 113–127. https://doi.org/10.1111/j.1469-8137.2005.01424.x

Jubic, L.M., Saile, S., Furzer, O.J., El Kasmi, F., Dangl, J.L., 2019. Help wanted: helper NLRs and plant immune responses. Current Opinion in Plant Biology 50, 82–94. https://doi.org/10.1016/j.pbi.2019.03.013

Kadota, Y., Sklenar, J., Derbyshire, P., Stransfeld, L., Asai, S., Ntoukakis, V., Jones, J.D., Shirasu, K., Menke, F., Jones, A., Zipfel, C., 2014. Direct Regulation of the NADPH Oxidase RBOHD by the PRR-Associated Kinase BIK1 during Plant Immunity. Molecular Cell 54, 43–55. https://doi.org/10.1016/j.molcel.2014.02.021

Kadota, Y., Shirasu, K., Zipfel, C., 2015. Regulation of the NADPH Oxidase RBOHD During Plant Immunity. Plant Cell Physiol 56, 1472–1480. https://doi.org/10.1093/pcp/pcv063

Kaku, H., Nishizawa, Y., Ishii-Minami, N., Akimoto-Tomiyama, C., Dohmae, N., Takio, K., Minami, E., Shibuya, N., 2006. Plant cells recognize chitin fragments for defense signaling through a plasma membrane receptor. Proceedings of the National Academy of Sciences 103, 11086–11091. https://doi.org/10.1073/pnas.0508882103

Kaling, M., Schmidt, A., Moritz, F., Rosenkranz, M., Witting, M., Kasper, K., Janz, D., Schmitt-Kopplin, P., Schnitzler, J.-P., Polle, A., 2018. Mycorrhiza-Triggered Transcriptomic and Metabolomic Networks Impinge on Herbivore Fitness. Plant Physiol. 176, 2639–2656. https://doi.org/10.1104/pp.17.01810

Kawasaki, T., Yamada, K., Yoshimura, S., Yamaguchi, K., 2017. Chitin receptor-mediated activation of MAP kinases and ROS production in rice and Arabidopsis. Plant Signaling & Behavior 12, e1361076. https://doi.org/10.1080/15592324.2017.1361076

Kearse, M., Moir, R., Wilson, A., Stones-Havas, S., Cheung, M., Sturrock, S., Buxton, S., Cooper, A., Markowitz, S., Duran, C., Thierer, T., Ashton, B., Meintjes, P., Drummond, A., 2012. Geneious Basic: An integrated and extendable desktop software platform for the organization and analysis of sequence data. Bioinformatics 28, 1647–1649. https://doi.org/10.1093/bioinformatics/bts199

Kohler, A., Rinaldi, C., Duplessis, S., Baucher, M., Geelen, D., Duchaussoy, F., Meyers, B.C., Boerjan, W., Martin, F., 2008. Genome-wide identification of NBS resistance genes in Populus trichocarpa. Plant Mol Biol 66, 619–636. https://doi.org/10.1007/s11103-008-9293-9

Kouchi, H., Shimomura, K., Hata, S., Hirota, A., Wu, G., Kumagai, H., Tajima, S., Suganuma, N., Suzuki, A., Aoki, T., Hayashi, M., Yokoyama, T., Ohyama, T., Asamizu, E., Kuwata, C., Shibata, D., Tabata, S., 2004. Large-Scale Analysis of Gene Expression Profiles during Early Stages of Root Nodule Formation in a Model Legume, *Lotus japonicus*. DNA Research 11, 263–274. https://doi.org/10.1093/dnares/11.4.263

Kouzai, Y., Nakajima, K., Hayafune, M., Ozawa, K., Kaku, H., Shibuya, N., Minami, E., Nishizawa, Y., 2014a. CEBiP is the major chitin oligomer-binding protein in rice and plays a main role in the perception of chitin oligomers. Plant Mol Biol 84, 519–528. https://doi.org/10.1007/s11103-013-0149-6

Kouzai, Y., Mochizuki, S., Nakajima, K., Desaki, Y., Hayafune, M., Miyazaki, H., Yokotani, N., Ozawa, K., Minami, E., Kaku, H., Shibuya, N., Nishizawa, Y., 2014b. Targeted Gene Disruption of OsCERK1 Reveals Its Indispensable Role in Chitin Perception and Involvement in the Peptidoglycan Response and Immunity in Rice. MPMI 27, 975–982. https://doi.org/10.1094/MPMI-03-14-0068-R

Kunz, J., Fuelling, A., Kolbe, L., Anderson, R.A., 2002. Stereo-specific Substrate Recognition by Phosphatidylinositol Phosphate Kinases Is Swapped by Changing a Single Amino Acid Residue. Journal of Biological Chemistry 277, 5611–5619. https://doi.org/10.1074/jbc.M110775200

Lassowskat, I., Böttcher, C., Eschen-Lippold, L., Scheel, D., Lee, J., 2014. Sustained mitogen-activated protein kinase activation reprograms defense metabolism and phosphoprotein profile in Arabidopsis thaliana. Front. Plant Sci. 5. https://doi.org/10.3389/fpls.2014.00554

Laurans, F., Pilate, G., 1999. Histological Aspects of a Hypersensitive Response in Poplar to *Melampsora larici-populin*a. Phytopathology 89, 233–238. https://doi.org/10.1094/PHYTO.1999.89.3.233

Lebedev, V.G., Faskhiev, V.N., Kovalenko, N.P., Shestibratov, K.A., Miroshnikov, A.I., 2016. Testing transgenic aspen plants with bar gene for herbicide resistance under semi-natural conditions. Acta Naturae 8(2):29, 92-101. URL: https://cyberleninka.ru/article/n/testing-transgenic-aspen-plants-with-bar-gene-for-herbicide-resistance-under-semi-natural-conditions (19.10.2021).

Lee, W.-S., Rudd, J.J., Hammond-Kosack, K.E., Kanyuka, K., 2014. Mycosphaerella graminicola LysM Effector-Mediated Stealth Pathogenesis Subverts Recognition Through Both CERK1 and CEBiP Homologues in Wheat. MPMI 27, 236–243. https://doi.org/10.1094/MPMI-07-13-0201-R

Lefebvre, B., Klaus-Heisen, D., Pietraszewska-Bogiel, A., Hervé, C., Camut, S., Auriac, M.-C., Gasciolli, V., Nurisso, A., Gadella, T.W.J., Cullimore, J., 2012. Role of N-Glycosylation Sites and CXC Motifs in Trafficking of *Medicago truncatula* Nod Factor Perception Protein to Plasma Membrane. Journal of Biological Chemistry 287, 10812–10823. https://doi.org/10.1074/jbc.M111.281634

Leppyanen, I., Shakhnazarova, V., Shtark, O., Vishnevskaya, N., Tikhonovich, I., Dolgikh, E., 2017. Receptor-Like Kinase LYK9 in Pisum sativum L. Is the CERK1-Like Receptor that Controls Both Plant Immunity and AM Symbiosis Development. IJMS 19, 8. https://doi.org/10.3390/ijms19010008

Levine, A., Tenhaken, R., Dixon, R., Lamb, C., 1994. H2O2 from the oxidative burst orchestrates the plant hypersensitive disease resistance response. Cell 79, 583–593. https://doi.org/10.1016/0092-8674(94)90544-4

Li, J., Wen, J., Lease, K.A., Doke, J.T., Tax, F.E., Walker, J.C., 2002. BAK1, an Arabidopsis LRR Receptor-like Protein Kinase, Interacts with BRI1 and Modulates Brassinosteroid Signaling. Cell 110, 213–222. https://doi.org/10.1016/S0092-8674(02)00812-7

Li, G., Meng, X., Wang, R., Mao, G., Han, L., Liu, Y., Zhang, S., 2012a. Dual-Level Regulation of ACC Synthase Activity by MPK3/MPK6 Cascade and Its Downstream WRKY Transcription Factor during Ethylene Induction in Arabidopsis. PLoS Genet 8, e1002767. https://doi.org/10.1371/journal.pgen.1002767

Li, W., Zhao, Y., Liu, C., Yao, G., Wu, S., Hou, C., Zhang, M., Wang, D., 2012b. Callose deposition at plasmodesmata is a critical factor in restricting the cell-to-cell movement of Soybean mosaic virus. Plant Cell Rep 31, 905–916. https://doi.org/10.1007/s00299-011-1211-y

Li, J., Manghwar, H., Sun, L., Wang, P., Wang, G., Sheng, H., Zhang, J., Liu, H., Qin, L., Rui, H., Li, B., Lindsey, K., Daniell, H., Jin, S., Zhang, X., 2019. Whole genome sequencing reveals rare off-target mutations and considerable inherent genetic or/and somaclonal variations in CRISPR /Cas9-edited cotton plants. Plant Biotechnol J 17, 858–868. https://doi.org/10.1111/pbi.13020

Liang, Y., Cao, Y., Tanaka, K., Thibivilliers, S., Wan, J., Choi, J., Kang, C. h., Qiu, J., Stacey, G., 2013. Nonlegumes Respond to Rhizobial Nod Factors by Suppressing the Innate Immune Response. Science 341, 1384–1387. https://doi.org/10.1126/science.1242736

Liang, Y., Tóth, K., Cao, Y., Tanaka, K., Espinoza, C., Stacey, G., 2014. Lipochitooligosaccharide recognition: an ancient story. New Phytol 204, 289–296. https://doi.org/10.1111/nph.12898

Liao, D., Sun, X., Wang, N., Song, F., Liang, Y., 2018. Tomato LysM Receptor-Like Kinase SlLYK12 Is Involved in Arbuscular Mycorrhizal Symbiosis. Front. Plant Sci. 9, 1004. https://doi.org/10.3389/fpls.2018.01004

Limpens, E., Franken, C., Smit, P., Willemse, J., Bisseling, T., Geurts, R., 2003. LysM Domain Receptor Kinases Regulating Rhizobial Nod Factor-Induced Infection. Science 302, 630–633. https://doi.org/10.1126/science.1090074

Limpens, E., van Zeijl, A., Geurts, R., 2015. Lipochitooligosaccharides Modulate Plant Host Immunity to Enable Endosymbioses. Annu. Rev. Phytopathol. 53, 311–334. https://doi.org/10.1146/annurev-phyto-080614-120149

Littlewood, J., Guo, M., Boerjan, W., Murphy, R.J., 2014. Bioethanol from poplar: a commercially viable alternative to fossil fuel in the European Union. Biotechnol Biofuels 7, 113. https://doi.org/10.1186/1754-6834-7-113

Liu, Y., Zhang, S., 2004. Phosphorylation of 1-Aminocyclopropane-1-Carboxylic Acid Synthase by MPK6, a Stress-Responsive Mitogen-Activated Protein Kinase, Induces Ethylene Biosynthesis in Arabidopsis. The Plant Cell 16, 3386–3399. https://doi.org/10.1105/tpc.104.026609

Liu, J., Maldonado-Mendoza, I., Lopez-Meyer, M., Cheung, F., Town, C.D., Harrison, M.J., 2007. Arbuscular mycorrhizal symbiosis is accompanied by local and systemic alterations in gene expression and an increase in disease resistance in the shoots: Local and systemic alterations in transcript profiles in AM symbiosis. The Plant Journal 50, 529–544. https://doi.org/10.1111/j.1365-313X.2007.03069.x

Liu, T., Liu, Z., Song, C., Hu, Y., Han, Z., She, J., Fan, F., Wang, J., Jin, C., Chang, J., Zhou, J.-M., Chai, J., 2012a. Chitin-Induced Dimerization Activates a Plant Immune Receptor. Science 336, 1160–1164. https://doi.org/10.1126/science.1218867

Liu, B., Li, J.-F., Ao, Y., Qu, J., Li, Z., Su, J., Zhang, Y., Liu, J., Feng, D., Qi, K., He, Y., Wang, J., Wang, H.-B., 2012b. Lysin Motif–Containing Proteins LYP4 and LYP6 Play Dual Roles in Peptidoglycan and Chitin Perception in Rice Innate Immunity. Plant Cell 24, 3406–3419. https://doi.org/10.1105/tpc.112.102475

Liu, T., Sheng, M., Wang, C.Y., Chen, H., Li, Z., Tang, M., 2015. Impact of arbuscular mycorrhizal fungi on the growth, water status, and photosynthesis of hybrid poplar under drought stress and recovery. Photosynt. 53, 250–258. https://doi.org/10.1007/s11099-015-0100-y

Liu, D., Zhang, J., Dong, Y., Zhang, X., Yang, M., Gao, B., 2016a. Genetic transformation and expression of Cry1Ac–Cry3A–NTHK1 genes in Populus × euramericana "Neva." Acta Physiol Plant 38, 177. https://doi.org/10.1007/s11738-016-2195-6

Liu, S., Wang, J., Han, Z., Gong, X., Zhang, H., Chai, J., 2016b. Molecular Mechanism for Fungal Cell Wall Recognition by Rice Chitin Receptor OsCEBiP. Structure 24, 1192–1200. https://doi.org/10.1016/j.str.2016.04.014

Liu, J., Liu, B., Chen, S., Gong, B.-Q., Chen, L., Zhou, Q., Xiong, F., Wang, M., Feng, D., Li, J.-F., Wang, H.-B., Wang, J., 2018. A Tyrosine Phosphorylation Cycle Regulates Fungal Activation of a Plant Receptor Ser/Thr Kinase. Cell Host & Microbe 23, 241-253.e6. https://doi.org/10.1016/j.chom.2017.12.005

Lu, J., Zhao, H., Wei, J., He, Y., Shi, C., Wang, H., Song, Y., 2004. Lignin reduction in transgenic poplars by expressing antisense CCoAOMT gene. Progress in Natural Sc. 14, 1060–1063. https://doi.org/10.1080/10020070412331344801

Luna, E., Pastor, V., Robert, J., Flors, V., Mauch-Mani, B., Ton, J., 2011. Callose Deposition: A Multifaceted Plant Defense Response. MPMI 24, 183–193. https://doi.org/10.1094/MPMI-07-10-0149

Lv, Z., Huang, Y., Ma, B., Xiang, Z., He, N., 2018. LysM1 in MmLYK2 is a motif required for the interaction of MmLYP1 and MmLYK2 in the chitin signaling. Plant Cell Rep 37, 1101–1112. https://doi.org/10.1007/s00299-018-2295-4

Ma, X., Zhang, Q., Zhu, Q., Liu, W., Chen, Yan, Qiu, R., Wang, B., Yang, Z., Li, H., Lin, Y., Xie, Y., Shen, R., Chen, S., Wang, Z., Chen, Yuanling, Guo, J., Chen, L., Zhao, X., Dong, Z., Liu, Y.-G., 2015. A Robust CRISPR/Cas9 System for Convenient, High-Efficiency Multiplex Genome Editing in Monocot and Dicot Plants. Molecular Plant 8, 1274–1284. https://doi.org/10.1016/j.molp.2015.04.007

Macho, A.P., Zipfel, C., 2014. Plant PRRs and the Activation of Innate Immune Signaling. Molecular Cell 54, 263–272. https://doi.org/10.1016/j.molcel.2014.03.028

Madeira, F., Park, Y. mi, Lee, J., Buso, N., Gur, T., Madhusoodanan, N., Basutkar, P., Tivey, A.R.N., Potter, S.C., Finn, R.D., Lopez, R., 2019. The EMBL-EBI search and sequence analysis tools APIs in 2019. Nucleic Acids Research 47, W636–W641. https://doi.org/10.1093/nar/gkz268

Madsen, E.B., Madsen, L.H., Radutoiu, S., Olbryt, M., Rakwalska, M., Szczyglowski, K., Sato, S., Kaneko, T., Tabata, S., Sandal, N., Stougaard, J., 2003. A receptor kinase gene of the LysM type is involved in legume perception of rhizobial signals. Nature 425, 637–640. https://doi.org/10.1038/nature02045

Madsen, E.B., Antolín-Llovera, M., Grossmann, C., Ye, J., Vieweg, S., Broghammer, A., Krusell, L., Radutoiu, S., Jensen, O.N., Stougaard, J., Parniske, M., 2011. Autophosphorylation is essential for the in vivo function of the *Lotus japonicus* Nod factor receptor 1 and receptor-mediated signalling in cooperation with Nod factor receptor 5: NFR1 and NFR5 phosphorylation and signalling. The Plant Journal 65, 404–417. https://doi.org/10.1111/j.1365-313X.2010.04431.x

Maillet, F., Poinsot, V., André, O., Puech-Pagès, V., Haouy, A., Gueunier, M., Cromer, L., Giraudet, D., Formey, D., Niebel, A., Martinez, E.A., Driguez, H., Bécard, G., Dénarié, J., 2011. Fungal lipochitooligosaccharide symbiotic signals in arbuscular mycorrhiza. Nature 469, 58–63. https://doi.org/10.1038/nature09622

Malabarba, J., Chevreau, E., Dousset, N., Veillet, F., Moizan, J., Vergne, E., 2020. New Strategies to Overcome Present CRISPR/Cas9 Limitations in Apple and Pear: Efficient Dechimerization and Base Editing. IJMS 22, 319. https://doi.org/10.3390/ijms22010319

Mao, G., Meng, X., Liu, Y., Zheng, Z., Chen, Z., Zhang, S., 2011. Phosphorylation of a WRKY Transcription Factor by Two Pathogen-Responsive MAPKs Drives Phytoalexin Biosynthesis in Arabidopsis. The Plant Cell 23, 1639–1653. https://doi.org/10.1105/tpc.111.084996

Maqbool, A., Horler, R.S.P., Muller, A., Wilkinson, A.J., Wilson, K.S., Thomas, G.H., 2015. The substrate-binding protein in bacterial ABC transporters: dissecting roles in the evolution of substrate specificity. Biochemical Society Transactions 43, 1011–1017. https://doi.org/10.1042/BST20150135

Mélida, H., Sopeña-Torres, S., Bacete, L., Garrido-Arandia, M., Jordá, L., López, G., Muñoz-Barrios, A., Pacios, L.F., Molina, A., 2018. Non-branched β-1,3-glucan oligosaccharides trigger immune responses in Arabidopsis. Plant J 93, 34–49. https://doi.org/10.1111/tpj.13755

Mentag, R., Luckevich, M., Morency, M.-J., Seguin, A., 2003. Bacterial disease resistance of transgenic hybrid poplar expressing the synthetic antimicrobial peptide D4E1. Tree Physiology 23, 405–411. https://doi.org/10.1093/treephys/23.6.405

Meyermans, H., Morreel, K., Lapierre, C., Pollet, B., De Bruyn, A., Busson, R., Herdewijn, P., Devreese, B., Van Beeumen, J., Marita, J.M., Ralph, J., Chen, C., Burggraeve, B., Van Montagu, M., Messens, E., Boerjan, W., 2000. Modifications in Lignin and Accumulation of Phenolic Glucosides in Poplar Xylem upon Down-regulation of Caffeoyl-Coenzyme A O-Methyltransferase, an Enzyme Involved in Lignin Biosynthesis. Journal of Biological Chemistry 275, 36899–36909. https://doi.org/10.1074/jbc.M006915200

Meyers, B.C., Kozik, A., Griego, A., Kuang, H., Michelmore, R.W., 2003. Genome-Wide Analysis of NBS-LRR–Encoding Genes in Arabidopsis. The Plant Cell 15, 809–834. https://doi.org/10.1105/tpc.009308

Miranda, M., Ralph, S.G., Mellway, R., White, R., Heath, M.C., Bohlmann, J., Constabel, C.P., 2007. The Transcriptional Response of Hybrid Poplar (*Populus trichocarpa x P. deltoides*) to Infection by *Melampsora medusae* Leaf Rust Involves Induction of Flavonoid Pathway Genes Leading to the Accumulation of Proanthocyanidins. MPMI 20, 816–831. https://doi.org/10.1094/MPMI-20-7-0816

Mithöfer, A., 2002. Suppression of plant defence in rhizobia–legume symbiosis. Trends in Plant Science 7, 440–444. https://doi.org/10.1016/S1360-1385(02)02336-1

Miya, A., Albert, P., Shinya, T., Desaki, Y., Ichimura, K., Shirasu, K., Narusaka, Y., Kawakami, N., Kaku, H., Shibuya, N., 2007. CERK1, a LysM receptor kinase, is essential for chitin elicitor signaling in Arabidopsis. Proceedings of the National Academy of Sciences 104, 19613–19618. https://doi.org/10.1073/pnas.0705147104

Miyata, K., Kozaki, T., Kouzai, Y., Ozawa, K., Ishii, K., Asamizu, E., Okabe, Y., Umehara, Y., Miyamoto, A., Kobae, Y., Akiyama, K., Kaku, H., Nishizawa, Y., Shibuya, N., Nakagawa, T., 2014. The Bifunctional Plant Receptor, OsCERK1, Regulates Both Chitin-Triggered Immunity and Arbuscular Mycorrhizal Symbiosis in Rice. Plant and Cell Physiology 55, 1864–1872. https://doi.org/10.1093/pcp/pcu129

Miyata, K., Hayafune, M., Kobae, Y., Kaku, H., Nishizawa, Y., Masuda, Y., Shibuya, N., Nakagawa, T., 2016. Evaluation of the Role of the LysM Receptor-Like Kinase, OsNFR5/OsRLK2 for AM Symbiosis in Rice. Plant Cell Physiol 57, 2283–2290. https://doi.org/10.1093/pcp/pcw144

Moling, S., Pietraszewska-Bogiel, A., Postma, M., Fedorova, E., Hink, M.A., Limpens, E., Gadella, T.W.J., Bisseling, T., 2014. Nod Factor Receptors Form Heteromeric Complexes and Are Essential for Intracellular Infection in *Medicago* Nodules. Plant Cell 26, 4188–4199. https://doi.org/10.1105/tpc.114.129502

Mulder, L., Lefebvre, B., Cullimore, J., Imberty, A., 2006. LysM domains of *Medicago truncatula* NFP protein involved in Nod factor perception. Glycosylation state, molecular modeling and docking of chitooligosaccharides and Nod factors. Glycobiology 16, 801–809. https://doi.org/10.1093/glycob/cwl006

Murakami, E., Cheng, J., Gysel, K., Bozsoki, Z., Kawaharada, Y., Hjuler, C.T., Sørensen, K.K., Tao, K., Kelly, S., Venice, F., Genre, A., Thygesen, M.B., Jong, N. de, Vinther, M., Jensen, D.B., Jensen, K.J., Blaise, M., Madsen, L.H., Andersen, K.R., Stougaard, J., Radutoiu, S., 2018. Epidermal LysM receptor ensures robust symbiotic signalling in *Lotus japonicus*. eLife 7, e33506. https://doi.org/10.7554/eLife.33506

Ngou, B.P.M., Ahn, H.-K., Ding, P., Jones, J.D.G., 2021. Mutual potentiation of plant immunity by cell-surface and intracellular receptors. Nature. https://doi.org/10.1038/s41586-021-03315-7

Noël, A., Levasseur, C., Le, V.Q., Séguin, A., 2005. Enhanced resistance to fungal pathogens in forest trees by genetic transformation of black spruce and hybrid poplar with a *Trichoderma harzianum* endochitinase gene. Physiological and Molecular Plant Pathology 67, 92–99. https://doi.org/10.1016/j.pmpp.2005.09.010

Nühse, T.S., Bottrill, A.R., Jones, A.M.E., Peck, S.C., 2007. Quantitative phosphoproteomic analysis of plasma membrane proteins reveals regulatory mechanisms of plant innate immune responses: Quantitative phosphoproteomics for signalling pathways. The Plant Journal 51, 931–940. https://doi.org/10.1111/j.1365-313X.2007.03192.x

Ogasawara, Y., Kaya, H., Hiraoka, G., Yumoto, F., Kimura, S., Kadota, Y., Hishinuma, H., Senzaki, E., Yamagoe, S., Nagata, K., Nara, M., Suzuki, K., Tanokura, M., Kuchitsu, K., 2008. Synergistic Activation of the Arabidopsis NADPH Oxidase AtrbohD by Ca^{2+} and Phosphorylation. J. Biol. Chem. 283, 8885–8892. https://doi.org/10.1074/jbc.M708106200

Ortiz-Morea, F.A., He, P., Shan, L., Russinova, E., 2020. It takes two to tango – molecular links between plant immunity and brassinosteroid signalling. J Cell Sci 133, jcs246728. https://doi.org/10.1242/jcs.246728

Pan, C., Ye, L., Qin, L., Liu, X., He, Y., Wang, J., Chen, L., Lu, G., 2016. CRISPR/Cas9-mediated efficient and heritable targeted mutagenesis in tomato plants in the first and later generations. Sci Rep 6, 24765. https://doi.org/10.1038/srep24765

Pandey, S.P., Somssich, I.E., 2009. The Role of WRKY Transcription Factors in Plant Immunity. Plant Physiol. 150, 1648–1655. https://doi.org/10.1104/pp.109.138990

Petre, B., Morin, E., Tisserant, E., Hacquard, S., Da Silva, C., Poulain, J., Delaruelle, C., Martin, F., Rouhier, N., Kohler, A., Duplessis, S., 2012. RNA-Seq of Early-Infected Poplar Leaves by the Rust Pathogen *Melampsora larici-populina* Uncovers PtSultr3;5, a Fungal-Induced Host Sulfate Transporter. PLoS ONE 7, e44408. https://doi.org/10.1371/journal.pone.0044408

Petutschnig, E.K., Jones, A.M.E., Serazetdinova, L., Lipka, U., Lipka, V., 2010. The Lysin Motif Receptor-like Kinase (LysM-RLK) CERK1 Is a Major Chitin-binding Protein in Arabidopsis thaliana and Subject to Chitin-induced Phosphorylation. J. Biol. Chem. 285, 28902–28911. https://doi.org/10.1074/jbc.M110.116657

Petutschnig, E.K., Stolze, M., Lipka, U., Kopischke, M., Horlacher, J., Valerius, O., Rozhon, W., Gust, A.A., Kemmerling, B., Poppenberger, B., Braus, G.H., Nürnberger, T., Lipka, V., 2014. A novel Arabidopsis CHITIN ELICITOR RECEPTOR KINASE 1 (CERK1) mutant with enhanced pathogen-induced cell death and altered receptor processing. New Phytol 204, 955–967. https://doi.org/10.1111/nph.12920

Pierleoni, A., Martelli, P., Casadio, R., 2008. PredGPI: a GPI-anchor predictor. BMC Bioinformatics 9, 392. https://doi.org/10.1186/1471-2105-9-392

Pietraszewska-Bogiel, A., Lefebvre, B., Koini, M.A., Klaus-Heisen, D., Takken, F.L.W., Geurts, R., Cullimore, J.V., Gadella, T.W.J., 2013. Interaction of *Medicago truncatula* Lysin Motif Receptor-Like Kinases, NFP and LYK3, Produced in *Nicotiana benthamiana* Induces Defence-Like Responses. PLoS ONE 8, e65055. https://doi.org/10.1371/journal.pone.0065055

Pinon, J., and Frey, P. 2005. Interaction between poplar clones and *Melampsora* populations and their implication for breeding for durable resistance. In: Rust Diseases of Willow and Poplar. pp. 139–154. Pei, M. H., and McCracken, A.R., Eds., CABI Publishing, Cambridge.

Pitzschke, A., Djamei, A., Bitton, F., Hirt, H., 2009. A Major Role of the MEKK1–MKK1/2–MPK4 Pathway in ROS Signalling. Molecular Plant 2, 120–137. https://doi.org/10.1093/mp/ssn079

Prince, V.E., Pickett, F.B., 2002. Splitting pairs: the diverging fates of duplicated genes. Nat Rev Genet 3, 827–837. https://doi.org/10.1038/nrg928

Qi, J., Wang, J., Gong, Z., Zhou, J.-M., 2017. Apoplastic ROS signaling in plant immunity. Current Opinion in Plant Biology 38, 92–100. https://doi.org/10.1016/j.pbi.2017.04.022

Qiu, J.-L., Zhou, L., Yun, B.-W., Nielsen, H.B., Fiil, B.K., Petersen, K., MacKinlay, J., Loake, G.J., Mundy, J., Morris, P.C., 2008a. Arabidopsis Mitogen-Activated Protein Kinase Kinases MKK1 and MKK2 Have Overlapping Functions in Defense Signaling Mediated by MEKK1, MPK4, and MKS1. Plant Physiol. 148, 212–222. https://doi.org/10.1104/pp.108.120006

Qiu, J.-L., Fiil, B.K., Petersen, K., Nielsen, H.B., Botanga, C.J., Thorgrimsen, S., Palma, K., Suarez-Rodriguez, M.C., Sandbech-Clausen, S., Lichota, J., Brodersen, P., Grasser, K.D., Mattsson, O., Glazebrook, J., Mundy, J., Petersen, M., 2008b. Arabidopsis MAP kinase 4 regulates gene expression through transcription factor release in the nucleus. EMBO J 27, 2214–2221. https://doi.org/10.1038/emboj.2008.147

Radutoiu, S., Madsen, L.H., Madsen, E.B., Felle, H.H., Umehara, Y., Grønlund, M., Sato, S., Nakamura, Y., Tabata, S., Sandal, N., Stougaard, J., 2003. Plant recognition of symbiotic bacteria requires two LysM receptor-like kinases. Nature 425, 585–592. https://doi.org/10.1038/nature02039

Radutoiu, S., Madsen, L.H., Madsen, E.B., Jurkiewicz, A., Fukai, E., Quistgaard, E.M.H., Albrektsen, A.S., James, E.K., Thirup, S., Stougaard, J., 2007. LysM domains mediate lipochitin–oligosaccharide recognition and Nfr genes extend the symbiotic host range. EMBO J 26, 3923–3935. https://doi.org/10.1038/sj.emboj.7601826

Ramos-Sánchez, J.M., Triozzi, P.M., Alique, D., Geng, F., Gao, M., Jaeger, K.E., Wigge, P.A., Allona, I., Perales, M., 2019. LHY2 Integrates Night-Length Information to Determine Timing of Poplar Photoperiodic Growth. Current Biology 29, 2402-2406.e4. https://doi.org/10.1016/j.cub.2019.06.003

Rao, S., Zhou, Z., Miao, P., Bi, G., Hu, M., Wu, Y., Feng, F., Zhang, X., Zhou, J.-M., 2018. Roles of receptor-like cytoplasmic kinase VII members in pattern-triggered immune signaling. Plant Physiol. pp.00486.2018. https://doi.org/10.1104/pp.18.00486

Rasmussen, S.R., Füchtbauer, W., Novero, M., Volpe, V., Malkov, N., Genre, A., Bonfante, P., Stougaard, J., Radutoiu, S., 2016. Intraradical colonization by arbuscular mycorrhizal fungi triggers induction of a lipochitooligosaccharide receptor. Sci Rep 6, 29733. https://doi.org/10.1038/srep29733

Rey, T., André, O., Nars, A., Dumas, B., Gough, C., Bottin, A., Jacquet, C., 2019. Lipo-chitooligosaccharide signalling blocks a rapid pathogen-induced ROS burst without impeding immunity. New Phytol 221, 743–749. https://doi.org/10.1111/nph.15574

Rinaldi, C., Kohler, A., Frey, P., Duchaussoy, F., Ningre, N., Couloux, A., Wincker, P., Le Thiec, D., Fluch, S., Martin, F., Duplessis, S., 2007. Transcript Profiling of Poplar Leaves upon Infection with Compatible and Incompatible Strains of the Foliar Rust *Melampsora larici-populina*. Plant Physiol. 144, 347–366. https://doi.org/10.1104/pp.106.094987

Sannigrahi, P., Ragauskas, A.J., Tuskan, G.A., 2010. Poplar as a feedstock for biofuels: A review of compositional characteristics. Biofuels, Bioprod. Bioref. 4, 209–226. https://doi.org/10.1002/bbb.206

Saucet, S.B., Ma, Y., Sarris, P.F., Furzer, O.J., Sohn, K.H., Jones, J.D.G., 2015. Two linked pairs of Arabidopsis TNL resistance genes independently confer recognition of bacterial effector AvrRps4. Nat Commun 6, 6338. https://doi.org/10.1038/ncomms7338

Saur, I.M.L., Panstruga, R., Schulze-Lefert, P., 2021. NOD-like receptor-mediated plant immunity: from structure to cell death. Nat Rev Immunol 21, 305–318. https://doi.org/10.1038/s41577-020-00473-z

Schlöffel, M.A., Käsbauer, C., Gust, A.A., 2019. Interplay of plant glycan hydrolases and LysM proteins in plant—Bacteria interactions. International Journal of Medical Microbiology 309, 252–257. https://doi.org/10.1016/j.ijmm.2019.04.004

Segonzac, C., Feike, D., Gimenez-Ibanez, S., Hann, D.R., Zipfel, C., Rathjen, J.P., 2011. Hierarchy and Roles of Pathogen-Associated Molecular Pattern-Induced Responses in *Nicotiana benthamiana*. Plant Physiol. 156, 687–699. https://doi.org/10.1104/pp.110.171249

Shimizu, T., Nakano, T., Takamizawa, D., Desaki, Y., Ishii-Minami, N., Nishizawa, Y., Minami, E., Okada, K., Yamane, H., Kaku, H., Shibuya, N., 2010. Two LysM receptor molecules, CEBiP and OsCERK1, cooperatively regulate chitin elicitor signaling in rice: LysM receptors for rice chitin signaling. The Plant Journal 64, 204–214. https://doi.org/10.1111/j.1365-313X.2010.04324.x

Shinya, T., Motoyama, N., Ikeda, A., Wada, M., Kamiya, K., Hayafune, M., Kaku, H., Shibuya, N., 2012. Functional Characterization of CEBiP and CERK1 Homologs in Arabidopsis and Rice Reveals the Presence of Different Chitin Receptor Systems in Plants. Plant and Cell Physiology 53, 1696–1706. https://doi.org/10.1093/pcp/pcs113

Shinya, T., Yamaguchi, K., Desaki, Y., Yamada, K., Narisawa, T., Kobayashi, Y., Maeda, K., Suzuki, M., Tanimoto, T., Takeda, J., Nakashima, M., Funama, R., Narusaka, M., Narusaka, Y., Kaku, H., Kawasaki, T., Shibuya, N., 2014. Selective regulation of the chitin-induced defense response by the Arabidopsis receptor-like cytoplasmic kinase PBL27. Plant J 79, 56–66. https://doi.org/10.1111/tpj.12535

Squeglia, F., Berisio, R., Shibuya, N., Kaku, H., 2017. Defense Against Pathogens: Structural Insights into the Mechanism of Chitin Induced Activation of Innate Immunity. CMC 24. https://doi.org/10.2174/0929867323666161221124345

Stanton, B., Eaton, J., Johnson, J., Rice, D., Schuette, B., Moser, B., 2002. Hybrid Poplar in the Pacific Northwest: The Effects of Market-Driven Management. Journal of Forestry 100(4), 28–33. https://doi.org/10.1093/jof/100.4.28

Stirling, B., Newcombe, G., Vrebalov, J., Bosdet, I., Bradshaw, H.D., 2001. Suppressed recombination around the MXC3 locus, a major gene for resistance to poplar leaf rust: Theor Appl Genet 103, 1129–1137. https://doi.org/10.1007/s001220100721

Su, J., Zhang, M., Zhang, L., Sun, T., Liu, Y., Lukowitz, W., Xu, J., Zhang, S., 2017. Regulation of Stomatal Immunity by Interdependent Functions of a Pathogen-Responsive MPK3/MPK6 Cascade and Abscisic Acid. Plant Cell 29, 526–542. https://doi.org/10.1105/tpc.16.00577

Suarez-Rodriguez, M.C., Adams-Phillips, L., Liu, Y., Wang, H., Su, S.-H., Jester, P.J., Zhang, S., Bent, A.F., Krysan, P.J., 2007. MEKK1 Is Required for flg22-Induced MPK4 Activation in Arabidopsis Plants. Plant Physiol. 143, 661–669. https://doi.org/10.1104/pp.106.091389

Suzuki, N., Miller, G., Morales, J., Shulaev, V., Torres, M.A., Mittler, R., 2011. Respiratory burst oxidases: the engines of ROS signaling. Current Opinion in Plant Biology 14, 691–699. https://doi.org/10.1016/j.pbi.2011.07.014

Suzuki, M., Shibuya, M., Shimada, H., Motoyama, N., Nakashima, M., Takahashi, S., Suto, K., Yoshida, I., Matsui, S., Tsujimoto, N., Ohnishi, M., Ishibashi, Y., Fujimoto, Z., Desaki, Y., Kaku, H., Kito, K., Shibuya, N., 2016. Autophosphorylation of Specific Threonine and Tyrosine Residues in Arabidopsis CERK1 is Essential for the Activation of Chitin-Induced Immune Signaling. Plant Cell Physiol 57, 2312–2322. https://doi.org/10.1093/pcp/pcw150

Suzuki, M., Watanabe, T., Yoshida, I., Kaku, H., Shibuya, N., 2018. Autophosphorylation site Y428 is essential for the in vivo activation of CERK1. Plant Signaling & Behavior 13, e1435228. https://doi.org/10.1080/15592324.2018.1435228

Swain, P.S., Siggia, E.D., 2002. The Role of Proofreading in Signal Transduction Specificity. Biophysical Journal 82, 2928–2933. https://doi.org/10.1016/S0006-3495(02)75633-6

Takata, N., Saito, S., Tanaka Saito, C., Nanjo, T., Shinohara, K., Uemura, M., 2009. Molecular phylogeny and expression of poplar circadian clock genes, LHY1 and LHY2. New Phytologist 181, 808–819. https://doi.org/10.1111/j.1469-8137.2008.02714.x

Tanaka, K., Nguyen, C.T., Liang, Y., Cao, Y., Stacey, G., 2013. Role of LysM receptors in chitin-triggered plant innate immunity. Plant Signaling & Behavior 8, e22598. https://doi.org/10.4161/psb.22598

Tang, D., Innes, R.W., 2002. Overexpression of a kinase-deficient form of the EDR1 gene enhances powdery mildew resistance and ethylene-induced senescence in Arabidopsis. Plant J 32, 975–983. https://doi.org/10.1046/j.1365-313X.2002.01482.x

Tang, D., Wang, G., Zhou, J.-M., 2017. Receptor Kinases in Plant-Pathogen Interactions: More Than Pattern Recognition. Plant Cell 29, 618–637. https://doi.org/10.1105/tpc.16.00891

Taylor, G., 2002. *Populus*: Arabidopsis for Forestry. Do We Need a Model Tree? Annals of Botany 90, 681–689. https://doi.org/10.1093/aob/mcf255

Taylor, S.S., Kornev, A.P., 2011. Protein kinases: evolution of dynamic regulatory proteins. Trends in Biochemical Sciences 36, 65–77. https://doi.org/10.1016/j.tibs.2010.09.006

Taylor, S.S., Keshwani, M.M., Steichen, J.M., Kornev, A.P., 2012. Evolution of the eukaryotic protein kinases as dynamic molecular switches. Phil. Trans. R. Soc. B 367, 2517–2528. https://doi.org/10.1098/rstb.2012.0054

Thakur, A.K., Kumar, P., Parmar, N., Shandil, R.K., Aggarwal, G., Gaur, A., Srivastava, D.K., 2021. Achievements and prospects of genetic engineering in poplar: a review. New Forests. https://doi.org/10.1007/s11056-021-09836-3

Torres, M.A., Dangl, J.L., Jones, J.D.G., 2002. Arabidopsis gp91phox homologues AtrbohD and AtrbohF are required for accumulation of reactive oxygen intermediates in the plant defense response. Proceedings of the National Academy of Sciences 99, 517–522. https://doi.org/10.1073/pnas.012452499

Torres, M.A., Dangl, J.L., 2005. Functions of the respiratory burst oxidase in biotic interactions, abiotic stress and development. Current Opinion in Plant Biology 8, 397–403. https://doi.org/10.1016/j.pbi.2005.05.014

Tuskan, G.A., DiFazio, S., Jansson, S., Bohlmann, J., Grigoriev, I., Hellsten, U., Putnam, N., Ralph, S., Rombauts, S., Salamov, A., Schein, J., Sterck, L., Aerts, A., Bhalerao, R.R., Bhalerao, R.P., Blaudez, D., Boerjan, W., Brun, A., Brunner, A., Busov, V., Campbell, M., Carlson, J., Chalot, M., Chapman, J., Chen, G.-L., Cooper, D., Coutinho, P.M., Couturier, J., Covert, S., Cronk, Q., Cunningham, R., Davis, J., Degroeve, S., Dejardin, A., dePamphilis, C., Detter, J., Dirks, B., Dubchak, I., Duplessis, S., Ehlting, J., Ellis, B., Gendler, K., Goodstein, D., Gribskov, M., Grimwood, J., Groover, A., Gunter, L., Hamberger, B., Heinze, B., Helariutta, Y., Henrissat, B., Holligan, D., Holt, R., Huang, W., Islam-Faridi, N., Jones, S., Jones-Rhoades, M., Jorgensen, R., Joshi, C., Kangasjarvi, J., Karlsson, J., Kelleher, C., Kirkpatrick, R., Kirst, M., Kohler, A., Kalluri, U., Larimer, F., Leebens-Mack, J., Leple, J.-C., Locascio, P., Lou, Y., Lucas, S., Martin, F., Montanini, B., Napoli, C., Nelson, D.R., Nelson, C., Nieminen, K., Nilsson, O., Pereda, V., Peter, G., Philippe, R., Pilate, G., Poliakov, A., Razumovskaya, J., Richardson, P., Rinaldi, C., Ritland, K., Rouze, P., Ryaboy, D., Schmutz, J., Schrader, J., Segerman, B., Shin, H., Siddiqui, A., Sterky, F., Terry, A., Tsai, C.-J., Uberbacher, E., Unneberg, P., Vahala, J., Wall, K., Wessler, S., Yang, G., Yin, T., Douglas, C., Marra, M., Sandberg, G., Van de Peer, Y., Rokhsar, D., 2006. The Genome of Black Cottonwood, *Populus trichocarpa* (Torr. & Gray). Science 313, 1596–1604. https://doi.org/10.1126/science.1128691

Underwood, W., 2012. The Plant Cell Wall: A Dynamic Barrier Against Pathogen Invasion. Front. Plant Sci. 3. https://doi.org/10.3389/fpls.2012.00085

van der Hoorn, R.A.L., Kamoun, S., 2008. From Guard to Decoy: A New Model for Perception of Plant Pathogen Effectors. Plant Cell 20, 2009–2017. https://doi.org/10.1105/tpc.108.060194

Verlinden, M.S., Broeckx, L.S., Van den Bulcke, J., Van Acker, J., Ceulemans, R., 2013. Comparative study of biomass determinants of 12 poplar (*Populus*) genotypes in a high-density short-rotation culture. Forest Ecology and Management 307, 101–111. https://doi.org/10.1016/j.foreco.2013.06.062

Vishwanathan, K., Zienkiewicz, K., Liu, Y., Janz, D., Feussner, I., Polle, A., Haney, C.H., 2020. Ecto-mycorrhizal fungi induce systemic resistance against insects on a nonmycorrhizal plant in a CERK1-dependent manner. New Phytol 228, 728–740. https://doi.org/10.1111/nph.16715

Voigt, C.A., 2014. Callose-mediated resistance to pathogenic intruders in plant defense-related papillae. Front. Plant Sci. 5. https://doi.org/10.3389/fpls.2014.00168

Waese, J., Fan, J., Pasha, A., Yu, H., Fucile, G., Shi, R., Cumming, M., Kelley, L.A., Sternberg, M.J., Krishnakumar, V., Ferlanti, E., Miller, J., Town, C., Stuerzlinger, W., Provart, N.J., 2017. ePlant: Visualizing and Exploring Multiple Levels of Data for Hypothesis Generation in Plant Biology. Plant Cell 29, 1806–1821. https://doi.org/10.1105/tpc.17.00073

Walker, J.C., 1994. Structure and function of the receptor-like protein kinases of higher plants. Plant Mol Biol 26, 1599–1609. https://doi.org/10.1007/BF00016492

Wan, J., Zhang, X.-C., Neece, D., Ramonell, K.M., Clough, S., Kim, S., Stacey, M.G., Stacey, G., 2008. A LysM Receptor-Like Kinase Plays a Critical Role in Chitin Signaling and Fungal Resistance in Arabidopsis. The Plant Cell 20, 471–481. https://doi.org/10.1105/tpc.107.056754

Wan, J., Tanaka, K., Zhang, X.-C., Son, G.H., Brechenmacher, L., Nguyen, T.H.N., Stacey, G., 2012. LYK4, a Lysin Motif Receptor-Like Kinase, Is Important for Chitin Signaling and Plant Innate Immunity in Arabidopsis. Plant Physiol. 160, 396–406. https://doi.org/10.1104/pp.112.201699

Wang, B., Qiu, Y.-L., 2006. Phylogenetic distribution and evolution of mycorrhizas in land plants. Mycorrhiza 16, 299–363. https://doi.org/10.1007/s00572-005-0033-6

Wang, Y.C., Qu, G.Z., Li, H.Y., Wu, Y.J., Wang, C., Liu, G.F., Yang, C.P., 2010. Enhanced salt tolerance of transgenic poplar plants expressing a manganese superoxide dismutase from *Tamarix androssowii*. Mol Biol Rep 37, 1119–1124. https://doi.org/10.1007/s11033-009-9884-9

Wang, H., Xue, Y., Chen, Y., Li, R., Wei, J., 2012. Lignin modification improves the biofuel production potential in transgenic Populus tomentosa. Industrial Crops and Products 37, 170–177. https://doi.org/10.1016/j.indcrop.2011.12.014

Wang, G., Roux, B., Feng, F., Guy, E., Li, L., Li, N., Zhang, X., Lautier, M., Jardinaud, M.-F., Chabannes, M., Arlat, M., Chen, S., He, C., Noël, L.D., Zhou, J.-M., 2015. The Decoy Substrate of a Pathogen Effector and a Pseudokinase Specify Pathogen-Induced Modified-Self Recognition and Immunity in Plants. Cell Host & Microbe 18, 285–295. https://doi.org/10.1016/j.chom.2015.08.004

Wang, G., Dong, Y., Liu, X., Yao, G., Yu, X., Yang, M., 2018. The Current Status and Development of Insect-Resistant Genetically Engineered Poplar in China. Front. Plant Sci. 9, 1408. https://doi.org/10.3389/fpls.2018.01408

Wang, Jizong, Wang, Jia, Hu, M., Wu, S., Qi, J., Wang, G., Han, Z., Qi, Y., Gao, N., Wang, H.-W., Zhou, J.-M., Chai, J., 2019a. Ligand-triggered allosteric ADP release primes a plant NLR complex. Science 364, eaav5868. https://doi.org/10.1126/science.aav5868

Wang, Jizong, Hu, M., Wang, Jia, Qi, J., Han, Z., Wang, G., Qi, Y., Wang, H.-W., Zhou, J.-M., Chai, J., 2019b. Reconstitution and structure of a plant NLR resistosome conferring immunity. Science 364, eaav5870. https://doi.org/10.1126/science.aav5870

Wang, F., Zhang, N., Guo, Y., Gong, B., Li, J., 2020a. Split Nano luciferase complementation for probing protein-protein interactions in plant cells. J. Integr. Plant Biol 62, 1065–1079. https://doi.org/10.1111/jipb.12891

Wang, P., Zhou, L., Jamieson, P., Zhang, L., Zhao, Z., Babilonia, K., Shao, W., Wu, L., Mustafa, R., Amin, I., Diomaiuti, A., Pontiggia, D., Ferrari, S., Hou, Y., He, P., Shan, L., 2020b. The Cotton Wall-associated Kinase GhWAK7A Mediates Responses to Fungal Wilt Pathogens by Complexing with the Chitin Sensory Receptors. Plant Cell tpc.00950.2019. https://doi.org/10.1105/tpc.19.00950

Washburn, M.P., Wolters, D., Yates, J.R., 2001. Large-scale analysis of the yeast proteome by multidimensional protein identification technology. Nat Biotechnol 19, 242–247. https://doi.org/10.1038/85686

Waterhouse, A., Bertoni, M., Bienert, S., Studer, G., Tauriello, G., Gumienny, R., Heer, F.T., de Beer, T.A.P., Rempfer, C., Bordoli, L., Lepore, R., Schwede, T., 2018. SWISS-MODEL: homology modelling of protein structures and complexes. Nucleic Acids Research 46, W296–W303. https://doi.org/10.1093/nar/gky427

Wei, S., Wu, H., Li, X., Chen, Y., Yang, Y., Dai, M., Yin, T., 2020. Identification of Genes Underlying the Resistance to *Melampsora larici-populina* in an R Gene Supercluster of the *Populus deltoides* Genome. Plant Disease 104, 1133–1143. https://doi.org/10.1094/PDIS-08-19-1699-RE

Welker, C., Balasubramanian, V., Petti, C., Rai, K., DeBolt, S., Mendu, V., 2015. Engineering Plant Biomass Lignin Content and Composition for Biofuels and Bioproducts. Energies 8, 7654–7676. https://doi.org/10.3390/en8087654

Wells, J.A., Powers, D.B., Bott, R.R., Graycar, T.P., Estell, D.A., 1987. Designing substrate specificity by protein engineering of electrostatic interactions. Proceedings of the National Academy of Sciences 84, 1219–1223. https://doi.org/10.1073/pnas.84.5.1219

Widin, K.D., Schipper, A.L., 1981. Effect of *Melampsora medusae* leaf rust infection on yield of hybrid poplars in the north-central United States. Forest Pathol 11, 438–448. https://doi.org/10.1111/j.1439-0329.1981.tb00116.x

Williams, S.J., Sohn, K.H., Wan, L., Bernoux, M., Sarris, P.F., Segonzac, C., Ve, T., Ma, Y., Saucet, S.B., Ericsson, D.J., Casey, L.W., Lonhienne, T., Winzor, D.J., Zhang, X., Coerdt, A., Parker, J.E., Dodds, P.N., Kobe, B., Jones, J.D.G., 2014. Structural Basis for Assembly and Function of a Heterodimeric Plant Immune Receptor. Science 344, 299–303. https://doi.org/10.1126/science.1247357

Willmann, R., Lajunen, H.M., Erbs, G., Newman, M.-A., Kolb, D., Tsuda, K., Katagiri, F., Fliegmann, J., Bono, J.-J., Cullimore, J.V., Jehle, A.K., Gotz, F., Kulik, A., Molinaro, A., Lipka, V., Gust, A.A., Nurnberger, T., 2011. Arabidopsis lysin-motif proteins LYM1 LYM3 CERK1 mediate bacterial peptidoglycan sensing and immunity to bacterial infection. Proceedings of the National Academy of Sciences 108, 19824–19829. https://doi.org/10.1073/pnas.1112862108

Wolt, J.D., Wang, K., Sashital, D., Lawrence-Dill, C.J., 2016. Achieving Plant CRISPR Targeting that Limits Off-Target Effects. Plant Genome 9. https://doi.org/10.3835/plantgenome2016.05.0047

Wu, C.-H., Abd-El-Haliem, A., Bozkurt, T.O., Belhaj, K., Terauchi, R., Vossen, J.H., Kamoun, S., 2017. NLR network mediates immunity to diverse plant pathogens. Proc Natl Acad Sci USA 114, 8113–8118. https://doi.org/10.1073/pnas.1702041114

Xiang, T., Zong, N., Zou, Y., Wu, Y., Zhang, J., Xing, W., Li, Y., Tang, X., Zhu, L., Chai, J., Zhou, J.-M., 2008. *Pseudomonas syringae* Effector AvrPto Blocks Innate Immunity by Targeting Receptor Kinases. Current Biology 18, 74–80. https://doi.org/10.1016/j.cub.2007.12.020

Xie, K., Yang, Y., 2013. RNA-Guided Genome Editing in Plants Using a CRISPR–Cas System. Molecular Plant 6, 1975–1983. https://doi.org/10.1093/mp/sst119

Xing, D.-H., Lai, Z.-B., Zheng, Z.-Y., Vinod, K.M., Fan, B.-F., Chen, Z.-X., 2008. Stress- and Pathogen-Induced Arabidopsis WRKY48 is a Transcriptional Activator that Represses Plant Basal Defense. Molecular Plant 1, 459–470. https://doi.org/10.1093/mp/ssn020

Xu, J., Xie, J., Yan, C., Zou, X., Ren, D., Zhang, S., 2014. A chemical genetic approach demonstrates that MPK3/MPK6 activation and NADPH oxidase-mediated oxidative burst are two independent signaling events in plant immunity. Plant J 77, 222–234. https://doi.org/10.1111/tpj.12382

Xu, C., Wei, H., Wang, L., Yin, T., Zhuge, Q., 2019. Optimization of the cry1Ah1 Sequence Enhances the Hyper-Resistance of Transgenic Poplars to *Hyphantria cunea*. Front. Plant Sci. 10, 335. https://doi.org/10.3389/fpls.2019.00335

Xue, L.-J., Alabady, M.S., Mohebbi, M., Tsai, C.-J., 2015. Exploiting genome variation to improve next-generation sequencing data analysis and genome editing efficiency in *Populus tremula × alba* 717-1B4. Tree Genetics & Genomes 11, 82. https://doi.org/10.1007/s11295-015-0907-5

Xue, D.-X., Li, C.-L., Xie, Z.-P., Staehelin, C., 2019. LYK4 is a component of a tripartite chitin receptor complex in *Arabidopsis thaliana*. Journal of Experimental Botany 70, 5507–5516. https://doi.org/10.1093/jxb/erz313

Yadav, R., Arora, P., Kumar, S., Chaudhury, A., 2010. Perspectives for genetic engineering of poplars for enhanced phytoremediation abilities. Ecotoxicology 19, 1574–1588. https://doi.org/10.1007/s10646-010-0543-7

Yamada, K., Yamaguchi, K., Shirakawa, T., Nakagami, H., Mine, A., Ishikawa, K., Fujiwara, M., Narusaka, M., Narusaka, Y., Ichimura, K., Kobayashi, Y., Matsui, H., Nomura, Y., Nomoto, M., Tada, Y., Fukao, Y., Fukamizo, T., Tsuda, K., Shirasu, K., Shibuya, N., Kawasaki, T., 2016. The Arabidopsis CERK1-associated kinase PBL27 connects chitin perception to MAPK activation. EMBO J 35, 2468–2483. https://doi.org/10.15252/embj.201694248

Yamada, K., Yamaguchi, K., Yoshimura, S., Terauchi, A., Kawasaki, T., 2017. Conservation of Chitin-Induced MAPK Signaling Pathways in Rice and Arabidopsis. Plant and Cell Physiology 58, 993–1002. https://doi.org/10.1093/pcp/pcx042

Yan, L., Ma, Y., Liu, D., Wei, X., Sun, Y., Chen, X., Zhao, H., Zhou, J., Wang, Z., Shui, W., Lou, Z., 2012. Structural basis for the impact of phosphorylation on the activation of plant receptor-like kinase BAK1. Cell Res 22, 1304–1308. https://doi.org/10.1038/cr.2012.74

Yang, S., Lu, L., Ni, Y., 2006. Cloned poplar as a new fibre resource for the Chinese pulp and paper industry. Pulp and Paper Canada 107(2): 34-37.

Yang, R.L., Wang, A.X., Zhang, J., Dong, Y., Yang, M.S., Wang, J.M., 2016. Genetic transformation and expression of transgenic lines of Populus x euramericana with insect-resistance and salt-tolerance genes. Genet. Mol. Res. 15. https://doi.org/10.4238/gmr.15028635

Ye, S., Jiang, Y., Duan, Y., Karim, A., Fan, D., Yang, L., Zhao, X., Yin, J., Luo, K., Li, C., 2014. Constitutive expression of the poplar WRKY transcription factor PtoWRKY60 enhances resistance to *Dothiorella gregaria Sacc.* in transgenic plants. Tree Physiology 34, 1118–1129. https://doi.org/10.1093/treephys/tpu079

Yin, T. -M., DiFazio, S.P., Gunter, L.E., Jawdy, S.S., Boerjan, W., Tuskan, G.A., 2004. Genetic and physical mapping of Melampsora rust resistance genes in Populus and characterization of linkage disequilibrium and flanking genomic sequence. New Phytologist 164, 95–105. https://doi.org/10.1111/j.1469-8137.2004.01161.x

Yuan, M., Ngou, B.P.M., Ding, P., Xin, X.-F., 2021a. PTI-ETI crosstalk: an integrative view of plant immunity. Current Opinion in Plant Biology 62, 102030. https://doi.org/10.1016/j.pbi.2021.102030

Yuan, M., Jiang, Z., Bi, G., Nomura, K., Liu, M., Wang, Y., Cai, B., Zhou, J.-M., He, S.Y., Xin, X.-F., 2021b. Pattern-recognition receptors are required for NLR-mediated plant immunity. Nature. https://doi.org/10.1038/s41586-021-03316-6

Zhang, J., 2003. Evolution by gene duplication: an update. Trends in Ecology & Evolution 18, 292–298. https://doi.org/10.1016/S0169-5347(03)00033-8

Zhang, J., Shao, F., Li, Y., Cui, H., Chen, L., Li, H., Zou, Y., Long, C., Lan, L., Chai, J., Chen, S., Tang, X., Zhou, J.-M., 2007. A *Pseudomonas syringae* Effector Inactivates MAPKs to Suppress PAMP-Induced Immunity in Plants. Cell Host & Microbe 1, 175–185. https://doi.org/10.1016/j.chom.2007.03.006

Zhang, J., Li, W., Xiang, T., Liu, Z., Laluk, K., Ding, X., Zou, Y., Gao, M., Zhang, X., Chen, S., Mengiste, T., Zhang, Y., Zhou, J.-M., 2010. Receptor-like Cytoplasmic Kinases Integrate Signaling from Multiple Plant Immune Receptors and Are Targeted by a *Pseudomonas syringae* Effector. Cell Host & Microbe 7, 290–301. https://doi.org/10.1016/j.chom.2010.03.007

Zhang, Hui, Zhang, J., Wei, P., Zhang, B., Gou, F., Feng, Z., Mao, Y., Yang, L., Zhang, Heng, Xu, N., Zhu, J.-K., 2014. The CRISPR/Cas9 system produces specific and homozygous targeted gene editing in rice in one generation. Plant Biotechnol J 12, 797–807. https://doi.org/10.1111/pbi.12200

Zhang, X., Dong, W., Sun, J., Feng, F., Deng, Y., He, Z., Oldroyd, G.E.D., Wang, E., 2015. The receptor kinase CERK1 has dual functions in symbiosis and immunity signalling. Plant J 81, 258–267. https://doi.org/10.1111/tpj.12723

Zhong, R., Morrison, W.H., Himmelsbach, D.S., Poole, F.L., Ye, Z.-H., 2000. Essential Role of Caffeoyl Coenzyme A O-Methyltransferase in Lignin Biosynthesis in Woody Poplar Plants. Plant Physiology 124, 563–578. https://doi.org/10.1104/pp.124.2.563

Zhou, Z., Tian, Y., Cong, P., Zhu, Y., 2018. Functional characterization of an apple (*Malus x domestica*) LysM domain receptor encoding gene for its role in defense response. Plant Science 269, 56–65. https://doi.org/10.1016/j.plantsci.2018.01.006

Zhou, Q., Liu, J., Wang, Jingyi, Chen, S., Chen, L., Wang, Jinfa, Wang, H., Liu, B., 2019. The juxtamembrane domains of Arabidopsis CERK1, BAK1, and FLS2 play a conserved role in chitin-induced signaling. J. Integr. Plant Biol. 62, 556–562. https://doi.org/10.1111/jipb.12847

Zipfel, C., Oldroyd, G.E.D., 2017. Plant signalling in symbiosis and immunity. Nature 543, 328–336. https://doi.org/10.1038/nature22009

Zuo, J., Niu, Q.-W., Chua, N.-H., 2000. An estrogen receptor-based transactivator XVE mediates highly inducible gene expression in transgenic plants. Plant J 24, 265–273. https://doi.org/10.1046/j.1365-313x.2000.00868.x

6. Appendix

6.1 PcCERK1 expression analyses in leaves

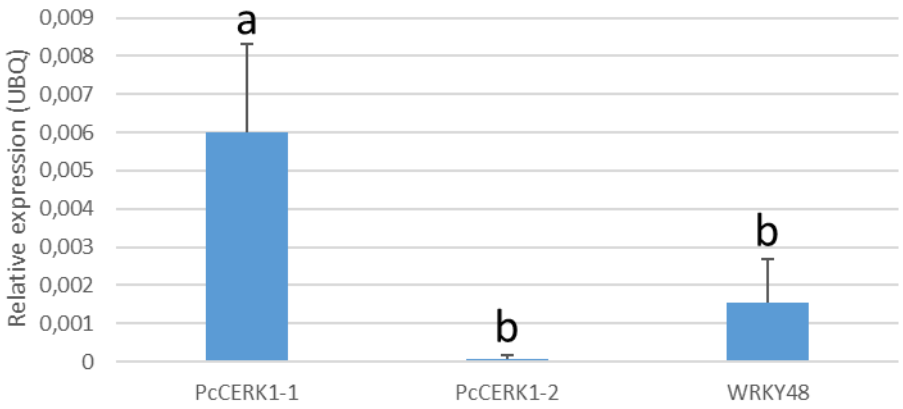

Supplemental Figure 1*: PcCERK1-1* exhibits a higher expression rate in leaves than *PcCERK1-2*. cDNA synthesized from RNA from leaves of *P. x canescens* was used as a template to perform qPCR. The chitin responsive gene WRKY48 was included as a control. The transcript abundance was determined relative to UBQ as a reference. Statistical analysis was conducted by one-way anova followed by Tukey's posthoc test. Different letters indicate statistically significant differences (P ≤ 0.05). **Data provided by Mo Awwanah.**

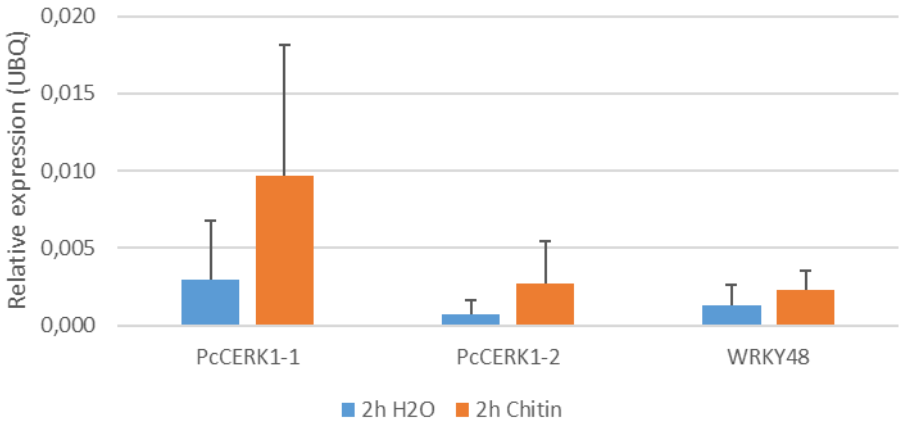

Supplemental Figure 2: *PcCERK1-1* and *PcCERK1-2* expression show a tendency to increase after chitin treatment. cDNA synthesized from RNA from leaves of *P. x canescens* was used as a template to perform qPCR. The chitin responsive gene WRKY48 was included as a control. The transcript abundance was determined relative to UBQ as a reference. Statistical analysis was performed with unpaired student's t-test (P ≤ 0.05). The data show a tendency for chitin-induced expression, but is not statistically significant. Data are means + SD (n = 3 biological replicates). **Data provided by Mo Awwanah.**

6.2 Transcript and protein sequences of *Populus x canescens* CERK1

Supplemental Table 1: Transcript and protein sequences of *PcCERK1-1* and *PcCERK1-2* of *Populus x canescens.* For complementation experiments in Arabidopsis the *P. tremula* allele was used for cloning the *pLexA:PcCERK1-1_mCitrine* construct and the *P. alba* allele for the *pAtCERK1:PcCERK1-2_mCitrine* construct. **Sequences provided by Mo Awwanah.**

PcCERK1-1
***P. alba* allele**
ATGAATCCCAAATTAGGATTTGGGTTTCTTCTTCTACTGTTACTCTGCTACTCAATCGACTCAAAATGCAGCA AAGGATGCGATTTGGCTCTAGCATCCTACTACGTTTGGCAAGGATCTAACCTTTCATTCATCGCCGAAGTTA TGCAATCAAGCATCTTAAGACTAACAGATTTCGACACCATCCTCAGCTACAATCCTCAAGTACTAAGCAAAG ACAGCCTCCCATCTTTCATCAGGATCAGCATCCCTTTCCCCTGCGACTGCATCAACGGTGAATTCCTCGGCCA CTTCTTCACCTACACCGTCAGAAGTCAAGACACTTATGACAAGGTCGCCGATCCATACTATGCCAATTTGAC CACGACTCAGTCGTTGAAAAACTTTAATAGCTACCCTGAGGTTAATATACCCGATAACGGAAAGCTTAATGT GAGTGTCAACTGTTCGTGTGGGGATAGCTCGGTTTCTAAGGATTACGGCTTGTTTATGACATACCCGCTCCG ACCCGAAGATACTTTGGCGTCGATTGCCAATCAGACCAATCTCACGCAGTCGCTGCTGCAGCGTTATAATGT TGGTTTCGATTTTAATCAAGGGAGTGGTGTGGTTTATATTCCGGCCAAAGATACAAATGGTAGCTACCGGC CCTTGAACTCGAGCACAGGAATAGCAGGTGGCGTTGTTGCTGGCATATGCATAGCAGCAGTAGCCGTGGC ACTGTTGTTGGCAGTTTTTATATATGCGAGATTTTACCGAAAGAAGAAGGTGAAGGAGGCAATAATGCTGT CACTCTCTCCACAAATTGTTCAAGTACCTGGAAGTGACTCCAATAAACCTGTGGATGCGACTGGGTCCCAAG GTCTTACAGGTATAACCGTGGACAAGTCTGTGGAGTTCTCTTATGAAGAACTTGCTAAGGCCACTGATGAC TTTAGTCTGGCAAATAAGATTGGTCAAGGAGGCTTTGGGGCTGTATACTATGCAGAACTGAGAGGCGAGA AAGCTGCCATTAAGAAGATGGACATGCAAGCATCAAAAGAATTCTTTGCTGAGCTCAAGGTTTTAACACAT GTTCACCACCTAAACCTGGTCCGATTGATAGGATATTGTGTTGAGGGTTCTCTTTTCCTTGTCTACGAATTTA TTGAAAATGGAAACTTAAGCCAACATTTGCGTGGCTCTGAGAAGGATCCATTGCCATGGTCTACAAGAGTG CAAATTGCCCTTGATTCAGCTAGAGGCCTTGAATACATCCATGAGCATACTGTCCCTGTTTATATTCATCGTG ATATTAAATCGGCAAACATACTGATCGACAAGAACTTCCGGGGAAAGGTTGCAGATTTTGGATTAACAAAA CTAACTGAGGTTGGAGGTGCATCACTCCCTACACGTCTTGTGGGTACATTTGGATACATGCCGCCAGAATAT GCTCAATATGGTGATGTTTCTCCGAAAGTAGATGTTTACGCACTCGGGGTTGTCCTCTATGAACTTATTTCT GCTAAAGAAGCTATCATCAAGACAAATGATTCTAGTGCTGAATCAAGGGGCCTTGTTGCTTTGTTTGAGGA TGTTCTTAATCAGCCTGATCCTAGGGAAGACCTTCGCAAAGTAGTTGATCCAAGGCTCGGAGAAGACTATC CACTCGATTCAGTTCGCAAGATGGCCCAGCTTGGCAAGGCATGCACCCAAGAGAATCCTCAGCTGCGGCCG AGTATGAGATCCATTGTGGTTGCTTTAATGACTCTTTCATCCGCCACGGAGGATTGGGATGTTGGCGCCTTC TATGAAAATCAAGCTCTTGTCAATCTAATGTCAGGAAGATAG
MNPKLGFGFLLLLLLCYSIDSKCSKGCDLALASYYVWQGSNLSFIAEVMQSSILRLTDFDTILSYNPQVLSKDSLPSF IRISIPFPCDCINGEFLGHFFTYTVRSQDTYDKVADPYYANLTTTQSLKNFNSYPEVNIPDNGKLNVSVNCSCGDSS VSKDYGLFMTYPLRPEDTLASIANQTNLTQSLLQRYNVGFDFNQGSGVVYIPAKDTNGSYRPLNSSTGIAGGVV AGICIAAVAVALLLAVFIYARFYRKKKVKEAIMLSLSPQIVQVPGSDSNKPVDATGSQGLTGITVDKSVEFSYEELA KATDDFSLANKIGQGGFGAVYYAELRGEKAAIKKMDMQASKEFFAELKVLTHVHHLNLVRLIGYCVEGSLFLVYE FIENGNLSQHLRGSEKDPLPWSTRVQIALDSARGLEYIHEHTVPVYIHRDIKSANILIDKNFRGKVADFGLTKLTEV GGASLPTRLVGTFGYMPPEYAQYGDVSPKVDVYALGVVLYELISAKEAIIKTNDSSAESRGLVALFEDVLNQPDPR EDLRKVVDPRLGEDYPLDSVRKMAQLGKACTQENPQLRPSMRSIVVALMTLSSATEDWDVGAFYENQALVNL MSGR
***P. tremula* allele**
ATGAATCCCAAATTAGGATTTGGGTTTCTTCTTCTACTGTTACTCTGCTACTCAATCGACTCAAAATGCAGCA AAGGATGCGATTTGGCTCTAGCATCCTACTACGTTTGGCAAGGATCTAACCTTTCATTCATCGCCGAAGTTA TGCAATCAAGCATCTTAAAACTAACAGATTTCGACACCATCCTCAGCTACAATCCTCAAGTACCAAGCAAAG ACAGCCTCCCATCTTTCATCAGGATCAGCATCCCTTTCCCCTGCGACTGCATCAACGGTGAATTCCTCGGCCA

CATCTTCTCCTACACCGTCAGAAGTCAAGACACTTATGACAAGGTCGCCGATACATACTATGCCAATTTGAC
AACGACTCAGTCGTTGAAAAACTTTAATAGCTACCCTGAGGTTAATATACCCGATAACGGAGTGCTTAATGT
GAGTGTCAACTGTTCGTGTGGGGATAGCGCGGTTTCTAAGGATTACGGCTTGTTTATGACATACCCGCTCC
GACCCGAAGATACTTTGGCGTCGATTGCCAATCAGACCAATCTCACGCAGTCGCTGCTGCAGCGTTATAAT
GTTGGTTTCGATTTTAATCAAGGAAGTGGTGTGGTTTATATTCCGGCCAAAGATACAAATGGTAGCTACCG
GCCCTTGAACTCGAGCACAGGAATAGCAGGTGGCGTTGTTGCTGGCATATGCATAGCAGCAGTAGCCGTG
GCACTGTTGTTGGCAGTTTTTATATATGCGGGATTTTACCGAAAGAAGAAGGTGAAGGAGGCAGTATTGGT
GTCACTCTCTCCACAAATTGTTCAAGTACCTGGAAGTGACTCCGATAAACCTGTGGATGCGACTGGGTCCCA
AGGTCTTAAAGGTATAACCGTGGACAAGTCTGTGGATTTCTCTTATGAAGAACTTGCTAAGGCCACTGATG
ACTTTAGTCTGGCAAATAAGATTGGTCAAGGAGGCTTTGGGGCTGTATACTATGCAGAACTGAGAGGCGA
GAAAGCTGCCATTAAGAAGATGGACATGCAAGCATCAAAAGAATTCTTTGCTGAGCTCAAGGTTTTAACAC
ATGTTCACCACCTAAACCTGGTCCGATTGATAGGATACTGTGTTGACGGTTCTCTTTTCCTTGTCTACGAATA
TATTGAAAATGGAAACTTAAGCCAACATTTGCGTGGATCTGAGAAGGATCCATTGCCATGGTCTACAAGAG
TGCAAATTGCCCTTGATTCAGCTAGAGGCCTTGAATACATCCATGAGCATACTGTCCCTGTTTATATTCATCG
TGATATTAAATCAGCAAACATACTGATCGACAAGAACTTCCGGGGAAAGGTTGCAGATTTCGGATTAACAA
AACTAACTGAGGTTGGAGGTGCATCACTCCCTACACGTCTTGTGGGTACATTTGGATACATGCCGCCAGAA
TATGCTCAATATGGTGATGTTTCTCCAAAAGTAGATGTTTACGCACTCGGGGTTGTCCTCTATGAACTTATTT
CTGCTAAAGAAGCTATTGTCAAGACAAATGATTCTAGTGCTGAATCAAGGGGCCTTGTTGCTTTGTTTGAG
GATGTTCTTAACCAGCCTGATCCTAGGGAAGACCTTCGCAAAGTAGTTGATCCAAGGCTCGGAGAAGACTA
TCCACTCGATTCAGTTCGCAAGATGGCCCAGCTCGGCAAGGCATGCACCCAAGAGAATCCTCAGCTGCGGC
CAAGTATGAGATCCATTGTGGTTGCTTTAATGACTCTTTCATCCGCCACGGAGGATTGGGATGTTGGCGCCT
TCTATGAAAATCAAGCTCTTGTCAATCTAATGTCAGGAAGATAG

MNPKLGFGFLLLLLLCYSIDSKCSKGCDLALASYYVWQGSNLSFIAEVMQSSILKLTDFDTILSYNPQVPSKDSLPSF
IRISIPFPCDCINGEFLGHIFSYTVRSQDTYDKVADTYYANLTTTQSLKNFNSYPEVNIPDNGVLNVSVNCSCGDSA
VSKDYGLFMTYPLRPEDTLASIANQTNLTQSLLQRYNVGFDFNQGSGVVYIPAKDTNGSYRPLNSSTGIAGGVV
AGICIAAVAVALLLAVFIYAGFYRKKKVKEAVLVSLSPQIVQVPGSDSDKPVDATGSQGLKGITVDKSVDFSYEELA
KATDDFSLANKIGQGGFGAVYYAELRGEKAAIKKMDMQASKEFFAELKVLTHVHHLNLVRLIGYCVDGSLFLVYE
YIENGNLSQHLRGSEKDPLPWSTRVQIALDSARGLEYIHEHTVPVYIHRDIKSANILIDKNFRGKVADFGLTKLTEV
GGASLPTRLVGTFGYMPPEYAQYGDVSPKVDVYALGVVLYELISAKEAIVKTNDSSAESRGLVALFEDVLNQPDP
REDLRKVVDPRLGEDYPLDSVRKMAQLGKACTQENPQLRPSMRSIVVALMTLSSATEDWDVGAFYENQALVN
LMSGR

PcCERK1-2

***P. alba* allele**

ATGAATCCCAAATTAGGGTTAGGTTTTATTCTTCTGCTTTTACTCTGCTACTCAATCGAATCAAAGTGCAGAA
AAGGCTGCGATTTGGCTCTAGCCTCCTACTACGTTTGGCAAGACGCAGACCTCACATTCATCGCCGAAGTTA
TGCAATCAAGCATCTTAAAATCATCAGATTTCGACACCATCCTCCGTTACAACCCTCAATTGCCAAGCAAAG
ACAGCCTCTCATCCTTCATCAGGATCAACATCCCTTTCCCCTGCGACTGCATCGAAGGTCAATTCCTCGGCCA
CTTCTTCAACTACAACGTCAGATCTCAAAACACTTACACTGACGTCGCTAATACATACTATGCCAATTTGACC
ACGATCCCGTCGTTGGTGTACTTCAATAACTACTCCGAGTTTAATATACCCGATAACGGAAAACTCAATGTG
AGTGTTAATTGTTCGTGTGGGGATAGCTCGGTTTCTAAGGATTATGGCCTGTTTATGACGTACCCGCTCCAA
CCCAACGATACTTTGGAGTCCATTGCCAAACAGAACAATGTTACTCAGGAGTTGCTGCAGCGGTATAATGT
TGGTTTCAATTTTAGTCGAGAGACTCAGACTGGTGTGGTTTATATTCCTACCAAAGATGCAGATGGTAGCTA
CCGGCCCTTGAAGTCGAGCACAGGAATAGCAGGTGGAGCTATTGCTGGCATAAGTATAGCAGCAGTAGCT
GTGGCACTGTTGTTGGCAGTTCTTATTTATGTGAGATTTTACCGAAAGAAGGAGAAGGGAGCAATATTGCT
GTCGGCATCTCCACAACTCTCTCCACGAATTCTTCATGTAACTGGAAGTAACTCCAATAGACCTGTGAATGC
GACTGGGTCTCAAGGTCTTACAGGCATAACTGTGGACAAATCTGTGGAATTCTCTTATGAAGAACTTGCTA
AGGCCACTGATGACTTTAGTCTTGCAAATAAGATTGGTGAAGGTGGCTTTGGGACTGTTTACTATGCAGAA
CTGAGAGGCGAGAAAGCTGCAATCAAGAAGATGGACGTGCAAGATTCAAAAGAATTTTTTGCTGAGCTCA
AGGTTTTAACACATGTTCACCACCTGAACCTGGTCCGATTAATAGGATATTGTGTGGAGGGTTCTCTTTTCG
TAGTTTACGAGTACATTGAAAATGGAAACTTAAGCCAACATTTGCGCGGCTCTGGGAAGGATCCATTGACA

TGGTCTACAAGAGTGCAAATTGCCCTTGATTCAGCTAGAGGTCTTGAATATATCCATGAGCATACTGTCCCT
GTTTATATTCATCGTGATATTAAATCAGCAAACATACTGATAGACAAGGACTTCAGGGGAAAGGTTGCAGA
TTTTGGATTAACAAAACTAACTAAGGTTGGAAGTGCATCTCTCCTTACACGTCTTGTGGGTACATTTGGATA
CATGTCGCCAGAATATGCTCAATATGGTGATGTTTCTCCAAAATTAGATGTTTTTGCATTTGGAGTTGTCCTC
TATGAACTTATTTCTGCTAAAGAAGCTATCGTCAAGGCAAATGATTCTAGTGCTGAATCAAGGGGCCTTATT
GCTTTGTTTGAGGATGTTCTAAATCAGCCTGATCCTGGAGAAGATCTTCGCAAATTAGTTGACCCAAGGCTT
GGAGAAGACTACCCACTCGATTCAGTTCGAAAGGTGGCCCAGCTTGCCAAGGCATGCACTCATGAGAATCC
TCAGGTGCGGCCGAGCATGAGATCCATTGTGGTTGCCTTAATGACTCTTTCATCATCGACCGAGGATTGGG
ATGTTGGCTCCTTCTATGAAAATCAAGCTCTCGTCAATCTGATGTCAGGAAGATGA

MNPKLGLGFILLLLLCYSIESKCRKGCDLALASYYVWQDADLTFIAEVMQSSILKSSDFDTILRYNPQLPSKDSLSSFI
RINIPFPCDCIEGQFLGHFFNYNVRSQNTYTDVANTYYANLTTIPSLVYFNNYSEFNIPDNGKLNVSVNCSCGDSS
VSKDYGLFMTYPLQPNDTLESIAKQNNVTQELLQRYNVGFNFSRETQTGVVYIPTKDADGSYRPLKSSTGIAGGA
IAGISIAAVAVALLLAVLIYVRFYRKKEKGAILLSASPQLSPRILHVTGSNSNRPVNATGSQGLTGITVDKSVEFSYEE
LAKATDDFSLANKIGEGGFGTVYYAELRGEKAAIKKMDVQDSKEFFAELKVLTHVHHLNLVRLIGYCVEGSLFVVY
EYIENGNLSQHLRGSGKDPLTWSTRVQIALDSARGLEYIHEHTVPVYIHRDIKSANILIDKDFRGKVADFGLTKLTK
VGSASLLTRLVGTFGYMSPEYAQYGDVSPKLDVFAFGVVLYELISAKEAIVKANDSSAESRGLIALFEDVLNQPDP
GEDLRKLVDPRLGEDYPLDSVRKVAQLAKACTHENPQVRPSMRSIVVALMTLSSSTEDWDVGSFYENQALVNL
MSGR

***P. tremula* allele**

ATGAATCCCAAATTAGGGTTAGGTTTTATTCTTCTGCTTTTACTCTGCTACTCAATCGAATCAAAGTGCAGAA
AAGGCTGCGATTTGGCTCTAGCCTCCTACTACGTTTGGCAAGACGCAACCCTCACATTCATCGCCGAAGTTA
TGCAATCAAGCATCTTACAATCATCAGATTTCGATACCATCCTCCGTTACAATCCTCAATTGCCAAGCAAAG
ACAGCCTCTCATCCTTCATCAGGATCAACATCCCTTTCCCCTGCGACTGCATCGAAGGTCAATTCCTCGGCCA
CTTATTCAACTACAACGTCAGATCTCAAAACACTTACACTGACGTCGCTAATACATACTATGCCAATTTGACC
ACGATCCCGTCGTTGGTGCACTTTAATAACTACTCCGAGTTTAATATACCCGATAACGGAAAACTCAATGTG
AGTGTTAATTGTTCGTGTGGGGATAGCTCGGTTTCTAAGGATTACGGCCTGTTTATGACGTACCCGCTCCAA
CCCAACGATACTTTGGAGTCCATTGCCAATCAGACCAATGTTACTCAGGAGTTGCTGCAGCAGTATAACGTT
GGTTTCAATTTTAGTCGAGAGACTGGTGTGGTTTATATTCCTACCAAAGATGTAGATGGTAGCTACCGGCC
CTTGAAGTCAAGCACAGGAATAGCAGGTGGAGCTATTGCTGGCATAAGTATAGCAGCAGTAGCTGTGGCA
CTGTTGTTGGCAGTTCTTATTTATGTGGGATTTTACCAAAAGAAGAAGGAGAAGAGAGCAATATTGCTGTC
GGCATCTCCACAACTCTCTCCACGAATTCTTCATGTAACTGGAAGCAACTCCAATAGACCTGTGAATGCGAC
TGGGTCTCAAGGTCTTACAGGCATAACTGTGGACAAATCTGTGGAATTCTCTTATGAAGAACTTGCTAAGG
CCACTGATGACTTTAGTCTTGCAAATAAGATTGGTGAAGGTGGCTTTGGGATTGTTTACTATGCAGAACTG
AGAGGCGAGAAAGCTGCAATCAAGAAGATGGACGTGCAAGATTCAAAAGAATTTTTTGCTGAGCTCAAGG
TTTTAACACATGTTCACCACCTGAACCTGGTCCGATTAATAGGATATTGTGTGGAGGGTTCTCTTTTTGTAG
TTTACGAGTACATTGAAAATGGAAACTTAAGCCAACATTTGCGTGGCTCTGGGAAGGATCCATTGACATGG
TCTACAAGAGTGCAAATTGCCCTTGATTCAGCTAGAGGTCTTGAATATATCCATGAGCATACTGTCCCTGTT
TATATTCATCGTGATATTAAATCAGCAAACATACTGATAGACAAGAACTTCAGGGGAAAGGTTGCAGATTT
TGGATTAACAAAACTAACTAAGGTTGGAAGTGCATCTCTCCTTACACGTCTTGTGGGTACATTTGGATACAT
GTCGCCAGAATATGCTCAATATGGTGATGTTTCTCCAAAATTAGATGTTTTTGCATTTGGAGTTGTCCTCTAT
GAACTTATTTCTGCTAAAGAAGCTATCGTCAAGGCAAATGATTCTAGAGCTGAATCAAGGGGCCTTATTGC
TTTGTTTGAGGATGTTCTAAATCAGCCTGATCCTGGAGAAGATCTTCGCAAATTAGTTGACCCAAGGCTTG
GAGAAGACTACCCACTCGATTCAGTTCGAAAGGTGGCCCAGCTTGCCAAGGCATGCACTCATGAGAATCCT
CAGGTGCGGCCGAGTATGAGATCCATTGTGGTTGCCTTAATGACTCTTTCATCATCGACCGAGGATTGGGA
TGTTGGCTCCTTCTATGAAAATCAAGCTCTTGTCAATCTGATGTCAGGAAGATGA

MNPKLGLGFILLLLLCYSIESKCRKGCDLALASYYVWQDATLTFIAEVMQSSILQSSDFDTILRYNPQLPSKDSLSSFI
RINIPFPCDCIEGQFLGHLFNYNVRSQNTYTDVANTYYANLTTIPSLVHFNNYSEFNIPDNGKLNVSVNCSCGDSS
VSKDYGLFMTYPLQPNDTLESIANQTNVTQELLQQYNVGFNFSRETGVVYIPTKDVDGSYRPLKSSTGIAGGAIA
GISIAAVAVALLLAVLIYVGFYQKKKEKRAILLSASPQLSPRILHVTGSNSNRPVNATGSQGLTGITVDKSVEFSYEE
LAKATDDFSLANKIGEGGFGIVYYAELRGEKAAIKKMDVQDSKEFFAELKVLTHVHHLNLVRLIGYCVEGSLFVVY
EYIENGNLSQHLRGSGKDPLTWSTRVQIALDSARGLEYIHEHTVPVYIHRDIKSANILIDKNFRGKVADFGLTKLTK

VGSASLLTRLVGTFGYMSPEYAQYGDVSPKLDVFAFGVVLYELISAKEAIVKANDSRAESRGLIALFEDVLNQPDP GEDLRKLVDPRLGEDYPLDSVRKVAQLAKACTHENPQVRPSMRSIVVALMTLSSSTEDWDVGSFYENQALVNL MSGR

6.3 Peptides identified in mass spectrometry analyses

6.3.1 Peptides identified for LysM-RLKs and LysM-RLPs in *Populus trichocarpa*

6.3.1.1 Tabular overview of detected peptides in protein samples of *Populus trichocarpa*

Supplemental Table 2: Peptides identified for CERK1 proteins of *Populus trichocarpa*. Proteins were extracted from leaf samples and mass spectrometry was performed after chitin affinity purification. Detected peptides, for which quantitative data are shown in Figure 6 (chapter 3.1.5), are listed below. Unique peptides for a protein are colored in black. Peptides shared between two proteins whose origin cannot be distinguished are highlighted in orange. Information about additional purification steps is listed in brackets behind the number of protein extraction. Addition of dowex, ascorbic acid and sephadex should reduce phenolic compounds. Microsomal fraction, chitin hexamer (C6mer) elution and double protein amount were used to enrich the presence of candidate proteins in the samples.

Protein extraction	PtCERK1-1	PtCERK1-3
# 1	-	-
# 2	DPDGSYLPLK DPDGSYLPLK DPDGSYLPLK DPDGSYLPLK DPDGSYLPLK DPDGSYLPLK DSLPSFIR DSLPSFIR VQIALDSAR YNVGFDFNQGSGVVYIPTK YNVGFDFNQGSGVVYIPTK	-
# 3 (microsomal fraction)	ATDDFSLANK ATDDFSLANK ATDDFSLANK ATDDFSLANK DSLPSFIR DSLPSFIR DSLPSFIR DSLPSFIR GLVALFEDVLNQPDPR GLVALFEDVLNQPDPR GLVALFEDVLNQPDPR GLVALFEDVLNQPDPR LGEDYPLDSVR LGEDYPLDSVR LGEDYPLDSVR LGEDYPLDSVR LGEDYPLDSVR LGEDYPLDSVR LVGTFGYmPPEYAQYGDVSPK LVGTFGYmPPEYAQYGDVSPK LVGTFGYmPPEYAQYGDVSPK LVGTFGYmPPEYAQYGDVSPK	IGQGGFGAVYYAELR IGQGGFGAVYYAELR IGQGGFGAVYYAELR IGQGGFGAVYYAELR IGQGGFGAVYYAELR IGQGGFGAVYYAELR SVEFSYEELAK SVEFSYEELAK

	VADFGLTK VADFGLTK VADFGLTK VADFGLTK VQIALDSAR VQIALDSAR VQIALDSAR VQIALDSAR VQIALDSAR	
# 4 (microsomal fraction/ C6mer elution)	DSLPSFIR DSLPSFIR DSLPSFIR DSLPSFIR DSLPSFIR DSLPSFIR GLVALFEDVLNQPDPR GLVALFEDVLNQPDPR GLVALFEDVLNQPDPR LGEDYPLDSVR LGEDYPLDSVR LGEDYPLDSVR LGEDYPLDSVR LGEDYPLDSVR LGEDYPLDSVR LVGTFGYmPPEYAQYGDVSPK LVGTFGYmPPEYAQYGDVSPK LVGTFGYmPPEYAQYGDVSPK LVGTFGYmPPEYAQYGDVSPK LVGTFGYmPPEYAQYGDVSPK LVGTFGYmPPEYAQYGDVSPK LVGTFGYmPPEYAQYGDVSPK LVGTFGYmPPEYAQYGDVSPK LVGTFGYmPPEYAQYGDVSPK LVGTFGYmPPEYAQYGDVSPK LVGTFGYmPPEYAQYGDVSPK LVGTFGYmPPEYAQYGDVSPK LVGTFGYmPPEYAQYGDVSPK LVGTFGYmPPEYAQYGDVSPK LVGTFGYmPPEYAQYGDVSPK VADFGLTK VDVYALGVVLYELISAK VDVYALGVVLYELISAK VDVYALGVVLYELISAK VDVYALGVVLYELISAK VDVYALGVVLYELISAK VDVYALGVVLYELISAK VDVYALGVVLYELISAK VDVYALGVVLYELISAK VDVYALGVVLYELISAK VDVYALGVVLYELISAK VQIALDSAR VQIALDSAR VQIALDSAR VQIALDSAR VQIALDSAR VQIALDSAR VQIALDSAR VQIALDSAR VQIALDSAR	IGQGGFGAVYYAELR IGQGGFGAVYYAELR IGQGGFGAVYYAELR IGQGGFGAVYYAELR IGQGGFGAVYYAELR IGQGGFGAVYYAELR IGQGGFGAVYYAELR IGQGGFGAVYYAELR IGQGGFGAVYYAELR IGQGGFGAVYYAELR SVEFSYEELAK SVEFSYEELAK
# 5	ATDDFSLANK DPDGSYLPLK DSLPSFIR DSLPSFIR EFLAELK	EFLAELK

	LTEVGSTSLPTR STDFDTILR STDFDTILR YNPQVTNK	
# 6	ATDDFSLANK EFLAELK LTEVGSTSLPTR STDFDTILR	EFLAELK
# 7 (Dowex)	ATDDFSLANK DSLPSFIR EFLAELK LGEDYPLDSVR LTEVGSTSLPTR SANILIDK STDFDTILR SVVFSYEELAK	EFLAELK SANILIDK
# 8 (Sephadex)	ATDDFSLANK DPDGSYLPLK EFLAELK LTEVGSTSLPTR SVVFSYEELAK VADFGLTK	EFLAELK
# 9	VQIALDSAR VQIALDSAR DPDGSYLPLK DPDGSYLPLK	-
# 10 (Dowex + Ascorbic Acid)	DSLPSFIR DSLPSFIR DYGLFmTYPLR DYGLFmTYPLR LGEDYPLDSVR LGEDYPLDSVR SANILIDK SANILIDK VQIALDSAR VQIALDSAR DPDGSYLPLK DPDGSYLPLK GAILLPASQELSPR GAILLPASQELSPR GAILLPASQELSPR LTEVGSTSLPTR LTEVGSTSLPTR SVVFSYEELAK SVVFSYEELAK	SANILIDK SANILIDK
# 11	DPDGSYLPLK DSLPSFIR STDFDTILR YNPQVTNK	-
# 12 (double protein amount)	DPDGSYLPLK DPDGSYLPLK DSLPSFIR DSLPSFIR STDFDTILR YNPQVTNK	-
# 13 (Sephadex)	DPDGSYLPLK	-
# 14 (Sephadex/ double protein amount)	DPDGSYLPLK DSLPSFIR STDFDTILR STDFDTILR	-

Supplemental Table 3: Peptides identified for LYK4 proteins of *Populus trichocarpa*. Proteins were extracted from leaf samples and mass spectrometry was performed after chitin affinity purification. Detected peptides, for which quantitative data are shown in Figure 6 (chapter 3.1.5), are listed below. Unique peptides for a protein are colored in black. Peptides shared between two proteins whose origin cannot be distinguished are highlighted in orange. Information about additional purification steps is listed in brackets behind the number of protein extraction. Addition of dowex, ascorbic acid and sephadex should reduce phenolic compounds. Microsomal fraction, chitin hexamer (C6mer) elution and double protein amount were used to enrich the presence of candidate proteins in the samples.

Protein extraction	PtLYK4-1	PtLYK4-2	PtLYK4-3	PtLYK4-4
# 1	-	-	-	-
# 2	-	-	-	-
# 3 (microsomal fraction)	-	-	-	-
# 4 (microsomal fraction/ C6mer elution	-	STDGPEGEFALTR STDGPEGEFALTR STDGPEGEFALTR STDGPEGEFALTR	-	-
# 5	-	-	-	INGSVYR INGSVYR
# 6	-	FGADIGR	-	-
# 7 (Dowex)	-	FGADIGR VYNYEDLK	-	-
# 8 (Sephadex)	-	-	-	-
# 9	-	-	-	-
# 10 (Dowex + Ascorbic Acid)	-	STDGPEGEFALTR STDGPEGEFALTR	-	-
# 11	-	-	-	INGSVYR
# 12 (double protein amount)	-	-	-	INGSVYR
# 13 (Sephadex)	SCQAYLIFR	FGADIGR FGADIGR SCQAYLIFR	-	INGSVYR INGSVYR
# 14 (Sephadex/ double protein amount)	QQPYVGK SCQAYLIFR	FGADIGR FGADIGR GRALEANEISEK QQPYVGK SCQAYLIFR	-	INGSVYR

Supplemental Table 4: Peptides identified for LYK5 proteins of *Populus trichocarpa*. Proteins were extracted from leaf samples and mass spectrometry was performed after chitin affinity purification. Detected peptides, for which quantitative data are shown in Figure 6 (chapter 3.1.5), are listed below. Unique peptides for a protein are colored in black. Peptides shared between two proteins whose origin cannot be distinguished are highlighted in orange. Information about additional purification steps is listed in brackets behind the number of protein extraction. Addition of dowex, ascorbic acid and sephadex should reduce phenolic compounds. Microsomal fraction, chitin hexamer (C6mer) elution and double protein amount were used to enrich the presence of candidate proteins in the samples.

Protein extraction	PtLYK5-1	PtLYK5-2
# 1	-	VLEGDNVR
# 2	-	-
# 3 (microsomal fraction)	-	GDVSSEINILK GDVSSEINILK GDVSSEINILK GDVSSEINILK TSNILLDANLR TSNILLDANLR TSNILLDANLR TSNILLDANLR
# 4 (microsomal fraction/ C6mer elution)	-	GDVSSEINILK GDVSSEINILK ILSSSLDWDPSDELNR ILSSSLDWDPSDELNR ILSSSLDWDPSDELNR ILSSSLDWDPSDELNR TSNILLDANLR TSNILLDANLR TSNILLDANLR TSNILLDANLR YEDLQVATGYFAQANLIK YEDLQVATGYFAQANLIK YEDLQVATGYFAQANLIK YEDLQVATGYFAQANLIK
# 5	-	-
# 6	-	-
# 7 (Dowex)	-	-
# 8 (Sephadex)	-	-
# 9	-	GDVSSEINILK LSSSNIIFPFTPILVPLPTEPTK LSSSNIIFPFTPILVPLPTEPTK LSSSNIIFPFTPILVPLPTEPTK LSSSNIIFPFTPILVPLPTEPTK SmPPYNSPVLIAYLLGVPQSATR SmPPYNSPVLIAYLLGVPQSATR SmPPYNSPVLIAYLLGVPQSATR SmPPYNSPVLIAYLLGVPQSATR
# 10 (Dowex + Ascorbic Acid)	-	GDVSSEINILK GDVSSEINILK LSSSNIIFPFTPILVPLPTEPTK LSSSNIIFPFTPILVPLPTEPTK LSSSNIIFPFTPILVPLPTEPTK LSSSNIIFPFTPILVPLPTEPTK LSSSNIIFPFTPILVPLPTEPTK LSSSNIIFPFTPILVPLPTEPTK SmPPYNSPVLIAYLLGVPQSATR SmPPYNSPVLIAYLLGVPQSATR SmPPYNSPVLIAYLLGVPQSATR SmPPYNSPVLIAYLLGVPQSATR TSNILLDANLR TSNILLDANLR

# 11	-	-
# 12 (double protein amount)	-	-
# 13 (Sephadex)	-	LSSSNIIFPFTPILVPLPTEPTK
# 14 (Sephadex/ double protein amount)	-	-

Supplemental Table 5: Peptides identified for NFP proteins of *Populus trichocarpa*. Proteins were extracted from leaf samples and mass spectrometry was performed after chitin affinity purification. Detected peptides, for which quantitative data are shown in Figure 6 (chapter 3.1.5), are listed below. Unique peptides for a protein are colored in black. Peptides shared between two proteins whose origin cannot be distinguished are highlighted in orange. Information about additional purification steps is listed in brackets behind the number of protein extraction. Addition of dowex, ascorbic acid and sephadex should reduce phenolic compounds. Microsomal fraction, chitin hexamer (C6mer) elution and double protein amount were used to enrich the presence of candidate proteins in the samples.

Protein extraction	PtNFP-1	PtNFP-2	PtNFP-3	PtNFP-4
# 1	-	-	-	-
# 2	-	-	SSNILLDSSMR SSNILLDSSMR	-
# 3 (microsomal fraction)	-	-	SSNILLDSSMR SSNILLDSSMR SSNILLDSSMR SSNILLDSSMR ASAPNFLDLASIGDLFSVSR ASAPNFLDLASIGDLFSVSR	-
# 4 (microsomal fraction/ C6mer elution)	-	-	SSNILLDSSMR SSNILLDSSMR VLWAEAIGVLEGNVEER	-
# 5	-	-	-	-
# 6	-	-	-	-
# 7 (Dowex)	-	-	-	-
# 8 (Sephadex)	-	-	-	-
# 9	-	-	-	-
# 10 (Dowex + Ascorbic Acid)	-	-	-	-
# 11	-	-	-	-
# 12 (double protein amount)	-	-	-	-
# 13 (Sephadex)	-	-	-	-
# 14 (Sephadex/ double protein amount)	-	-	-	-

Supplemental Table 6: Peptides identified for LYM2 proteins of *Populus trichocarpa*. Proteins were extracted from leaf samples and mass spectrometry was performed after chitin affinity purification. Detected peptides, for which quantitative data are shown in Figure 6 (chapter 3.1.5), are listed below. Unique peptides for a protein are colored in black. Peptides shared between two proteins whose origin cannot be distinguished are highlighted in orange. Information about additional purification steps is listed in brackets behind the number of protein extraction. Addition of dowex, ascorbic acid and sephadex should reduce phenolic compounds. Microsomal fraction, chitin hexamer (C6mer) elution and double protein amount were used to enrich the presence of candidate proteins in the samples.

Protein extraction	PtLYM2-1	PtLYM2-2.1	PtLYM2-2.2
# 1	QPIYTVQK QPIYTVQK	-	QPIYTVQK QPIYTVQK TLFSIK
# 2	-	SSTSPNYVIQEQQVIK SSTSPNYVIQEQQVIK	-
# 3 (microsomal fraction)	-	-	-
# 4 (microsomal fraction/ C6mer elution)	NQSIFTTLATR NQSIFTTLATR NQSIFTTLATR NQSIFTTLATR NQSIFTTLATR NQSIFTTLATR	-	LWIPLPCSCDDVDGVK LWIPLPCSCDDVDGVK LWIPLPCSCDDVDGVK LWIPLPCSCDDVDGVK
# 5	QPIYTVQK QPIYTVQK QPIYTVQK QPIYTVQK QPIYTVQK QPIYTVQK	-	QPIYTVQK QPIYTVQK QPIYTVQK QPIYTVQK QPIYTVQK QPIYTVQK TLFSIK TLFSIK TLFSIK
# 6	LLIPLPCNCDDVDGVK LLIPLPCNCDDVDGVK LLIPLPCNCDDVDGVK QPIYTVQK QPIYTVQK QPIYTVQK QPIYTVQK QPIYTVQK QPIYTVQK	NLHSLLGANNLR VVHYAHLVEEGSTVEEIAEK	QPIYTVQK QPIYTVQK QPIYTVQK QPIYTVQK QPIYTVQK QPIYTVQK TLFSIK TLFSIK VVHYGHVVEAGSSLEFIAQEYGTSR
# 7 (Dowex)	QPIYTVQK QPIYTVQK QPIYTVQK	NLHSLLGANNLR	QPIYTVQK QPIYTVQK QPIYTVQK TLFSIK TLFSIK
# 8 (Sephadex)	QPIYTVQK QPIYTVQK QPIYTVQK	NLHSLLGANNLR	QPIYTVQK QPIYTVQK QPIYTVQK TLFSIK TLFSIK
# 9	VVHYGHVVEAGSSLELIAQEYGTSTDTLVK LLIPLPCNCDDVDGVK LLIPLPCNCDDVDGVK LWIPLPCNCDDVDGVK LWIPLPCNCDDVDGVK LWIPLPCNCDDVDGVK LWIPLPCNCDDVDGVK	-	-
# 10 (Dowex + Ascorbic Acid)	LLIPLPCNCDDVDGVK LLIPLPCNCDDVDGVK LLIPLPCNCDDVDGVK	SSTSPNYVIQEQQVIK SSTSPNYVIQEQQVIK	-

	LWIPLPCNCDDVDGVK VVHYGHVVEAGSSLELIAQEYGTSTDTLVK VVHYGHVVEAGSSLELIAQEYGTSTDTLVK VVHYGHVVEAGSSLELIAQEYGTSTDTLVK VVHYGHVVEAGSSLELIAQEYGTSTDTLVK VVHYGHVVEAGSSLELIAQEYGTSTDTLVK		
# 11	LLIPLPCNCDDVDGVK LLIPLPCNCDDVDGVK QPIYTVQK QPIYTVQK QPIYTVQK QPIYTVQK QPIYTVQK QPIYTVQK	-	QPIYTVQK QPIYTVQK QPIYTVQK QPIYTVQK QPIYTVQK QPIYTVQK
# 12 (double protein amount)	LLIPLPCNCDDVDGVK LLIPLPCNCDDVDGVK LLIPLPCNCDDVDGVK LLIPLPCNCDDVDGVK LLIPLPCNCDDVDGVK LLIPLPCNCDDVDGVK QPIYTVQK QPIYTVQK QPIYTVQK QPIYTVQK QPIYTVQK QPIYTVQK QPIYTVQK	-	QPIYTVQK QPIYTVQK QPIYTVQK QPIYTVQK QPIYTVQK QPIYTVQK QPIYTVQK
# 13 (Sephadex)	LLIPLPCNCDDVDGVK LLIPLPCNCDDVDGVK QPIYTVQK QPIYTVQK QPIYTVQK QPIYTVQK QPIYTVQK	-	QPIYTVQK QPIYTVQK QPIYTVQK QPIYTVQK QPIYTVQK
# 14 (Sephadex/ double protein amount)	LLIPLPCNCDDVDGVK LLIPLPCNCDDVDGVK QPIYTVQK QPIYTVQK QPIYTVQK QPIYTVQK QPIYTVQK QPIYTVQK QPIYTVQK QPIYTVQK QPIYTVQK QPIYTVQK	-	QPIYTVQK QPIYTVQK QPIYTVQK QPIYTVQK QPIYTVQK QPIYTVQK QPIYTVQK QPIYTVQK QPIYTVQK QPIYTVQK

6.3.1.2 Detected peptides in protein samples of *Populus trichocarpa* assigned to protein subdomains

For some genes of *Populus trichocarpa* a second allele was found through sequence analysis in our department (Mo Awwanah, unpublished).

PtCERK1

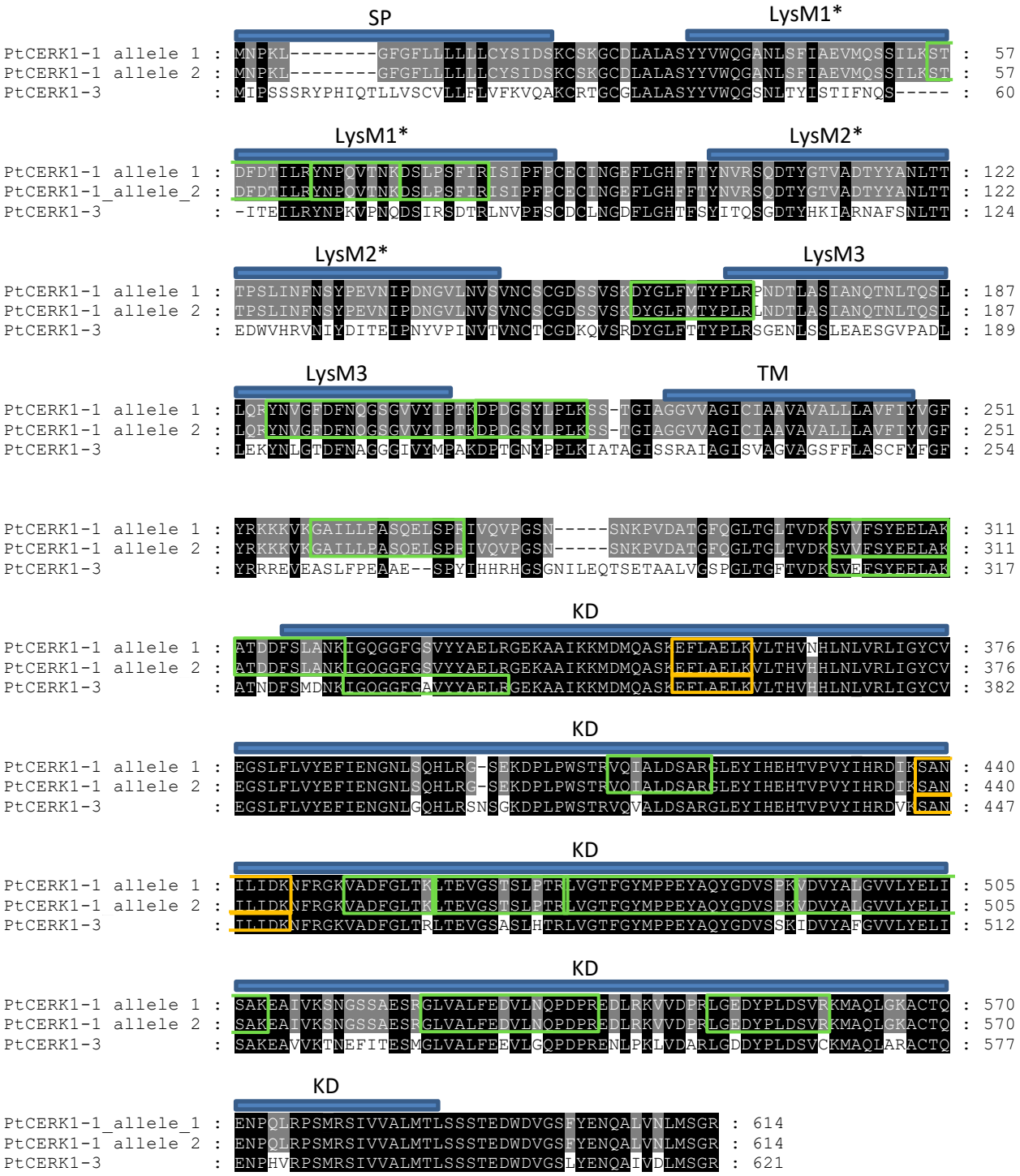

Supplemental Figure 3: Peptides identified for CERK1 proteins of *Populus trichocarpa*. A mass spectrometry analysis was performed with proteins from leave samples. Detected peptides are highlighted with a box. Unique peptides are colored in green and shared peptides in yellow. Domains are assigned with InterProScan integrated in Geneious® 8.1.9 (Kearse et al., 2012). Lysin motifs designated with an asterisk are predicted via sequence alignment with Arabidopsis CERK1 (Petutschnig et al., 2010). **SP:** signal peptide; **LysM:** lysin motif; **TM:** transmembrane domain; **KD:** kinase domain.

PtLYK4

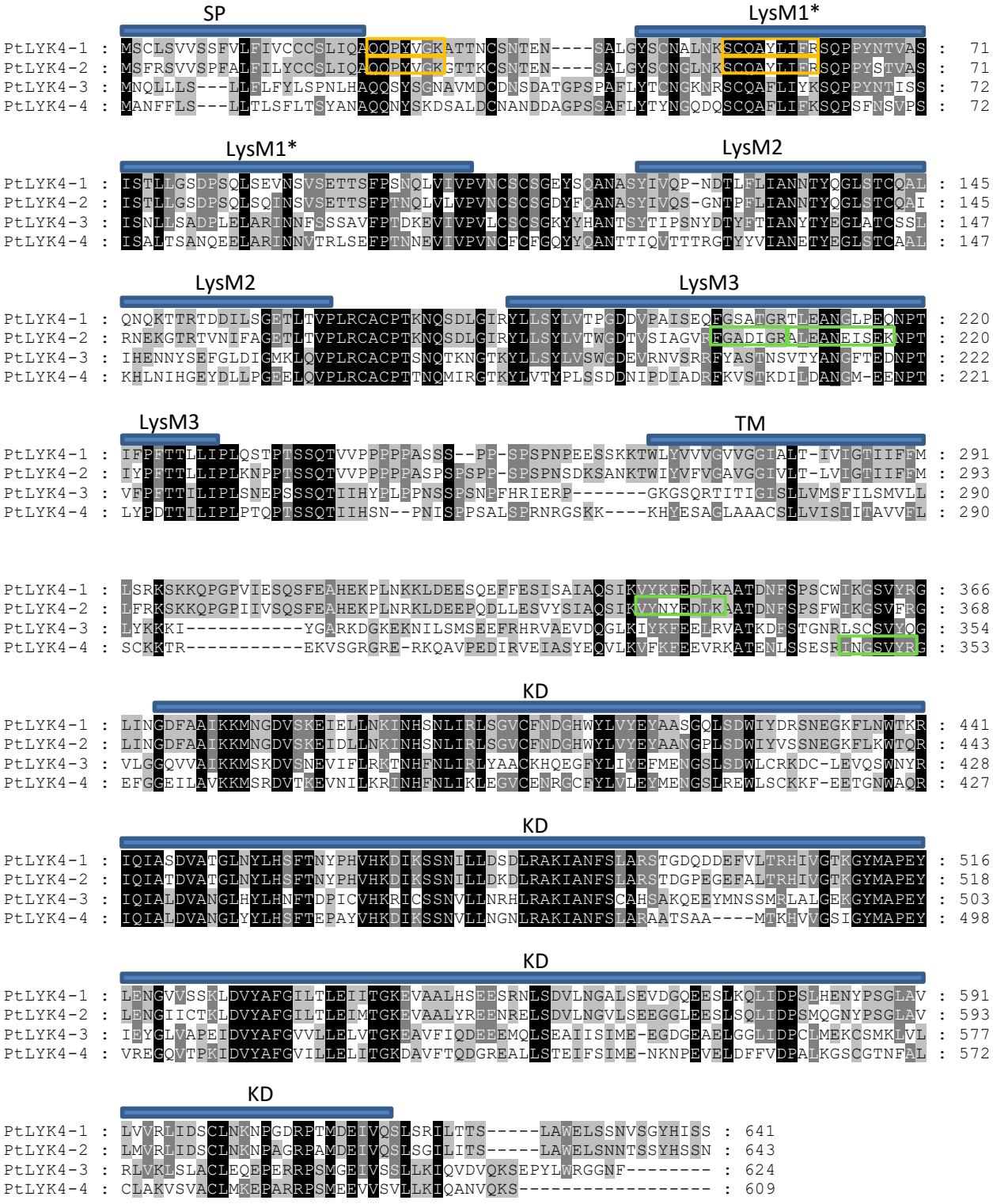

Supplemental Figure 4: Peptides identified for LYK4 proteins of *Populus trichocarpa*. A mass spectrometry analysis was performed with proteins from leave samples. Detected peptides are highlighted with a box. Unique peptides are colored in green and shared peptides in yellow. Domains are assigned with InterProScan integrated in Geneious® 8.1.9 (Kearse et al., 2012). Lysin motifs designated with an asterisk are predicted via sequence alignment with Arabidopsis CERK1 (Petutschnig et al., 2010). **SP:** signal peptide; **LysM:** lysin motif; **TM:** transmembrane domain; **KD:** kinase domain.

PtLYK5

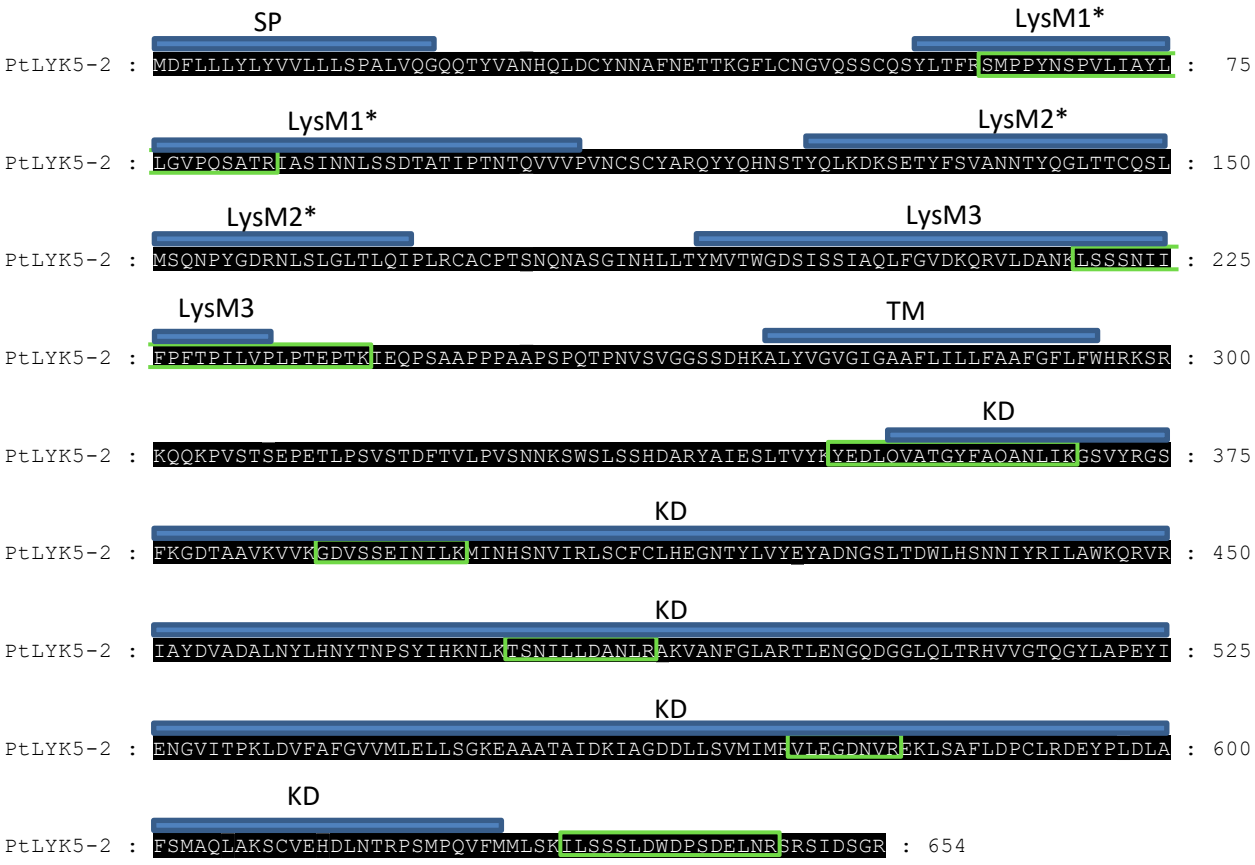

Supplemental Figure 5: Peptides identified for the LYK5-2 proteins of *Populus trichocarpa*. A mass spectrometry analysis was performed with proteins from leave samples. Detected peptides are highlighted with a box. Unique peptides are colored in green and shared peptides in yellow. Domains are assigned with InterProScan integrated in Geneious® 8.1.9 (Kearse et al., 2012). Lysin motifs designated with an asterisk are predicted via sequence alignment with Arabidopsis CERK1 (Petutschnig et al., 2010). **SP:** signal peptide; **LysM:** lysin motif; **TM:** transmembrane domain; **KD:** kinase domain.

PtNFP-3

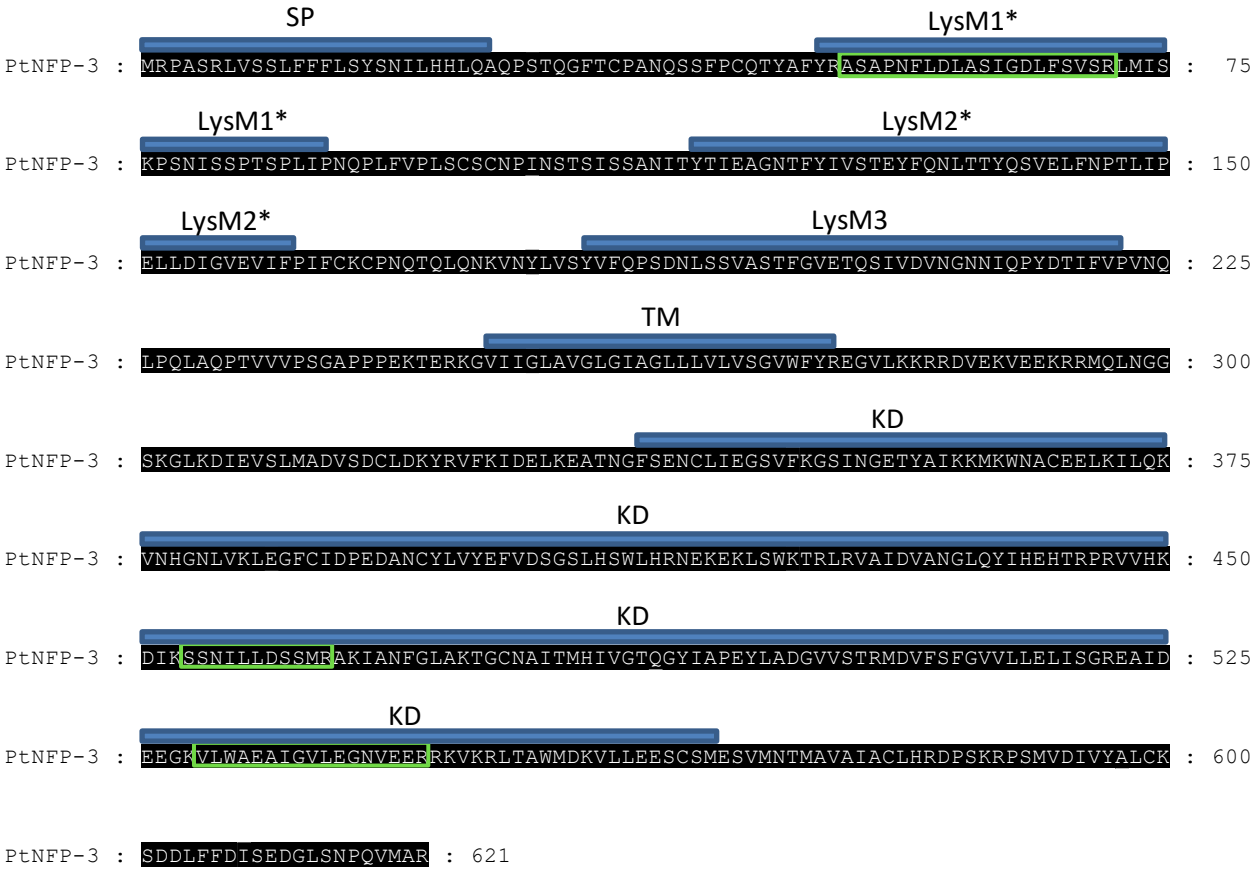

Supplemental Figure 6: Peptides identified for the NFP-3 protein of *Populus trichocarpa*. A mass spectrometry analysis was performed with proteins from leave samples. Detected peptides are highlighted with a box. Unique peptides are colored in green and shared peptides in yellow. Domains are assigned with InterProScan integrated in Geneious® 8.1.9 (Kearse et al., 2012). Lysin motifs designated with an asterisk are predicted via sequence alignment with Medicago truncatula NFP (Mulder et al., 2006). **SP:** signal peptide; **LysM:** lysin motif; **TM:** transmembrane domain; **KD:** kinase domain.

PtLYM2

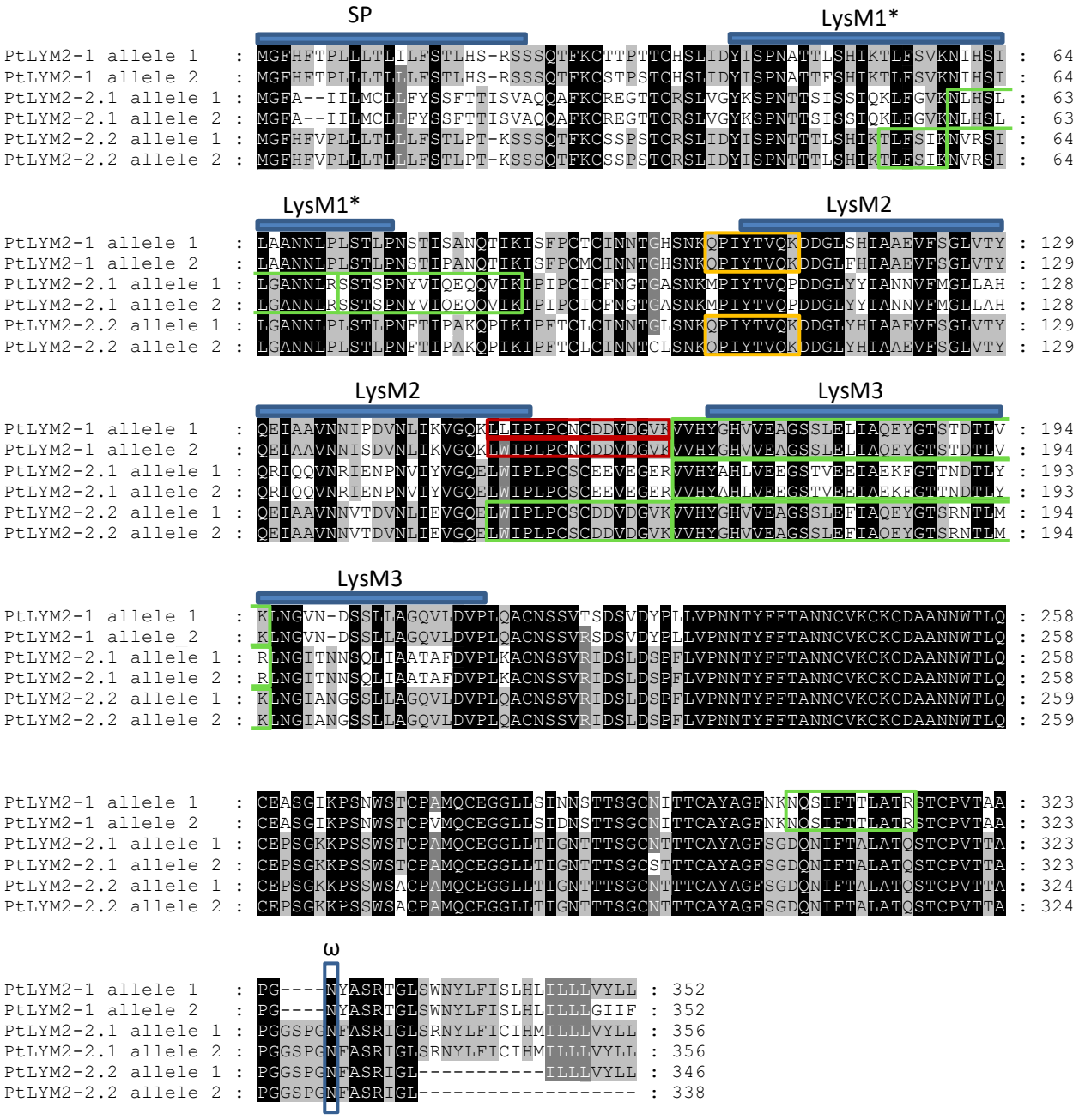

Supplemental Figure 7: Peptides identified for LYM2 proteins of *Populus trichocarpa*. A mass spectrometry analysis was performed with proteins from leave samples. Detected peptides are highlighted with a box. Unique peptides are colored in green and shared peptides in yellow. Peptides unique for a specific allele are colored in red. Domains are assigned with InterProScan integrated in Geneious® 8.1.9 (Kearse et al., 2012). Lysin motifs designated with an asterisk are predicted via sequence alignment with Oryza sativa CEBiP (Hayafune et al., 2014). For identification of the omega site as a GPI attachment signal the PredGPI tool (Pierleoni et al., 2008) was used. **SP:** signal peptide; **LysM:** lysin motif; **TM:** transmembrane domain; **KD:** kinase domain; **ω:** omega-site.

6.3.2 Peptides identified for LysM-RLKs and LysM-RLPs in *Populus x canescens*

6.3.1.1 Tabular overview of detected peptides in protein samples of *Populus x canescens*

Supplemental Table 7: Peptides identified for CERK1 proteins of *Populus x canescens*. Proteins were extracted from leaf samples and mass spectrometry was performed after chitin affinity purification. Detected peptides, for which quantitative data are shown in Figure 7 (chapter 3.1.5), are listed below. Unique peptides for a protein are colored in black. Peptides shared between two proteins whose origin cannot be distinguished are highlighted in orange. Information about additional purification steps is listed in brackets behind the number of protein extraction. Addition of dowex, ascorbic acid and sephadex should reduce phenolic compounds. Microsomal fraction and double protein amount were used to enrich the presence of candidate proteins in the samples.

Protein extraction	PcCERK1-1	PcCERK1-2
# 1	IGQGGFGAVYYAELR IGQGGFGAVYYAELR LGEDYPLDSVR LGEDYPLDSVR LTEVGGASLPTR LTEVGGASLPTR	LGEDYPLDSVR LGEDYPLDSVR
# 2 (microsomal fraction)	DSLPSFIR IGQGGFGAVYYAELR IGQGGFGAVYYAELR LGEDYPLDSVR LGEDYPLDSVR LTDFDTILSYNPQVPSK LTDFDTILSYNPQVPSK LTDFDTILSYNPQVPSK LTDFDTILSYNPQVPSK LTEVGGASLPTR LTEVGGASLPTR SVDFSYEELAK SVDFSYEELAK SVEFSYEELAK SVEFSYEELAK VDVYALGVVLYELISAK VDVYALGVVLYELISAK VQIALDSAR VQIALDSAR YNVGFDFNQGSGVVYIPAK YNVGFDFNQGSGVVYIPAK YNVGFDFNQGSGVVYIPAK YNVGFDFNQGSGVVYIPAK	LGEDYPLDSVR LGEDYPLDSVR SVEFSYEELAK SVEFSYEELAK VQIALDSAR VQIALDSAR
# 3	ATDDFSLANK ATDDFSLANK GSEKDPLPWSTR GSEKDPLPWSTR LGEDYPLDSVR LGEDYPLDSVR SVDFSYEELAK SVEFSYEELAK	ATDDFSLANK ATDDFSLANK LGEDYPLDSVR LGEDYPLDSVR SVEFSYEELAK
# 4	DSLPSFIR DSLPSFIR LGEDYPLDSVR LGEDYPLDSVR LTDFDTILSYNPQVPSK LTDFDTILSYNPQVPSK LTDFDTILSYNPQVPSKDSLPSFIR LTDFDTILSYNPQVPSKDSLPSFIR LTDFDTILSYNPQVPSKDSLPSFIR	LGEDYPLDSVR LGEDYPLDSVR VQIALDSAR VQIALDSAR

	LTDFDTILSYNPQVPSKDSLPSFIR LTEVGGASLPTR LTEVGGASLPTR SVDFSYEELAK SVDFSYEELAK VQIALDSAR VQIALDSAR YNVGFDFNQGSGVVYIPAK YNVGFDFNQGSGVVYIPAK YNVGFDFNQGSGVVYIPAK	
# 5 (Dowex + Ascorbic Acid)	DSLPSFIR DSLPSFIR DSLPSFIR LTDFDTILSYNPQVPSK LTDFDTILSYNPQVPSK LTDFDTILSYNPQVPSK LTDFDTILSYNPQVPSK SVDFSYEELAK SVDFSYEELAK VQIALDSAR YNVGFDFNQGSGVVYIPAK YNVGFDFNQGSGVVYIPAK	VQIALDSAR
# 6	LTDFDTILSYNPQVPSK YAGFYR	-
# 7 (double protein amount)	ATDDFSLANK DSLPSFIR DSLPSFIR EFFAELK LGEDYPLDSVR LGEDYPLDSVR LTDFDTILSYNPQVPSK SVDFSYEELAK YAGFYR YNVGFDFNQGSGVVYIPAK	ATDDFSLANK EFFAELK LGEDYPLDSVR LGEDYPLDSVR
# 8 (Sephadex)	LTDFDTILSYNPQVPSK YNVGFDFNQGSGVVYIPAK	-
# 9 (Sephadex/ double protein amount)	ATDDFSLANK LTDFDTILSYNPQVPSK LTDFDTILSYNPQVPSK LTDFDTILSYNPQVPSK YAGFYR YNVGFDFNQGSGVVYIPAK	ATDDFSLANK

Supplemental Table 8: Peptides identified for LYK4 proteins of *Populus x canescens*. Proteins were extracted from leaf samples and mass spectrometry was performed after chitin affinity purification. Detected peptides, for which quantitative data are shown in Figure 7 (chapter 3.1.5), are listed below. Unique peptides for a protein are colored in black. Peptides shared between two proteins whose origin cannot be distinguished are highlighted in orange. Information about additional purification steps is listed in brackets behind the number of protein extraction. Addition of dowex, ascorbic acid and sephadex should reduce phenolic compounds. Microsomal fraction and double protein amount were used to enrich the presence of candidate proteins in the samples.

Protein extraction	PcLYK4-1	PcLYK4-2	PcLYK4-3	PcLYK4-4
# 1	STGDLDGEFALTR STGDLDGEFALTR TNDIILSGETLTVPLR TNDIILSGETLTVPLR	STDGPEGEFALTR STDGPEGEFALTR	-	-
# 2 (microsomal fraction)	-	-	-	-
# 3	IANFSLAR IANFSLAR STGGLDGEFALTR	IANFSLAR IANFSLAR		INGSVYR INGSVYR
# 4	DITSSNILLDSDLR TNDIILSGETLTVPLR TNDIILSGETLTVPLR TNDIILSGETLTVPLR TNDIILSGETLTVPLR	-	-	-
# 5 (Dowex + Ascorbic Acid)	TNDIILSGETLTVPLR TNDIILSGETLTVPLR TNDIILSGETLTVPLR TNDIILSGETLTVPLR TNDIILSGETLTVPLR TNDIILSGETLTVPLR	-	-	-
# 6	IANFSLAR IANFSLAR SCQAYLIFR	IANFSLAR IANFSLAR	-	INGSVYR INGSVYR
# 7 (double protein amount)	-	-	-	INGSVYR
# 8 (Sephadex)	IANFSLAR QQPYVGK SCQAYLIFR	IANFSLAR QQPYVGK	-	INGSVYR INGSVYR INGSVYR
# 9 (Sephadex/ double protein amount)	IANFSLAR	IANFSLAR	-	INGSVYR INGSVYR

Supplemental Table 9: Peptides identified for LYK5 proteins of *Populus x canescens*. Proteins were extracted from leaf samples and mass spectrometry was performed after chitin affinity purification. Detected peptides, for which quantitative data are shown in Figure 7 (chapter 3.1.5), are listed below. Unique peptides for a protein are colored in black. Peptides shared between two proteins whose origin cannot be distinguished are highlighted in orange. Information about additional purification steps is listed in brackets behind the number of protein extraction. Addition of dowex, ascorbic acid and sephadex should reduce phenolic compounds. Microsomal fraction and double protein amount were used to enrich the presence of candidate proteins in the samples.

Protein extraction	PcLYK5-1	PcLYK5-2
# 1	-	TLENDQDGGLQLTR TLENDQDGGLQLTR TLENDQDGGLQLTR TLENDQDGGLQLTR TSNILLDANLR TSNILLDANLR TSNILLDANLR TSNILLDANLR
# 2 (microsomal fraction)	-	LSSSDIIFPFTPILVPLPTNPTK LSSSDIIFPFTPILVPLPTNPTK LSSSDIIFPFTPILVPLPTNPTK LSSSDIIFPFTPILVPLPTNPTK
# 3	-	GDVSSEINILK GLNLQIPLR SWSLSPNDAR TSNILLDANLR VLEGDNVR YAIESLTVYK
# 4	-	GLNLQIPLR GLNLQIPLR GLNLQIPLR GLNLQIPLR LSSSDIIFPFTPILVPLPTNPTK LSSSDIIFPFTPILVPLPTNPTK LSSSDIIFPFTPILVPLPTNPTK LSSSDIIFPFTPILVPLPTNPTK LSSSDIIFPFTPILVPLPTNPTK LSSSDIIFPFTPILVPLPTNPTK LSSSDIIFPFTPILVPLPTNPTK LSSSDIIFPFTPILVPLPTNPTK ILSSSLDWDPSDELNR
# 5 (Dowex + Ascorbic Acid)	-	GLNLQIPLR GLNLQIPLR LSSSDIIFPFTPILVPLPTNPTK LSSSDIIFPFTPILVPLPTNPTK LSSSDIIFPFTPILVPLPTNPTK LSSSDIIFPFTPILVPLPTNPTK
# 6	-	GLNLQIPLR
# 7 (double protein amount)	-	GLNLQIPLR LSSSDIIFPFTPILVPLPTNPTK
# 8 (Sephadex)	-	LSSSDIIFPFTPILVPLPTNPTK LSSSDIIFPFTPILVPLPTNPTK
# 9 (Sephadex/ double protein amount)	-	EAAATAIDK GLNLQIPLR LSSSDIIFPFTPILVPLPTNPTK VLEGDNVR

Supplemental Table 10: Peptides identified for LYM2 proteins of *Populus x canescens*. Proteins were extracted from leaf samples and mass spectrometry was performed after chitin affinity purification. Detected peptides, for which quantitative data are shown in Figure 7 (chapter 3.1.5), are listed below. Unique peptides for a protein are colored in black. Peptides shared between two proteins whose origin cannot be distinguished are highlighted in orange. Information about additional purification steps is listed in brackets behind the number of protein extraction. Addition of dowex, ascorbic acid and sephadex should reduce phenolic compounds. Microsomal fraction and double protein amount were used to enrich the presence of candidate proteins in the samples.

Protein extraction	PcLYM2-1	PcLYM2-2.1	PcLYM2-2.2
# 1	-	VVHYAHLVEEGSTVEEIAEK VVHYAHLVEEGSTVEEIAEK VVHYAHLVEEGSTVEEIAEK VVHYAHLVEEGSTVEEIAEK VVHYAHLVEEGSTVEEIAEK VVHYAHLVEEGSTVEEIAEK	-
# 2 (microsomal fraction)	DDGLSHIATEVFSGLVTYQEIAAVNNIPDVNLIK DDGLSHIATEVFSGLVTYQEIAAVNNIPDVNLIK DDGLSHIATEVFSGLVTYQEIAAVNNIPDVNLIK DDGLSHIATEVFSGLVTYQEIAAVNNIPDVNLIK NQSIFTTLATR NQSIFTTLATR VVHYGHVVEAGSSLELIAQEYGTSTDTLVK VVHYGHVVEAGSSLELIAQEYGTSTDTLVK VVHYGHVVEAGSSLELIAQEYGTSTDTLVK VVHYGHVVEAGSSLELIAQEYGTSTDTLVK VVHYGHVVEAGSSLELIAQEYGTSTDTLVK VVHYGHVVEAGSSLELIAQEYGTSTDTLVK LWIPLPCSCDDVDGVK LWIPLPCSCDDVDGVK	-	LWIPLPCSCDDVDGVK LWIPLPCSCDDVDGVK SILGANNLALSTLPNFTIPAK VVHYGHVVEAGSSLEVIAQEYGTSR VVHYGHVVEAGSSLEVIAQEYGTSR VVHYGHVVEAGSSLEVIAQEYGTSR VVHYGHVVEAGSSLEVIAQEYGTSR VVHYGHVVEAGSSLEVIAQEYGTSR VVHYGHVVEAGSSLEVIAQEYGTSR VVHYGHVVEAGSSLEVIAQEYGTSR
# 3	QPIYTVQK QPIYTVQK QPIYTVQK	VVHYAHLVEEGSTVEEIAEK	QPIYTVQK QPIYTVQK QPIYTVQK TLFSIK
# 4	LWIPLPCSCDDVDGVK LWIPLPCSCDDVDGVK LWIPLPCSCDDVDGVK LWIPLPCSCDDVDGVK	VVHYAHLVEEGSTVEEIAEK VVHYAHLVEEGSTVEEIAEK	LWIPLPCSCDDVDGVK LWIPLPCSCDDVDGVK LWIPLPCSCDDVDGVK LWIPLPCSCDDVDGVK
# 5 (Dowex + Ascorbic Acid)	-	-	-
# 6	-	-	-
# 7 (double protein amount)	LWIPLPCSCDDVDGVK QPIYTVQK	-	CSSPLTCR LWIPLPCSCDDVDGVK QPIYTVQK TLFSIK
# 8 (Sephadex)	QPIYTVQK	-	QPIYTVQK
# 9 (Sephadex/ double protein amount)	QPIYTVQK QPIYTVQK QPIYTVQK QPIYTVQK	-	CSSPLTCR QPIYTVQK QPIYTVQK QPIYTVQK QPIYTVQK TLFSIK TLFSIK

6.3.1.2 Detected peptides in protein samples of *Populus x canescens* assigned to protein subdomains

Populus x canescens is a natural hybrid of *Populus tremula* x *Populus alba.* For each gene both alleles are listed. Sequences are obtained by sequence analysis in our department. Transcript and protein sequences for PcCERK1 are published in this work (see section 6.2) and for PcLYK4, PcLYK5 and PcLYM2 in Awwanah (2020).

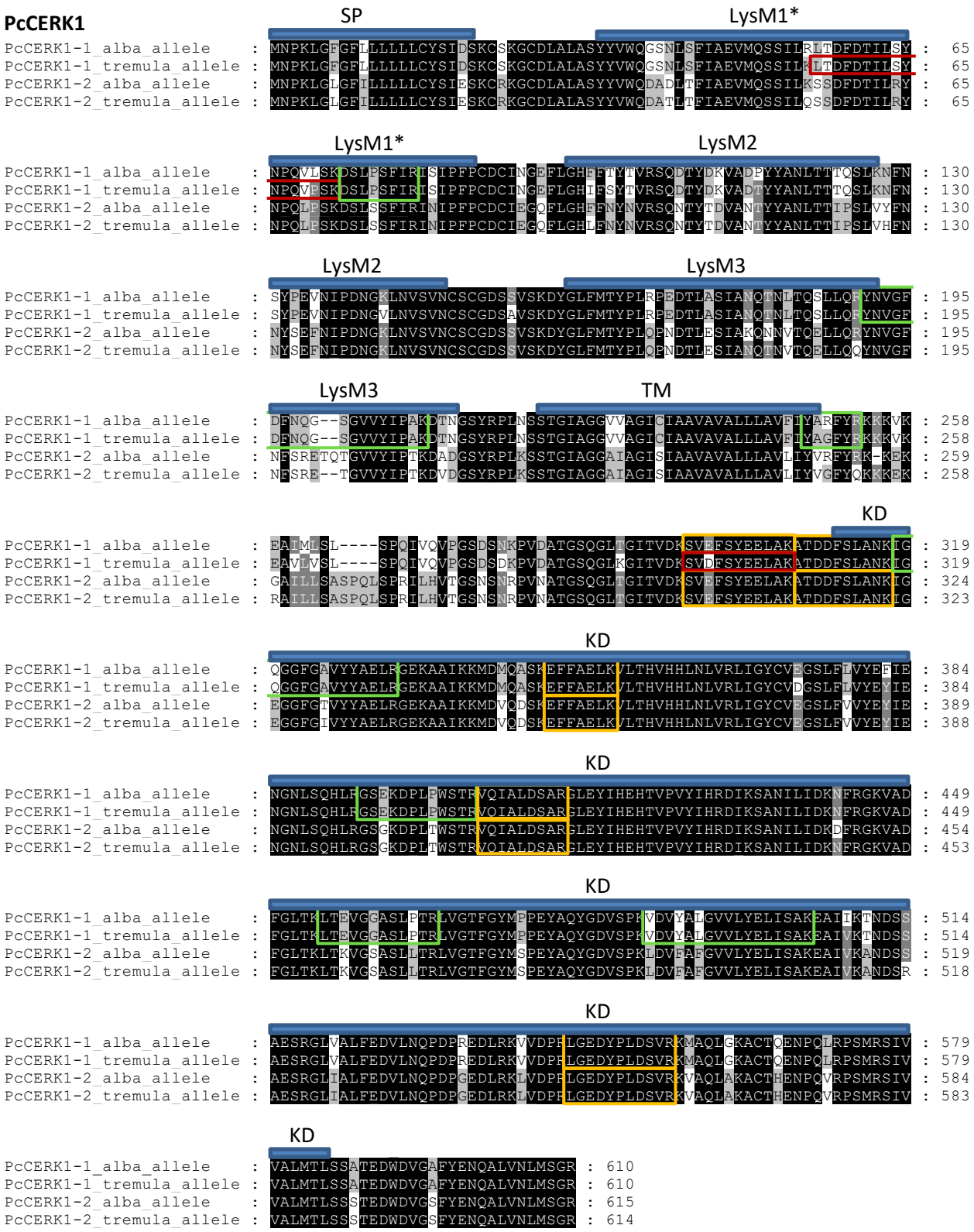

Supplemental Figure 8: Peptides identified for CERK1 proteins of *Populus x canescens*. A mass spectrometry analysis was performed with proteins from leave samples. Detected peptides are highlighted with a box. Unique peptides are colored in green and shared peptides in yellow. Peptides unique for a specific allele are colored in red. Domains are assigned with InterProScan integrated in Geneious® 8.1.9 (Kearse et al., 2012). Lysin motifs designated with an asterisk are predicted via sequence alignment with Arabidopsis CERK1 (Petutschnig et al., 2010). **SP:** signal peptide; **LysM:** lysin motif; **TM:** transmembrane domain; **KD:** kinase domain.

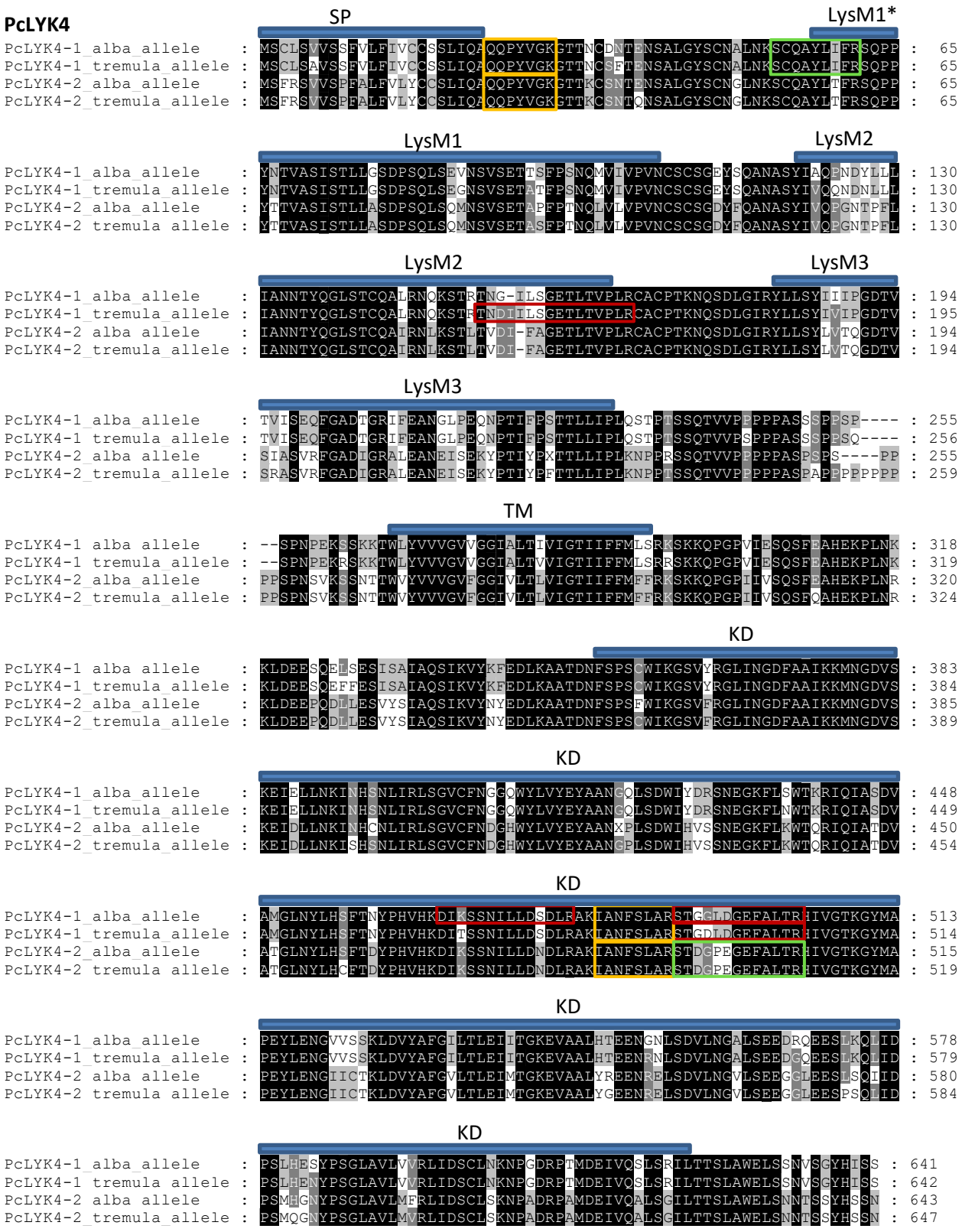

Supplemental Figure 9: Peptides identified for LYK4 proteins of *Populus x canescens*. A mass spectrometry analysis was performed with proteins from leave samples. Detected peptides are highlighted with a box. Unique peptides are colored in green and shared peptides in yellow. Peptides unique for a specific allele are colored in red. Domains are assigned with InterProScan integrated in Geneious® 8.1.9 (Kearse et al., 2012). Lysin motifs designated with an asterisk are predicted via sequence alignment with Arabidopsis CERK1 (Petutschnig et al., 2010). **SP:** signal peptide; **LysM:** lysin motif; **TM:** transmembrane domain; **KD:** kinase domain.

PcLYK5-2

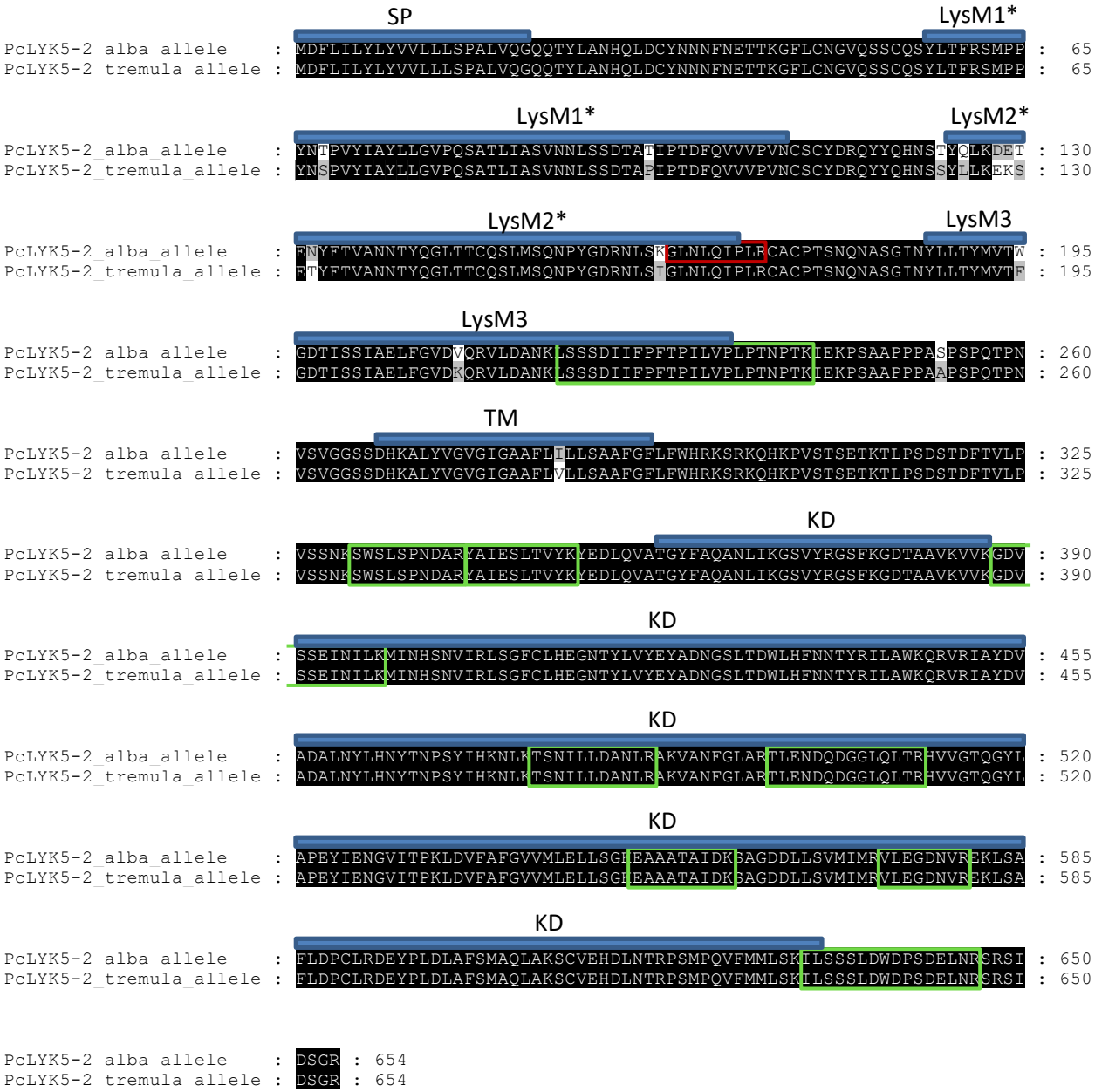

Supplemental Figure 10: Peptides identified for the LYK5-2 protein of *Populus x canescens*. A mass spectrometry analysis was performed with proteins from leave samples. Detected peptides are highlighted with a box. Unique peptides are colored in green and shared peptides in yellow. Peptides unique for a specific allele are colored in red. Domains are assigned with InterProScan integrated in Geneious® 8.1.9 (Kearse et al., 2012). Lysin motifs designated with an asterisk are predicted via sequence alignment with Arabidopsis CERK1 (Petutschnig et al., 2010). **SP:** signal peptide; **LysM:** lysin motif; **TM:** transmembrane domain; **KD:** kinase domain.

PcLYM2

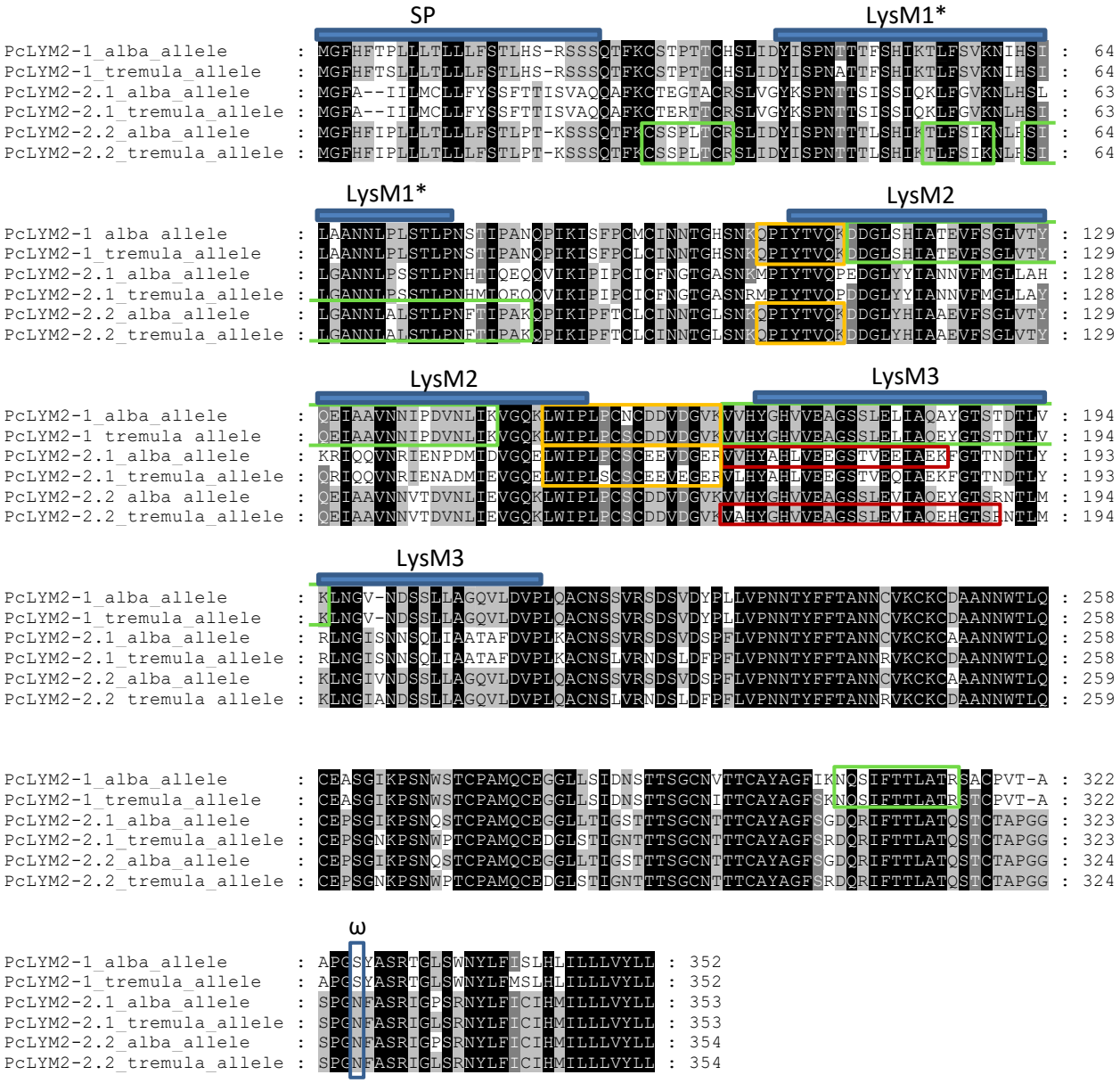

Supplemental Figure 11: Peptides identified for LYM2 proteins of *Populus x canescens*. A mass spectrometry analysis was performed with proteins from leave samples. Detected peptides are highlighted with a box. Unique peptides are colored in green and shared peptides in yellow. Peptides unique for a specific allele are colored in red. Domains are assigned with InterProScan integrated in Geneious® 8.1.9 (Kearse et al., 2012). Lysin motifs designated with an asterisk are predicted via sequence alignment with Oryza sativa CEBiP (Hayafune et al., 2014). For identification of the omega site as a GPI attachment signal the PredGPI tool (Pierleoni et al., 2008) was used. **SP:** signal peptide; **LysM:** lysin motif; **TM:** transmembrane domain; **KD:** kinase domain; **ω:** omega-site.

6.4 Flagellin induced ROS bursts

6.4.1 Flagellin induced ROS bursts of complementation experiments

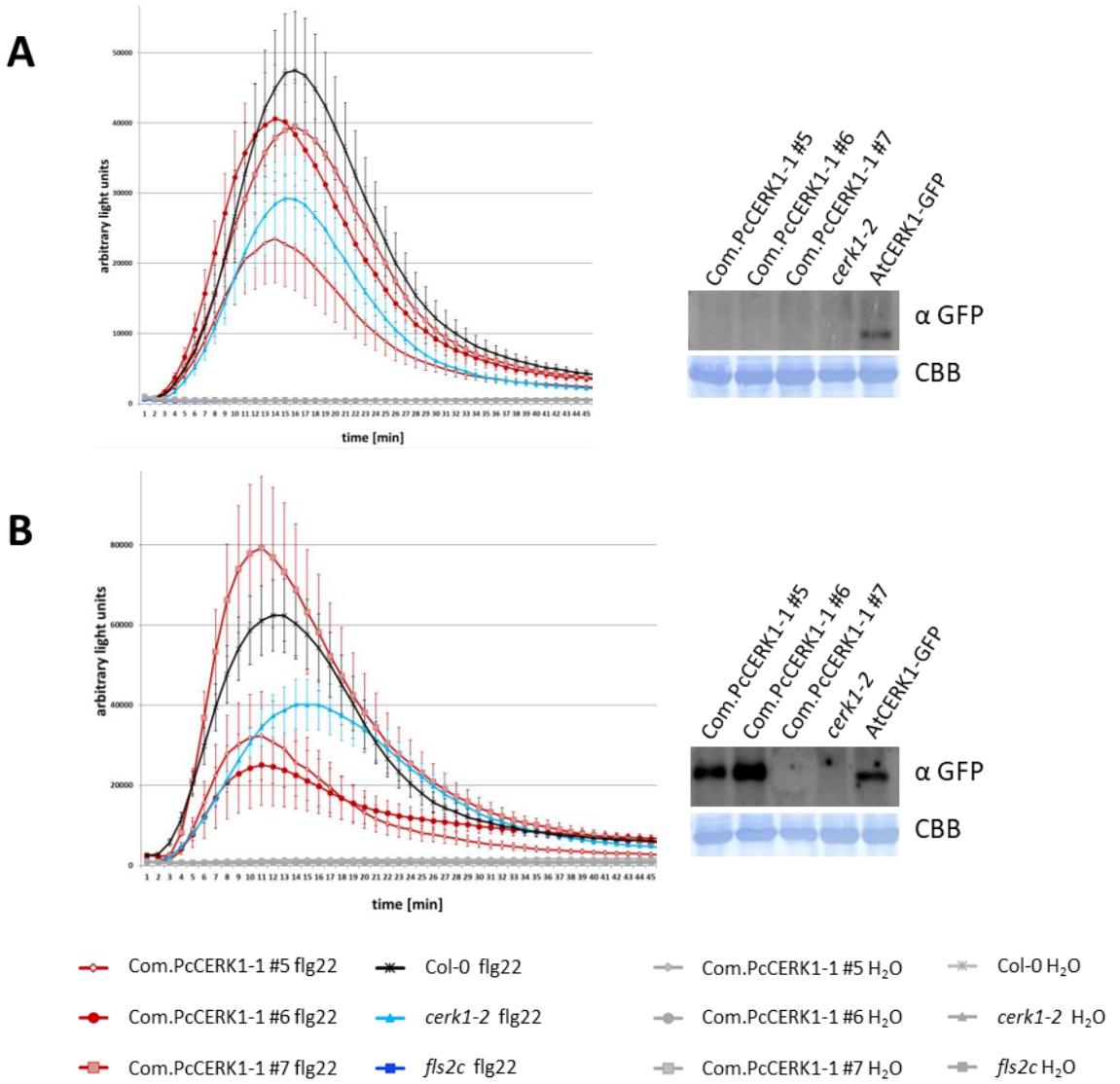

Supplemental Figure 12: The *pLexA:PcCERK1-1_mCitrine* lines react with a flagellin induced ROS burst similar to the wildtype response. Leaf discs were treated with 100 nM flg22 or water as a control. To visualize ROS generation a luminol based assay was used. Data represent the mean of 8 leaf discs ± SEM. To test if the *PcCERK1-1* gene expression was induced after applying estradiol, a Western Blot was performed detecting the mCitrine tagged protein with a GFP antibody. **A:** samples sprayed with water; **B:** samples sprayed with 25 µM estradiol; **Com.PcCERK1-1 #5, #6, #7**: individual lines of *pLexA:PcCERK1-1_mCitrine* transformed into *cerk1-2* mutant; **Col-0**: Arabidopsis wildtype; ***cerk1-2***: Arabidopsis CERK1 knockout mutant that lacks chitin response; ***fls2c*:** Arabidopsis FLS2c knockout mutant that lacks flagellin response; **AtCERK1-GFP:** *pAtCERK1:AtCERK1_GFP* transformed into *cerk1-2* mutant, used as a control for detection of PcCERK1-mCitrine fusions that are recognized by the GFP antibody; **CBB**: Coomassie Brilliant Blue-stained membrane.

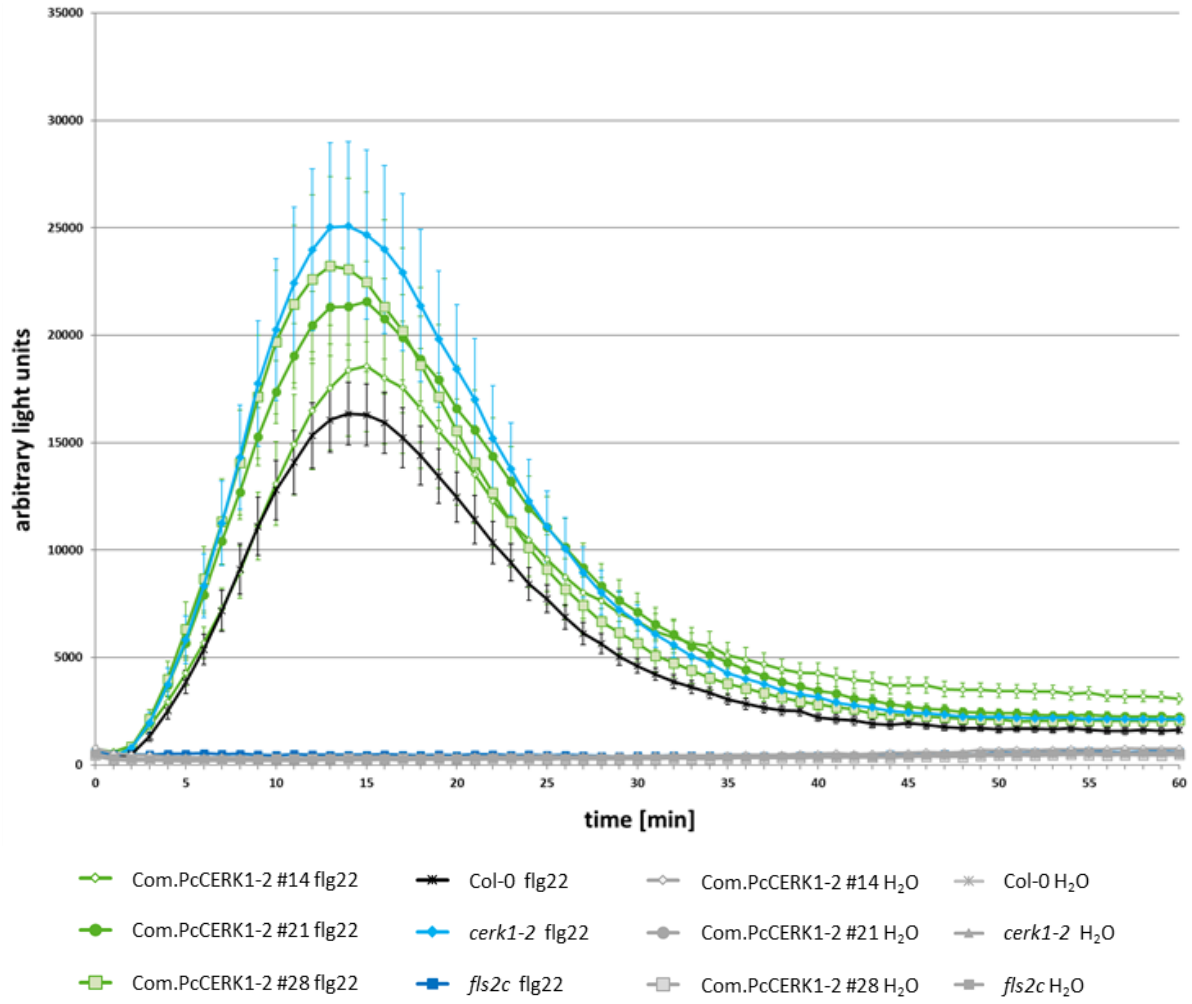

Supplemental Figure 13: Arabidopsis *cerk1-2* plants expressing *PcCERK1-2* show a flagellin induced ROS burst similar to the wildtype response. Leaf discs were treated with either 100 nM flg22 or water as a control. To visualize ROS generation a luminol based assay was used. Data represent the mean of 8 leaf discs ± SEM. **Com.PcCERK1-2 #14, #21, #28**: individual lines of *pAtCERK1:PcCERK1-2_mCitrine* transformed into *cerk1-2* mutant; **Col-0:** Arabidopsis wildtype; ***cerk1-2*:** Arabidopsis CERK1 knockout mutant that lacks chitin response; ***fls2c*:** Arabidopsis FLS2C knockout mutant that lacks flagellin response.

6.4.2 Flagellin induced ROS burst of overexpression lines of a cerk1 loss of function gene

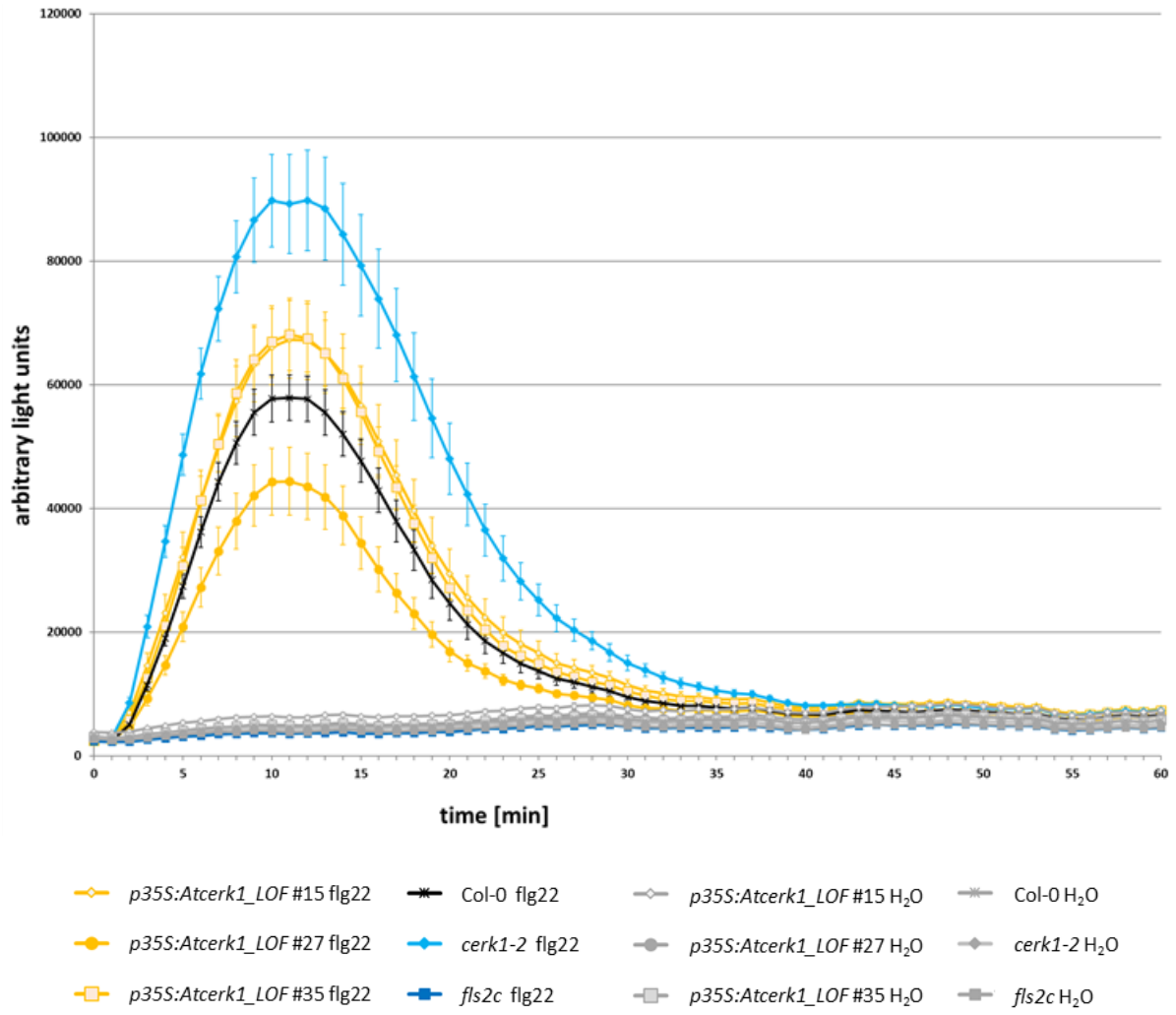

Supplemental Figure 14: The overexpression of a cerk1 loss of function gene in Arabidopsis does not affect the flagellin induced ROS burst response. Leaf discs were treated with either 100 nM flg22 or water as a control. To visualize ROS generation a luminol based assay was used. Data represent the mean of 8 leaf discs ± SEM. ***p35S:Atcerk1_LOF* #15, #27, #35**: individual lines overexpressing a kinase dead version of CERK1 in Col-0; **Col-0**: Arabidopsis wildtype; ***cerk1-2***: Arabidopsis CERK1 knockout mutant that lacks chitin response; ***fls2c***: Arabidopsis FLS2C knockout mutant that lacks flagellin response.

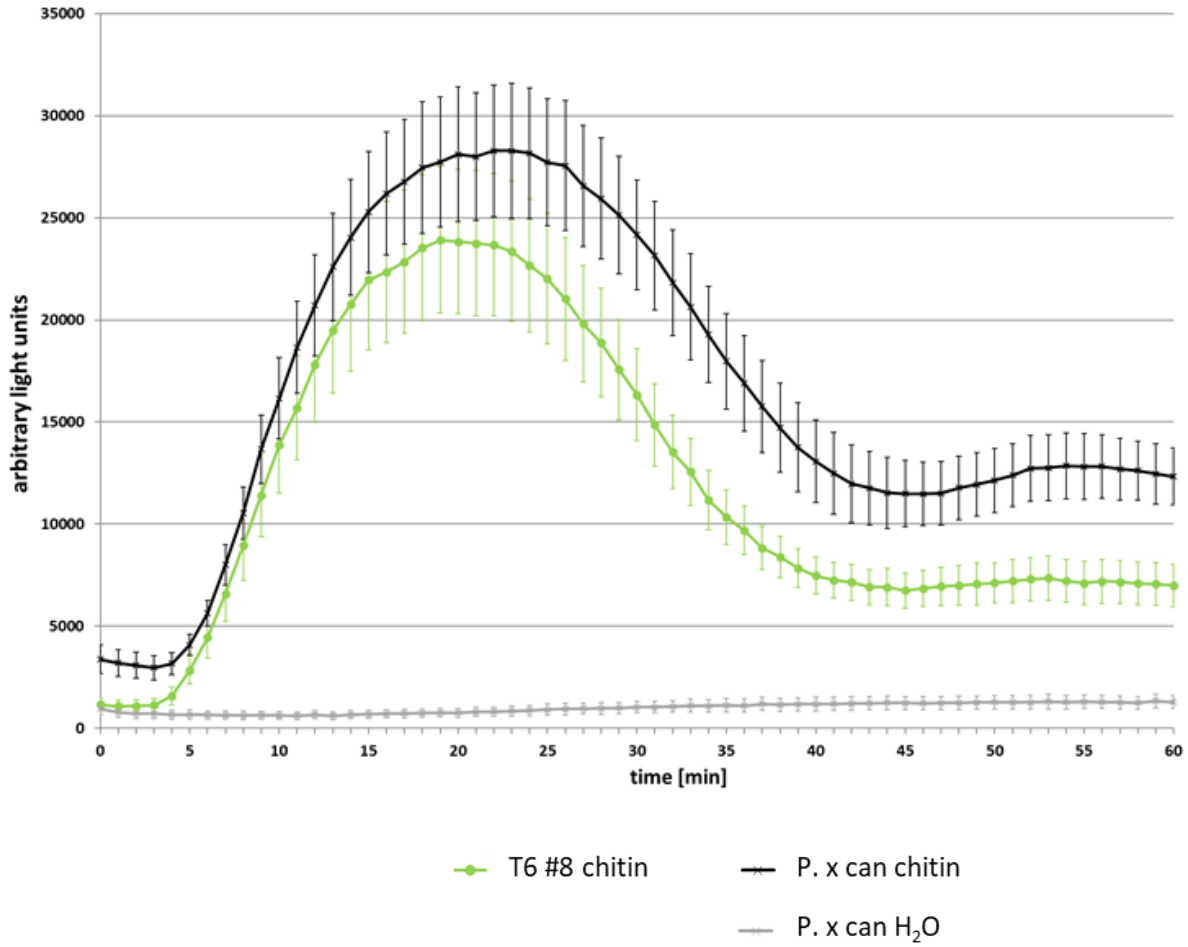

Supplemental Figure 15: The overexpression of a Pccerk1-1 loss of function gene in wildtype *P. x canescens* shows a flagellin induced ROS burst similar to the wildtype response. Leaf discs were treated with either 100 nM flg22 solution or water as a control. To visualize ROS generation a luminol based assay was used. Data represent the mean of 8 leaf discs ± SEM. **T6 #8**: *p35S:Pccerk1-1_LOF* line overexpressing a kinase dead version of CERK1 in *P. x canescens*; **P. x can**: wildtype *Populus x canescens*.

6.4.3 Flagellin induced ROS burst of poplar CRISPR/Cas9 knockout lines

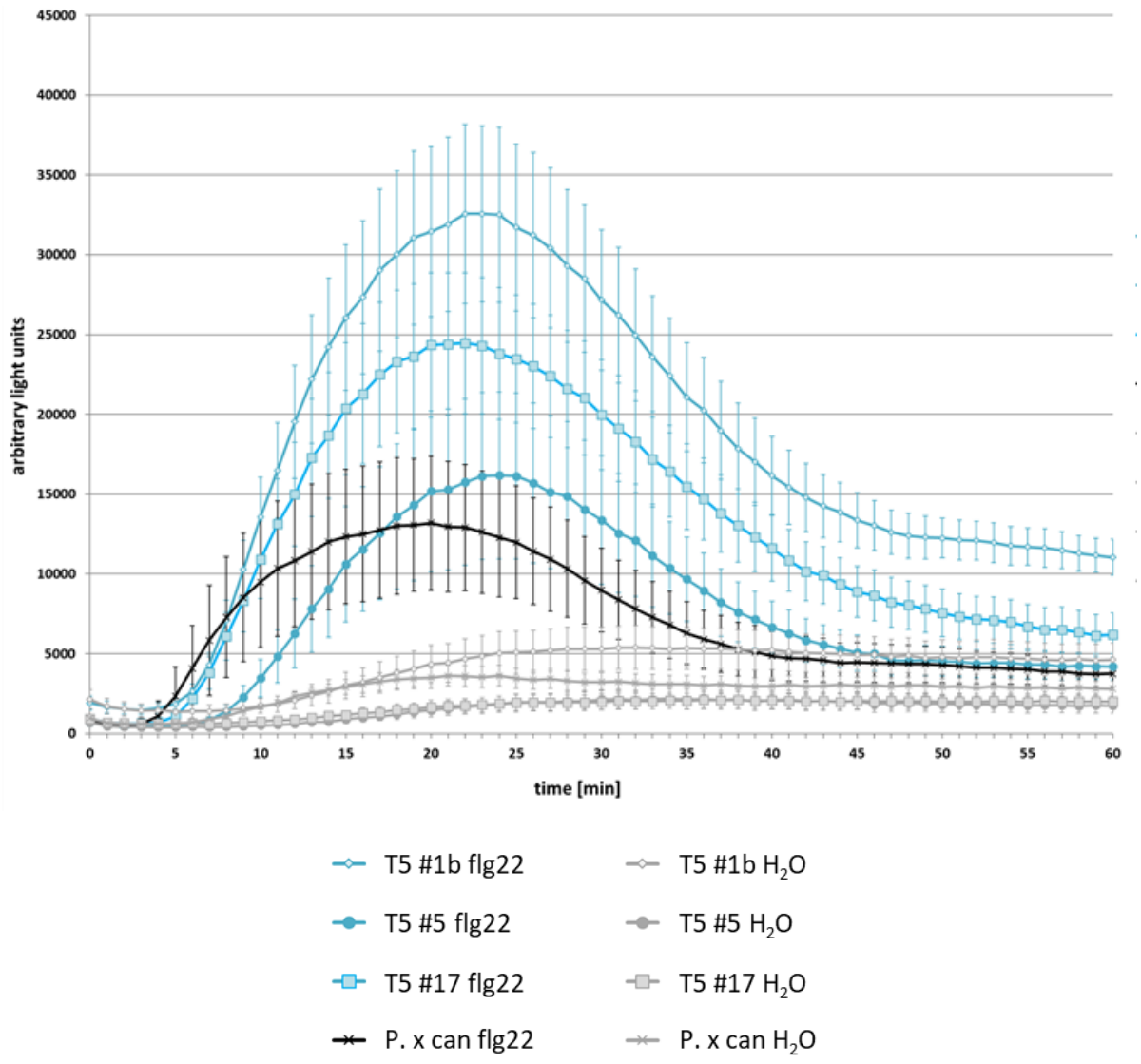

Supplemental Figure 16: *Pccerk1-1* CRISPR/Cas9 knockout lines show a flagellin induced ROS burst similar to the wildtype response. Leaf discs were treated with either 100 nM flg22 or water as a control. To visualize ROS generation a luminol based assay was used. Data represent the mean of 8 leaf discs ± SEM. **T5 #1b, T5 #5, T5 #17**: individual *Pccerk1-1* CRISPR/Cas9 knockout lines; **P. x can**: wildtype *Populus x canescens*.

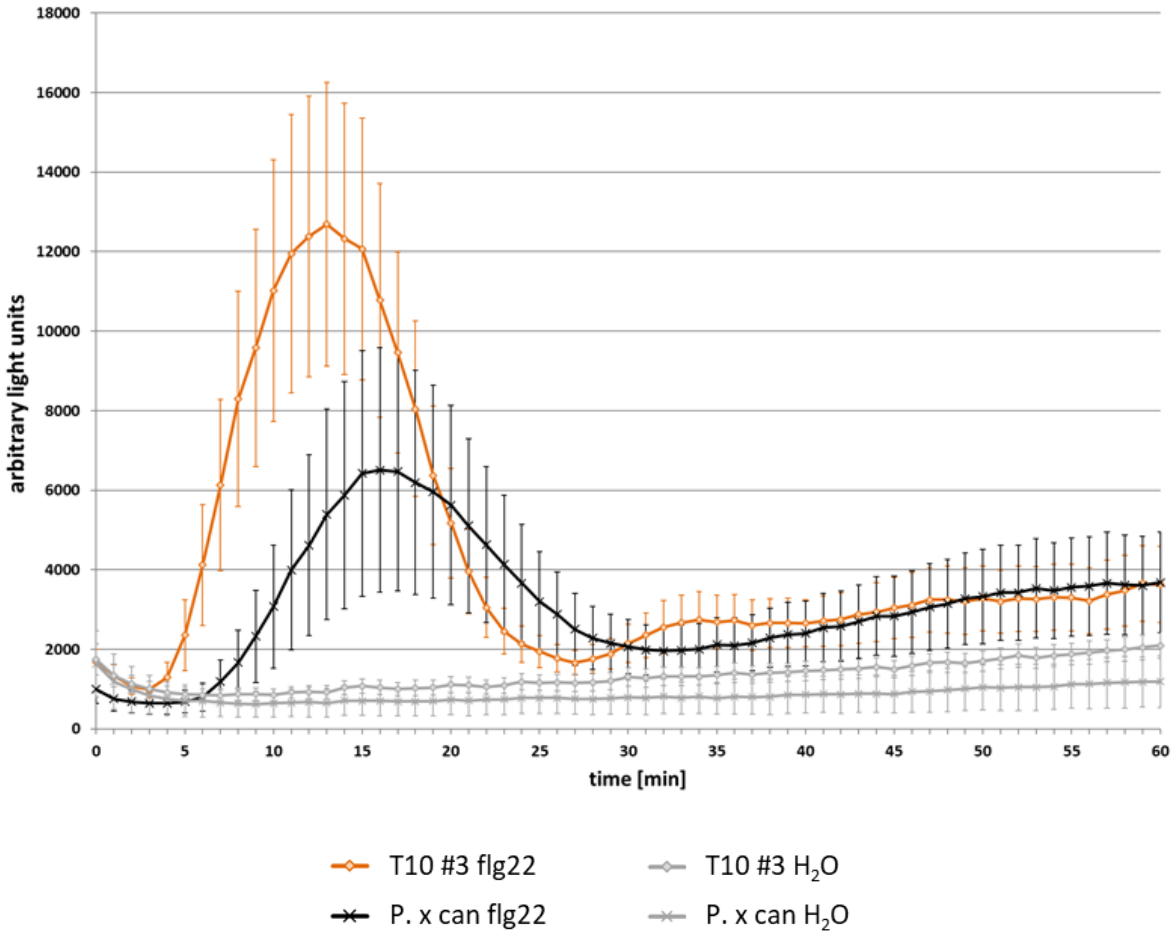

Supplemental Figure 17: The *Pccerk1-2* CRISPR/Cas9 knockout line show a flagellin induced ROS burst similar to the wildtype response. Leaf discs were treated with either 100 nM flg22 or water as a control. To visualize ROS generation a luminol based assay was used. Data represent the mean of 8 leaf discs ± SEM. **T10 #3**: *Pccerk1-2* CRISPR/Cas9 knockout line; **P. x can**: wildtype *Populus x canescens*.

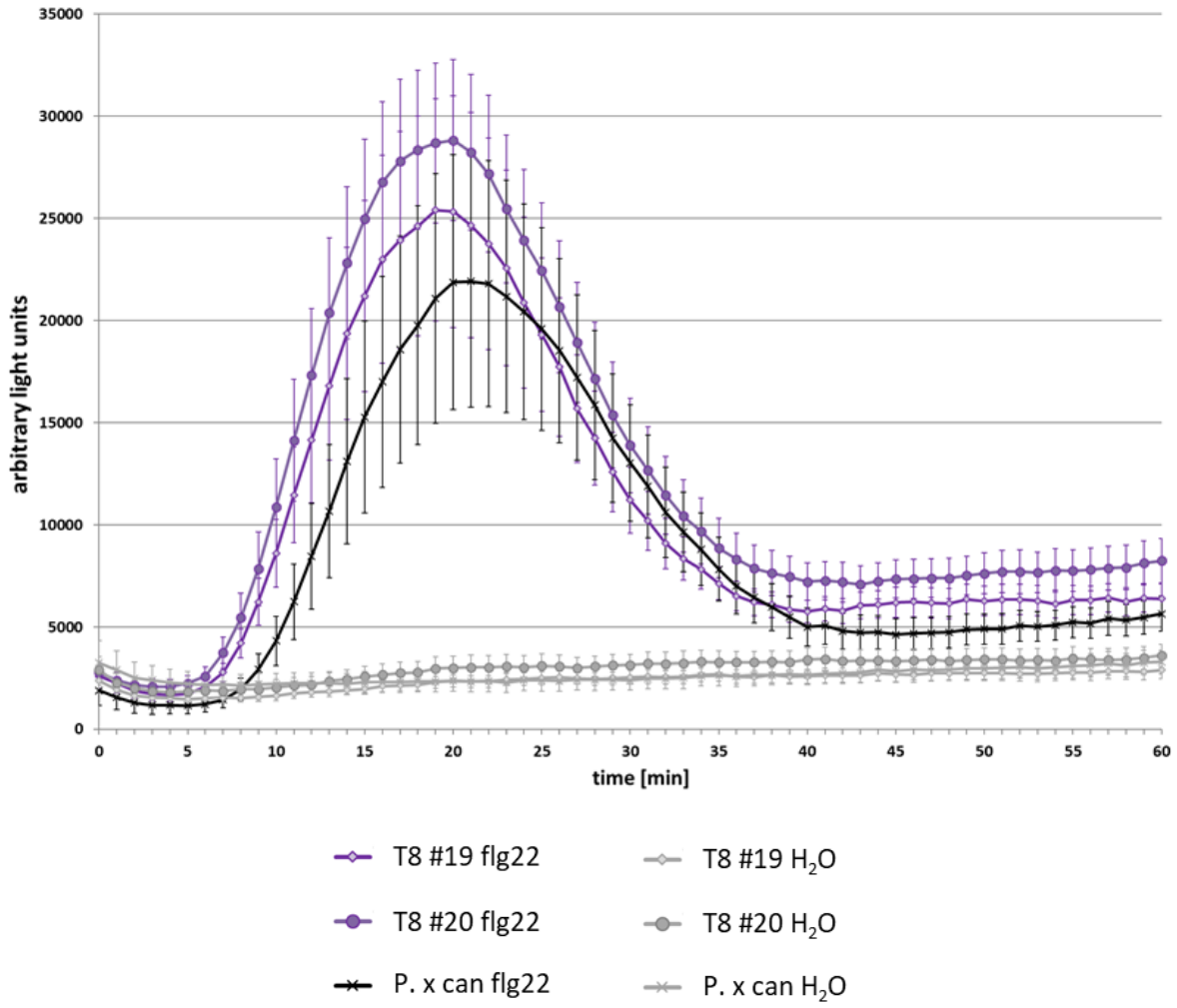

Supplemental Figure 18*: Pccerk1-1 Pccerk1-2* CRISPR/Cas9 double knockout lines exhibit a flagellin induced ROS burst similar to the wildtype response. Leaf discs were treated with either 100 nM flg22 or water as a control. To visualize ROS generation a luminol based assay was used. Data represent the mean of 8 leaf discs ± SEM. **T8 #19, T8 #20**: individual *Pccerk1-1* and *Pccerk1-2* CRISPR/Cas9 double knockout lines; **P. x can**: wildtype *Populus x canescens*.

6.5 Editing of CRISPR/Cas9 knockout lines

6.5.1 Sequence analyses of edited sites in *Pccerk1-1* CRISPR/Cas9 knockout lines

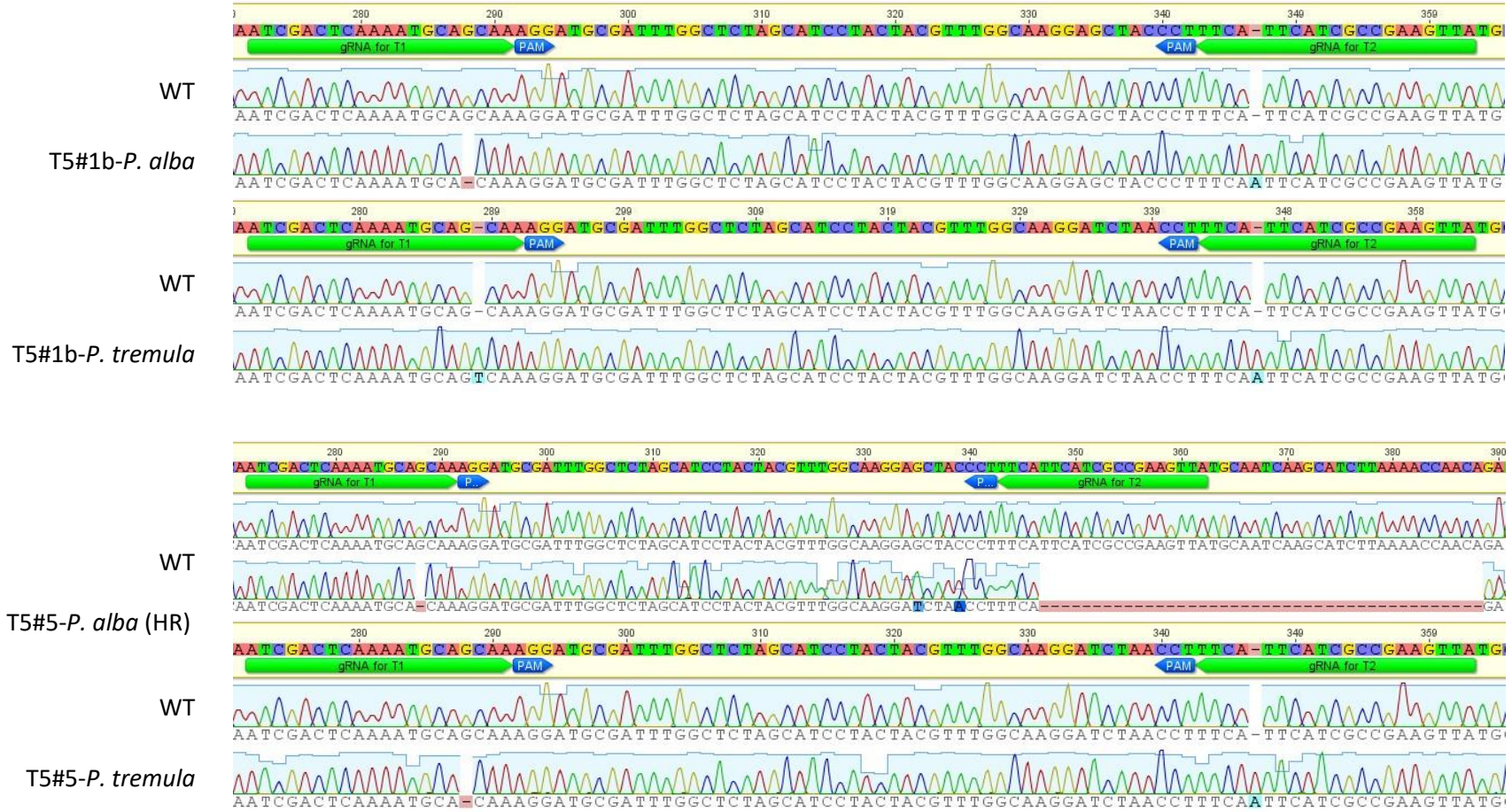

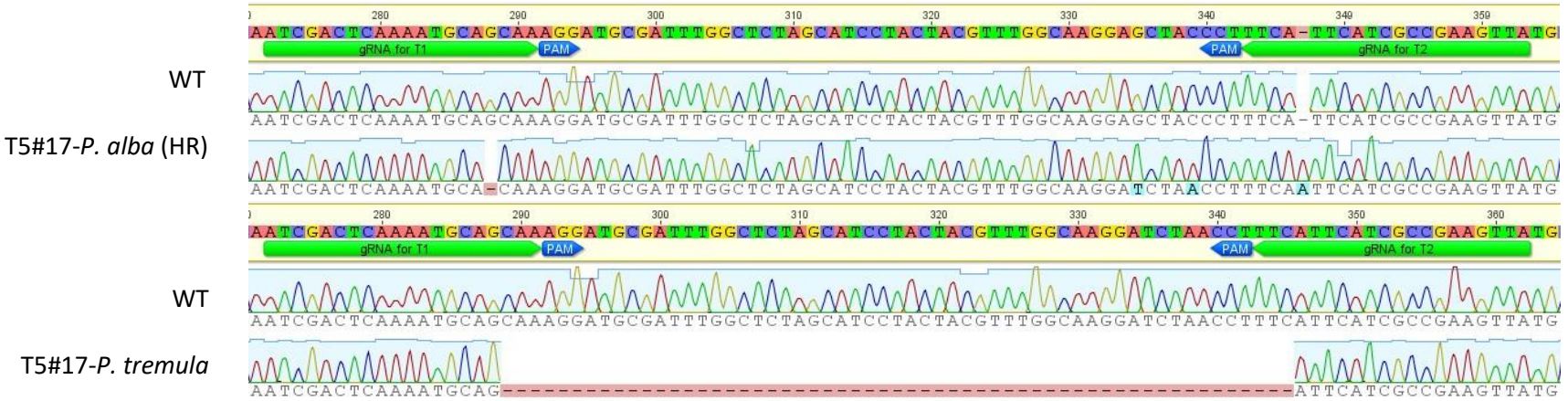

Supplemental Figure 19: Sequence analyses of edited sites in *Pccerk1-1* CRISPR/Cas9 knockout lines. *P. tremula* and *P. alba* alleles were amplified with allele specific primers to sequence the target sites. Sequences were analysed with the software Geneious® 8.1.9 (Kearse et al., 2012). Nucleotides highlighted in blue are different from the wildtype sequence due to substitutions or insertions. Red dashes indicate deletions. The letters **HR** in brackets indicate alba alleles that were repaired by homologous recombination with the tremula allele and then have been edited again. This can be concluded from the whole sequence alignment because changed nucleotides between the guide RNAs correspond to nucleotides of the tremula allele while the rest of the sequence refers still to the alba allele. **T5 #1b, T5 #5, T5 #17**: individual *Pccerk1-1* CRISPR/Cas9 knockout lines; **WT:** wildtype *Populus x canescens*.

6.5.2 Sequence analyses of edited sites in the *Pccerk1-2* CRISPR/Cas9 knockout line

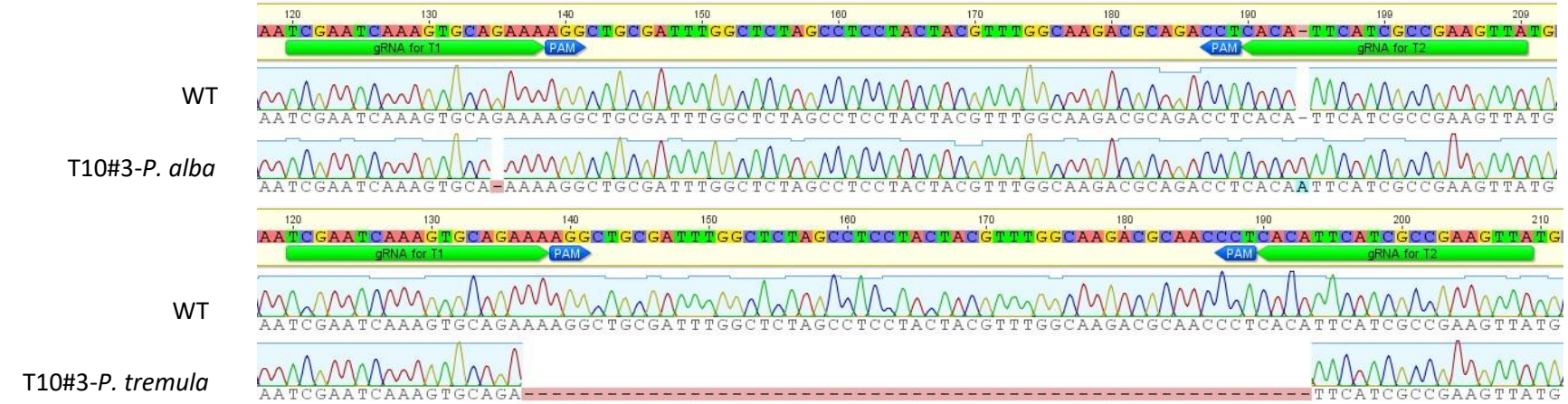

Supplemental Figure 20: Sequence analyses of edited sites in *Pccerk1-2* CRISPR/Cas9 knockout line. *P. tremula* and *P. alba* alleles were amplified with allele specific primers to sequence the target sites. Sequences were analysed with the software Geneious® 8.1.9 (Kearse et al., 2012). Nucleotides highlighted in blue are different from the wildtype sequence due to insertions. Red dashes indicate deletions. **T10 #3**: *Pccerk1-2* CRISPR/Cas9 knockout line; **WT:** wildtype *Populus x canescens*.

6.5.3 Sequence analyses of edited sites in *Pccerk1-1 Pccerk1-2* CRISPR/Cas9 double knockout lines

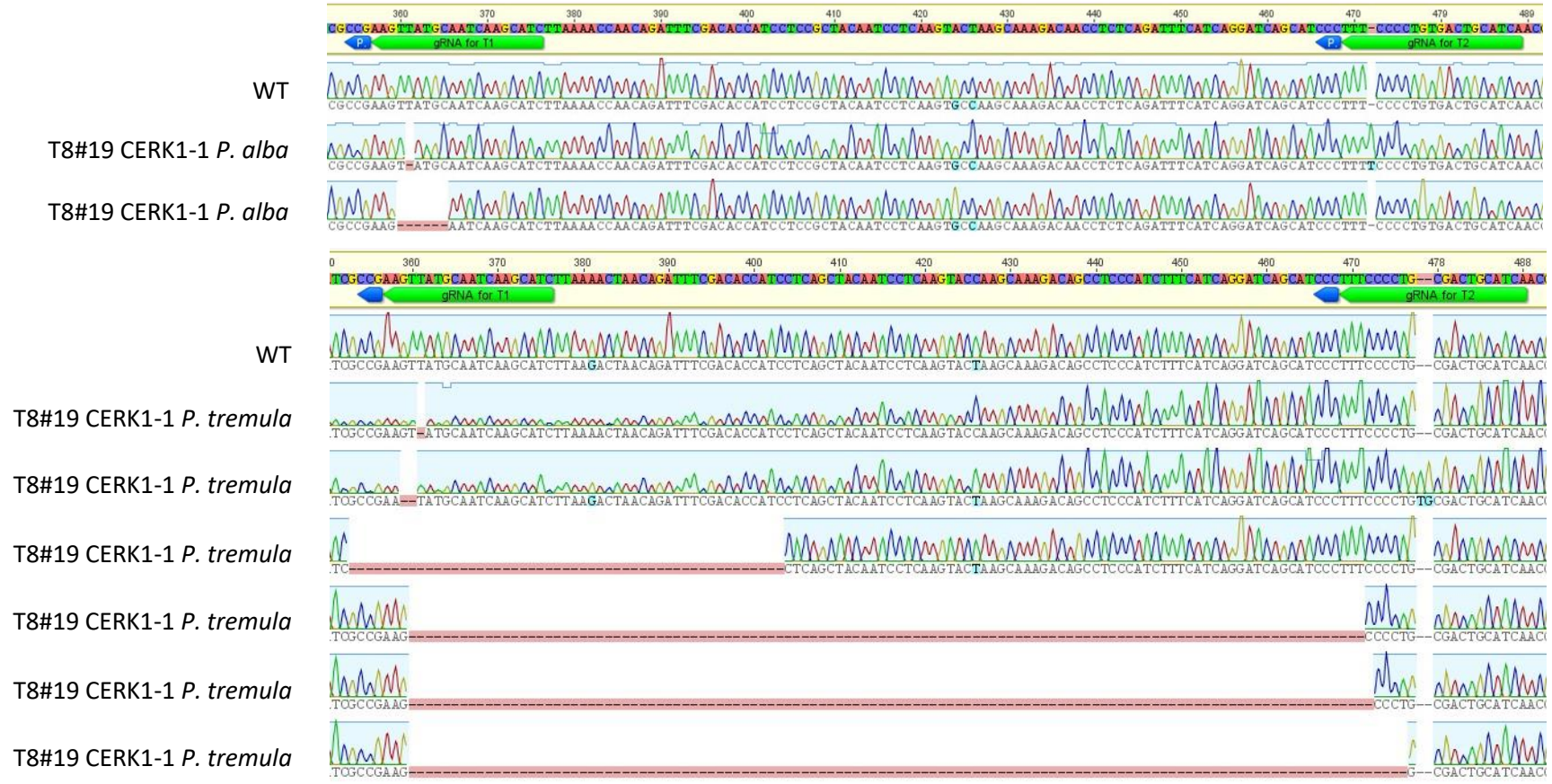

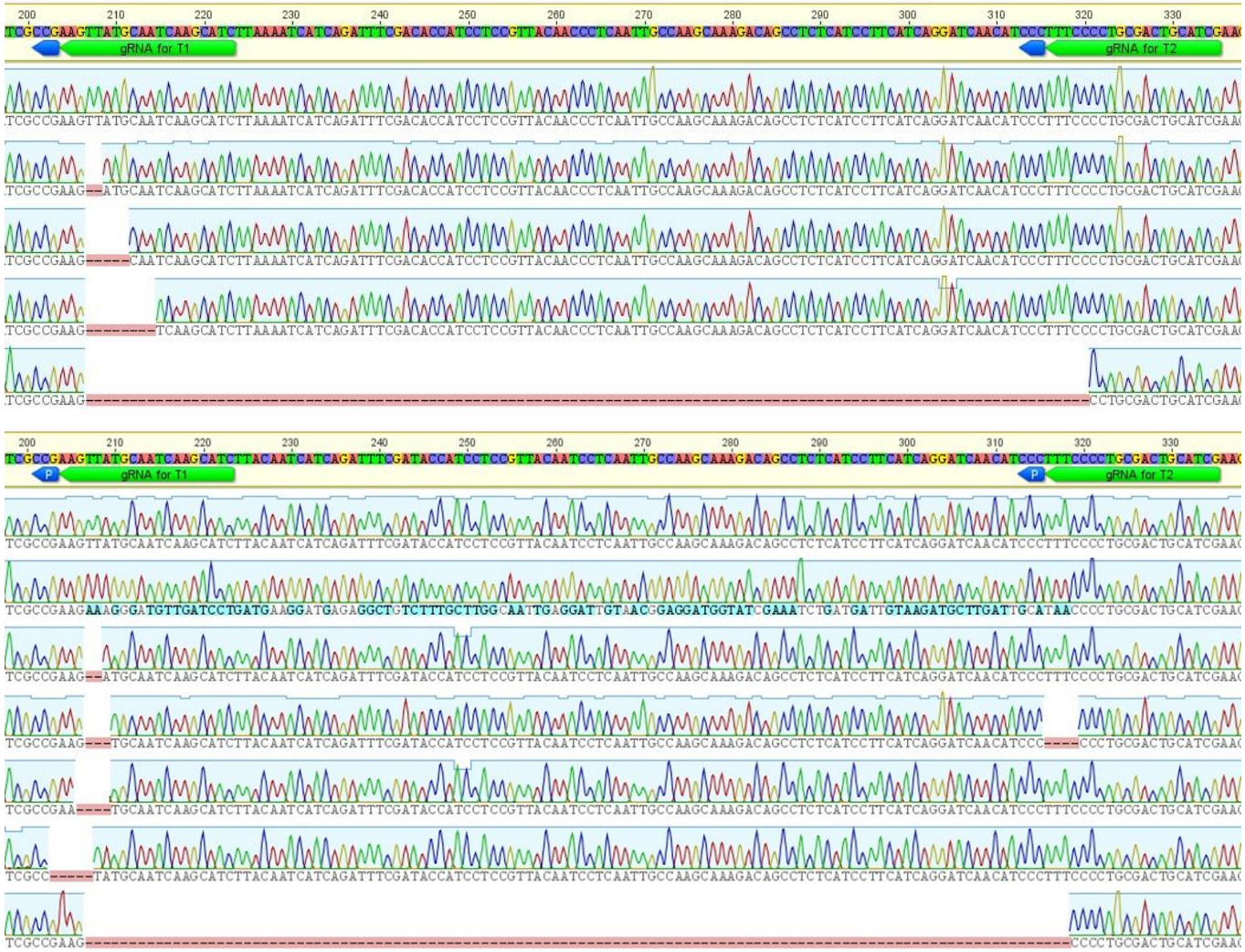
WT
T8#19 CERK1-2 *P. alba*
T8#19 CERK1-2 *P. alba*
T8#19 CERK1-2 *P. alba*
T8#19 CERK1-2 *P. alba*
WT
T8#19 CERK1-2 *P. tremula*
T8#19 CERK1-2 *P. tremula*
T8#19 CERK1-2 *P. tremula*
T8#19 CERK1-2 *P. tremula*
T8#19 CERK1-2 *P. tremula*
T8#19 CERK1-2 *P. tremula*
gRNA for T1
gRNA for T2


WT
T8#20 CERK1-1 *P. alba*
T8#20 CERK1-1 *P. alba*
gRNA for T1
gRNA for T2
WT
T8#20 CERK1-1 *P. tremula*
T8#20 CERK1-1 *P. tremula*
T8#20 CERK1-1 *P. tremula*

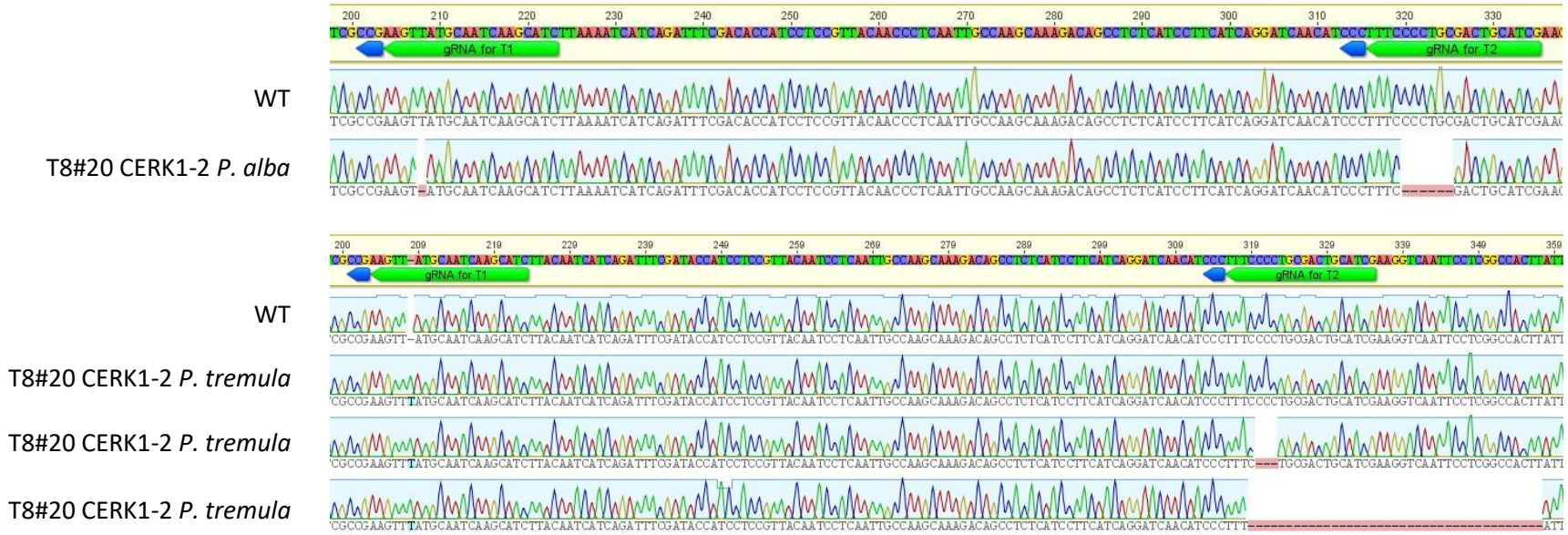

Supplemental Figure 21: Sequence analyses of edited sites in *Pccerk1-1 Pccerk1-2* CRISPR/Cas9 double knockout lines. *P. tremula* and *P. alba* alleles were amplified with allele specific primers to sequence the target sites. Sequences were analysed with the software Geneious® 8.1.9 (Kearse et al., 2012). Nucleotides highlighted in blue are different from the wildtype sequence due to substitutions or insertions. Red dashes indicate deletions. **T8 #19, T8 #20**: *Pccerk1-1 Pccerk1-2* CRISPR/Cas9 double knockout lines; **WT:** wildtype *Populus x canescens*.

List of Figures

List of Tables

List of Supplemental Figures

List of Supplemental Tables

Danksagung

PD Dr. Thomas Teichmann möchte ich herzlich für die gute Betreuung während der Doktorarbeit danken. Sein ehrliches Interesse am Fortschritt dieses Forschungsprojekts hat mir sehr geholfen selbst in schwierigen Phasen motiviert zu bleiben. Außerdem bedanke ich mich dafür, dass er immer ein offenes Ohr für Probleme hatte und einem mit vielen guten Ratschlägen zur Seite stand.

Prof. Dr. Volker Lipka danke ich für die Möglichkeit in seiner Abteilung meine Experimente durchzuführen und ebenso für sein Interesse und den hilfreichen Input während zahlreicher Besprechungen meiner aktuellen Ergebnisse.

Prof. Dr. Andrea Polle danke ich für die kurzfristige Übernahme des Zweitgutachtens. Ebenso danke ich allen weiteren Mitgliedern der Prüfungskommission (Prof. Dr. Volker Lipka, Prof. Dr. Ivo Feußner, Prof. Dr. Christiane Gatz und PD Dr. Marcel Wiermer) für die Bereitschaft bei meiner Disputation als Prüfer zu fungieren.

Ein großes Dankeschön geht auch an Dr. Elena Petutschnig, die mir als Expertin für alle Fragen bezüglich der Massenspektrometrie und Proteinaufreinigung zur Seite gestanden hat und hilfreiche Tipps zur Verbesserung des Proteinaufreinigungsprotokolls geliefert hat.

Dr. Merlin Muhr danke ich für seine fachliche Expertise in der Anfangsphase dieses Dissertationsvorhabens und die Einführung in die Pappeltransformation. Und dafür das du mich mit deiner fröhlichen Art so verzaubert hast, dass wir jetzt glücklich verheiratet sind ;-)

Bei Maria Paulat, unserer biologisch-technischen Assistentin, bedanke ich mich für die Unterstützung bei diversen molekularbiologischen Arbeiten und der intensiven Pflege unserer *in-vitro* Pappelkulturen.

I want to thank Mo Awwanah for being the best college one can wish for: always motivated and in a good mood. Working with you has always been fun because we shared so much laughter ☺ So sad, that we are living now on different continents. I really hope we will manage to see each other again in the future.

Ein ganz besonderer Dank geht auch an Patricia Rohnstock, meine super fleißige Masterstudentin und Hiwi-Kraft. Trotz stressiger Zeiten hast du mir immer bestens gelaunt geholfen, meine Experimente noch rechtzeitig vor dem Mutterschutz fertig zu stellen. Danke vor allem für die zahlreichen Westernblots und das mitfiebern, ob diese das erhoffte Ergebnis zeigen. Außerdem hast du mit deinen lustigen Geschichten immer unsere Pausenzeiten aufgewertet.

Bei Roberto Palm bedanke ich mich dafür, dass du im Rahmen deiner Bachelorarbeit mit großer Begeisterung deine Experimente durchgeführt hast und somit auch einen wertvollen Beitrag für diese Arbeit geleistet hast.

Ich bedanke mich auch herzlich bei Andrzej Majcherczyk und Oliver Valerius für ihre Unterstützung bei der massenspektrometrischen Messung meiner Proteinproben.

Unseren fleißigen Gärtnerinnen, Feli und Susanne, danke ich für die hervorragende Betreuung unserer getopften Pappelpflanzen und die Bereitstellung zahlreicher Pflanztöpfchen für die Arabidopsisanzucht.

Bei den Mitgliedern des ChitoPop Projekts – Mathias Fladung, Khira Lettkemann, Stefanie Werner und Christine Hallmann – bedanke ich mich für ihre wertvollen Diskussions-Beiträge zu meinen Ergebnissen während unserer regelmäßigen Treffen.

Ebenso bedanke ich mich bei allen Mitdoktoranden (Denise, Daniel, Chrissi, Sina, Julia, Lena, Leonie und Mohamed) für die angenehme Arbeits-Atmosphäre und gegenseitige Unterstützung.

Bei Hanna Berger, Joram Schwartzmann and Matthias Arlt von der „Plant2030 Acadamy“ möchte ich mich für die stets gut organisierten, informativen Kurse und Exkursionen bedanken und auch dass sie dadurch eine hervorragende Möglichkeit geschaffen haben, sich mit Doktoranden anderer Universitäten auszutauschen.

Diese Arbeit mit zwei kleinen Kindern zu schreiben, hat sich als eine extrem große Herausforderung herausgestellt. Mit einem erheblichen Schlaf- und Konzentrationsmangel war es nicht immer einfach, die nötige Motivation zu finden etwas Sinnvolles zu Papier zu bringen. Zuletzt möchte ich mich daher auch noch bei all denjenigen bedanken, die mich in dieser schwierigen Zeit unterstützt haben: bei meinen Mann Merlin, dafür, dass du mich bei schlechter Laune immer erfolgreich wieder aufgemuntert hast und zahlreiche Wochenenden allein mit den Kindern unterwegs warst, um mir die nötige Ruhe zum Schreiben zu verschaffen; bei meiner Familie (Renate, Uli, Janka und Mitja), dass ihr nie daran gezweifelt habt, dass ich dieses Projekt noch abschließen werde und bei meiner allerbesten Freundin Sonja, dafür, dass du immer ein offenes Ohr für meine Probleme hattest und dich nie beschwert hast, wenn ich mal wieder voll im Stress war und wochenlang nichts habe von mir hören lassen.